PPAR Research

Biological Network Analysis of PPAR and Related Signaling Pathways

Lead Guest Editor: Hongbao Cao
Guest Editors: Ancha Baranova, Anastasia Nesterova, and Fuquan Zhang

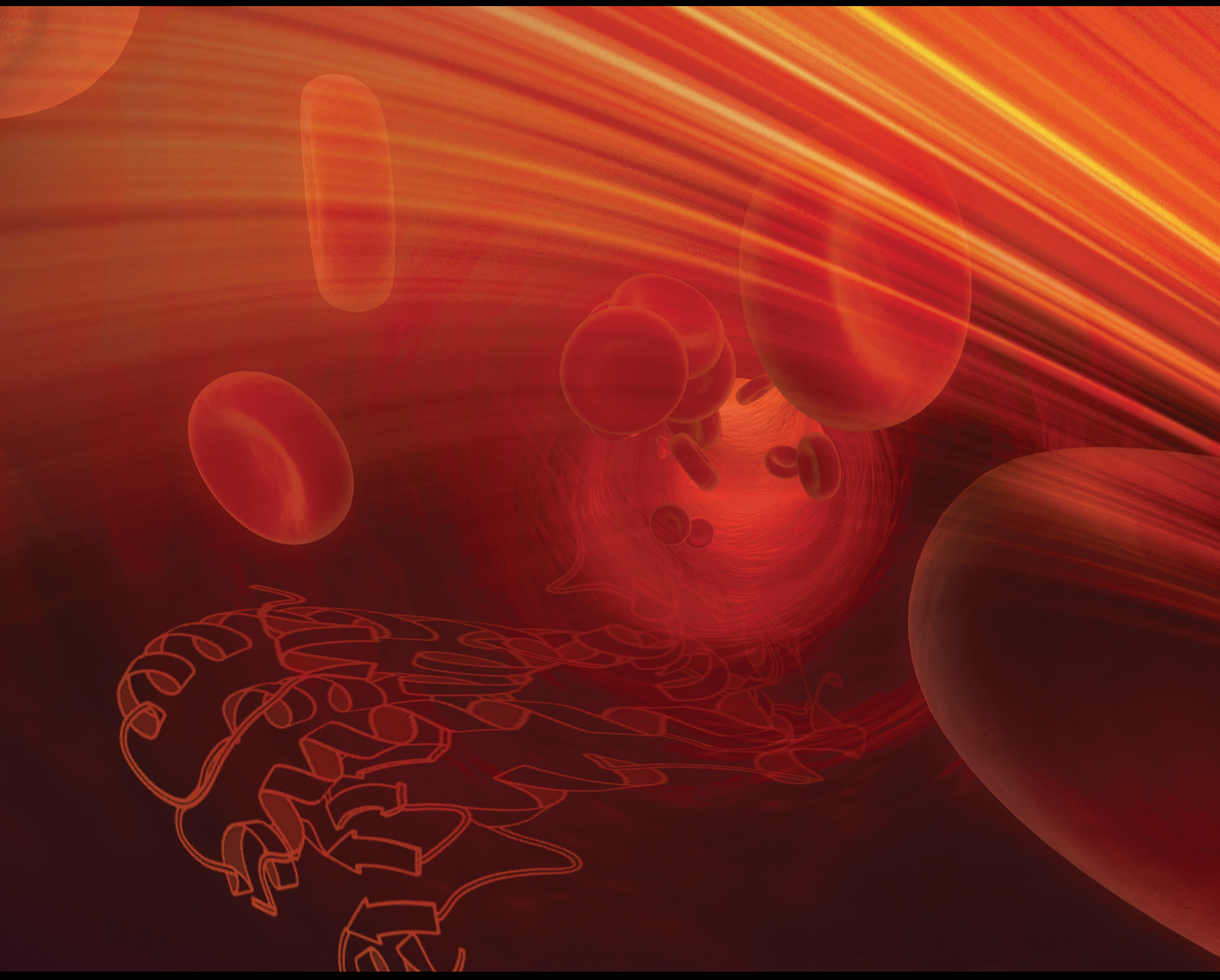

Biological Network Analysis of PPAR and Related Signaling Pathways

PPAR Research

Biological Network Analysis of PPAR and Related Signaling Pathways

Lead Guest Editor: Hongbao Cao
Guest Editors: Ancha Baranova, Anastasia Nesterova, and Fuquan Zhang

Contents

***Pparg* may Promote Chemosensitivity of Hypopharyngeal Squamous Cell Carcinoma**
Meng Lian, Jiaming Chen, Xixi Shen, Lizhen Hou, and Jugao Fang
Research Article (6 pages), Article ID 6452182, Volume 2020 (2020)

Comparative Study of PPAR*γ* Targets in Human Extravillous and Villous Cytotrophoblasts
Fulin Liu, Christine Rouault, Mickael Guesnon, Wencan Zhu, Karine Clément, Séverine A. Degrelle, and Thierry Fournier
Research Article (18 pages), Article ID 9210748, Volume 2020 (2020)

Hindawi
PPAR Research
Volume 2020, Article ID 8859017, 15 pages
https://doi.org/10.1155/2020/8859017

Review Article

Role of PPARs in Progression of Anxiety: Literature Analysis and Signaling Pathways Reconstruction

Olga I. Rudko,[1,2] Artemii V. Tretiakov,[1,2] Elena A. Naumova,[1,2] and Eugene A. Klimov[1,2]

[1]*Faculty of Biology, Lomonosov Moscow State University, Moscow 119234, Russia*
[2]*Sirius University of Science and Technology, Sochi 354340, Russia*

Correspondence should be addressed to Eugene A. Klimov; klimov_eugeney@mail.ru

Received 17 September 2020; Revised 26 October 2020; Accepted 17 November 2020; Published 30 November 2020

Academic Editor: Hongbao Cao

Peroxisome proliferator-activated receptor (PPAR) group includes three isoforms encoded by PPARG, PPARA, and PPARD genes. High concentrations of PPARs are found in parts of the brain linked to anxiety development, including hippocampus and amygdala. Among three PPAR isoforms, PPARG demonstrates the highest expression in CNS, where it can be found in neurons, astrocytes, and glial cells. Herein, the highest PPARG expression occurs in amygdala. However, little is known considering possible connections between PPARs and anxiety behavior. We reviewed possible connections between PPARs and anxiety. We used the Pathway Studio software (Elsevier). Signal pathways were created according to previously developed algorithms. SNEA was performed in Pathway Studio. Current study revealed 14 PPAR-regulated proteins linked to anxiety. Possible mechanism of PPAR involvement in neuroinflammation protection is proposed. Signal pathway reconstruction and reviewing aimed to reveal possible connection between PPARG and CCK-ergic system was conducted. Said analysis revealed that PPARG-dependent regulation of MME and ACE peptidase expression may affect levels of nonhydrolysed, i.e., active CCK-4. Impairments in PPARG regulation and following MME and ACE peptidase expression impairments in amygdala may be the possible mechanism leading to pathological anxiety development, with brain CCK-4 accumulation being a key link. Literature data analysis and signal pathway reconstruction and reviewing revealed two possible mechanisms of peroxisome proliferator-activated receptors involvement in pathological anxiety: (1) cytokine expression and neuroinflammation mechanism and (2) regulation of peptidases targeted to anxiety-associated neuropeptides, primarily CCK-4, mechanism.

1. Introduction

1.1. Anxiety and Anxiety Disorders. Anxiety disorders (including generalized anxiety disorders or panic disorders) are the most widespread mental diseases which are at the same time difficult to treat [1, 2]. Main characteristic of panic disorder is presence of repetitive sudden panic attacks [3]. According to large scale surveys, percentage of population suffering from the anxiety disease throughout lifetime is up to 33.7% [4, 5].

Many researchers report that anxiety disorders cause even more severe decrease in patient's quality of life and psychosocial functions than other chronic diseases including diabetes, cardiovascular diseases, and lung diseases [6–8]. Both environmental factors and genetic factors are believed to be involved in the development of panic disorders [9, 10].

Last decade studies showed that anxiety and anxiety disorder are associated with amygdala functioning and various types of its dysfunction that lead to a decrease in its activity [11–15]. Hypothalamus is also often associated with anxiety [16, 17]. Thus, it was shown that the anorexigenic neuropeptide CCK4 is able to directly interact with the hypothalamus [18].

Most modern studies of the molecular basis underlying F40-F48 series (ICD-10) mental disorders focus on polymorphisms in genes encoding the main neurotransmitter system proteins, i.e., catecholamine and GABAergic [19]. However, it is already clear that they are not the primary link in the fine

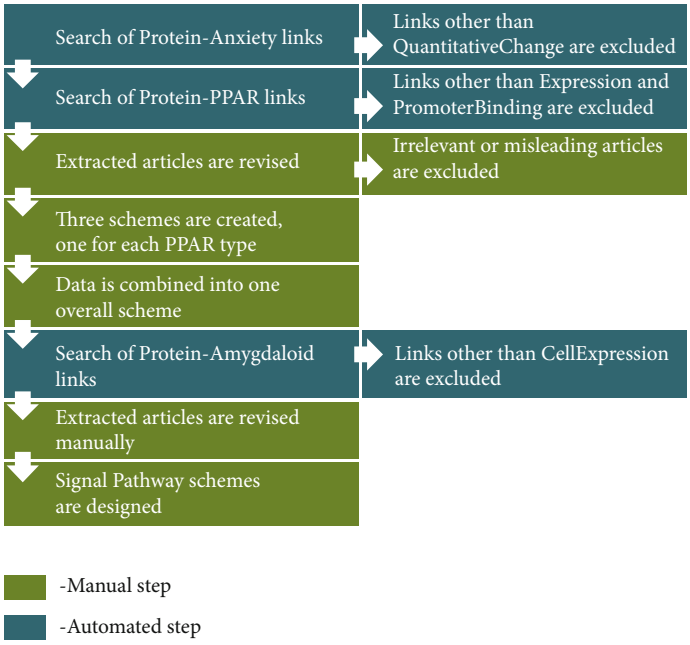

Figure 1: Workflow used in our study. Description in the text.

regulation of the formation, severity, and direction of anxious emotions.

1.2. Peroxisome Proliferator-Activated Receptors. Peroxisome proliferator-activated receptor (PPAR) subfamily belongs to nuclear receptor family. Three isoforms encoded by individual genes are known: PPARγ, PPARα, and PPARδ. PPARs are ligand-dependent transcription factors that regulate target gene expression by binding to specific peroxisome proliferator response elements (PPREs) in the enhancer sites of regulated genes. Each receptor binds to its PPRE as a heterodimer with a retinoid X receptor (RXR). Upon binding of the agonist, PPAR conformation changes and stabilizes, after which transcriptional coactivators contribute to activation of target genes [20].

The PPARs possess the canonical domain structure common to other nuclear receptor family members, including the amino-terminal AF-1 transactivation domain, followed by a DNA-binding domain and a dimerization and ligand binding domain with a ligand-dependent transactivation function AF-2 located at the carboxy-terminal region [21].

PPARs regulate expression of genes actively involved in lipid and carbohydrate metabolism, vascular homeostasis, tissue repair, cell proliferation and differentiation, and sexual dimorphism [22].

PPARs are expressed in almost all mammalian tissues and organs. The expression patterns of PPARα, PPARβ/δ, and PPARγ differ, although intersections do occur. A high expression level of all PPARs is observed in tissues with active fatty acid metabolism. PPARβ/δ is constitutively expressed in almost all tissues [22, 23]. PPARγ among all 3 isoforms has the highest expression in the nervous system, where it was found in neurons, astrocytes, and glial cells [24]. Moreover, all three PPA receptors are expressed both in amygdala and in the hypothalamus [24]. PPAR association with various diseases is also shown [25]. However, the association with anxiety is poorly understood.

This study for the first time analyzes the relationship between PPARs and anxiety. Our results will allow to look at molecular-genetic basis of anxiety disorders pathogenesis, underlying mechanisms and related problems from a new angle.

2. Materials and Methods

We used the Pathway Studio® 9 desktop software with ResNet® 14 database and web version of the Pathway Studio software (https://mammalcedfx.pathwaystudio.com) (Elsevier). Additional search of information was performed by using PubMed (http://www.ncbi.nlm.nih.gov/pubmed/), TargetInsights (https://demo.elseviertextmining.com/), and Google Scholar (https://scholar.google.ru/). Signal pathways were created according to previously developed algorithms [26].

Search algorithm and workflow scheme are presented in Figure 1. Detailed description is given along in Results for better understanding.

3. Results and Discussion

3.1. A Search for Common PPARs and Anxiety Targets. During the first step of our work, we used text-mining and signaling pathway analysis for revealing possible role of PPARs in the development of anxiety.

We used the Pathway Studio® 9 desktop software with ResNet® 14 database and web version of the Pathway Studio software (https://mammalcedfx.pathwaystudio.com) (Elsevier).

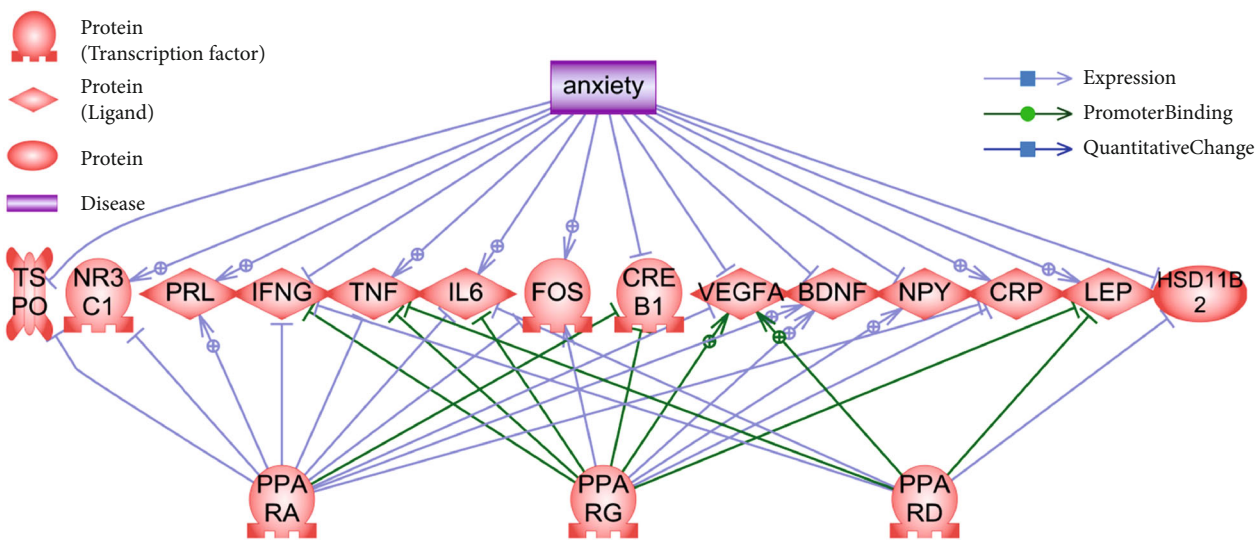

Figure 2: Common targets of anxiety and PPARs. Legend given on the picture.

The search algorithm for anxiety-protein-PPAR links was as follows:

(1) Searching proteins linked to anxiety through concentration change. Linkage type: QuantitativeChange was used in Pathway Studio. This type allows to search for proteins with reported concentration alterations in patients with anxiety. Total of 304 proteins were found

(2) 304 proteins discovered on the previous step were taken into further analysis by searching linkage between protein and each of the three PPARs independently. We had chosen to search for PPAR connections separately to avoid too complicated pathways. Linkage types: Expression and PromoterBinding were used in Pathway Studio. These two types imply direct PPAR effect on protein concentration through promoter binding or other direct interaction which makes them the most relevant

(3) On the next step, all the supporting references were manually revised; at first by reviewing Pathway Studio text-mined "Sentences" section, and after that, if necessary, by studying the whole text for additional details

(4) This analysis resulted in three schemes which include all the proteins linked to both anxiety and PPARs. Each scheme was representing one PPAR isoform

(5) Three schemes created on the previous step were combined into one for better data representation and reducing number of figures

For describing proteins and their role, search engines highlighted in Materials and Methods were used.

Thus, lists of proteins with confirmed quantity changes in anxiety, and proteins connected to PPARs were obtained. Figure 2 and Table 1 show combined target lists.

3.2. Common Target Descriptions and Possible Underlying Mechanisms. Only cytokines (IFNG, IL6, and TNF) and vascular endothelial growth factor A (VEGFA) are regulated by all three PPARs. In most cases, connection to PPARα is present. In one case, HSD11B2, only connection to PPARD is present.

Thus, 14 PPAR-regulated proteins with altered concentration in anxiety are known:

3.2.1. BDNF (Brain-Derived Neurotrophic Factor). Protein's main function is nerve growth and neuron homeostasis [27]. Both BDNF polymorphisms and concentration alterations are linked to variety of mental and neurological diseases [28]. In our case, reduced BDNF product concentration is observed in both animal models ([29], see supplementary (available here)) and patients ([30], see supplementary). The BDNF expression is positively regulated by PPARA ([31], see supplementary) and PPARG ([32], see supplementary). If PPARs-independent BDNF expression regulation pathways are unaltered, lower PPARA and PPARG levels are to be expected as well.

3.2.2. CREB1 (CAMP Responsive Element Binding Protein 1). This is a transcription factor which induces target gene transcription in response to hormonal stimulation via the cAMP pathway. This protein is involved in many cellular processes and is expressed in all tissues (https://www.ncbi.nlm.nih.gov/gene/1385). CREB1 activity is important for brain neuron development and maintenance [33, 34]. Thus, its linkage to mental diseases' pathogenesis is widely studied [35, 36]. The CREB1 expression is known to be lowered in animal models of anxiety [37, 38]. PPARA and PPARG activate CREB1 transcription by binding to its promoter. Exact in-promoter targets of PPARA are known [39, 40], which points out its important role on CREB1 regulation. PPARG was shown to be able to bind to CREB1 promoter bearing certain nucleotide sequence and block its expression [41]. However, other mechanisms leading to CREB1 activation along with

Table 1: List of 14 anxiety-associated proteins–targets of PPARs.

Protein	Full name	Functional class	PPARs
BDNF	Brain derived neurotrophic factor	Growth factor	PPARA PPARG
CREB1	cAMP responsive element binding protein 1	Class bZIP transcription factor	PPARA PPARG
CRP	C-reactive protein	Plasma protein	PPARA PPARG
FOS	FOS proto-oncogene, AP-1 transcription factor subunit	Class bZIP transcription factor	PPARA PPARG
HSD11B2	Hydroxysteroid 11-beta dehydrogenase 2	Steroid metabolism protein	PPARD
IFNG	Interferon gamma	Inflammatory cytokine	PPARA PPARD PPARG
IL6	Interleukin 6	Inflammatory cytokine	PPARA PPARD PPARG
LEP	Leptin	Adipokine	PPARD PPARG
NPY	Neuropeptide Y	Neuropeptide	PPARG
NR3C1	Nuclear receptor subfamily 3 group C member 1	Nuclear steroid hormone receptor family	PPARA
PRL	Prolactin	Glycopeptide hormone (gonadotropins)	PPARA
TNF	Tumor necrosis factor	Inflammatory cytokine/adipokine	PPARA PPARD PPARG
TSPO	Translocator protein	Mitochondrial damage protein	PPARA
VEGFA	Vascular endothelial growth factor A	Growth factor	PPARA PPARD PPARG

PPARG activation are known, i.e., PKCA (protein kinase C, alpha) activation with further CREB1 activation [42]. Interestingly, CREB1 activation via cAMP-PKCA signaling provokes binding of CREB1 to a cAMP responsive element-like site in PPARG gene promoter region [43] which allows to speculate of mutual regulation of these factors.

3.2.3. CRP (C-Reactive Protein). This protein is involved in several host defence-related functions based on its ability to recognize foreign pathogens and damaged host cells and initiate their elimination by interacting with humoral and cellular effector systems in the blood (https://www.ncbi.nlm.nih.gov/gene/1401). CRP linkage to anxiety was shown in several studies. Patients with anxiety were shown to have increased CRP levels [44–46], wherein all authors point out the alterations in patients' immune status. This can be explained by possible interactions between the central nervous system and the immune system in neuropsychiatric disorders. CRP regulation via PPARs is negative in both PPARA ([47, 48], see supplementary) and PPARG ([49, 50], see supplementary) cases. There is no information on PPARD-CRP interactions. Thus, in case of anxiety, we can observe an increase of CRP levels despite PPARA and PPARG blocking it. The reasons may lie in either other CRP activation signal pathways or tissue effects insofar CRP is expressed in the liver. This is the only protein in this list which lacks expression brain regions of interest.

3.2.4. FOS. FOS proteins are members of the transcription factor complex AP-1. FOS proteins were implicated as cell proliferation, differentiation, and transformation regulators. FOS gene is expressed in almost every tissue (https://www.ncbi.nlm.nih.gov/gene/2353). One of the most thorough research of this gene is focused on neuronal plasticity [51, 52]. Animal models of anxiety, fear, and depression show increased FOS in the brain areas linked to the formation of these behavioral reactions in animals [53–55]. Negative effect of PPARA activation on the FOS expression is known [56, 57]. It is also known that PPARG regulates the FOS expression [58–61], but there is no univocal opinion wherever this regulation is positive or negative. It is most likely that several signal pathways involving PPARG and FOS are present. Most of the PPARG-FOS interaction studies are using osteogenesis models, which makes it impossible to

speculate about PPARs-FOS-anxiety linkage. This linkage is the least evidence-supported among this list.

3.2.5. HSD11B2. The corticosteroid 11-beta-dehydrogenase is a microsomal enzyme complex responsible for the interconversion of glucocorticoid cortisol and its inactive metabolite cortisone; this conversion prevents illicit activation of the mineralocorticoid receptor (https://www.ncbi.nlm.nih.gov/gene/3291). Cortisol is intricately linked to anxiety as increases in its concentration correlates with anxiety and its symptoms [62, 63]. Insofar, as HSD11B2 enzyme is directly involved in processes related to cortisol, its role is pathogenesis of diseases characterized by increased cortisol levels is important [64]. Animal models with HSD11B2 gene knockout have inborn predisposition to increased anxiety [65]. Thus, reduced HSD11B2 activity leads to increased cortisol and anxiety phenotype development. Main organs expressing HSD11B2 are the kidneys, intestines, and salivary glands. Only three of PPAR receptors regulate the HSD11B2 expression wherein this regulation is negative. PPARD is known to bind to HSD11B2 promotor in trophoblasts of the placenta and inhibits its expression [66–68]. We have no knowledge of studies describing PPARD and HSD11B2 interactions in other tissues. However, as far as PPARD is expressed in all tissues, both genes are expressed in the kidney which is the most interesting organ from the point of cortisol accumulation. Thus, in case of HSD11B2, one of peroxisome proliferator-activated receptors (PPARD) may be linked to one of the clinical anxiety manifestations, i.e., increased cortisol.

3.2.6. IFNG. Interferon gamma is soluble cytokine that is a member of the type II interferon class, secreted by cells of both the innate and adaptive immune systems (https://www.ncbi.nlm.nih.gov/gene/3458). Its expression is limited by immune system cells. Interferon gamma may modulate anxiety and depressive states via its role in brain plasticity [69]. Other study suggests that decreased INFG in patients with anxiety disorder is not a cause but a result of the disease [70]. However, all PPARs regulate its expression negatively via INFG promotor binding and blocking its transcriptional activity ([71–75], see supplementary). Thus, link between PPARs and INFG regulation is unequivocal, but determining if decreased INFG concentration is a disease's cause, or a consequence is a subject for further studies. It is possible that decrease of INFG concentration is a result of prolonged anxiety.

3.2.7. IL6 (Interleukin 6). This cytokine plays role in inflammation and maturation of B cells; encoded protein was shown to be an endogenous pyrogen capable of inducing fever in people with autoimmune diseases or infections (https://www.ncbi.nlm.nih.gov/gene/3569). Increase of the IL6 expression in patients with anxiety/depression is well known [76–80]. However, some studies show decrease of IL6 levels in states characterized by pathological anxiety [81, 82]. Thus, IL6 anxiety link is possible but requires further studies. All three PPARs negatively regulate IL6 ([83–85], see supplementary). Further understanding PPARs and IL6 interaction requires evaluation of IL6 role in anxiety.

3.2.8. LEP. Leptin is secreted by white adipocytes into the circulation and plays a major role in the regulation of energy homeostasis; it binds to the leptin receptor in the brain, which activates downstream signaling pathways that inhibit feeding and promote energy expenditure (https://www.ncbi.nlm.nih.gov/gene/3952). Leptin concentration is increased in patients with emotional anxiety and reaches its peak in conditions of moderate anxiety [86]. Other studies also show high levels of leptin which correlates with anxiety levels [87–89]. Leptin administration resulted in dose-dependent anxiety decrease [86, 90]. This data points out the positive link between leptin and anxiety. Among three PPARs, two receptors regulate LEP gene expression, i.e., delta and gamma. PPARD binds to the LEP promotor and inhibits its expression [91–93]. Thus, one of the mechanisms of leptin increase in anxiety may be linked to PPARD and PPARG decrease.

3.2.9. NPY. Neuropeptide Y is a neuropeptide that is widely expressed in the central nervous system and influences many physiological processes, including cortical excitability, stress response, food intake, circadian rhythms, and cardiovascular function (https://www.ncbi.nlm.nih.gov/gene/4852). Neuropeptide Y deficiency is significantly linked to anxiety development in all animals including fish and human ([94–97], see supplementary). The NPY expression is linked to only one PPAR—gamma; its positive effect on the NPY expression is known in arcuate hypothalamus [98]. We can speculate that NPY decrease may be linked to alterations in PPARG activation/functioning.

3.2.10. NR3C1. Glucocorticoid receptor can function both as a transcription factor that binds to glucocorticoid response elements in the promoters of glucocorticoid responsive genes to activate their transcription and as a regulator of other transcription factors and involved in inflammatory responses, cellular proliferation, and differentiation in target tissues (https://www.ncbi.nlm.nih.gov/gene/2908). Increase of the NR3C1 expression was linked to anxiety increases in rats [99]; antagonist administration resulted in reduction of anxiety-like behavior in rats [100]. Increased glucocorticoid leads to increased anxiety via activation of receptor NR3C1 [101, 102]. Among all peroxisome proliferator-activated receptors, only PPARA is linked to the NR3C1 expression regulation as it reduces it [103–105]. Wherein mutual gene regulation is known as NR3C1 is capable of activating the PPARA expression [106]. Thus, PPARA is capable of regulating NR3C1-dependent anxiety.

3.2.11. PRL. Prolactin is a hormonal growth regulator for many tissues, including cells of the immune system, essential for lactation (https://www.ncbi.nlm.nih.gov/gene/5617). An increase in prolactin levels is associated with anxiety in women during lactation [107], as well as in paratroopers before jumping [108]. In roman low-avoidance rats with an increased level of anxiety, an increased level of the PRL gene expression in the amygdala was shown [109]. PPARA is the

only PPAR able of activating the PRL expression [110–112]. It is also noted that gene is not necessarily activated via PPARA binding to PRL promotor [111, 113]. Thus, one of the mechanisms leading to the increased PRL in anxiety may be explained due to PPARA activity.

3.2.12. TNF. Tumor necrosis factor is a multifunctional pro-inflammatory cytokine that belongs to the tumor necrosis factor superfamily; it is mainly secreted by macrophages and involved in the regulation of a wide spectrum of biological processes including cell proliferation, differentiation, apoptosis, lipid metabolism, and coagulation (https://www.ncbi.nlm.nih.gov/gene/7124). Serum TNF levels are elevated in patients with anxiety symptoms [114], as well as in patients with generalized anxiety disorder [115]. TNF knockout mice showed a low level of anxiety [116]. Cited works indicate a reliable association of TNF elevation with anxiety. All three PPARs block the expression of TNF, as well as the rest of the cytokines identified in our work ([92, 117–121], see supplementary for additional links). Thus, the explanation of increased TNF in anxiety patients lays either in the malfunction/decreased activity of PPARs or in the activation of another mechanism for regulating the TNF expression.

3.2.13. TSPO. Translocator protein is a key factor in the flow of cholesterol into mitochondria to permit the initiation of steroid hormone synthesis and interacts with some benzodiazepines (https://www.ncbi.nlm.nih.gov/gene/706). The level of TSPO was significantly reduced in both patients with anxiety and anxiety mice models [122–125] and increased after treatment [126]. Since the benzodiazepines are used in the treatment of anxiety and anxiety disorder [127], the association of their molecular target TSPO with anxiety is beyond doubt. The TSPO expression is negatively regulated by PPARA ([128, 129], see supplementary). It can be assumed that PPARA activity may adversely affect the development of anxiety due to a decrease in the TSPO expression.

3.2.14. VEGFA (Vascular Endothelial Growth Factor A). It is a growth factor which induces proliferation and migration of vascular endothelial cells; essential for angiogenesis (https://www.ncbi.nlm.nih.gov/gene/7422). A decrease in VEGFA concentration in patients with anxiety [130, 131] and a high VEGFA level accompanying low anxiety [30] were reported. The VEGFA expression is regulated by all PPARs: delta and gamma bind to the promoter, activating the translation ([132], see supplementary), alpha, on the contrary, blocks VEGFA promoter, reducing expression ([133], see supplementary). Thus, activation and blockade of the VEGFA gene expression are also regulated by transcription factor PPARs. Since the VEGFA expression is reduced in patients with increased anxiety, it can be assumed that in this case, both PPARA activation and a decrease in PPAR delta and gamma activity may occur. Table 2 summarizes above said.

In our analysis, two groups of proteins are the most presented:

(i) Inflammatory cytokines—three members (IL6, INFG, and TNF)

Table 2: Anxiety-associated proteins and PPARs—directions of regulation.

Target	PPARA	PPARD	PPARG
BDNF	↑		↑
CREB1	↓		↓
CRP	↓		↓
FOS	↓		|
HSD11B2		↓	
IFNG	↓	↓	↓
IL6	↓	↓	↓
LEP		↓	↓
NPY			↑
NR3C1	↓		
PRL	↑		
TNF	↓	↓	↓
TSPO	↓		
VEGFA	↓	↑	↑

↑—positive regulation (increased expression), ↓—negative regulation (decreased expression), |—exact effect it unclear, empty field—interaction of this target gene with PPAR is unknown. Italics—decreased expression in anxiety, bold—increased expression in anxiety.

(ii) Transcription factors—three members (CREB1, FOS, and NR3C1)

Interestingly, all PPARs are linked to the inflammatory cytokine expression, while only PPARA and PPARG are involved linked to transcription factor expression. Transcriptional targets of PPARD are involved in immune response and body homeostasis (HSD11B2, LEP, and VEGFA). It expresses in all brain tissues at the same level [24], which indicates the probable absence of its participation in the development of most behavioral reactions, including anxiety.

3.3. PPARs, Common Target, and Amygdala. Proteins, identified in the previous step, were reviewed for expression in amygdaloid:

(1) Amygdaloid was added to the list, and all the amygdaloid-protein links were extracted

(2) All the links except for CellExpression type were excluded

(3) All the supporting references were manually revised at first by reviewing Pathway Studio text-mined "Sentences" section, and after that, if necessary, by studying the whole text for additional details

All detected proteins, except for CRP (C-reactive protein), are expressed in amygdala (Figure 3).

Information about the environment is acquired via sensory organs and is transferred to the thalamus nuclei of the limbic system and then to the cortical sections of the sensory analyzer (auditory, visual, tactile cortex):

(i) The limbic system responds to the image that the brain has perceived and recognized. In particular,

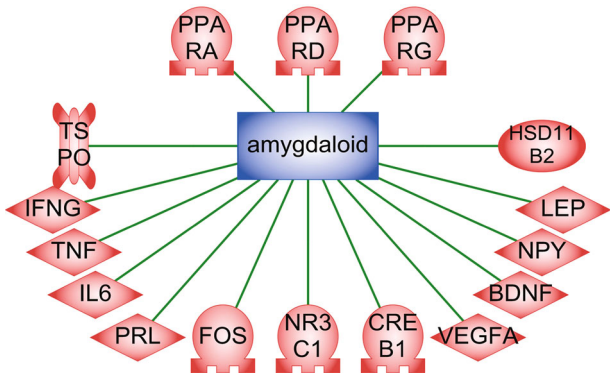

Figure 3: The association of proteins with amygdala. Relation type—CellExpression.

amygdala is responsible for the defensive reaction, fear, and aggression

(ii) The amygdala sends a signal to the prefrontal cortex, which evaluates the situation. Its main function in this cascade is to develop a rescue plan in a situation of perceived danger. This path functions inappropriately in case of phobias, which leads to the development of a sense of fear for the stimuli that are not harmful. The amygdala is a key link in the anxiety formation; it is known that the groups of cells of the amygdala are activated when there is fear or aggression. The central nucleus of the amygdala has direct connections with the hypothalamus and brain stem—areas also responsible for fear.

Thus, the amygdala is currently defined as the main part of the brain responsible for the formation of anxiety and fear [13, 134, 135].

PPARs and retinoid X receptor are expressed in the central nervous system. Delta is widely expressed in all parts of the brain, while alpha and gamma show selective expression:

(i) Gamma is not expressed in the structures of the olfactory bulb, in the part of the olfactory cortex, part of the neocortex, some structures of the thalamus, nuclei of the solitary tract, dorsal motor nuclei of the vagus, and Purkinje cells

(ii) Alpha is not expressed in the hypothalamus [24]

All 3 isoforms are actively expressed in the basal ganglia to which amygdala belongs [24, 136, 137]. Thus, PPARs in high concentration are located in the brain areas involved in the formation of anxiety, including those that are widely represented in the hippocampus and amygdala.

3.4. Enrichment Analysis. To further elucidate role of PPARs in anxiety, we conducted Sub-Network Enrichment Analysis (SNEA) using the Pathway Studio® software using list of genes obtained during the first stage of our study. We found considerable number of pathways/gene sets in almost every search subgroup (SNEA: for compounds regulators (branch-drugs), for compounds regulators, for phenotypes and processes (all), with anatomy, with expression regulators) for every gene associated with anxiety disorder.

Table 3 lists top 10 of 100 substances obtained after the SNEA Compounds Regulators Enriched analysis. Compound regulators were chosen as the most representative search subgroup. All these substances (ginsenoside, epinephrine, corticosterone, norepinephrine, Li+, serotonin, n-3 polyunsaturated fatty acid, dehydroepiandrosterone), either have an antistress, antidepressant, neuroprotective, and neurogenic effects or regulate blood pressure, carbohydrate, and lipid metabolism (according to https://pubchem.ncbi.nlm.nih.gov/). Some of them are found in cellular membranes and blood vessel walls. Despite the low Jaccard similarity, which may be explained by relatively low number of searched genes (17), according to enrichment analysis, good ratio of 9/10 of Gene Set Seed related to neurological regulation is observed. This means that 9 substances out of 10 are related to neurological regulation through underlying pathways. This result points out the significant role these genes play in pathogenesis of psychoneurological diseases.

In this set of 10 substances, genes BDNF, FOS, VEGFA, IFNG, IL6, TNF, and PPAR (A, D, G) are present in 100% of underlying pathways. PPARG is present in 80% of them, while PPARA in 70% cases and PPARD in 50%. This tendency is persists in full list of 100 substances obtained after SNEA Compounds Regulators Enriched analysis with BDNF presence in 77%; FOS, 76%; VEGFA, 82%; IFNG, 76%; IL6, 96%; TNF, 96%; and PPAR (A, D, G), 78%. Among PPARs, PPARA is present in 52% and PPARD in 27%; most presented is PPARG in 71%, wherein only 18% out of 100 substances lack any PPARs in their underlying pathway.

This result is an indirect evidence of PPAR role in the anxiety development.

3.5. Neuroinflammation, PPARs, and Anxiety. Recently, the theory of neuroinflammation as the cause of anxiety development was discussed [138–141]. We performed a signal pathway analysis which revealed possible mechanism explaining the role of PPARs in the development of neuroinflammation (Figure 4).

Signal pathway schemes were designed manually using data available in the ResNet database describing links between objects. Annotated schemes available in the Pathway Studio software were used as well.

We suggest that ligand-activated PPARs block the activity of the NF-kappa B family of transcription factors [142, 143]. Coactivators of PPARs-retinoid-X receptor subfamily [144] and PPARG coactivator 1 alpha (PPARGC1A) [145] are also involved in this process. NF-kappa B activates the transcription of number of proinflammatory cytokines, including those that change their expression during anxiety, i.e., IL6 [146], TNF [147], and IFNG [148]. Thus, PPARs normally block the development of neuroinflammation [149, 150].

3.6. Peroxisome Proliferator-Activated Receptor Gamma (PPARG) and Cholecystokininergic Systems in Anxiety. In recent years, PPARG was shown to be involved in the development of pathological anxiety [151–153]. This surge of

Table 3: Top 10 for compound regulators subnetworks enriched for anxiety disorder-associated genes.

Gene Set Seed	Total number of neighbours	Overlap	Percent overlap	*P* value	Jaccard similarity
Ginsenoside	106	11	10	1.97889*E*-14	0.098214
Alpha-MSH	179	12	6	1.50466*E*-13	0.065217
Epinephrine	292	13	4	1.50691*E*-12	0.043919
Corticosterone	510	15	2	2.00908*E*-12	0.029297
Norepinephrine	412	14	3	3.86353*E*-12	0.033735
Li+	418	14	3	4.72452*E*-12	0.033254
Serotonin	239	12	5	4.9582*E*-12	0.04918
n-3 Polyunsaturated fatty acid	426	14	3	6.14958*E*-12	0.032634
Dehydroepiandrosterone	330	13	3	7.35581*E*-12	0.038922

P value was calculated using Fisher's exact test. Enrichment analysis that does not include experimental values when calculating enrichment from a list. The Jaccard similarity index (Jaccard similarity coefficient) compares members for two sets to see which members are shared and which are distinct. It is a measure of similarity for the two sets of data, with a range from 0% to 100%.

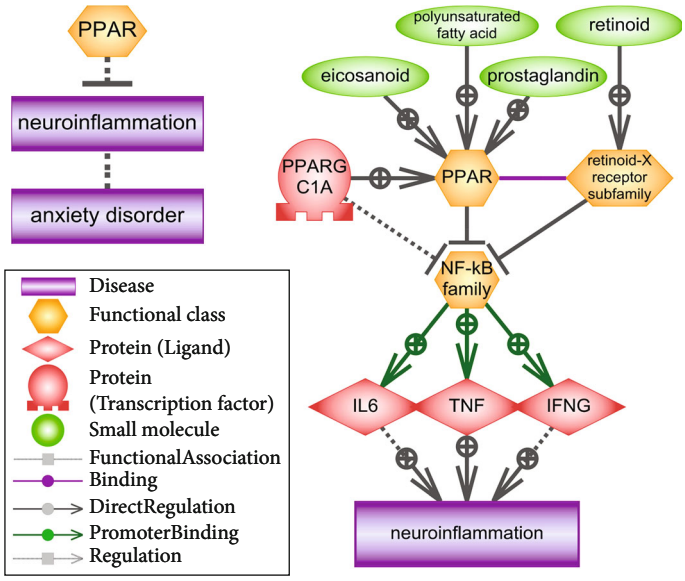

(a) (b)

Figure 4: The association of PPARs with neuroinflammation. (a) The effect of PPARs on neuroinflammation and the association of neuroinflammation with anxiety. (b) The signaling pathway of the blockade by activated PPARs of the transcription factor NF-kappa B, an activator of transcription of cytokines IL6, TNF, and IFNG. The legend in the figure.

research was initiated by Domi et al., whose aim was to study the role of PPARG in the regulation of GABAergic transmission [154]. The work revealed the role of PPARG in the regulation of mood disorders, indicating that weakened signal transmission can contribute to exacerbation of anxiety and the negative effects of stress. Authors suggest that activation of PPARG may be useful in the treatment of psychiatric conditions related to stress and, in particular, anxiety disorders [154].

At the same time, PPARG is most actively expressed in the amygdala [154–158].

Cholecystokinin (CCK) is a neuropeptide which may be found in high concentrations throughout the central nervous system, where it is involved in numerous physiological functions [159]. The role of CCK, especially its smallest functional peptide, CCK-4, in the induction and maintenance of anxiety and major depression is well known [160–162]. The increase in CCK-4 is associated with loss of motivation, anxiety, and panic attacks [159, 163, 164].

The amygdala is firmly connected with the cholecystokininergic system. It was shown that CCK-4 is synthesized and released into amygdala, hippocampal formation, and cerebral cortex [165, 166]. Both CCK-4 receptors are expressed in the amygdala: CCKAR [167, 168] and CCKBR [168, 169].

In this part of the work, we carried out an analysis of signaling pathways in order to identify a possible connection between the cholecystokininergic system and PPARG.

We used the Pathway Studio® 9 desktop software with the ResNet®14 database and web version of the Pathway Studio software (https://mammalcedfx.pathwaystudio.com)

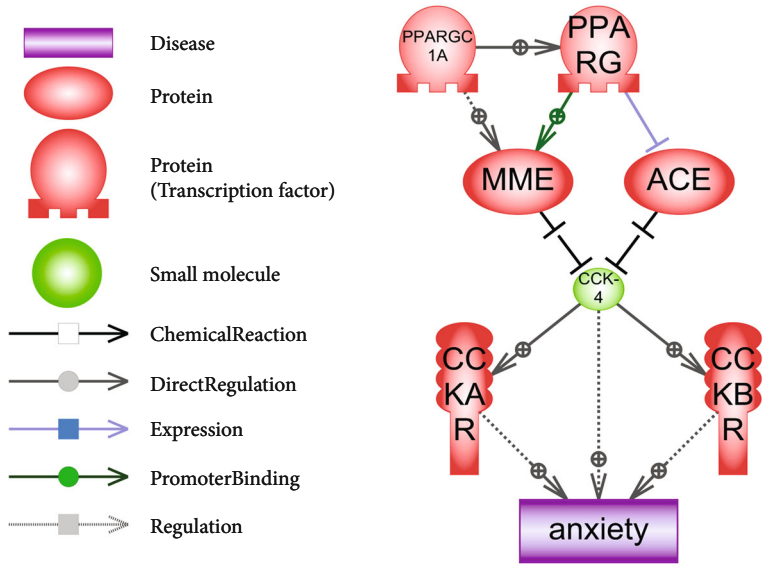

Figure 5: Hypothetical signaling pathway for PPARG in the regulation of anxiety. Legend in the figure.

(Elsevier). Signal pathways were created according to the algorithms we developed [170]. The results are presented in Figure 5 and are described below.

PPARG and PPARGC1A are involved in MME transcription regulation [171]. Simultaneously, PPARG inhibits the ACE expression [172].

CCK-4 hydrolysis (Trp-Met-Asp-Phe = WMDF) may be carried out by two enzymes: membrane metalloendopeptidase (MME, also known as NEP, EC 3.4.24.11) and angiotensin I converting enzyme (ACE, EC 3.4.15.1) [173]. MME and ACE cut 2 terminal amino acids (DF) from CCK-4 and CCK-8 which leads to forming of unfunctional peptides (or dipeptides WM and DF in case of CCK-4) [174, 175].

Thus, PPARG-related MME and ACE expression regulation affect levels of active nonhydrolysed CCK-4. Dysregulation of PPARG and the following alteration of peptidase expression in amygdala may be a possible mechanism of pathological anxiety development, with a CCK-4 accumulation as a main cause. This may explain Domi et al. results [154].

4. Conclusions

We examined possible associations of PPARs with anxiety. An analysis of the data and signaling pathways available in the literature suggests two mechanisms for the participation of peroxisome proliferator-activated receptors in the formation of anxiety: (1) expression of cytokines and neuroinflammation and (2) regulation of the expression of peptidases, the targets of which are neuropeptides associated with anxiety (CCK-4 in the first place). Further research in these areas will help to better understand the role of PPARs in the development of anxiety.

Data Availability

All supplemental materials (Excel file) are available to download from ResearchGate resource by the link https://www.researchgate.net/publication/340418909_Supplemental_Materials_Role_of_PPARs_in_progression_of_anxiety. Additional data is available from the corresponding author upon reasonable request.

Conflicts of Interest

The authors declare that there is no conflict of interest regarding the publication of this paper.

Acknowledgments

The reported study was funded by RFBR, project number 19-34-51045.

Supplementary Materials

The supplement file was provided for this study (an excel file), including following information: PPARs and neuroinflammation relation sheet, PPARs and CCK4 relation sheet, PPARs and anxiety common target sheet, and amygdaloid expressed gene sheet. The data on relations between objects on pathways. The downloadable online version can be accessed via ResearchGate: https://www.researchgate.net/publication/340418909_Supplemental_Materials_Role_of_PPARs_in_progression_of_anxiety. *(Supplementary Materials)*

References

[1] D. J. Kupfer, "Anxiety and DSM-5," *Dialogues in Clinical Neuroscience*, vol. 17, no. 3, pp. 245-246, 2015.

[2] F. Thibaut, "Anxiety disorders: a review of current literature," *Dialogues in Clinical Neuroscience*, vol. 19, no. 2, pp. 87-88, 2017.

[3] C. Cackovic, S. Nazir, and R. Marwaha, "Panic disorder (attack)," in *StatPearls*, StatPearls Publishing, Treasure Island, FL, USA, 2020.

[4] B. Bandelow and S. Michaelis, "Epidemiology of anxiety disorders in the 21st century," *Dialogues in Clinical Neuroscience*, vol. 17, no. 3, pp. 327–335, 2015.

[5] H.-U. Wittchen, "Generalized anxiety disorder: prevalence, burden, and cost to society," *Depression and Anxiety*, vol. 16, no. 4, pp. 162–171, 2002.

[6] J. Davidoff, S. Christensen, D. N. Khalili, J. Nguyen, and W. W. IsHak, "Quality of life in panic disorder: looking beyond symptom remission," *Quality of Life Research*, vol. 21, no. 6, pp. 945–959, 2012.

[7] M. V. Mendlowicz and M. B. Stein, "Quality of life in individuals with anxiety disorders," *The American Journal of Psychiatry*, vol. 157, no. 5, pp. 669–682, 2000.

[8] A. E. Meuret, N. Tunnell, and A. Roque, "Anxiety disorders and medical comorbidity: treatment implications," *Advances in Experimental Medicine and Biology*, vol. 1191, pp. 237–261, 2020.

[9] R. B. Goldstein, P. J. Wickramaratne, E. Horwath, and M. M. Weissman, "Familial aggregation and phenomenology of 'Early'-Onset (at or before age 20 years)," *Archives of General Psychiatry*, vol. 54, no. 3, pp. 271–278, 1997.

[10] J. M. Hettema, M. C. Neale, and K. S. Kendler, "A review and meta-analysis of the genetic epidemiology of anxiety disorders," *The American Journal of Psychiatry*, vol. 158, no. 10, pp. 1568–1578, 2001.

[11] S. Chakraborty, S. J. Tripathi, T. R. Raju, and B. S. Shankaranarayana Rao, "Brain stimulation rewarding experience attenuates neonatal clomipramine-induced adulthood anxiety by reversal of pathological changes in the amygdala," *Progress in Neuro-Psychopharmacology & Biological Psychiatry*, vol. 103, article 110000, 2020.

[12] X. Li and X. Li, "The antidepressant effect of light therapy from retinal projections," *Neuroscience Bulletin*, vol. 34, no. 2, pp. 359–368, 2018.

[13] C. Ottaviani, D. Cevolani, V. Nucifora et al., "Amygdala responses to masked and low spatial frequency fearful faces: a preliminary fMRI study in panic disorder," *Psychiatry Research*, vol. 203, no. 2-3, pp. 159–165, 2012.

[14] O. T. Ousdal, O. A. Andreassen, A. Server, and J. Jensen, "Increased amygdala and visual cortex activity and functional connectivity towards stimulus novelty is associated with state anxiety," *PLoS One*, vol. 9, no. 4, article e96146, 2014.

[15] L. Zhang, K. Wang, C. Zhu, F. Yu, and X. Chen, "Trait anxiety has effect on decision making under ambiguity but not decision making under risk," *PLoS One*, vol. 10, no. 5, article e0127189, 2015.

[16] J. H. Jiang, Y. L. Peng, P. J. Zhang et al., "The ventromedial hypothalamic nucleus plays an important role in anxiolytic-like effect of neuropeptide S," *Neuropeptides*, vol. 67, pp. 36–44, 2018.

[17] J. C. Jimenez, K. Su, A. R. Goldberg et al., "Anxiety cells in a hippocampal-hypothalamic circuit," *Neuron*, vol. 97, no. 3, pp. 670–683.e6, 2018.

[18] V. Cano, E. Caicoya, and M. Ruiz-Gayo, "Effect of peripheral cholecystokinin receptor agonists on c-Fos expression in brain sites mediating food consumption in rats," *Neuroscience Letters*, vol. 343, no. 1, pp. 13–16, 2003.

[19] J. D. A. Olivier and B. Olivier, "Translational studies in the complex role of neurotransmitter systems in anxiety and anxiety disorders," *Advances in Experimental Medicine and Biology*, vol. 1191, pp. 121–140, 2020.

[20] J. Berger and D. E. Moller, "The mechanisms of action of PPARs," *Annual Review of Medicine*, vol. 53, no. 1, pp. 409–435, 2002.

[21] V. Zoete, A. Grosdidier, and O. Michielin, "Peroxisome proliferator-activated receptor structures: ligand specificity, molecular switch and interactions with regulators," *Biochimica et Biophysica Acta (BBA) - Molecular and Cell Biology of Lipids*, vol. 1771, no. 8, pp. 915–925, 2007.

[22] L. Michalik, J. Auwerx, J. P. Berger et al., "International Union of Pharmacology. LXI. Peroxisome proliferator-activated receptors," *Pharmacological Reviews*, vol. 58, no. 4, pp. 726–741, 2006.

[23] W. Wahli and L. Michalik, "PPARs at the crossroads of lipid signaling and inflammation," *Trends in Endocrinology and Metabolism*, vol. 23, no. 7, pp. 351–363, 2012.

[24] S. Moreno, S. Farioli-Vecchioli, and M. P. Cerù, "Immunolocalization of peroxisome proliferator-activated receptors and retinoid X receptors in the adult rat CNS," *Neuroscience*, vol. 123, no. 1, pp. 131–145, 2004.

[25] S. Tyagi, P. Gupta, A. S. Saini, C. Kaushal, and S. Sharma, "The peroxisome proliferator-activated receptor: a family of nuclear receptors role in various diseases," *Journal of Advanced Pharmaceutical Technology & Research*, vol. 2, no. 4, pp. 236–240, 2011.

[26] A. P. Nesterova, A. Yuryev, E. A. Klimov et al., *Disease Pathways: An Atlas of Human Disease Signaling Pathways*, Elsevier, Waltham, 1st edition, 2019.

[27] M. Zagrebelsky, C. Tacke, and M. Korte, "BDNF signaling during the lifetime of dendritic spines," *Cell and Tissue Research*, vol. 382, no. 1, pp. 185–199, 2020.

[28] C.-C. Lin and T.-L. Huang, "Brain-derived neurotrophic factor and mental disorders," *Biomedical Journal*, vol. 43, no. 2, pp. 134–142, 2020.

[29] D. Olsen, M. Kaas, O. Schwartz, A. Nykjaer, and S. Glerup, "Loss of BDNF or its receptors in three mouse models has unpredictable consequences for anxiety and fear acquisition," *Learning & Memory*, vol. 20, no. 9, pp. 499–504, 2013.

[30] I. Aksu, B. Baykara, S. Ozbal et al., "Maternal treadmill exercise during pregnancy decreases anxiety and increases prefrontal cortex VEGF and BDNF levels of rat pups in early and late periods of life," *Neuroscience Letters*, vol. 516, no. 2, pp. 221–225, 2012.

[31] Y. Fu, J. Zhen, and Z. Lu, "Synergetic neuroprotective effect of docosahexaenoic acid and aspirin in SH-Y5Y by inhibiting miR-21 and activating RXRα and PPARα," *DNA and Cell Biology*, vol. 36, no. 6, pp. 482–489, 2017.

[32] T. Kariharan, G. Nanayakkara, K. Parameshwaran et al., "Central activation of PPAR-gamma ameliorates diabetes induced cognitive dysfunction and improves BDNF expression," *Neurobiology of Aging*, vol. 36, no. 3, pp. 1451–1461, 2015.

[33] Y. H. Belgacem and L. N. Borodinsky, "CREB at the crossroads of activity-dependent regulation of nervous system development and function," *Advances in Experimental Medicine and Biology*, vol. 1015, pp. 19–39, 2017.

[34] T. Laviv, B. Scholl, P. Parra-Bueno et al., "In vivo imaging of the coupling between neuronal and CREB activity in the mouse brain," *Neuron*, vol. 105, no. 5, pp. 799–812.e5, 2020.

[35] H. Wang, J. Xu, P. Lazarovici, R. Quirion, and W. Zheng, "cAMP response element-binding protein (CREB): a possible signaling molecule link in the pathophysiology of

schizophrenia," *Frontiers in Molecular Neuroscience*, vol. 11, p. 255, 2018.

[36] C. Yu, Y. X. Bai, X. P. Xu et al., "Behavioral abnormality along with NMDAR-related CREB suppression in rat hippocampus after shortwave exposure," *Biomedical and Environmental Sciences*, vol. 32, no. 3, pp. 189–198, 2019.

[37] M. Barrot, D. L. Wallace, C. A. Bolaños et al., "Regulation of anxiety and initiation of sexual behavior by CREB in the nucleus accumbens," *Proceedings National Academy of Sciences United States of America*, vol. 102, no. 23, pp. 8357–8362, 2005.

[38] T. Rubino, C. Guidali, D. Vigano et al., "CB1 receptor stimulation in specific brain areas differently modulate anxiety-related behaviour," *Neuropharmacology*, vol. 54, no. 1, pp. 151–160, 2008.

[39] A. Roy, M. Jana, G. T. Corbett et al., "Regulation of cyclic AMP response element binding and hippocampal plasticity-related genes by peroxisome proliferator-activated receptor α," *Cell Reports*, vol. 4, no. 4, pp. 724–737, 2013.

[40] A. Roy and K. Pahan, "PPARα signaling in the hippocampus: crosstalk between fat and memory," *Journal of Neuroimmune Pharmacology*, vol. 10, no. 1, pp. 30–34, 2015.

[41] C. Sharma, A. Pradeep, R. G. Pestell, and B. Rana, "Peroxisome proliferator-activated receptor gamma activation modulates cyclin D1 transcription via beta-catenin-independent and cAMP-response element-binding protein-dependent pathways in mouse hepatocytes," *The Journal of Biological Chemistry*, vol. 279, no. 17, pp. 16927–16938, 2004.

[42] J. Vamecq, J.-M. Colet, J. J. Vanden Eynde, G. Briand, N. Porchet, and S. Rocchi, "PPARs: interference with Warburg' effect and clinical anticancer trials," *PPAR Research*, vol. 2012, Article ID 304760, 23 pages, 2012.

[43] X. He, J.-L. Hu, J. Li et al., "A feedback loop in PPARγ-adenosine A2A receptor signaling inhibits inflammation and attenuates lung damages in a mouse model of LPS-induced acute lung injury," *Cellular Signalling*, vol. 25, no. 9, pp. 1913–1923, 2013.

[44] R. Hou, G. Ye, Y. Liu et al., "Effects of SSRIs on peripheral inflammatory cytokines in patients with Generalized Anxiety Disorder," *Brain, Behavior, and Immunity*, vol. 81, pp. 105–110, 2019.

[45] T. Liukkonen, P. Räsänen, J. Jokelainen et al., "The association between anxiety and C-reactive protein (CRP) levels: results from the Northern Finland 1966 birth cohort study," *European Psychiatry*, vol. 26, no. 6, pp. 363–369, 2011.

[46] C. Pitsavos, D. B. Panagiotakos, C. Papageorgiou, E. Tsetsekou, C. Soldatos, and C. Stefanadis, "Anxiety in relation to inflammation and coagulation markers, among healthy adults: the ATTICA study," *Atherosclerosis*, vol. 185, no. 2, pp. 320–326, 2006.

[47] M. C. Cave, H. B. Clair, J. E. Hardesty et al., "Nuclear receptors and nonalcoholic fatty liver disease," *Biochimica et Biophysica Acta (BBA) - Gene Regulatory Mechanisms*, vol. 1859, no. 9, pp. 1083–1099, 2016.

[48] M. H. Davidson and P. P. Toth, "Comparative effects of lipid-lowering therapies," *Progress in Cardiovascular Diseases*, vol. 47, no. 2, pp. 73–104, 2004.

[49] A. Laudisio, M. R. Lo Monaco, D. L. Vetrano et al., "Association of metabolic syndrome with falls in patients with Parkinson's disease," *Clinical Nutrition*, vol. 36, no. 2, pp. 559–563, 2017.

[50] J. Plutzky, "Peroxisome proliferator-activated receptors as therapeutic targets in inflammation," *Journal of the American College of Cardiology*, vol. 42, no. 10, pp. 1764–1766, 2003.

[51] F. T. Gallo, C. Katche, J. F. Morici, J. H. Medina, and N. V. Weisstaub, "Immediate early genes, memory and psychiatric disorders: focus on c-Fos, Egr1 and Arc," *Frontiers in Behavioral Neuroscience*, vol. 12, p. 79, 2018.

[52] J. Jaworski, K. Kalita, and E. Knapska, "c-Fos and neuronal plasticity: the aftermath of Kaczmarek's theory," *Acta Neurobiologiae Experimentalis (Wars)*, vol. 78, no. 4, pp. 287–296, 2018.

[53] C. E. O'Neill, R. J. Newsom, J. Stafford et al., "Adolescent caffeine consumption increases adulthood anxiety-related behavior and modifies neuroendocrine signaling," *Psychoneuroendocrinology*, vol. 67, pp. 40–50, 2016.

[54] L. G. Staples, "Predator odor avoidance as a rodent model of anxiety: learning-mediated consequences beyond the initial exposure," *Neurobiology of Learning and Memory*, vol. 94, no. 4, pp. 435–445, 2010.

[55] B. Xiao, F. Han, H.-T. Wang, and Y.-X. Shi, "Single-prolonged stress induces increased phosphorylation of extracellular signal-regulated kinase in a rat model of post-traumatic stress disorder," *Molecular Medicine Reports*, vol. 4, pp. 445–449, 2011.

[56] C.-B. Li, X.-X. Li, Y.-G. Chen et al., "Effects and mechanisms of PPARalpha activator fenofibrate on myocardial remodelling in hypertension," *Journal of Cellular and Molecular Medicine*, vol. 13, no. 11-12, pp. 4444–4452, 2009.

[57] T. Nakamachi, T. Nomiyama, F. Gizard et al., "PPARalpha agonists suppress osteopontin expression in macrophages and decrease plasma levels in patients with type 2 diabetes," *Diabetes*, vol. 56, no. 6, pp. 1662–1670, 2007.

[58] S. Lim, C. J. Jin, M. Kim et al., "PPARγ gene transfer sustains apoptosis, inhibits vascular smooth muscle cell proliferation, and reduces neointima formation after balloon injury in rats," *Arteriosclerosis, Thrombosis, and Vascular Biology*, vol. 26, no. 4, pp. 808–813, 2006.

[59] A. Nakanishi and I. Tsukamoto, "n-3 polyunsaturated fatty acids stimulate osteoclastogenesis through PPARγ-mediated enhancement of c-Fos expression, and suppress osteoclastogenesis through PPARγ-dependent inhibition of NFkB activation," *The Journal of Nutritional Biochemistry*, vol. 26, no. 11, pp. 1317–1327, 2015.

[60] Y. Wan, L.-W. Chong, and R. M. Evans, "PPAR-gamma regulates osteoclastogenesis in mice," *Nature Medicine*, vol. 13, no. 12, pp. 1496–1503, 2007.

[61] Y.-X. Wu, Y. Sun, Y.-P. Ye et al., "Iguratimod prevents ovariectomy-induced bone loss and suppresses osteoclastogenesis via inhibition of peroxisome proliferator-activated receptor-γ," *Molecular Medicine Reports*, vol. 16, no. 6, pp. 8200–8208, 2017.

[62] B. Dierckx, G. Dieleman, J. H. M. Tulen et al., "Persistence of anxiety disorders and concomitant changes in cortisol," *Journal of Anxiety Disorders*, vol. 26, no. 6, pp. 635–641, 2012.

[63] S. Fischer and A. J. Cleare, "Cortisol as a predictor of psychological therapy response in anxiety disorders-systematic review and meta-analysis," *Journal of Anxiety Disorders*, vol. 47, pp. 60–68, 2017.

[64] P. C. White, "Alterations of cortisol metabolism in human disorders," *Hormone Research in Pædiatrics*, vol. 89, no. 5, pp. 320–330, 2018.

[65] M. C. Holmes, C. T. Abrahamsen, K. L. French, J. M. Paterson, J. J. Mullins, and J. R. Seckl, "The mother or the fetus? 11beta-hydroxysteroid dehydrogenase type 2 null mice provide evidence for direct fetal programming of behavior by endogenous glucocorticoids," *The Journal of Neuroscience*, vol. 26, no. 14, pp. 3840–3844, 2006.

[66] T. Fournier, V. Tsatsaris, K. Handschuh, and D. Evain-Brion, "PPARs and the placenta," *Placenta*, vol. 28, no. 2-3, pp. 65–76, 2007.

[67] P. He, Z. Chen, Q. Sun, Y. Li, H. Gu, and X. Ni, "Reduced expression of 11β-hydroxysteroid dehydrogenase type 2 in preeclamptic placentas is associated with decreased PPARγ but increased PPARα expression," *Endocrinology*, vol. 155, no. 1, pp. 299–309, 2014.

[68] L. Julan, H. Guan, J. P. van Beek, and K. Yang, "Peroxisome proliferator-activated receptor delta suppresses 11beta-hydroxysteroid dehydrogenase type 2 gene expression in human placental trophoblast cells," *Endocrinology*, vol. 146, no. 3, pp. 1482–1490, 2005.

[69] A. C. Campos, G. N. Vaz, V. M. Saito, and A. L. Teixeira, "Further evidence for the role of interferon-gamma on anxiety- and depressive-like behaviors: involvement of hippocampal neurogenesis and NGF production," *Neuroscience Letters*, vol. 578, pp. 100–105, 2014.

[70] R. Tükel, B. A. Arslan, B. A. Ertekin et al., "Decreased IFN-γ and IL-12 levels in panic disorder," *Journal of Psychosomatic Research*, vol. 73, no. 1, pp. 63–67, 2012.

[71] J. Fenimore and H. A. Young, "Regulation of IFN-γ expression," *Advances in Experimental Medicine and Biology*, vol. 941, pp. 1–19, 2016.

[72] P. Libby and J. Plutzky, "Inflammation in diabetes mellitus: role of peroxisome proliferator-activated Receptor–α and peroxisome proliferator-activated Receptor–γ agonists," *The American Journal of Cardiology*, vol. 99, no. 4, pp. 27–40, 2007.

[73] Y. Liu, J. Wang, S. Luo, Y. Zhan, and Q. Lu, "The roles of PPARγ and its agonists in autoimmune diseases: a comprehensive review," *Journal of Autoimmunity*, vol. 113, article 102510, 2020.

[74] Y. Okabayashi, S. Nagasaka, G. Kanzaki, N. Tsuboi, T. Yokoo, and A. Shimizu, "Group 1 innate lymphoid cells are involved in the progression of experimental anti-glomerular basement membrane glomerulonephritis and are regulated by peroxisome proliferator-activated receptor α," *Kidney International*, vol. 96, no. 4, pp. 942–956, 2019.

[75] H.-J. Park and J.-M. Choi, "Sex-specific regulation of immune responses by PPARs," *Experimental & Molecular Medicine*, vol. 49, no. 8, article e364, 2017.

[76] O. Y. Alshogran, A. A. Khalil, A. O. Oweis, S. M. Altawalbeh, and M. A. Y. Alqudah, "Association of brain-derived neurotrophic factor and interleukin-6 serum levels with depressive and anxiety symptoms in hemodialysis patients," *General Hospital Psychiatry*, vol. 53, pp. 25–31, 2018.

[77] E. Avolio, G. Fazzari, M. Mele et al., "Unpredictable chronic mild stress paradigm established effects of pro- and anti-inflammatory cytokine on neurodegeneration-linked depressive states in hamsters with brain endothelial damages," *Molecular Neurobiology*, vol. 54, no. 8, pp. 6446–6458, 2017.

[78] J. Lasselin, S. Elsenbruch, M. Lekander et al., "Mood disturbance during experimental endotoxemia: predictors of state anxiety as a psychological component of sickness behavior," *Brain, Behavior, and Immunity*, vol. 57, pp. 30–37, 2016.

[79] B. Leonard and M. Maes, "Mechanistic explanations how cell-mediated immune activation, inflammation and oxidative and nitrosative stress pathways and their sequels and concomitants play a role in the pathophysiology of unipolar depression," *Neuroscience and Biobehavioral Reviews*, vol. 36, no. 2, pp. 764–785, 2012.

[80] Z. Zou, B. Zhou, Y. Huang, J. Wang, W. Min, and T. Li, "Differences in cytokines between patients with generalised anxiety disorder and panic disorder," *Journal of Psychosomatic Research*, vol. 133, article 109975, 2020.

[81] S. T. H. Lee, "Inflammation, depression, and anxiety disorder: a population-based study examining the association between interleukin-6 and the experiencing of depressive and anxiety symptoms," *Psychiatry Research*, vol. 285, article 112809, 2020.

[82] E.-Y. N. Wagner, M.-P. F. Strippoli, V. Ajdacic-Gross et al., "Generalized anxiety disorder is prospectively associated with decreased levels of interleukin-6 and adiponectin among individuals from the community," *Journal of Affective Disorders*, vol. 270, pp. 114–117, 2020.

[83] H. Chang, F. Zhao, X. Xie et al., "PPARα suppresses Th17 cell differentiation through IL-6/STAT3/RORγt pathway in experimental autoimmune myocarditis," *Experimental Cell Research*, vol. 375, no. 1, pp. 22–30, 2019.

[84] G. Kökény, L. Calvier, E. Legchenko, P. Chouvarine, M. M. Mózes, and G. Hansmann, "PPARγ is a gatekeeper for extracellular matrix and vascular cell homeostasis," *Current Opinion in Nephrology and Hypertension*, vol. 29, no. 2, pp. 171–179, 2020.

[85] Z. Kunicka, A. Kurzyńska, A. Szydłowska, B. Kaczyńska, and I. Bogacka, "PPARβ/δ ligands regulate the expression of immune response mediators in the porcine endometrium - an in vitro study," *Theriogenology*, vol. 134, pp. 112–120, 2019.

[86] D. J. Haleem, Z. Haque, Q.-A. Inam, H. Ikram, and M. A. Haleem, "Behavioral, hormonal and central serotonin modulating effects of injected leptin," *Peptides*, vol. 74, pp. 1–8, 2015.

[87] M. E. Byrne, M. Tanofsky-Kraff, M. Jaramillo et al., "Relationships of trait anxiety and loss of control eating with serum leptin concentrations among youth," *Nutrients*, vol. 11, no. 9, p. 2198, 2019.

[88] S. Cernea, E. Both, A. Huțanu, F. L. Şular, and A. L. Roiban, "Correlations of serum leptin and leptin resistance with depression and anxiety in patients with type 2 diabetes," *Psychiatry and Clinical Neurosciences*, vol. 73, no. 12, pp. 745–753, 2019.

[89] J. Liu, M. Guo, and X.-Y. Lu, "Leptin/LepRb in the ventral tegmental area mediates anxiety-related behaviors," *The International Journal of Neuropsychopharmacology*, vol. 19, no. 2, article pyv115, 2016.

[90] S. M. Tyree, R. G. K. Munn, and N. McNaughton, "Anxiolytic-like effects of leptin on fixed interval responding," *Pharmacology, Biochemistry, and Behavior*, vol. 148, pp. 15–20, 2016.

[91] L. V. d'Uscio, T. He, A. V. R. Santhanam, L.-J. Tai, R. M. Evans, and Z. S. Katusic, "Mechanisms of vascular dysfunction in mice with endothelium-specific deletion of the PPAR-δ gene," *American Journal of Physiology-Heart and Circulatory Physiology*, vol. 306, no. 7, pp. H1001–H1010, 2014.

[92] A. Magadum and F. B. Engel, "PPARβ/δ: linking metabolism to regeneration," *International Journal of Molecular Sciences*, vol. 19, no. 7, p. 2013, 2018.

[93] K.-D. Wagner, M. Benchetrit, L. Bianchini, J.-F. Michiels, and N. Wagner, "Peroxisome proliferator-activated receptor β/δ (PPARβ/δ) is highly expressed in liposarcoma and promotes migration and proliferation," *The Journal of Pathology*, vol. 224, no. 4, pp. 575–588, 2011.

[94] R. Sah and T. D. Geracioti, "Neuropeptide Y and posttraumatic stress disorder," *Molecular Psychiatry*, vol. 18, no. 6, pp. 646–655, 2013.

[95] S. Sayed, N. T. Van Dam, S. R. Horn et al., "A randomized dose-ranging study of neuropeptide Y in patients with posttraumatic stress disorder," *The International Journal of Neuropsychopharmacology*, vol. 21, no. 1, pp. 3–11, 2018.

[96] S. N. Schmeltzer, J. P. Herman, and R. Sah, "Neuropeptide Y (NPY) and posttraumatic stress disorder (PTSD): a translational update," *Experimental Neurology*, vol. 284, pp. 196–210, 2016.

[97] K. Shiozaki, M. Kawabe, K. Karasuyama et al., "Neuropeptide Y deficiency induces anxiety-like behaviours in zebrafish (Danio rerio)," *Scientific Reports*, vol. 10, no. 1, p. 5913, 2020.

[98] J. T. Garretson, B. J. W. Teubner, K. L. Grove, A. Vazdarjanova, V. Ryu, and T. J. Bartness, "Peroxisome proliferator-activated receptor γ controls ingestive behavior, agouti-related protein, and neuropeptide Y mRNA in the arcuate hypothalamus," *The Journal of Neuroscience*, vol. 35, no. 11, pp. 4571–4581, 2015.

[99] N. J. Grundwald and P. J. Brunton, "Prenatal stress programs neuroendocrine stress responses and affective behaviors in second generation rats in a sex-dependent manner," *Psychoneuroendocrinology*, vol. 62, pp. 204–216, 2015.

[100] N. Calvo, M. Cecchi, M. Kabbaj, S. J. Watson, and H. Akil, "Differential effects of social defeat in rats with high and low locomotor response to novelty," *Neuroscience*, vol. 183, pp. 81–89, 2011.

[101] S. Hellwig and K. Domschke, "Anxiety in late life: an update on pathomechanisms," *Gerontology*, vol. 65, no. 5, pp. 465–473, 2019.

[102] J. V. Zorn, R. R. Schür, M. P. Boks, R. S. Kahn, M. Joëls, and C. H. Vinkers, "Cortisol stress reactivity across psychiatric disorders: a systematic review and meta-analysis," *Psychoneuroendocrinology*, vol. 77, pp. 25–36, 2017.

[103] N. Bougarne, R. Paumelle, S. Caron et al., "PPARα blocks glucocorticoid receptor α-mediated transactivation but cooperates with the activated glucocorticoid receptor α for transrepression on NF-κB," *Proceedings National Academy of Sciences United States of America*, vol. 106, no. 18, pp. 7397–7402, 2009.

[104] X. Chen, M. Li, W. Sun et al., "Peroxisome proliferator-activated receptor alpha agonist-induced down-regulation of hepatic glucocorticoid receptor expression in SD rats," *Biochemical and Biophysical Research Communications*, vol. 368, no. 4, pp. 865–870, 2008.

[105] T. Varga, Z. Czimmerer, and L. Nagy, "PPARs are a unique set of fatty acid regulated transcription factors controlling both lipid metabolism and inflammation," *Biochimica et Biophysica Acta (BBA) - Molecular Basis of Disease*, vol. 1812, no. 8, pp. 1007–1022, 2011.

[106] G. Rando, C. K. Tan, N. Khaled et al., "Glucocorticoid receptor-PPARα axis in fetal mouse liver prepares neonates for milk lipid catabolism," *eLife*, vol. 5, 2016.

[107] B. L. Parry, L. F. Martínez, E. L. Maurer, A. M. López, D. Sorenson, and C. J. Meliska, "Sleep, rhythms and women's mood. Part I. Menstrual cycle, pregnancy and postpartum," *Sleep Medicine Reviews*, vol. 10, no. 2, pp. 129–144, 2006.

[108] R. T. Chatterton, K. M. Vogelsong, Y. C. Lu, and G. A. Hudgens, "Hormonal responses to psychological stress in men preparing for skydiving," *The Journal of Clinical Endocrinology and Metabolism*, vol. 82, no. 8, pp. 2503–2509, 1997.

[109] M. Sabariego, M. J. Gómez, I. Morón et al., "Differential gene expression between inbred Roman high- (RHA-I) and low- (RLA-I) avoidance rats," *Neuroscience Letters*, vol. 504, no. 3, pp. 265–270, 2011.

[110] B. König, C. Rauer, S. Rosenbaum, C. Brandsch, K. Eder, and G. I. Stangl, "Fasting upregulates PPARα target genes in brain and influences pituitary hormone expression in a PPARα dependent manner," *PPAR Research*, vol. 2009, Article ID 801609, 9 pages, 2009.

[111] R. M. Tolón, A. I. Castillo, and A. Aranda, "Activation of the prolactin gene by peroxisome proliferator-activated receptor-alpha appears to be DNA binding-independent," *The Journal of Biological Chemistry*, vol. 273, no. 41, pp. 26652–26661, 1998.

[112] R. M. Tolón, A. I. Castillo, A. M. Jiménez-Lara, and A. Aranda, "Association with Ets-1 causes ligand- and AF2-independent activation of nuclear receptors," *Molecular and Cellular Biology*, vol. 20, no. 23, pp. 8793–8802, 2000.

[113] C. Tomkiewicz, F. Muzeau, A. D. Edgar, R. Barouki, and M. Aggerbeck, "Opposite regulation of the rat and human cytosolic aspartate aminotransferase genes by fibrates," *Biochemical Pharmacology*, vol. 67, no. 2, pp. 213–225, 2004.

[114] M. Postal, A. T. Lapa, N. A. Sinicato et al., "Depressive symptoms are associated with tumor necrosis factor alpha in systemic lupus erythematosus," *Journal of Neuroinflammation*, vol. 13, no. 1, p. 5, 2016.

[115] R. Hou, M. Garner, C. Holmes et al., "Peripheral inflammatory cytokines and immune balance in Generalised Anxiety Disorder: case-controlled study," *Brain, Behavior, and Immunity*, vol. 62, pp. 212–218, 2017.

[116] M. L. Camara, F. Corrigan, E. J. Jaehne et al., "TNF-α and its receptors modulate complex behaviours and neurotrophins in transgenic mice," *Psychoneuroendocrinology*, vol. 38, no. 12, pp. 3102–3114, 2013.

[117] C. Ciavarella, I. Motta, S. Valente, and G. Pasquinelli, "Pharmacological (or synthetic) and nutritional agonists of PPAR-γ as candidates for cytokine storm modulation in COVID-19 disease," *Molecules*, vol. 25, no. 9, p. 2076, 2020.

[118] A. Dutta and N. Sharma-Walia, "Curbing lipids: impacts on cancer and viral infection," *International Journal of Molecular Sciences*, vol. 20, no. 3, p. 644, 2019.

[119] O. Y. Kytikova, J. M. Perelman, T. P. Novgorodtseva et al., "Peroxisome proliferator-activated receptors as a therapeutic target in asthma," *PPAR Research*, vol. 2020, Article ID 8906968, 18 pages, 2020.

[120] Y. Ma, M. Shi, Y. Wang, and J. Liu, "PPARγ and its agonists in chronic kidney disease," *International Journal of Nephrology*, vol. 2020, Article ID 2917474, 10 pages, 2020.

[121] N. Wagner and K.-D. Wagner, "PPAR beta/delta and the hallmarks of cancer," *Cell*, vol. 9, no. 5, p. 1133, 2020.

[122] D. Li, J. Zheng, M. Wang et al., "Changes of TSPO-mediated mitophagy signaling pathway in learned helplessness mice," *Psychiatry Research*, vol. 245, pp. 141–147, 2016.

[123] X.-B. Li, A. Liu, L. Yang et al., "Antidepressant-like effects of translocator protein (18 kDa) ligand ZBD-2 in mouse models

of postpartum depression," *Molecular Brain*, vol. 11, no. 1, p. 12, 2018.

[124] S. Taliani, I. Pugliesi, and F. Da Settimo, "Structural requirements to obtain highly potent and selective 18 kDa Translocator Protein (TSPO) Ligands," *Current Topics in Medicinal Chemistry*, vol. 11, no. 7, pp. 860–886, 2011.

[125] L. Veenman and M. Gavish, "The peripheral-type benzodiazepine receptor and the cardiovascular system. Implications for drug development," *Pharmacology & Therapeutics*, vol. 110, no. 3, pp. 503–524, 2006.

[126] T. Barichello, L. R. Simões, A. Collodel et al., "The translocator protein (18kDa) and its role in neuropsychiatric disorders," *Neuroscience and Biobehavioral Reviews*, vol. 83, pp. 183–199, 2017.

[127] R. Balon and V. Starcevic, "Role of benzodiazepines in anxiety disorders," *Advances in Experimental Medicine and Biology*, vol. 1191, pp. 367–388, 2020.

[128] A. Batarseh and V. Papadopoulos, "Regulation of translocator protein 18 kDa (TSPO) expression in health and disease states," *Molecular and Cellular Endocrinology*, vol. 327, no. 1-2, pp. 1–12, 2010.

[129] M. Gazouli, Z.-X. Yao, N. Boujrad, J. C. Corton, M. Culty, and V. Papadopoulos, "Effect of peroxisome proliferators on Leydig cell peripheral-type benzodiazepine receptor gene expression, hormone-stimulated cholesterol transport, and steroidogenesis: role of the peroxisome proliferator-activator receptor α," *Endocrinology*, vol. 143, no. 7, pp. 2571–2583, 2002.

[130] O. Petyunina, M. Kopytsya, I. Kuznetsov, and I. Vyshnevska, "Prognostication of clinical outcomes after stemi: the role of vascular endothelial growth factor-A," *Georgian Medical news*, vol. 279, pp. 79–86, 2018.

[131] T. Tomita, N. Yasui-Furukori, S. Tsuchimine, A. Kaneda, and S. Kaneko, "Relationships between vascular endothelial growth factor levels and temperament and character inventory traits in healthy Japanese subjects," *Neuropsychobiology*, vol. 69, no. 1, pp. 1–5, 2014.

[132] C. Röhrl, U. Kaindl, I. Koneczny et al., "Peroxisome-proliferator-activated receptors γ and β/δ mediate vascular endothelial growth factor production in colorectal tumor cells," *Journal of Cancer Research and Clinical Oncology*, vol. 137, no. 1, pp. 29–39, 2011.

[133] R. Grau, C. Punzón, M. Fresno, and M. A. Iñiguez, "Peroxisome-proliferator-activated receptor alpha agonists inhibit cyclo-oxygenase 2 and vascular endothelial growth factor transcriptional activation in human colorectal carcinoma cells via inhibition of activator protein-1," *The Biochemical Journal*, vol. 395, no. 1, pp. 81–88, 2006.

[134] J. M. Spielberg, J. M. Schwarz, and M. A. Matyi, "Anxiety in transition: neuroendocrine mechanisms supporting the development of anxiety pathology in adolescence and young adulthood," *Frontiers in Neuroendocrinology*, vol. 55, article 100791, 2019.

[135] S. P. A. Wolfensberger, D. J. Veltman, W. J. G. Hoogendijk, D. I. Boomsma, and E. J. C. de Geus, "Amygdala responses to emotional faces in twins discordant or concordant for the risk for anxiety and depression," *NeuroImage*, vol. 41, no. 2, pp. 544–552, 2008.

[136] G.-Q. Chang, O. Karatayev, O. Lukatskaya, and S. F. Leibowitz, "Prenatal fat exposure and hypothalamic PPAR β/δ: possible relationship to increased neurogenesis of orexigenic peptide neurons," *Peptides*, vol. 79, pp. 16–26, 2016.

[137] J. Yong, L. Yan, J. Wang, H. Xiao, and Q. Zeng, "Effects of compound 21, a non-peptide angiotensin II type 2 receptor agonist, on general anesthesia-induced cerebral injury in neonatal rats," *Molecular Medicine Reports*, vol. 18, pp. 5337–5344, 2018.

[138] B. M. Flannery, J. L. Silverman, D. A. Bruun et al., "Behavioral assessment of NIH Swiss mice acutely intoxicated with tetramethylenedisulfotetramine," *Neurotoxicology and Teratology*, vol. 47, pp. 36–45, 2015.

[139] N. Haji, G. Mandolesi, A. Gentile et al., "TNF-α-mediated anxiety in a mouse model of multiple sclerosis," *Experimental Neurology*, vol. 237, no. 2, pp. 296–303, 2012.

[140] K. Sanchez, S. P. Guerin, and L. K. Fonken, "Anxiety in obesity: is neuroinflammation the critical link?," *Brain, Behavior, and Immunity*, vol. 78, pp. 7-8, 2019.

[141] B. Willekens, G. Perrotta, P. Cras, and N. Cools, "Into the moment: does mindfulness affect biological pathways in multiple sclerosis?," *Frontiers in Behavioral Neuroscience*, vol. 12, p. 103, 2018.

[142] J. Korbecki, R. Bobiński, and M. Dutka, "Self-regulation of the inflammatory response by peroxisome proliferator-activated receptors," *Inflammation Research*, vol. 68, no. 6, pp. 443–458, 2019.

[143] H. Shen, E. Oesterling, A. Stromberg, M. Toborek, R. Mac Donald, and B. Hennig, "Zinc deficiency induces vascular pro-inflammatory parameters associated with NF-kappaB and PPAR signaling," *Journal of the American College of Nutrition*, vol. 27, no. 5, pp. 577–587, 2008.

[144] N. Martin, X. Ma, and D. Bernard, "Regulation of cellular senescence by retinoid X receptors and their partners," *Mechanisms of Ageing and Development*, vol. 183, article 111131, 2019.

[145] J.-J. Zhou, J.-D. Ma, Y.-Q. Mo et al., "Down-regulating peroxisome proliferator-activated receptor-gamma coactivator-1 beta alleviates the proinflammatory effect of rheumatoid arthritis fibroblast-like synoviocytes through inhibiting extracellular signal-regulated kinase, p38 and nuclear factor-kappaB activation," *Arthritis Research & Therapy*, vol. 16, no. 5, p. 472, 2014.

[146] Y. Lin, M. Sun, S. M. Fuentes, C. D. Keim, T. Rothermel, and B. He, "Inhibition of interleukin-6 expression by the V protein of parainfluenza virus 5," *Virology*, vol. 368, no. 2, pp. 262–272, 2007.

[147] W. Zou, A. Amcheslavsky, S. Takeshita, H. Drissi, and Z. Bar-Shavit, "TNF-alpha expression is transcriptionally regulated by RANK ligand," *Journal of Cellular Physiology*, vol. 202, no. 2, pp. 371–378, 2005.

[148] L. Wang, J. Zhu, S. Shan et al., "Repression of interferon-gamma expression in T cells by Prospero-related homeobox protein," *Cell Research*, vol. 18, no. 9, pp. 911–920, 2008.

[149] T. Maeda and S. Kishioka, "Chapter 13 PPAR and pain," *International Review of Neurobiology*, vol. 85, pp. 165–177, 2009.

[150] R. A. Quintanilla, E. Utreras, and F. A. Cabezas-Opazo, "Role of PPAR γ in the differentiation and function of neurons," *PPAR Research*, vol. 2014, Article ID 768594, 9 pages, 2014.

[151] A. Domi, S. Stopponi, E. Domi, R. Ciccocioppo, and N. Cannella, "Sub-dimensions of alcohol use disorder in alcohol preferring and non-preferring rats, a comparative study," *Frontiers in Behavioral Neuroscience*, vol. 13, p. 3, 2019.

[152] J. D. Jones, S. D. Comer, V. E. Metz et al., "Pioglitazone, a PPARγ agonist, reduces nicotine craving in humans, with marginal effects on abuse potential," *Pharmacology, Biochemistry, and Behavior*, vol. 163, pp. 90–100, 2017.

[153] T. Zimmermann, J. C. Bartsch, A. Beer et al., "Impaired anandamide/palmitoylethanolamide signaling in hippocampal glutamatergic neurons alters synaptic plasticity, learning, and emotional responses," *Neuropsychopharmacology*, vol. 44, no. 8, pp. 1377–1388, 2019.

[154] E. Domi, S. Uhrig, L. Soverchia et al., "Genetic deletion of neuronal PPARγ enhances the emotional response to acute stress and exacerbates anxiety: an effect reversed by rescue of amygdala PPARγ function," *The Journal of Neuroscience*, vol. 36, no. 50, pp. 12611–12623, 2016.

[155] K. Boes, V. Russmann, T. Ongerth et al., "Expression regulation and targeting of the peroxisome proliferator-activated receptor γ following electrically-induced status epilepticus," *Neuroscience Letters*, vol. 604, pp. 151–156, 2015.

[156] E. Domi, F. F. Caputi, P. Romualdi et al., "Activation of PPARγ attenuates the expression of physical and affective nicotine withdrawal symptoms through mechanisms involving amygdala and hippocampus neurotransmission," *The Journal of Neuroscience*, vol. 39, no. 49, pp. 9864–9875, 2019.

[157] J. C. Gaspar, B. N. Okine, A. Llorente-Berzal, M. Roche, and D. P. Finn, "Pharmacological blockade of PPAR isoforms increases conditioned fear responding in the presence of nociceptive tone," *Molecules*, vol. 25, no. 4, article 1007, 2020.

[158] S. Sánchez-Iglesias, A. Fernández-Liste, C. Guillín-Amarelle et al., "Does seipin play a role in oxidative stress protection and peroxisome biogenesis? New insights from human brain autopsies," *Neuroscience*, vol. 396, pp. 119–137, 2019.

[159] O. Okonkwo and A. Adeyinka, "Biochemistry, cholecystokinin (CCK)," in *StatPearls*, StatPearls Publishing, Treasure Island, FL, USA, 2020.

[160] M. Javanmard, J. Shlik, S. H. Kennedy, F. J. Vaccarino, S. Houle, and J. Bradwejn, "Neuroanatomic correlates of CCK-4-induced panic attacks in healthy humans: a comparison of two time points," *Biological Psychiatry*, vol. 45, no. 7, pp. 872–882, 1999.

[161] M. Kellner, "Experimental panic provocation in healthy man-a translational role in anti-panic drug development?," *Dialogues in Clinical Neuroscience*, vol. 13, no. 4, pp. 485–493, 2011.

[162] P. Zwanzger, K. Domschke, and J. Bradwejn, "Neuronal network of panic disorder: the role of the neuropeptide cholecystokinin," *Depression and Anxiety*, vol. 29, no. 9, pp. 762–774, 2012.

[163] J. Andre, B. Zeau, M. Pohl, F. Cesselin, J.-J. Benoliel, and C. Becker, "Involvement of cholecystokininergic systems in anxiety-induced hyperalgesia in male rats: behavioral and biochemical studies," *The Journal of Neuroscience*, vol. 25, no. 35, pp. 7896–7904, 2005.

[164] Y. Clement and G. Chapouthier, "Biological bases of anxiety," *Neuroscience and Biobehavioral Reviews*, vol. 22, no. 5, pp. 623–633, 1998.

[165] C. Del Boca, P. E. Lutz, J. Le Merrer, P. Koebel, and B. L. Kieffer, "Cholecystokinin knock-down in the basolateral amygdala has anxiolytic and antidepressant-like effects in mice," *Neuroscience*, vol. 218, pp. 185–195, 2012.

[166] F. Noble, S. A. Wank, J. N. Crawley et al., "International Union of Pharmacology. XXI. Structure, distribution, and functions of cholecystokinin receptors," *Pharmacological Reviews*, vol. 51, no. 4, pp. 745–781, 1999.

[167] S. Ballaz, "The unappreciated roles of the cholecystokinin receptor CCK (1) in brain functioning," *Reviews in the Neurosciences*, vol. 28, no. 6, pp. 573–585, 2017.

[168] L. Lu, B. Zhang, Z. Liu, and Z. Zhang, "Reactivation of cocaine conditioned place preference induced by stress is reversed by cholecystokinin-B receptors antagonist in rats," *Brain Research*, vol. 954, no. 1, pp. 132–140, 2002.

[169] G. R. Wunderlich, R. Raymond, N. J. DeSousa, J. N. Nobrega, and F. J. Vaccarino, "Decreased CCK (B) receptor binding in rat amygdala in animals demonstrating greater anxiety-like behavior," *Psychopharmacology*, vol. 164, no. 2, pp. 193–199, 2002.

[170] A. P. Nesterova, E. A. Klimov, M. Zharkova et al., "Introduction," in *Disease Pathways*, pp. 3–32, Elsevier, 2020.

[171] L. Katsouri, C. Parr, N. Bogdanovic, M. Willem, and M. Sastre, "PPARγ co-activator-1α (PGC-1α) reduces amyloid-β generation through a PPARγ-dependent mechanism," *Journal of Alzheimer's Disease*, vol. 25, no. 1, pp. 151–162, 2011.

[172] S. Takai, D. Jin, M. Kimura et al., "Inhibition of vascular angiotensin-converting enzyme by telmisartan via the peroxisome proliferator-activated receptor gamma agonistic property in rats," *Hypertension Research*, vol. 30, no. 12, pp. 1231–1237, 2007.

[173] A. Kaloudi, B. A. Nock, E. Lymperis et al., "In vivo inhibition of neutral endopeptidase enhances the diagnostic potential of truncated gastrin (111)In-radioligands," *Nuclear Medicine and Biology*, vol. 42, no. 11, pp. 824–832, 2015.

[174] P. Dubreuil, P. Fulcrand, M. Rodriguez, H. Fulcrand, J. Laur, and J. Martinez, "Novel activity of angiotensin-converting enzyme. Hydrolysis of cholecystokinin and gastrin analogues with release of the amidated C-terminal dipeptide," *Biochemical Journal*, vol. 262, no. 1, pp. 125–130, 1989.

[175] K. A. Zuzel, C. Rose, and J. C. Schwartz, "Assessment of the role of "enkephalinase" in cholecystokinin inactivation," *Neuroscience*, vol. 15, no. 1, pp. 149–158, 1985.

Hindawi
PPAR Research
Volume 2020, Article ID 6529057, 11 pages
https://doi.org/10.1155/2020/6529057

Research Article

The Model of *PPARγ*-Downregulated Signaling in Psoriasis

Vladimir Sobolev,[1,2] Anastasia Nesterova,[3] Anna Soboleva,[2] Evgenia Dvoriankova,[2] Anastas Piruzyan,[2] Dzerassa Mildzikhova,[2] Irina Korsunskaya,[2] and Oxana Svitich[1]

[1]*I. Mechnikov Research Institute for Vaccines and Sera RAMS, 5 Malyy Kazennyy Pereulok, 105064 Moscow, Russia*
[2]*Centre of Theoretical Problems of Physico-Chemical Pharmacology, Russian Academy of Sciences, Russian Academy of Sciences, 4 Kosygin street, 119334 Moscow, Russia*
[3]*Life Science Research and Development Department, Elsevier Inc., Rockville, USA*

Correspondence should be addressed to Anastasia Nesterova; nesterova.anastasia@gmail.com

Received 3 April 2020; Revised 2 September 2020; Accepted 18 September 2020; Published 9 October 2020

Academic Editor: Pascal Froment

Interactions of genes in intersecting signaling pathways, as well as environmental influences, are required for the development of psoriasis. Peroxisome proliferator-activated receptor gamma (*PPARγ*) is a nuclear receptor and transcription factor which inhibits the expression of many proinflammatory genes. We tested the hypothesis that low levels of *PPARγ* expression promote the development of psoriatic lesions. We combined experimental results and network functional analysis to reconstruct the model of *PPARγ*-downregulated signaling in psoriasis. We hypothesize that the expression of *IL17*, *STAT3*, *FOXP3*, and *RORC* and *FOSL1* genes in psoriatic skin is correlated with the level of *PPARγ* expression, and they belong to the same signaling pathway that regulates the development of psoriasis lesion.

1. Introduction

Psoriasis is an example of chronic inflammatory skin disorder with a complex multifactorial origin. Multiple genes cause heterogeneous heredity of psoriasis [1, 2]. Interactions of predisposing genes, as well as environmental influences, are required for the development of the disease.

Family genotyping supports the hypothesis that different phenotypes or manifestations of psoriasis are determined by different genetic loci [3]. These loci are associated with psoriasis and located at least on 13 different chromosomes and are named PSORS (psoriasis susceptibility), PSORS1-PSORS13 ([4]). Each PSORS contains a list with several revealed genes candidates [5].

Peroxisome proliferator-activated receptors (PPARs) do not get on lists of gene candidates for psoriasis; however, the important role of PPARs in antiinflammatory and immunomodulatory cellular signaling pathways has been established. Recently, association of proline12/alanine gene polymorphism (rs1801282) in peroxisome proliferator-activated receptor gamma (*PPARγ*, NCBI Gene ID: 5468) was found to be associated with psoriasis and obesity in Egyptian patients [6].

PPARs perform function primarily as ligand-dependent transcription factors which activate genes with PPAR-responsive elements (PPREs) in their promoter. *PPARγ* is detected mostly in well-differentiated suprabasal keratinocytes within the human epidermis [7]. Human hair follicle epithelial stem cells also express *PPARγ* which maintains their survival in normal conditions [8]. Skin adipocytes and sebocytes are the next large *PPARγ* depositions [9, 10], and the protein is vital for their differentiation [11, 12]. The *PPARγ* expression was reported to be downregulated in the psoriatic skin of mice, and DDH1 dose dependently could restore the gene expression [13]. In vitro experimental models of psoriasis showed that the expression of other PPARs (PPARa) was also decreased in the skin, while PPARb and PPARd expressions were increased [14]. Mice model of inflammatory skin diseases revealed that the expression of *PPARγ* and PPARa was decreased in the skin due to the absence of the *Dlx3* gene [15]. The medical suppression of *PPARγ* improved the health of the mice model of atopic

dermatitis [16]. Wang et al. reported that gene *PPARγ* had high level of expression in the skin of IMQ-induced psoriasis mice, and a *PPARγ*-selective antagonist GSK3787 was able to decrease the inflammation in the skin [17]. Finally, another animal model research showed that mutant mice with deleted *PPARγ* did not have sebaceous glands and normal hair follicles (HF) and developed scarring alopecia and skin inflammation [18]. There is no experimental evidence about *PPARγ* activity level in human skin of patients with psoriasis to our knowledge.

PPARγ signaling in psoriasis has been studied at a good level, but conflicting experimental results do not allow describing a clear picture of protein-protein interactions and pathological changes in cell pathways leading to the development of psoriasis (read below section "Pathway Model of PPARγ Signaling in Psoriasis").

In this work, we tested a hypothesis that low levels of *PPARγ* may change the activity of cellular signaling pathways in the skin and facilitate the chronic inflammatory and immune response in psoriatic lesion in humans. Based on the literature-based protein-protein interactome (PPI) and pathway analysis, we proposed that low *PPARγ* activity promotes the development of psoriatic lesions due to changes in the inflammatory signaling pathways regulated by STAT3, RORC, FOXP3, FOSL1, and IL17A. To check the hypothesis, we measured the expression of these genes altogether with *PPARγ* on the mRNA level in the skin of patients with psoriasis before and after low-intensity laser treatment.

2. Materials and Methods

2.1. Protein-Protein Interactome (PPI) Analysis and Pathway Model Reconstruction. To reconstruct the *PPARγ*-psoriasis interactome, we used the literature-based database PSD (Resnet-2020 ®, Elsevier Pathway Studio database). PSD is a mammal-centered database where relationships between biological terms and molecules extracted from published papers with natural language processing (NLP) technology. Data from public databases with experimental types of connections are also present in PSD. Resnet-2020 contains over one million objects and more than 12 million relationships with more than 55 million supporting sentences ([19], http://www.pathwaystudio.com/).

For PPI analysis, we used SQL language and ran queries to filter PSD connections and found inhibited by *PPARγ* expression targets that simultaneously have positive relationships with psoriasis (see "*PPARγ* targets and regulators" file, list 1 in supplemental materials). To find *PPARγ* regulators, we selected genes that negatively regulate expression of *PPARγ* and simultaneously negatively regulate *PPARγ* expression targets (see "*PPARγ* targets and regulators" file, list 2 in supplemental materials). To focus only on gene expression signaling and exclude other molecular types of interaction, we considered only two types of relationships in PSD that indexed sentences about the changing of mRNA or gene expression ("Expression" and "PromoterBinding"). Queries and other parameters of network filtering are available by a request.

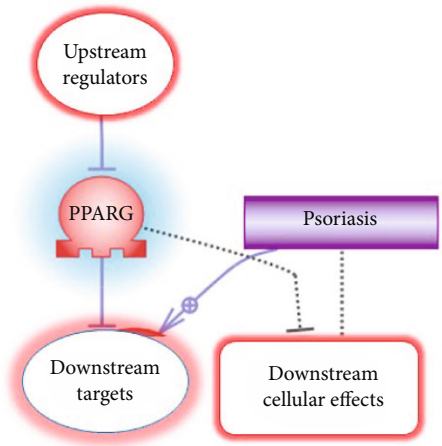

Figure 1: The logic of discovering the members of *PPARγ*-downregulated subnetwork associated with psoriasis.

We used the Pathway Studio software to reconstruct the model of *PPARγ* signaling. Models are interactive networks which describe connections between molecules and related phenotype or biological processes. Models are kept in RNEF format, connected with PSD, and included different annotations of molecules and relationships (synonymes, identificators, references, sentences, effects, mechanism of actions, and more). All files can be found in supplemental materials (see below).

2.2. Pathway Functional Analysis. List of proteins that we had identified in the PPI analysis was set up with subnetwork enrichment analysis (SNEA, Pathways Studio), Fisher's exact test, Enrichr tool [20], and KEGG mapping tool [21]. SNEA was used to find cell processes statistically enriched with genes from list 1 and 2. SNEA is the modification of gene set enrichment analysis that accounts for relationships between genes in the network [22]. Fisher's test was used to find associated Pathway Studio pathways and Gene Ontology (GO) functional gene groups [23]. We found the associated KEGG pathways with the KEGG mapping tool, and we found the other associations with the Enrichr tool.

Cell processes were selected if more than 5 genes from the list 3 (combined genes from list 1 and list 2) were overlapped with total genes associated with the pathway and if more than 5% genes from the lists 1 and 2 were overlapped with a subnetwork or GO group. We selected top subnetworks and KEGG pathways filtered by rank and top PS pathways and GO groups filtered by Jaccard index. For the comparison of methods, we selected top 50 subnetworks, 50 pathways, and 50 GO groups after manual filtering off unrelated diseases (such as cancer), viral, and bacterial KEGG pathways. See supplemental materials for results of pathway functional analysis ("PPARG network analysis" file and "PPARG Enrichr analysis" file).

2.3. Microarray In Silico Analysis. Public microarray data (GEO, GSE13355) was used to verify the reconstructed model of *PPARγ* signaling in psoriasis. GSE13355 contains

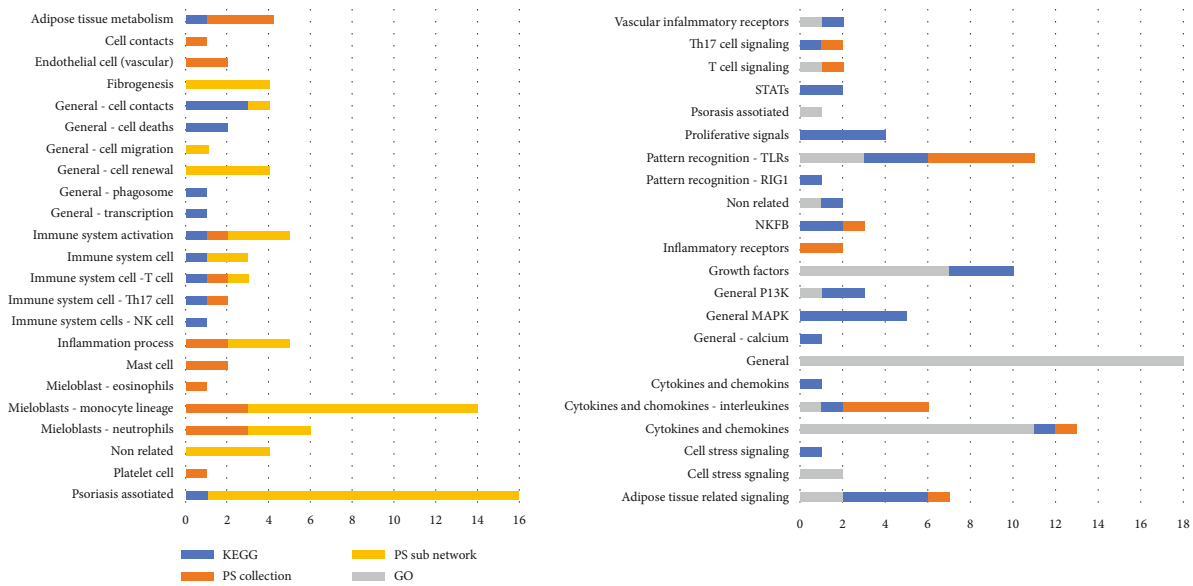

Figure 2: Cellular processes associated with members of PPARγ-downregulated signaling associated with psoriasis. Numbers are for the sum of pathways, subnetworks, or GO groups in each category. Different sources are highlighted with blue (KEGG database), orange (Pathway Studio Pathway Collection), light orange (Resnet-2020 database), and grey (GO). For the complete list of results, see supplemental materials ("PPARG network analysis" file).

data about the expression of the human genome in skin samples of 58 patients with psoriasis [24]. DEs (differentially expressed genes) were identified with a two-class unpaired t-test between samples of lesional skin of each patient (PP samples) and nonlesional skin uninvolved samples (PN samples). Multiple probes were averaged by the best p value or maximum magnitude. The Pathway Studio software was used for calculation of DE and pathway analysis.

2.4. Supplemental Materials. All supplemental materials are available to download from ResearchGate resource by the link https://www.researchgate.net/publication/340427568_Supplemental_Materials_The_role_of_PPARg_downregulated_signaling_in_psoriasis [25]. All pathway models and their annotations are available for browsing and can be downloaded at http://www.transgene.ru/ppar-pathways.

3. Results and Discussion

3.1. Reconstruction of Downregulated PPARγ Pathway Model Associated with Psoriasis. For testing the hypothesis that low levels of *PPARγ* trigger inflammatory signaling pathways in the skin, we analysed the protein-protein interaction literature-based network (PSD, Elsevier Pathway Studio) and several public ontologies and databases (Gene Ontology, Human Protein Atlas, KEGG, Reactome).

First, in the PSD network, we identified *PPARγ* downstream expression targets and upstream regulators (inhibitors) of *PPARγ* expression. For researching the downstream targets, we looked for the genes and proteins which were reported to be inhibited by *PPARγ* and simultaneously were positive biomarkers for psoriasis. 146 associated with psoriasis genes and gene families whose expressions are repressed by *PPARγ* had been found. For researching the upstream of *PPARγ* signaling, we focused on the transcriptional factors which can inhibit both the expression of *PPARγ* and his direct targets. 99 associated with psoriasis unique negative regulators of *PPARγ* had been identified. Then we combine regulators with targets to obtain 182 names of unique genes forming the *PPARγ*-downregulated subnetwork associated with psoriasis (see supplemental materials, "PPARG regulators and targets" file, list 3) (Figure 1).

3.2. Comparative Pathway Analysis of PPARγ-Downregulated Signaling Associated with Psoriasis. Several methods of pathway analysis were performed to explore the functional roles of 182 targets, and regulators of *PPARγ* revealed in PPI analysis. Methods of pathway functional analysis are widely used for discovering cellular processes and signalings that are statistically associated with the list of genes or proteins [26].

We compared results from pathway functional analysis with three resources: Gene Ontology, Elsevier Pathways, and KEGG Pathways. Gene Ontology is the source of groups of proteins or genes manually assigned by their different functional roles. Elsevier Pathways and KEGG Pathways are manually reconstructed schemas or models of interactions between proteins describing molecular mechanisms of one or several biological processes. Gene Set Enrichment Analysis (GSEA) is a well-known method to analyse predefined and manually created collections of gene groups and pathways [27]. Besides GSEA, we used SNEA method which allows finding associated cellular processes based on literature-based PPI network. SNEA does not use predefined groups of genes or pathways and is considered less biased [22, 26].

According to the results of comparative pathway analysis, *PPARγ*-downregulated signaling is associated with

Table 1: Cell processes directly related to psoriasis and enriched with genes and proteins from the *PPARγ*-downregulated signaling. See complete results with additional statistics in supplemental materials, "PPRAG network analysis" file.

Name of the process or signaling	Source	Rank or Jaccard similarity (the closer to 10%, the more similarity)	Category
Keratinocyte activation in psoriatic arthritis	PS Collection	9.13%	Disease
Lesion size	PS subnetwork	46	Targets neighbors
Keratinocyte proliferation	PS subnetwork	100	Targets neighbors
Skin fibrosis	PS Collection	9.09%	Disease
T cell differentiation block in psoriasis	PS Collection	8.88%	Disease
Th17 cell and Th1 immune response in psoriatic arthritis	PS Collection	8.82%	Disease
Dendritic cell dysfunction in psoriatic arthritis	PS Collection	8.44%	Disease
T cell cytotoxic response against melanocytes in vitiligo	PS Collection	6.20%	Disease
Synovial fibroblast activation in psoriatic arthritis	PS Collection	8.18%	Disease
Inflammatory reaction in acne vulgaris	PS Collection	5.70%	Disease
Apoptotic keratinocyte clearance recession in systemic lupus erythematosus	PS Collection	5.69%	Disease
Atopic dermatitis	PS Collection	5.62%	Disease
Hair follicle keratinocyte apoptosis	PS Collection	5.56%	Disease
Vitiligo	PS Collection	5.07%	Disease
Melanogenesis—Homo sapiens	KEGG	n/a	Pathway
Positive regulation of timing of anagen	GO	1.10%	GO: biological_process
Glycosaminoglycan binding	GO	4.24%	GO: molecular_ function

adipogenesis, activation of myeloid proinflammatory cells (with a predominance of mast cells and dendritic cells), and activation of overall immune system response (with a predominance of Th17 cells). Also, fibrogenesis, cell-to-cell contacts, vascular-related processes, and universal cell processes, such as cell proliferation or cell death, were identified (Figure 2). Cellular possesses directly associated with psoriasis were present in results from each source that we compared (Table 1).

Top subnetworks from SNEA were neighbors of adipogenesis and adipocyte differentiation, followed by the immune response, and T-development. The subnetworks "neighbours of monocyte recruitment or differentiation" and "macrophage differentiation" had the most percent (9%) of overlapped genes from *PPARγ*-downregulated signaling.

GSEA analysis of PS Pathway Collection and KEGG pathways resulted in many cancer-related processes. The disease taxonomy filtering with PS pathways about skin and immune system identified processes related to adipokines and IL17 signaling (Table 2). The signaling of aryl hydrocarbon receptor (AHR) in Th17 cells was the pathway with the biggest percent (48%) of overlapped genes from *PPARγ*-downregulated signaling.

Among the top KEGG pathways enriched with our gene list, we identified general MAPK and PI3K signaling and cancer-related pathways (for example, "hsa05200 Pathways in cancer - Homo sapiens"). TNF signaling pathway (hsa04668), as well as Th17 cell (hsa04659) and IL17 pathway (hsa04657), was also in the top 10 results. The cytokine-cytokine receptor interaction (hsa05200) and PI3K-Akt signaling (hsa04151) had the highest number of overlapped entities (48 and 34).

The list of revealed in pathway analysis molecular cascades completes the lists of cell processes.

There was no surprise that activation of general cellular flows like ERK/MAPK, RAS/ACT1, and adipose cells related with AMPK, MTOR, and cAMP cascades was associated with the list of *PPARγ* targets and regulators. Also, among the top of associated molecular signalings, there were well predictable inflammatory cascades like Toll-like receptors, interleukins, and interleukin receptors signaling (IL17, IL1B, IL6, and IL1R1) altogether with all-purpose cytokines and cytokine receptors signaling (CXCR3, CCR1, and TNF). Signalings related to transcription factors NFKB and STATs also were significantly associated with the analysed list. GO functional group "GO: glycosaminoglycan binding"; "IL1R1 signaling in Pneumocytes" from PS Pathway Collection; and "ErbB signaling pathway" (hsa04012) from KEGG had the maximum rank (see complete results with additional statistics in supplemental materials, "PPRAG network analysis" file). Glycosaminoglycans are essential for skin functioning. IL1R1 is a receptor commonly activated in any nonspecific inflammatory processes. Finally, the ERb-B/EGFR family is involved in cell proliferation and tumor development.

Additional comparison of pathway analysis results with other pathways databases (WikiPathways, Reactome, and Biocarta analysed with Enrichr tool) confirmed results obtained with PS Pathway Collection (Figure 3). Pathways

Table 2: List of PS pathways associated with members of PPARγ-downregulated signaling associated with psoriasis. See complete results with additional statistics in supplemental materials, "PPRAG network analysis" file.

Pathway name	# of entities	Overlap	Percent overlap	*p* value	Jaccard similarity	Pathway taxonomy top category
EGFR—expression targets in skin	98	26	26	4.68*E*-11	10.28%	Biomarkers
GPCRs family—expression targets in lymphoid system and blood	89	24	26	1.97*E*-10	9.76%	Biomarkers
Adipokine production by adipocyte	58	20	34	4.8*E*-16	9.13%	Biological process
Skin fibrosis	83	22	26	3.29*E*-17	9.09%	Disease
Scavenger receptor OLR1 in inflammation-related endothelial dysfunction	73	21	28	2.8*E*-17	9.01%	Disease
T cell differentiation block in psoriasis	52	19	36	5.87*E*-18	8.88%	Disease
Adipokine production by adipocyte impaired in obesity	56	19	33	2.99*E*-17	8.72%	Disease
CD40—expression targets in thymus	58	19	32	4.67*E*-10	8.64%	Biomarkers
Lymphocyte-mediated myocardial injury in myocarditis	84	21	25	6.67*E*-16	8.61%	Disease
IL17 signaling in psoriasis	49	18	36	4.08*E*-17	8.49%	Disease
Th17 cell differentiation	73	19	26	8.94*E*-13	8.09%	Biological process

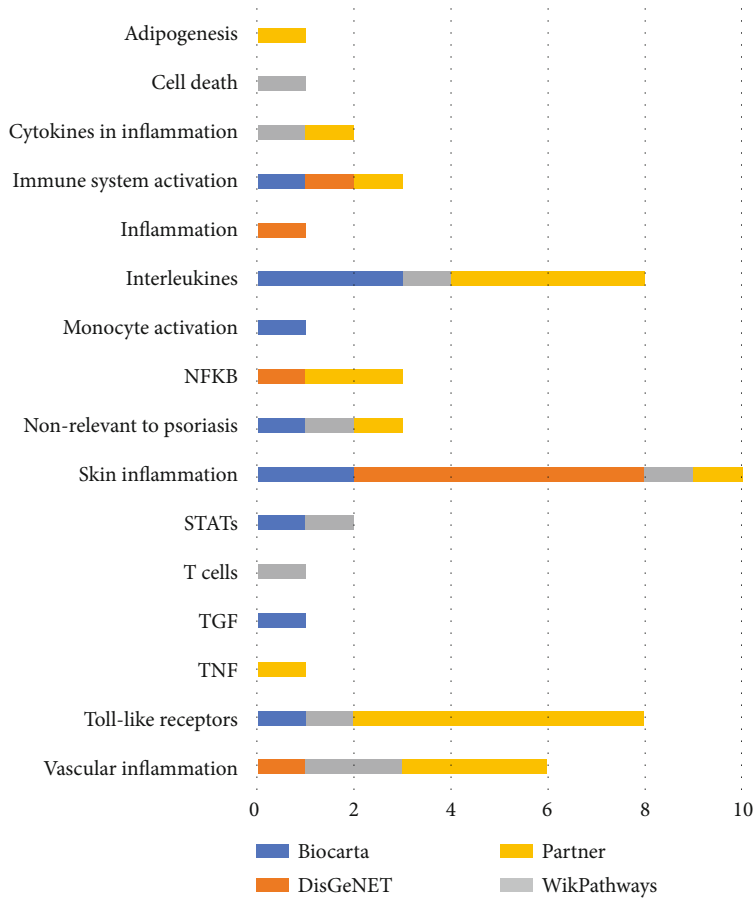

Figure 3: Comparison of results of pathway analysis (GSEA) with different sources for PPARγ-downregulated signaling associated with psoriasis. Results were calculated with the Enrichr tool. Numbers are for the sum of pathways in each category. Different sources are highlighted with blue (Biocarta database), grey (Partner database), orange (DisGeNET), and yellow (WikiPathways).

from all sources revealed skin inflammatory processes, TLRs, and interleukin-related cascades. However, the list of molecules was different compared with PS and KEGG results presenting IL10 and IL22R and no IL17 associations. In addition, analysis with DisGeNET [28] confirmed that the *PPARγ* regulators and targets are connected with psoriasis since top diseases associated with the list 3 were as follows: psoriasis, epithelial hyperplasia of skin, and inflammatory dermatosis.

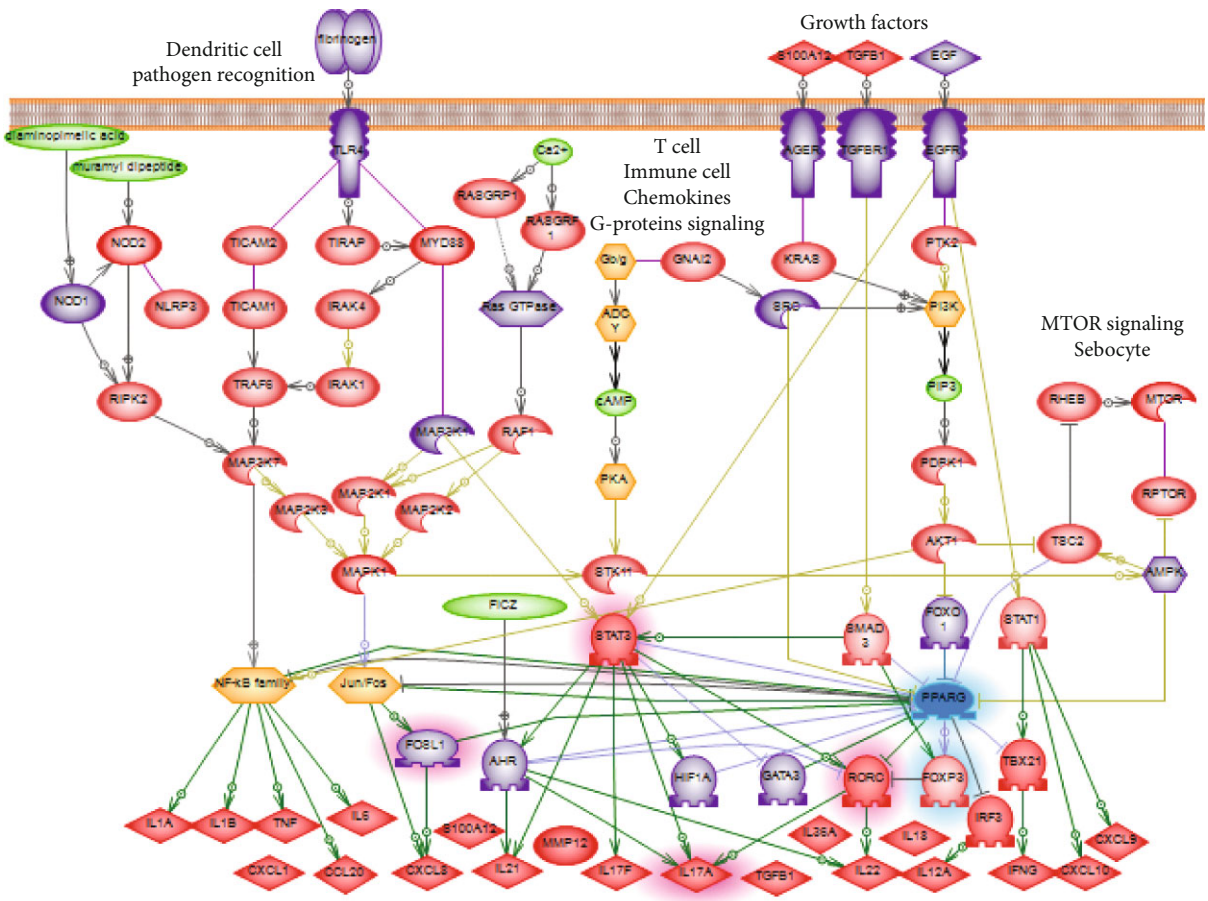

Figure 4: Model of downregulated *PPARγ* signaling in psoriasis. *PPARγ* which expression is downregulated in psoriasis is colored blue. Regulators that may inhibit the expression of *PPARγ* (data based on PPI and pathway functional analysis) are colored in violet. Targets which may be overexpressed in psoriasis due to the decrease of the negative impact of *PPARγ* are colored in bright red. *FOXP3*, *STAT3*, *IL17A*, *RORC*, and *FOSL1* are highlighted according to own experiments (read section "Preliminary analysis of *PPARγ* signaling in human psoriatic skin"). Downexpressed genes (*PPARγ* and *FOXP3*) are highlighted in blue, and overexpressed genes are highlighted in red.

Allergic reaction, neutrophilia, and vascular diseases were also in the top 10 results (see supplemental materials, file "PPARG Enrichr analysis" file).

3.3. Pathway Model of PPARγ Signaling in Psoriasis. Considering results of PPI network and functional pathway analysis, we build a hypothetical model that describes cellular molecular mechanisms of involvement of *PPARγ* in the maintenance of chronic inflammatory and immune response in human psoriatic skin. Literature-based network (PSD) was used to build the model. Figure 4 described the adopted for the publication-simplified version of the downregulated PPARγ pathway model. See supplemental materials for the completed version of the pathway model.

Based on the model, reducing the level of the *PPARγ* gene expression may be a result of the overregulation of several cascades. Pattern recognition receptors (TLRs, NOD1, NOD2, and CLEC7A) that sensor pathogens and highly expressed in keratinocytes and monocytes during the infection may be one of such cascades. All-purpose cellular cascades like growth factor signaling, G-proteins, and MTOR signaling also were reported to be inhibitors of *PPARγ* expression in literature and revealed in our analysis. Moreover, transcription factors including NF-kBs, JUN-FOS, AHR, GATA3, HIF1A, FOXO1, and FOSL1 can directly inhibit *PPARγ* expression. All these transcription factors are overstimulated in the inflammatory and immune response. For example, it is reported that NF-kBs are stimulated in systemic inflammatory processes in general and in psoriasis as well [29, 30].

In healthy skin, *PPARγ* inhibits mentioned transcriptional factors in a feedback regulation loop. *PPARγ* may directly bind and suppress transcriptional factors STAT3 and RORC, by thus blocking the synthesis of proinflammatory cytokines including IL17. Less quantity of expressed cytokines decreases the Th17 cell proliferation, minimises chemotaxis of neutrophils and monocytes, and results in the reduction of inflammation in psoriatic lesions.

IL17 which is produced mostly by TH17 cells plays the central role in the development of psoriasis because it stimulates keratinocytes to secrete proinflammatory cytokines and antibacterial peptides [31]. IL17 pathway and Th17 cells had a strong association with *PPARγ*-downregulated signaling confirmed by our network and functional analysis.

Th17 cells need robust activity of STAT3 gene for their function and differentiation. Also, STAT3 is described as an

#	Gene set seed	Percent overlap	*p* value
1	Epithelial cell	5	2.50*E*-62
2	Keratinocyte	8	1.91*E*-58
3	Vascular smooth muscle cell	10	5.08*E*-57
4	Umbilical vein endothelial cell	12	1.39*E*-56
5	Monocyte	5	2.55*E*-51
6	Endometrial stromal cell	24	1.58*E*-50
7	Alveolar macrophage	10	6.13*E*-50
8	Synoviocyte	21	2.17*E*-49
9	Macrophage	3	3.44*E*-49
10	Adipocyte	7	2.61*E*-48
11	Activated monocyte	18	8.78*E*-48
12	Fibroblast	4	8.18*E*-47
13	Airway epithelial cell	12	2.55*E*-46
14	PBMC	6	1.66*E*-45
15	Stromal cell	7	5.12*E*-45
16	Airway smooth muscle cell	23	6.18*E*-44
17	Osteoblast	7	7.00*E*-44
18	Pneumocyte	10	7.14*E*-44
19	Endometium cell	23	3.11*E*-43
20	Microglia	6	1.15*E*-42

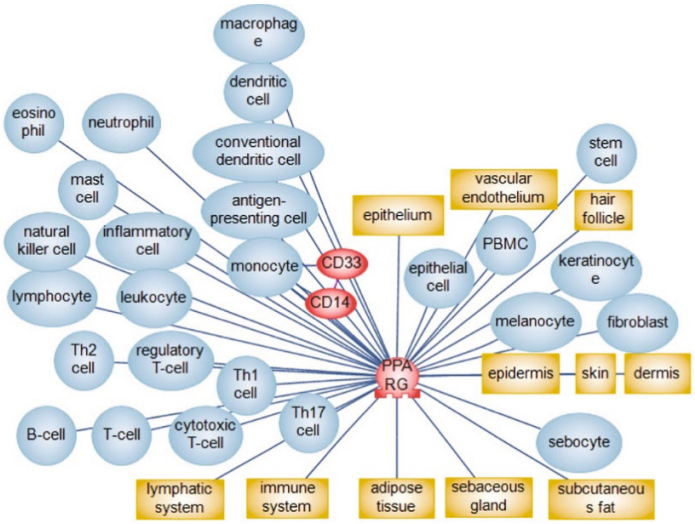

Figure 5: Cells associated with downregulated *PPARγ* signaling. SNEA method and Pathway Studio were used to calculate the results. See the complete list with statistics in supplemental materials, "PPARG and cell" file.

important linkage between keratinocytes and immune cells [32]. Previously, the expression of *STAT3* was shown to be repressed due to *PPARγ* activation [33]. *STAT3* may also act as a regulator of *PPARγ* expression; however, it is not clear whether with positive or negative effect [34].

As a transcription factor, STAT3 is reported to be a strong activator of RORC (ROR*γ*) and, probably, IL17 gene expression. From the other side, gene RORC is the major inductor of the expression of IL17 cytokine family [35]. *PPARγ* was shown to bind the *RORC* promoter and suppress its expression altogether with *RORC*-mediated Th17 cell differentiation [36].

Transcription factor FOXP3 is closely associated with psoriasis and the diminishing of Treg cell number [37, 38]. It was shown that activated *PPARγ* induces the stable *FOXP3* expression by strong inhibiting effect on DNA methyltransferases. The activating effect of *PPARγ* on FOXP3 results in the proliferation of iTreg cells [39].

FOSL1 is the transcriptional factor which plays an important role in many processes related to cell differentiation and tissue remodeling ([40–42]). *FOSL1* (FOS-like antigen 1) is expressed in low level in healthy tissues; however, its expression rises due to presence of mitogens or toxins. The accumulation of the FOSL1 protein in the skin depends on the stage of the keratinocyte differentiation [43]. Markers of stratum corneum differentiation like gene IVL are the main expression targets of FOSL1 [44].

The degree of the pathogenicity of downregulated *PPARγ* in psoriatic lesion depends on the cell type. It is known that *PPARγ* is expressed in Th17 cells as well as in keratinocytes, sebocytes, and other cells of the psoriatic lesion [7, 8, 10–12]. Functional and network analysis supported the association of *PPARγ*-downregulated signaling with keratinocytes, vascular endothelium, vascular smooth muscle cells, macrophages, fibroblasts and adipocytes, and monocytes lineage (particular with CD33+ and CD14+ monocytes) (Figure 5). However, we did not attempt to separate the *PPARγ* pathway model by appropriate cell types which is a disadvantage of this work. There is no reliable way to take in account cell specificity in our modeling paradigm. Moreover, we expect that most of the revealed from the literature network analysis cascades will be equal for different human cells due to insufficient experimental studies.

For additional evaluation of the reconstructed model, we analysed the public microarray data (GEO:GSE13355). In that experiment, biopsies from 58 psoriatic patients were run on Affymetrix microarrays contain more than 50000 gene probes [45]. We uploaded raw data from GEO and calculated differentially expressed genes (DEs) between samples of psoriatic skin and unaltered samples for all patients. Then, we used the pathway analysis to explore the difference in the expression for genes of the *PPARγ* model we build (Figure 6).

PPARγ gene was slightly downregulated in psoriatic lesions comparing to nonaltered lesions in GSE13355 microarray data (Figure 6, *PPARγ* expression diagram).

We assumed that regulators of *PPARγ* signaling should have higher expression in psoriatic lesion than in normal skin. Only S100A12 (S100 calcium-binding protein A12) had a significantly higher level of expression in analysed microarray data comparing with all regulators of *PPARγ* that we selected for the model (Figures 6 and 7). S100A12 binds to the AGER receptor which belongs to the immunoglobulin superfamily and is involved in many processes of inflammation and immune response. S100A12 is thought to be the most prominent biomarker of psoriasis [46]. Also, polymorphisms in AGER receptor were found to be associated with psoriasis [47].

The EGFR signaling almost completely was downexpressed in this microarray data including the *FOXO1* expression which is one of the direct inhibitors of *PPARγ*. Therefore, EGFR/-FOXO1 signaling probably does not play an important role in the regulation of *PPARγ* in psoriasis (Figure 7).

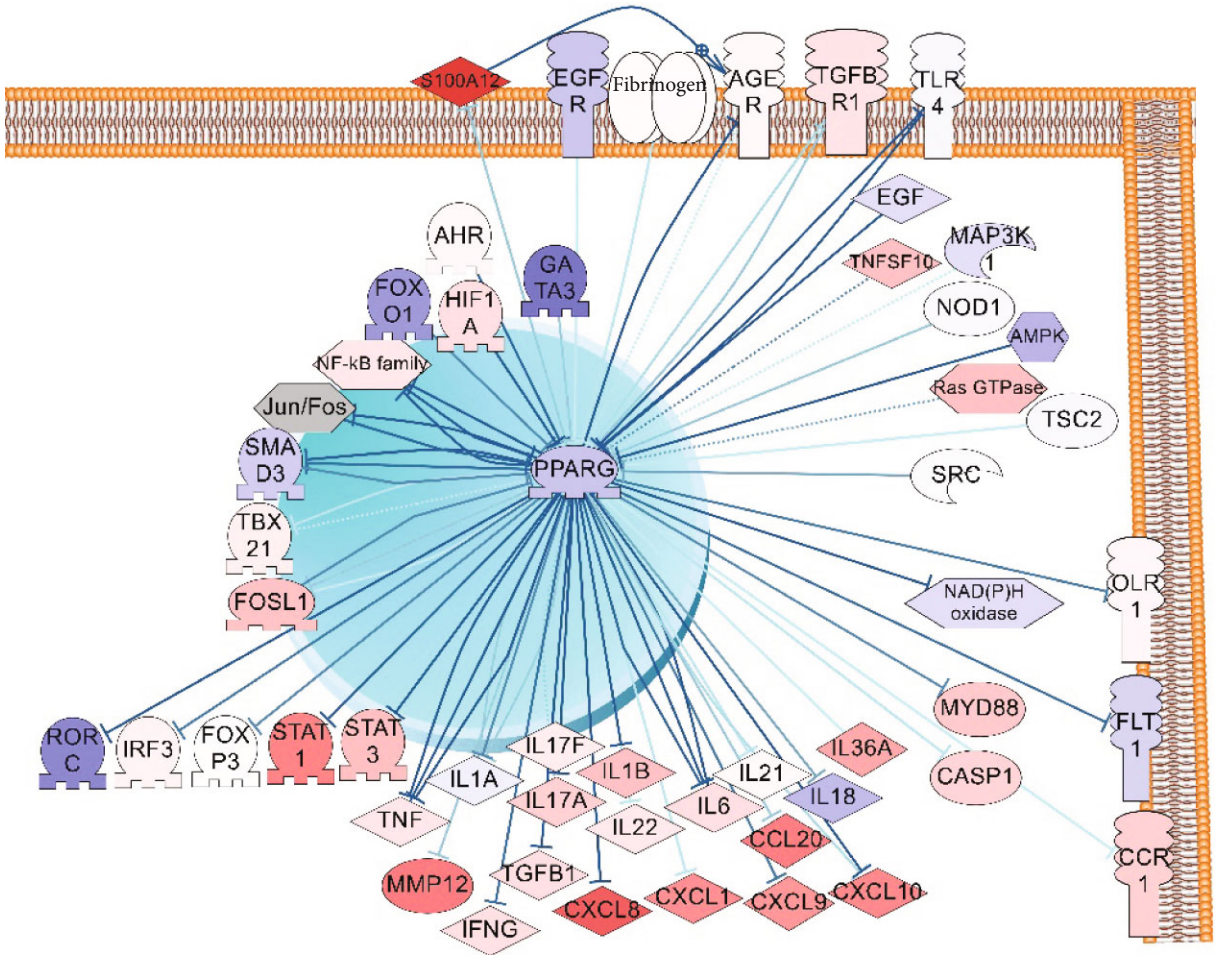

Figure 6: Evaluation of *PPARγ*-downregulated subnetwork (selected *PPARγ* regulators and targets) associated with psoriasis using microarray data analysis (results of differential expression analysis of psoriatic lesions vs. unaltered lesions). The saturation in blue indicates the degree of gene downexpression in psoriatic samples in comparison with unaltered samples. The saturation in red indicates the degree of gene overexpression. The list of targets and regulators can be seen in supplemental materials, "PPARG regulators and targets," list 3.

4. Conclusion

In our previous work, we reviewed the recent progress in psoriasis pathways and published two pathway models. The first pathway model described the shift to TH17 cell production during the differentiation of psoriatic T cells. The primary cause of the shift of the T cell differentiation is supposed to be genetic mutations, for example, in IL23R receptors. The second model showed how elevated levels of IL17 and IL22 may activate keratinocytes to release different cytokines and chemokines for attracting neutrophils and other inflammatory cells in the psoriatic lesion [19].

In this work, we tested the hypothesis that *PPARγ* signaling when downregulated may promote psoriasis. We built the model of *PPARγ*-dependent pathways involved in the development of the psoriatic lesions. However, we used a different approach for reconstructing the pathway model and selected key members with bioinformatic analysis. We included in the pathway model the top statistically significant regulators of *PPARγ* gene expression and *PPARγ*-depended expression targets. Then, we included significant molecular cascades and cell processes from results of the functional analysis (IL17 signaling, TLRs signaling, activation of STAT3 or NFKB transcription factors, and others). We tested the model with analysis of published microarray data.

While the prominent role of *RORC* in psoriasis as the major controller of Th17 cell differentiation is well described, however, the evidence of *RORC* expression in psoriasis is controversial and supported by work where mice T cells and dendritic cells had increased STAT3/RORC expression [48]; still, patients with psoriasis had elevated level of *RORC* (RORG-t isoform) [49]. In analysed published microarray data, the level of expression of *RORC* was downregulated in most of 58 patients.

We detected downregulation of *PPARγ* gene expression in human psoriatic skin from 23 patients with real-time PCR method (data not shown). Our results are similar to the data from microarray on 58 patients where average *PPARγ* gene expression also is slightly downregulated in psoriatic lesions [45]. Our results do not confirm the work of Westergaard et al. which described the slightly higher level of the *PPARγ* expression in human psoriatic skin compared to normal skin. However, the level of *PPARγ* mRNA was close to the detection limit in their research [39]. This

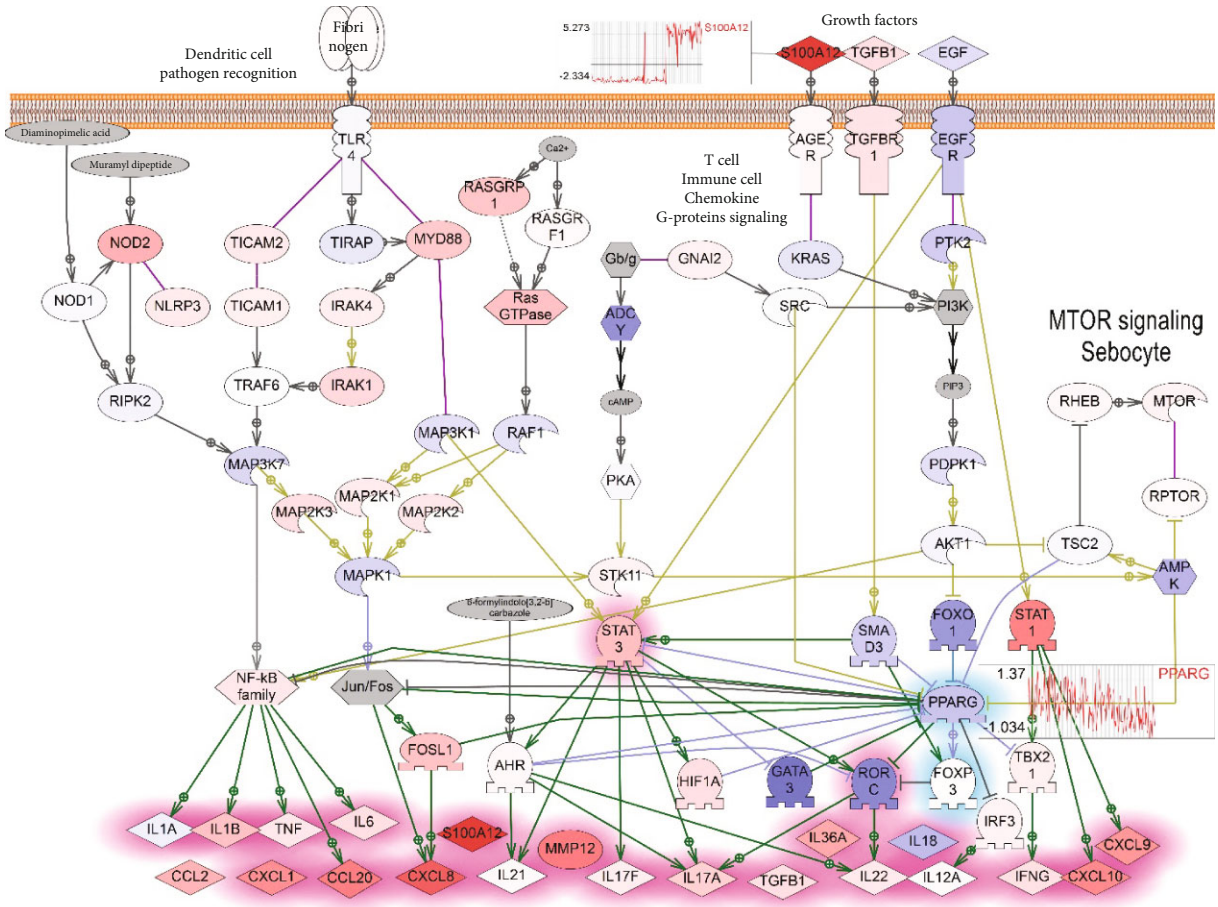

Figure 7: Evaluation of *PPARγ*-downregulated model associated with psoriasis using microarray data analysis (results of differential expression analysis of psoriatic lesions vs. unaltered lesions from GEO:GSE13355). The saturation in blue indicates the degree of gene downexpression in psoriatic samples in comparison with unaltered samples. The saturation in red indicates the degree of gene overexpression. The plots of expression pattern in psoriatic lesions compared with healthy skins samples are shown for *PPARγ* and *S100A12* genes.

difference may be due the detection of different isoforms of *PPARγ* which all have different patterns of the expression [50]. More research on protein level is needed to conclude whether *PPARγ* gene expression is downregulated in psoriatic lesions.

Within the framework of the model validation, we hypothesize that signaling related to repressed *PPARγ* activity is correlated with the development of psoriasis. IL17A, STATS3, and RORC (RORg) are statistically significant *PPARγ* negative targets, and we detected higher levels of their mRNA in psoriatic lesion of 23 patients and moreover, the decrease of their expression levels after laser treatment (preliminary results not shown). The alignment of our preliminary experimental results with microarray data and PPI network analysis shows that the reconstructed model of *PPARγ*-downregulated signaling in psoriasis can be useful for further research.

Data Availability

All supplemental materials (four excel files) are available to download from ResearchGate resource by the link https://www.researchgate.net/publication/340427568_Supplemental_Materials_The_role_of_PPARg_downregulated_signaling_in_psoriasis. All pathways models and their annotations are available for browsing and can be downloaded at http://www.transgene.ru/ppar-pathways." Preprint has posted on bioRxiv: https://biorxiv.org/cgi/content/short/2020.09.01.274753v1.

Conflicts of Interest

The authors declare that they have no conflicts of interest.

Acknowledgments

We thank the "University Diagnostic Laboratory" LLC for funding along with Elsevier Inc. and Pathway Studio® for software and the database.

Supplementary Materials

Supplementary materials include 3 files with results of network and pathways analysis in Pathway Studio software, one file with results of GSEA in Enrichr tool, and one file with

preliminary results of experimental validations (real-time gene expression analysis) of the model. *(Supplementary Materials)*

References

[1] B. J. Nickoloff and F. O. Nestle, "Recent insights into the immunopathogenesis of psoriasis provide new therapeutic opportunities," *The Journal of Clinical Investigation*, vol. 113, no. 12, pp. 1664–1675, 2004.

[2] B. P. Peters, F. G. Weissman, and M. A. Gill, "Pathophysiology and treatment of psoriasis," *American Journal of Health-System Pharmacy*, vol. 57, no. 7, pp. 645–659, 2000.

[3] L. Samuelsson, F. Enlund, Å. Torinsson et al., "A genome-wide search for genes predisposing to familial psoriasis by using a stratification approach," *Human Genetics*, vol. 105, no. 6, pp. 523–529, 1999.

[4] H. M. Merve, "Psoriasis and genetics," in *Büyük Başak (Tran.), Psoriasis*, K. Sevilay, Ed., p. 1, IntechOpen, Rijeka, 2017.

[5] J. N. W. N. Barker, "Genetic aspects of psoriasis," *Clinical and Experimental Dermatology*, vol. 26, no. 4, pp. 321–325, 2001.

[6] I. Seleit, O. Bakry, E. Abd El Gayed, and M. Ghanem, "Peroxisome proliferator-activated receptor-γ gene polymorphism in psoriasis and its relation to obesity, metabolic syndrome, and narrowband ultraviolet B response: a case–control study in Egyptian patients," *Indian Journal of Dermatology*, vol. 64, no. 3, pp. 192–200, 2019.

[7] G. Icre, W. Wahli, and L. Michalik, "Functions of the peroxisome proliferator-activated receptor (PPAR) α and β in skin homeostasis, epithelial repair, and morphogenesis," *Journal of Investigative Dermatology Symposium Proceedings*, vol. 11, no. 1, pp. 30–35, 2006.

[8] N. Billoni, B. Buan, and B. Gauti, "Expression of peroxisome proliferator activated receptors (PPARs) in human hair follicles and PPARα involvement in hair growth," *Acta Dermato-Venereologica*, vol. 80, no. 5, pp. 329–334, 2000.

[9] T. Alestas, R. Ganceviciene, S. Fimmel, K. Müller-Decker, and C. C. Zouboulis, "Enzymes involved in the biosynthesis of leukotriene B4 and prostaglandin E2 are active in sebaceous glands," *Journal of Molecular Medicine*, vol. 84, no. 1, pp. 75–87, 2006.

[10] T. Inoue, Y. Miki, S. Kakuo et al., "Expression of steroidogenic enzymes in human sebaceous glands," *Journal of Endocrinology*, vol. 222, no. 3, pp. 301–312, 2014.

[11] K. Nehrenheim, I. Meyer, H. Brenden, G. Vielhaber, J. Krutmann, and S. Grether-Beck, "Dihydrodehydrodiisoeugenol enhances adipocyte differentiation and decreases lipolysis in murine and human cells," *Experimental Dermatology*, vol. 22, no. 10, pp. 638–643, 2013.

[12] R. Paus, J. Klein, P. A. Permana et al., "What are subcutaneous adipocytes *really* good for…?," *Experimental Dermatology*, vol. 16, no. 1, pp. 45–47, 2007.

[13] K. Kitahata, K. Matsuo, Y. Hara et al., "Ascorbic acid derivative DDH-1 ameliorates psoriasis-like skin lesions in mice by suppressing inflammatory cytokine expression," *Journal of Pharmacological Sciences*, vol. 138, no. 4, pp. 284–288, 2018.

[14] P. Friedmann, H. Cooper, and E. Healy, "Peroxisome proliferator-activated receptors and their relevance to dermatology," *Acta Dermato-Venereologica*, vol. 85, no. 3, pp. 194–202, 2005.

[15] J. Hwang, R. Kita, H.-S. Kwon et al., "Epidermal ablation of Dlx3 is linked to IL-17-associated skin inflammation," *Proceedings of the National Academy of Sciences*, vol. 108, no. 28, pp. 11566–11571, 2011.

[16] K. Jung, A. Tanaka, H. Fujita et al., "Peroxisome proliferator–activated receptor γ–mediated suppression of dendritic cell function prevents the onset of atopic dermatitis in NC/Tnd mice," *Journal of Allergy and Clinical Immunology*, vol. 127, no. 2, pp. 420–429.e6, 2011.

[17] X. Wang, Y. Hao, X. Wang et al., "A PPARδ-selective antagonist ameliorates IMQ-induced psoriasis-like inflammation in mice," *International Immunopharmacology*, vol. 40, pp. 73–78, 2016.

[18] C. Sardella, C. Winkler, L. Quignodon et al., "Delayed hair follicle morphogenesis and hair follicle dystrophy in a lipoatrophy mouse model of Pparg total deletion," *Journal of Investigative Dermatology*, vol. 138, no. 3, pp. 500–510, 2018.

[19] A. P. Nesterova, A. Yuryev, E. A. Klimov et al., *Disease Pathways: An Atlas of Human Disease Signaling Pathways*, Elsevier, Waltham, 1st ed edition, 2019.

[20] E. Y. Chen, C. M. Tan, Y. Kou et al., "Enrichr: interactive and collaborative HTML5 gene list enrichment analysis tool," *BMC Bioinformatics*, vol. 14, no. 1, p. 128, 2013.

[21] M. Kanehisa and Y. Sato, "KEGG Mapper for inferring cellular functions from protein sequences," *Protein Science*, vol. 29, no. 1, pp. 28–35, 2019.

[22] E. Kotelnikova, A. Yuryev, I. Mazo, and N. Daraselia, "Computational approaches for drug repositioning and combination therapy design," *Journal of Bioinformatics and Computational Biology*, vol. 8, no. 3, pp. 593–606, 2011.

[23] M. Ashburner, C. A. Ball, J. A. Blake et al., "Gene ontology: tool for the unification of biology," *Nature Genetics*, vol. 25, no. 1, pp. 25–29, 2000.

[24] J. Ding, J. E. Gudjonsson, L. Liang et al., "Gene expression in skin and lymphoblastoid cells: refined statistical method reveals extensive overlap in cis-eQTL signals," *American Journal of Human Genetics*, vol. 87, no. 6, pp. 779–789, 2010.

[25] V. Sobolev, *Supplemental Materials [WWW Document]*, Research Gate, 2020, URL https://www.researchgate.net/publication/340427568_Supplemental_Materials_The_role_of_PPARg_downregulated_signaling_in_psoriasis.

[26] A. P. Nesterova, E. A. Klimov, M. Zharkova et al., "Chapter 14-applications of disease pathways in biology and medicine," in *Disease Pathways*, A. P. Nesterova, E. A. Klimov, M. Zharkova, S. Sozin, V. Sobolev, N. V. Ivanikova, M. Shkrob, and A. Yuryev, Eds., pp. 629–668, Elsevier, 2020.

[27] A. Subramanian, P. Tamayo, V. K. Mootha et al., "Gene set enrichment analysis: a knowledge-based approach for interpreting genome-wide expression profiles," *Proceedings. National Academy of Sciences. United States of America*, vol. 102, no. 43, pp. 15545–15550, 2005.

[28] J. Piñero, À. Bravo, N. Queralt-Rosinach et al., "DisGeNET: a comprehensive platform integrating information on human disease-associated genes and variants," *Nucleic Acids Research*, vol. 45, no. D1, pp. D833–D839, 2017.

[29] T. Tang, J. Zhang, J. Yin et al., "Uncoupling of inflammation and insulin resistance by NF-κB in transgenic mice through elevated energy expenditure," *The Journal of Biological Chemistry*, vol. 285, no. 7, pp. 4637–4644, 2010.

[30] X. Xu, M. He, T. Liu, Y. Zeng, and W. Zhang, "Effect of salusin-ß on peroxisome proliferator-activated receptor

gamma gene expression in vascular smooth muscle cells and its possible mechanism," *Cellular Physiology and Biochemistry*, vol. 36, no. 6, pp. 2466–2479, 2015.

[31] A. Srivastava, P. Nikamo, W. Lohcharoenkal et al., "MicroRNA-146a suppresses IL-17–mediated skin inflammation and is genetically associated with psoriasis," *Journal of Allergy and Clinical Immunology*, vol. 139, no. 2, pp. 550–561, 2017.

[32] S. Chowdhari and N. Saini, "Hsa-miR-4516 mediated downregulation of STAT3/CDK6/UBE2N plays a role in PUVA induced apoptosis in keratinocytes," *Journal of Cellular Physiology*, vol. 229, no. 11, pp. 1630–1638, 2014.

[33] H.-T. Hsu, M.-T. Sung, C.-C. Lee et al., "Peroxisome proliferator-activated receptor γ expression is inversely associated with macroscopic vascular invasion in human hepatocellular carcinoma," *International Journal of Molecular Sciences*, vol. 17, no. 8, p. 1226, 2016.

[34] H. Tuna, R. G. Avdiushko, V. J. Sindhava et al., "Regulation of the mucosal phenotype in dendritic cells by PPARγ: role of tissue microenvironment," *Journal of Leukocyte Biology*, vol. 95, no. 3, pp. 471–485, 2014.

[35] M. Takaishi, M. Ishizaki, K. Suzuki, T. Isobe, T. Shimozato, and S. Sano, "Oral administration of a novel RORγt antagonist attenuates psoriasis-like skin lesion of two independent mouse models through neutralization of IL-17," *Journal of Dermatological Science*, vol. 85, no. 1, pp. 12–19, 2017.

[36] N. Hermann-Kleiter, M. Meisel, F. Fresser et al., "Nuclear orphan receptor NR2F6 directly antagonizes NFAT and RORγt binding to the Il17a promoter," *Journal of Autoimmunity*, vol. 39, no. 4, pp. 428–440, 2012.

[37] H. Jorn Bovenschen, P. C. van de Kerkhof, P. E. van Erp, R. Woestenenk, I. Joosten, and H. J. P. M. Koenen, "Foxp3+ regulatory T cells of psoriasis patients easily differentiate into IL-17A-producing cells and are found in lesional skin," *Journal of Investigative Dermatology*, vol. 131, no. 9, pp. 1853–1860, 2011.

[38] Y. Shu, Q. Hu, H. Long, C. Chang, Q. Lu, and R. Xiao, "Epigenetic variability of CD4+CD25+ Tregs contributes to the pathogenesis of autoimmune diseases," *Clinical Reviews in Allergy & Immunology*, vol. 52, no. 2, pp. 260–272, 2017.

[39] J. Lei, H. Hasegawa, T. Matsumoto, and M. Yasukawa, "Peroxisome proliferator-activated receptor α and γ agonists together with TGF-β convert human CD4 $^{+}$ CD25 $^{-}$ T cells into functional Foxp3 $^{+}$ regulatory T cells," *The Journal of Immunology*, vol. 185, no. 12, pp. 7186–7198, 2010.

[40] V. V. Sobolev, A. D. Zolotorenko, A. G. Soboleva et al., "Effects of expression of transcriptional factor AP-1 FOSL1 gene on psoriatic process," *Bulletin of Experimental Biology and Medicine*, vol. 150, no. 5, pp. 632–634, 2011.

[41] V. V. Sobolev, A. D. Zolotarenko, A. G. Soboleva et al., "Expression of the FOSL1," *Genetika*, vol. 46, no. 1, pp. 104–110, 2010.

[42] M. R. Young and N. H. Colburn, "Fra-1 a target for cancer prevention or intervention," *Gene*, vol. 379, pp. 1–11, 2006.

[43] D. Mehic, L. Bakiri, M. Ghannadan, E. F. Wagner, and E. Tschachler, "Fos and Jun proteins are specifically expressed during differentiation of human keratinocytes," *Journal of Investigative Dermatology*, vol. 124, no. 1, pp. 212–220, 2005.

[44] G. Adhikary, J. Crish, J. Lass, and R. L. Eckert, "Regulation of involucrin expression in normal human corneal epithelial cells: a role for activator protein one," *Investigative Ophthalmology & Visual Science*, vol. 45, no. 4, p. 1080, 2004.

[45] R. P. Nair, K. C. Duffin, C. Helms et al., "Genome-wide scan reveals association of psoriasis with IL-23 and NF-kappaB pathways," *Nature Genetics*, vol. 41, no. 2, pp. 199–204, 2009.

[46] D. Wilsmann-Theis, J. Wagenpfeil, D. Holzinger et al., "Among the S100 proteins, S100A12 is the most significant marker for psoriasis disease activity," *Journal of the European Academy of Dermatology and Venereology*, vol. 30, no. 7, pp. 1165–1170, 2016.

[47] L. Puig and A. López-Ferrer, "The AGEs of psoriasis: a biomarker for severity and a pathogenetic link to comorbidities," *Acta Dermato-Venereologica*, vol. 97, no. 7, p. 775, 2017.

[48] A. Nadeem, N. O. Al-Harbi, M. A. Ansari et al., "Psoriatic inflammation enhances allergic airway inflammation through IL-23/STAT3 signaling in a murine model," *Biochemical Pharmacology*, vol. 124, pp. 69–82, 2017.

[49] G. J. Mendoza, O. Almeida, and L. Steinfeld, "Intermittent fetal bradycardia induced by midpregnancy fetal ultrasonographic study," *American Journal of Obstetrics and Gynecology*, vol. 160, no. 5, pp. 1038–1040, 1989.

[50] A. Meirhaeghe and P. Amouyel, "Impact of genetic variation of PPARγ in humans," *Molecular Genetics and Metabolism*, vol. 83, no. 1-2, pp. 93–102, 2004.

[51] P. Avci, A. Gupta, M. Sadasivam et al., "Low-level laser (light) therapy (LLLT) in skin: stimulating, healing, restoring," *restoring. Semin Cutan Med Surg*, vol. 32, no. 1, pp. 41–52, 2013.

[52] Y. Yao, L. Richman, C. Morehouse et al., "Type I interferon: potential therapeutic target for psoriasis?," *PLoS One*, vol. 3, no. 7, article e2737, 2008.

Hindawi
PPAR Research
Volume 2020, Article ID 6937475, 13 pages
https://doi.org/10.1155/2020/6937475

Research Article

A New Prognostic Risk Model Based on PPAR Pathway-Related Genes in Kidney Renal Clear Cell Carcinoma

Yingkun Xu,[1] Xiunan Li,[1,2] Yuqing Han,[3] Zilong Wang,[1] Chenglin Han,[1] Ningke Ruan,[4] Jianyi Li,[1] Xiao Yu,[1] Qinghua Xia,[1,5] and Guangzhen Wu[2]

[1]*Department of Urology, Shandong Provincial Hospital, Cheeloo College of Medicine, Shandong University, Jinan, Shandong 250021, China*
[2]*Department of Urology, The First Affiliated Hospital of Dalian Medical University, Dalian, Liaoning 116011, China*
[3]*Department of Radiology, Shandong Provincial Hospital, Cheeloo College of Medicine, Shandong University, Jinan, Shandong 250021, China*
[4]*The Nursing College of Zhengzhou University, Zhengzhou, Henan 450001, China*
[5]*Department of Urology, Shandong Provincial Hospital Affiliated to Shandong First Medical University, Jinan, Shandong 250021, China*

Correspondence should be addressed to Qinghua Xia; xqhgege@hotmail.com and Guangzhen Wu; wuguang0613@hotmail.com

Received 16 June 2020; Revised 29 August 2020; Accepted 1 September 2020; Published 22 September 2020

Academic Editor: Hongbao Cao

Objective. This study is aimed at using genes related to the peroxisome proliferator-activated receptor (PPAR) pathway to establish a prognostic risk model in kidney renal clear cell carcinoma (KIRC). *Methods*. For this study, we first found the PPAR pathway-related genes on the gene set enrichment analysis (GSEA) website and found the KIRC mRNA expression data and clinical data through TCGA database. Subsequently, we used R language and multiple R language expansion packages to analyze the expression, hazard ratio analysis, and coexpression analysis of PPAR pathway-related genes in KIRC. Afterward, using the Search Tool for the Retrieval of Interacting Genes/Proteins (STRING) website, we established the protein-protein interaction (PPI) network of genes related to the PPAR pathway. After that, we used LASSO regression curve analysis to establish a prognostic survival model in KIRC. Finally, based on the model, we conducted correlation analysis of the clinicopathological characteristics, univariate analysis, and multivariate analysis. *Results*. We found that most of the genes related to the PPAR pathway had different degrees of expression differences in KIRC. Among them, the high expression of 27 genes is related to low survival rate of KIRC patients, and the high expression of 13 other genes is related to their high survival rate. Most importantly, we used 13 of these genes successfully to establish a risk model that could accurately predict patients' prognosis. There is a clear correlation between this model and metastasis, tumor, stage, grade, and fustat. *Conclusions*. To the best of our knowledge, this is the first study to analyze the entire PPAR pathway in KIRC in detail and successfully establish a risk model for patient prognosis. We believe that our research can provide valuable data for future researchers and clinicians.

1. Introduction

Renal malignancies are the twelfth most common tumors occurring worldwide [1]. Renal cell carcinoma (RCC) is the most common primary malignant tumor of the kidney, accounting for 90% to 95% of all cases of renal cancer [2]. Kidney renal clear cell carcinoma (KIRC) is the most common subtype of RCC [3]. Surgery is the primary treatment for early kidney cancer; however, it usually results in unsatisfactory outcomes, because 20% to 50% of the patients will relapse after surgery, and about 30% of the patients, though they miss local recurrence after surgery, end up having distant metastasis [4]. Renal cell carcinoma is highly resistant to radiotherapy and chemotherapy. Immunotherapy is extraordinarily inefficient and has apparent side effects [5, 6]. Molecular-targeted drug therapy is the primary treatment for advanced renal cancer [7]. In recent years, targeted drugs such as sunitinib have shown sound therapeutic effects and

have become first-line treatment for patients with advanced kidney cancer. However, a considerable number of patients with kidney cancer show the original primary resistance and secondary resistance. Therefore, there is an urgent need to find new molecular therapeutic targets. Molecules such as VHL and VEGF were discovered as part of this ongoing quest for new targets for cancer therapy. However, more in-depth understanding of cancer shows that the occurrence of the disease is not the result of uncontrolled single or several oncogenes or tumor suppressors. Oncogenesis is the result of a complex mechanism, which may involve typical serial changes in many critical biological pathways, involving groups of highly related molecules [8, 9]. We use this new understanding to explore the potential role played by entire pathways in kidney cancer, to potentially arrive at successful therapeutic modes of action. Such research helps to understand the pathogenesis of renal cancer and provide personalized treatment.

As a biological pathway mediated by specific receptors, the peroxisome proliferator-activated receptor (PPAR) pathway plays a key role in cell differentiation, development, metabolism (sugar, lipid, and protein), and tumorigenesis. KIRC is also known as clear cell renal cell carcinoma (ccRCC) because its cells contain a large amount of deposited lipids and present a special transparent appearance. PPAR is a nuclear hormone receptor activated by fatty acids and their derivatives [10]. Therefore, we have reason to believe that the PPAR pathway plays an important role in the progress of KIRC. PPAR has three subtypes (PPARα, PPARβ, and PPARγ), which show different expressions in vertebrates [11]. They are each encoded by a separate gene and combine fatty acids and eicosanoids. PPARα plays a role in clearing circulating lipids or cellular lipids by regulating the expression of genes involved in lipid metabolism in liver and skeletal muscle. PPARβ is involved in lipid oxidation and cell proliferation. PPARγ promotes the differentiation of adipocytes, thereby increasing blood glucose uptake. The PPAR pathway is also considered to be a regulatory pathway for various cancers. PPARα is a potential drug target for the treatment of kidney cancer. In renal cancer cell lines, the PPARα antagonist GW6471 can arrest the cell cycle in G0/G1 phase by attenuating cell cycle regulatory proteins, thereby inducing cell apoptosis. GW6471 can also attenuate fatty acid oxidation and oxidative phosphorylation by inhibiting glycolysis, and thereby inhibit the growth of kidney cancer cells. However, PPARα has been controversial in the regulation of cell growth, proliferation, and tumorigenesis [12, 13]. Some studies have shown that in colorectal cancer, PPARα activated by fenofibrate can stall the progress of colorectal cancer by inhibiting the expression of proinflammatory factors and by increasing the antioxidant capacity of cells [14]. Additionally, activated PPARα can play an anti-inflammatory function by reducing the production of cytokines, which may lead to the downregulation of NF-κB and COX-2 [15, 16]. It has been reported that after the retinoic acid/PPARα pathway is disrupted, it will affect oxidative damage and change the expression of tumor suppressors, which may lead to colorectal tumors caused by low folic acid intake [17]. Shaw et al. found that retinoic acid could also bind to PPARβ to promote tumor cell growth and inhibit apoptosis [18]. Previous studies have found that some PPARγ agonists can inhibit tumor cell proliferation, induce tumor cell apoptosis, and inhibit tumor angiogenesis. If used in combination with chemotherapeutics, it is also thought to increase the antitumor effect of the latter [19, 20]. However, some studies have found that activation of PPARγ can promote tumor development [21–25]. All this shows that PPARs and the PPAR pathway are closely related to the occurrence and development of tumors and may become a potential target for tumor treatment.

In our study, we conducted an in-depth and detailed analysis of genes related to the PPAR pathway in KIRC. We analyzed the expression of these genes in KIRC, and found that most of them had apparent expression differences. After conducting hazard ratio (HR) analysis, we found that most of them played a role as a promoter or inhibitor in the occurrence and development of KIRC. We then established a prognostic model composed of 13 PPAR pathway-related genes. The ROC curve results show that this model has good prediction accuracy. In the future, we hope that our research can provide accurate data for later researchers, and at the same time, can help doctors make proper clinical diagnosis and treatment decisions for patients.

2. Materials and Methods

2.1. Data Collection. In May 2020, we obtained mRNA expression data and clinical data set of KIRC through TCGA database. Then we found the PPAR pathway through the GSEA analysis website (https://www.gsea-msigdb.org/gsea/index.jsp) and evaluated the genes in this pathway. The standard name of this path is KEGG_PPAR_signaling_pathway, and the systematic name is M13088.

2.2. Generation of Protein-Protein Interaction Networks. The Search Tool for the Retrieval of Interacting Genes/Proteins (STRING) website can be used to predict the functional correlation between different proteins (https://string-db.org/) [26]. The STRING is a continuously updated biological database that contains comprehensive and easily accessible interactive information, some of which are obtained through experiments and others through predictive analysis. In this study, we used the website's online tool to map the protein-protein interaction (PPI) network between molecules related to the PPAR pathway.

2.3. The Human Protein Atlas (HPA) Website. This database (http://www.proteinatlas.org/) contains protein distribution information including those of multiple human tissues and organs and provides tissue and cell expression levels of nearly 20,000 human proteins [27, 28]. We used this website to explore the protein expression of CPT2 in normal kidney tissues and kidney cancer tissues.

2.4. Renal Cancer Cell Lines and Plasmid Transfection. In this study, renal cancer cell lines 786-O and ACHN were purchased from the Institute of Cell Research, Chinese Academy of Sciences. These two cell lines were cultured in the presence of penicillin and streptomycin at 37°C in an

atmosphere containing 5% CO_2. We harvested 2×10^5 786-O and ACHN cells during the logarithmic growth period and seeded them into 6-well plates. The plasmid was transfected the next day. Subsequently, Lipofectamine 2000 (Invitrogen) and plasmid fragments were diluted in serum-free medium, and a pipette was used to add 100 μL of the mixture to the 6-well plates. After 6 hours of incubation at 37°C, the medium containing serum was changed to continue the culture until 24 hours. Finally, the cells were digested with trypsin and collected for proliferation experiments.

2.5. Cell Counting Kit-8 (CCK-8) Experiment. First, we cultured 1×10^3 786-O and ACHN cells per well in a 96-well culture plates (4 replicate wells per group). Subsequently, we added 10 μL of the CCK-8 reagent to each well according to the instructions of Cell Counting Kit-8 (Dojindo, Japan) and incubated it in a 37°C incubator for 1-2 hours. Finally, we used a microplate reader to measure the optical density (OD) of each well at 450 nm, record, analyze, and draw the corresponding histogram.

2.6. Data Processing and Analysis. In May 2020, we downloaded RNA-seq transcriptome data of KIRC through the R/Bioconductor software package from TCGAbiolinks, which contains 72 normal kidney tissues and 539 tumor tissues. The clinical information of KIRC patients including age, survival status, grade, stage, tumor (T), and metastasis (M) were all downloaded from TCGAbiolinks and analyzed using Perl language and R studio. We then constructed a heat map that reflects the expression of PPAR pathway-related genes in KIRC. The "pheatmap" expansion package was used to draw heat maps, and the "limma" expansion package was used to analyze mRNA differences. We then performed a hazard ratio (HR) analysis of these molecules in KIRC to show the relationship these molecules have with kidney cancer progression. Afterward, we used the "corrplot" expansion package to plot the coexpression relationship among the PPAR pathway-related genes. Then we used the "glmnet" and "survival" extension packages to draw the LASSO regression curve and survival curve. To verify this model's accuracy, we used the "survival ROC" expansion package to bring a five-year and ten-year ROC curve. Subsequently, based on this model, we analyzed the correlation with the pathological characteristics of renal cell carcinoma patients and depicted it in the form of a heat map. The "rms" software package was used to draw the nomogram. Finally, we combined the clinical data of KIRC patients with the model through the "survival" expansion package for univariate and multivariate analysis.

2.7. Statistical Analyses. One-way ANOVA was used to compare the expression of PPAR pathway-related genes in tumor and normal tissue samples. The Student's t-test was used to compare the expression of PPAR pathway-related genes in the KIRC dataset according to gender, age, stage, tumor (T), and metastasis (M). Node (N) was not included in the study because it was not verified for a large number of samples in TCGA database. The cut-off value of each risk score in the tumor group was determined using the "survminer" expansion package, and the patients were divided into high- and low-risk groups according to the best cut-off threshold value. The R studio package was used for all statistical analyses. $P < 0.05$ was considered statistically significant.

3. Results

3.1. The Expression of PPAR-Related Genes in KIRC and the Univariate Cox Regression Analysis in KIRC. To explore the expression of PPAR pathway-related genes in KIRC, we individually plotted their related heat maps (Figure 1(a)). We observed that the vast majority of PPAR pathway-related genes differed significantly in tumor tissues and normal tissues. It can be inferred from this that any change in this pathway plays a significant role in tumorigenesis and progress of the cancer. Then, we performed the univariate Cox regression analysis of these PPAR pathway-related molecules in KIRC (Figure 1(b)). The results show the hazard ratios with 95% confidence intervals (CI) and P values for the PPAR pathway-related genes. The results showed that high expression of PCK2, PPARG/PPARγ, ACOX2, PLIN2, CYP27A1, SORBS1, PDPK1, GK, PPARA/PPARα, SLC27A2, CPT1A, SCD5, CYP4A11, ACOX1, ACAA1, CD36, EHHADH, PCK1, RXRA, SCP2, ACADM, ACADL, CYP4A22, LPL, ILK, ACSL1, and CPT2 correlated with better survival rates; in contrast, high expression of MMP1, FABP5, ACOX3, NR1H3, DBI, PLIN4, ACSBG1, PLTP, ADIPOQ, PLIN1, CPT1B, CPT1C, and UCP1 correlated with worse survival rates in KIRC patients.

3.2. PPI Network and Coexpression Analysis between PPAR Pathway-Related Molecules. To explore the interaction between PPAR pathway-related molecules, we used the online tool of the STRING website to illustrate the PPI network (Figure 2(a)). We observed that there were relatively close interactions between the various molecules on the PPAR pathway. When the expansion package on the R language was used to draw an image showing coexpression between molecules (Figure 2(b); Supplementary Table S1 and S2), we observed that there was a highly positive coexpression relationship between the four molecules APOA1, APOA5, APOC3, and CYP7A1. There was a clear positive correlation between PPARA/PPARα and CPT1A, ACSL1, PCK1, PCK2, ACOX2, ACAA1, GK, ACOX1, ACADM, SLC27A2, EHHADH, and so on. Among them, CPT1A was the representative. CPT1A is an important rate-limiting enzyme for fatty acid transport into mitochondria to participate in fatty acid β-oxidation, suggesting that PPARA/PPARα may play an important role in lipid metabolism. Additionally, previous studies have shown that CPT1A may be a potential therapeutic target in KIRC [29]. As we all know, KIRC is also known as clear cell renal cell carcinoma because this kidney cancer cell contains many lipid droplets. The presence of apparent abnormalities in fatty acid metabolism in kidney cancer is recognized. In our previous studies, it was found that breaking the lipid homeostasis in this type of kidney cancer could significantly limit tumor progression [30]. Of course,

Figure 1: (a) Heat map of PPAR pathway-related gene expression and (b) analysis of their risk factors in KIRC. $^{*}P < 0.05$; $^{**}P < 0.01$; $^{***}P < 0.001$.

many molecules clearly express correlations, and because of the limited space, they are not listed here.

3.3. Using LASSO Regression to Establish a Risk Model Related to the Prognosis of Patients in KIRC. To explore whether it was possible to use PPAR pathway-related molecules to establish a model in KIRC that could predict the clinical outcome of patients, we conducted a LASSO regression curve analysis (Figures 3(a) and 3(b)). We derived a model composed of thirteen molecules PDPK1, ACADM, SCP2, SLC27A2, EHHADH, CPT2, SCD5, SORBS1, PLTP, FABP5, PLIN1, and PLIN4. We then used this model to divide KIRC patients into a high-risk group and a low-risk group. We observed that the overall survival rate of patients

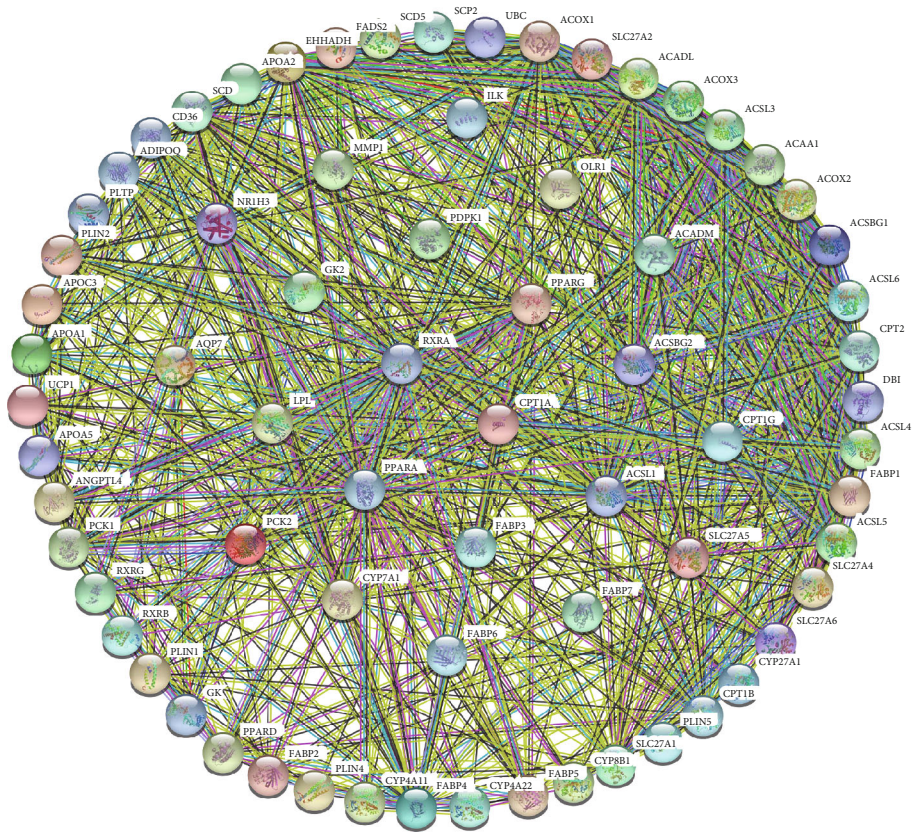

(a)

(b)

Figure 2: Interactions and correlations between PPAR pathway molecules. PPI network (a) and coexpression analysis (b) between PPAR pathway-related genes.

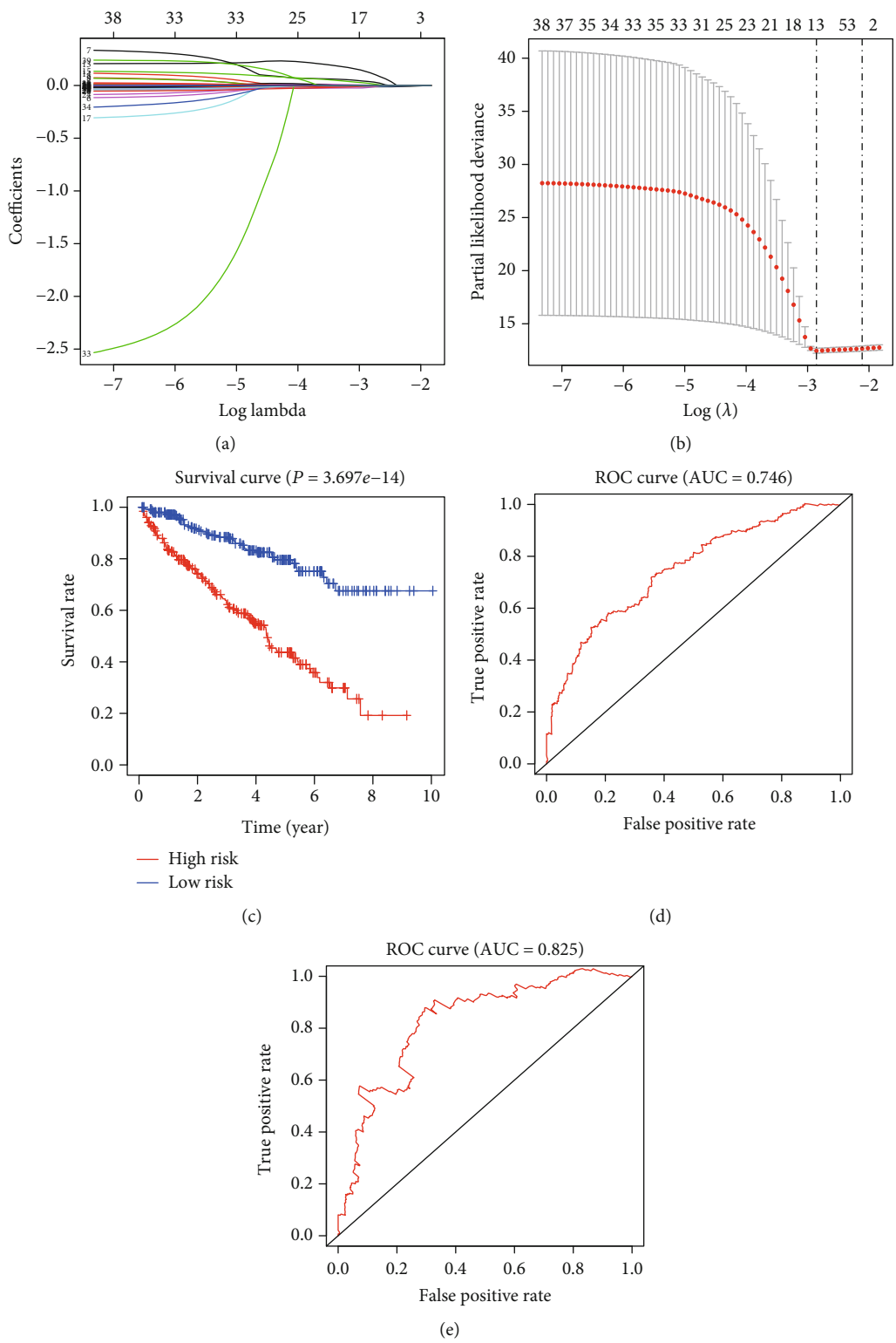

Figure 3: The establishment of the risk model and analysis of its prediction accuracy. (a, b) Target gene selection using LASSO logistic regression. (c) Based on this model, we conducted survival analysis in KIRC. (d) Five-year ROC curve. (e) Ten-year ROC curve.

in the high-risk group was significantly lower than that in the low-risk group ($P = 3.697e\text{-}14$) (Figure 3(c)). Additionally, we performed ROC curve analysis to analyze the prognostic prediction performance of the new survival model in KIRC patients and obtained a five-year AUC score of 0.746 (Figure 3(d)) and a ten-year AUC score of 0.825

(Figure 3(e)), which indicated that the risk score calculated by the model could accurately predict the 5-year and 10-year survival rates of KIRC patients.

3.4. Model-Based Correlation Analysis with Clinicopathological Characteristics, Univariate Cox Regression Analysis, and Multivariate Cox Regression Analysis. We plotted a heat map between these target molecules and clinical data to explore the correlation between this risk model and clinicopathological features (Figure 4(a)). In this heat map, we found a relationship between this risk model and the patient's M, T, stage, grade, and fustat. Then we conducted univariate Cox regression analysis (Figure 4(b)) and multivariate Cox regression analysis (Figure 4(c)) and found that this risk model played a risk factor in both different regression analyses. And the hazard ratio of the risk model is higher than that of other clinicopathological features.

3.5. Draw a Novel Nomogram Based on Logistic Regression and Verify In Vitro Experiments. The nomogram predicts the risk of KIRC patients (Figure 5). The value of each variable gets a score on the dot scale axis. The nomogram generates a total of nine rows. The second, third, fourth, and fifth lines represent age, grade, stage, and risk score, respectively. The total score in the sixth row is obtained from the sum of each score assigned to age, grade, stage, and the risk score, and the five-year, seven-year, and ten-year survival rates of KIRC patients can be easily estimated from the total score. Additionally, in order to add validity to our conclusions, we conducted in vitro experiments.

By consulting the literature, we found that CPT2 has not been studied in KIRC thus far; hence, we chose CPT2 as a target molecule for subsequent exploration. We explored the expression of CPT2 between normal kidney tissue and renal tumor tissue through the HPA website. We found that the protein expression level of CPT2 in KIRC tissue was significantly lower than that in normal kidney tissue (Figure 6(a)). Subsequently, we used a plasmid transfection technology to establish CPT2 overexpressing renal cancer cell lines (786-O and ACHN cell lines) and conducted CCK-8 experiments. The experimental results showed that the cell proliferation of 786-O and ACHN cells overexpressing CPT2 was significantly inhibited (Figures 6(b) and 6(c)). These results indicate that CPT2 may become a potential therapeutic target in the treatment of renal cancer in the future.

4. Discussion

Over the past decade, the research on molecules related to the PPAR pathway in cancer has been ongoing, but the results remain unclear. Some reports suggest that the PPAR pathway plays a protective factor in tumorigenesis, and the primary mechanism is achieved by inhibiting the activity of inflammation or angiogenesis [31, 32]. At the same time, other researchers regard it as a promoter of tumorigenesis [33]. Recently, another study showed that PPARG/PPARγ overexpression might help to better treat patients with CRC by inhibiting the process of EMT (epithelial-mesenchymal transition) [34]. PPARA/PPARα in KIRC can overcome sunitinib resistance by regulating the NF-κB pathway [35]. PPARG/PPARγ in KIRC can promote cell apoptosis and inhibit cell migration and proliferation by inhibiting SIX2 [36, 37]. Similarly, in this investigation, the hazard ratio results show that PPARG/PPARγ plays a protective factor in KIRC. This study aims at integrating PPAR pathway-related genes and determining a model that can predict patients' survival. In our study, we first investigated the expression and prognosis of PPAR pathway-related genes in KIRC. Subsequently, the interaction and coexpression of these molecules were analyzed and through the LASSO regression and cross-validation, the novel thirteen-gene model was determined. This model divides KIRC patients into high-risk and low-risk groups through the risk score, and survival curve analysis shows that the survival of patients in the high-risk group is significantly worse than that of the low-risk group patients. The ROC curve shows that this model has good five-year and ten-year survival prediction accuracy. Multivariate Cox regression analysis shows that this new 13-gene prognostic model is an independent risk factor for KIRC.

The occurrence and development of clear cell renal cell carcinoma is a complex process regulated by genetic changes of multiple molecules. To date, there have been many previous studies exploring the prognostic role of risk models in predicting KIRC patients [38–41]. The clinical application results based on multiple gene expression profiles indicate that genetic risk model may be a promising clinical diagnosis and treatment method [42–44]. In this study, we successfully used 13 genes of PDPK1, ACADM, SCP2, SLC27A2, EHHADH, CPT2, SCD5, SORBS1, PLTP, FABP5, PLIN1, and PLIN4 to construct risk models related to the prognosis of KIRC patients. Its five-year ROC curve has an AUC value of 0.746, and its ten-year ROC curve has an AUC value of 0.825. Generally, a risk model with an AUC value over 0.7 indicates a very high prediction accuracy.

PDPK1 is a regulated protein kinase from the AGC protein kinase family, which can activate multiple downstream effectors associated with various pathways of tumorigenesis [45]. Previous researchers found that inhibiting PDPK1 expression in small cell lung cancer and melanoma can inhibit tumor progression [46, 47]. ACADM can catalyze the first dehydrogenation process of β-oxidation of fatty acyl-CoA [48]. In KIRC, the low expression of ACADM may affect the metabolism of medium-chain fatty acids, and then the metabolism of triglycerides, and play an essential role in apoptosis through the function of light chains [49, 50]. Previous studies have shown that SCP2 plays a critical role in stabilizing PML expression. Low expression of SCP2 will increase the phosphorylation level of PMLS518, thereby reducing PML. The downregulation of PML is related to the occurrence and development of high-grade tumors [51]. In endometrial and ovarian cancer, researchers found that SLC27A2 can play a biological role in regulating chemical resistance [52, 53]. EHHADH can encode a bifunctional enzyme and is one of the four enzymes for peroxisomal β-oxidation [54]. In the studies of Cablé et al. and Suto et al., it was found that EHHADH had a significantly low expression in colon cancer and hepatocellular carcinoma and could be used as a potential prognostic marker [55, 56].

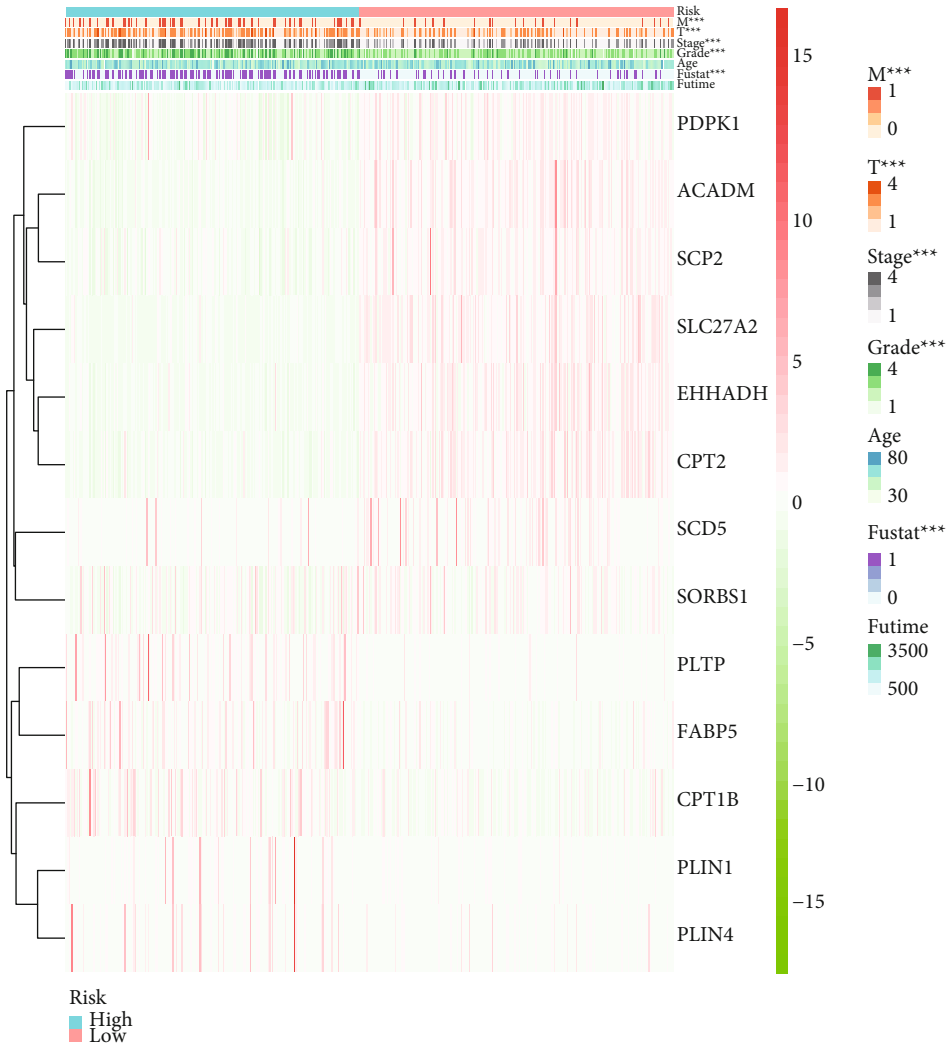

(a)

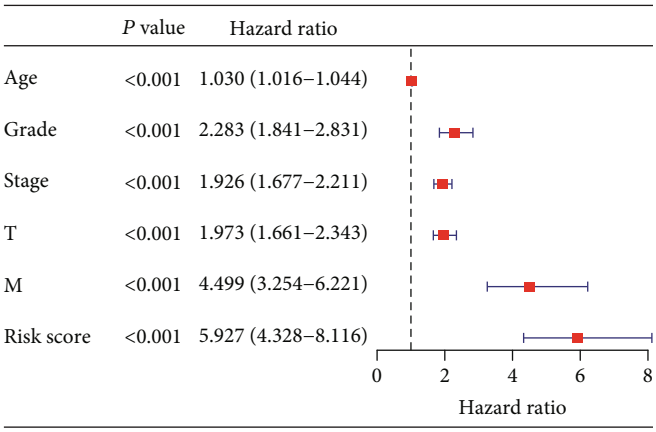

(b)

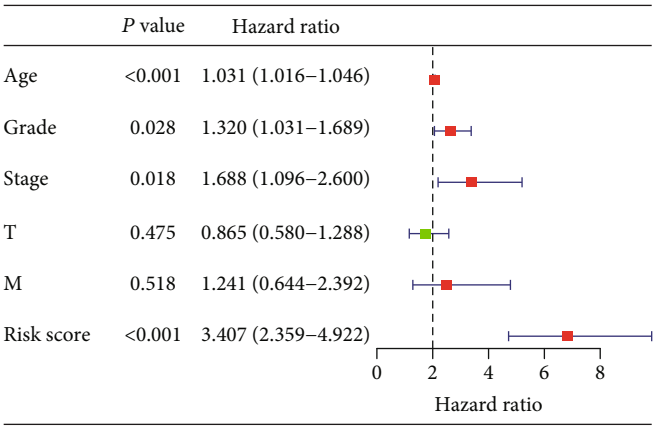

(c)

Figure 4: (a) Based on this risk model, the analysis correlates with the clinicopathological characteristics. (b) Univariate Cox regression analysis. The results of univariate Cox regression analysis showed clinicopathological parameters such as age, grade, stage, T (tumor), M (metastasis), and risk score of the new survival model with the OS of KIRC patients. (c) Multivariate Cox regression analysis. The results of multivariate Cox regression analysis showed clinicopathological parameters such as age, grade, stage, and risk score of the new survival model with the OS of KIRC patients. $^{***}P < 0.001$.

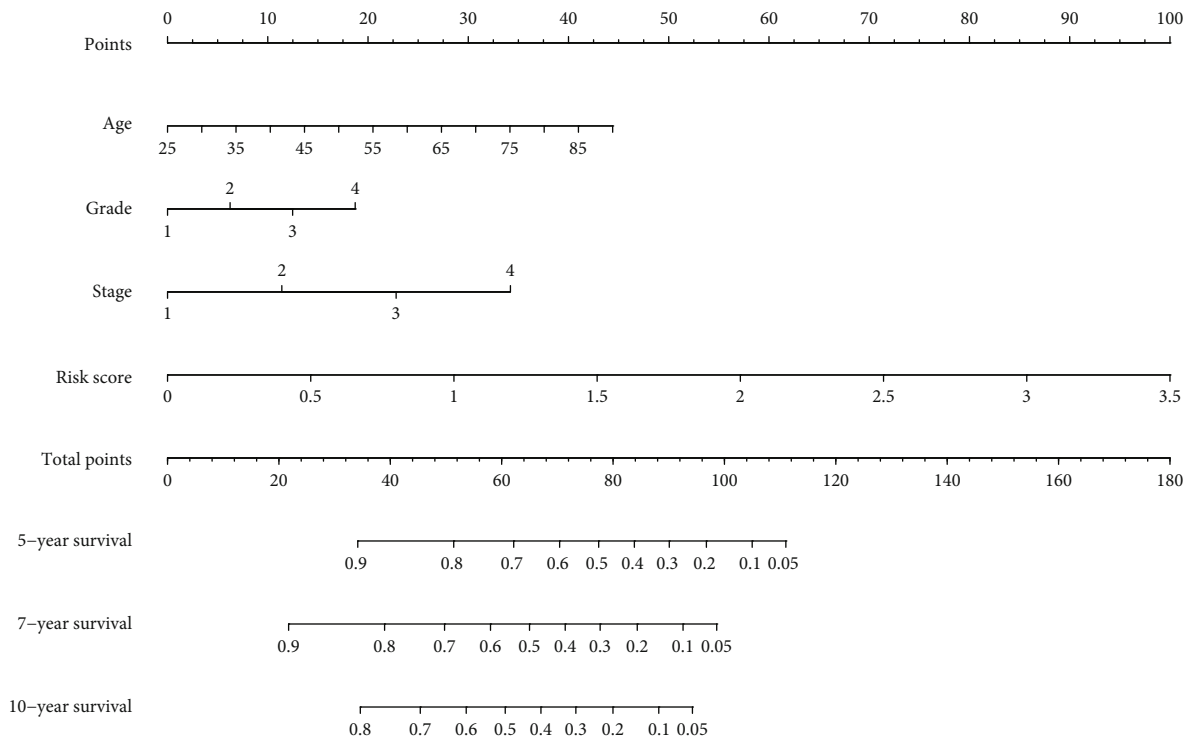

Figure 5: The novel nomogram was constructed based on the risk model for predicting 5-, 7-, or 10-year survival rates in KIRC. The value of each variable gets a score on the dot scale axis. The total score can be easily calculated by adding up each individual score and projecting the total score to a lower total score system, and we can estimate the risk of KIRC patients.

PPARA/PPARα mainly regulates the expression of CPT2. Studies have shown that in hepatocellular carcinoma, CPT2 is the rate-limiting enzyme for fatty acid oxidation. Its expression level is related to the proliferation and invasion of liver cancer cells. Silencing CPT2 can induce chemical resistance to cisplatin [57]. Some researchers have found that downregulating the expression of CPT2 helps to avoid the lipid toxicity caused by the lipid-rich cell environment [58]. SCD5 is a protein-coding gene that can regulate neuronal cell growth and differentiation by regulating key fat-generating pathways. SCD5 may play an important role through the PPAR pathway in breast cancer chemotherapy [59]. The activity of SCD5 is also correlated with the activity of multiple cancer pathways such as AKT, WNT, and EGFR [60].

SORBS1, also known as Cap/Ponsin protein, can regulate biological processes such as growth factor signaling, cell adhesion, and cancer metastasis [61]. The primary function of the protein encoded by PLTP is to transfer phospholipids from triglyceride-rich lipoproteins to high-density lipoproteins. Studies have shown that PLTP can induce anti-inflammatory responses by activating the ABCA1/STAT3 pathway [62, 63]. FABP5 is a member of the FABP family [64]. Some researchers have found that it can affect the progress of tumors by affecting the activity of the PI3K/AKT signaling pathway in KIRC [65], and that it plays a role as an oncogene in KIRC [66]. CPT1B is one of three CPT1 subtypes. The researchers found that knocking down the expression of CPT1B in BLCA could increase the ability of tumor proliferation and invasion by inhibiting FAO [67]. Overexpression of PLIN1 can inhibit the proliferation, migration, and invasion of breast cancer cells. The expression level of PLIN1 is correlated with the prognosis of breast cancer patients and is expected to become a potential new gene therapy target for breast cancer [68]. PLIN1 may affect tumor progression through PPARG/PPARγ pathway in breast cancer [69]. At the same time, another member of the same family, PLIN4, has also been identified as a therapeutic target for triple-negative breast cancer [70].

It can be inferred from the above-mentioned information that the target gene used to establish this model in this study has received varying degrees of attention and research in various tumors. However, there are parameters like CPT2, SORBS1, PLIN1, and PLIN4 that have not been studied in KIRC. These biomarkers may be worthy of attention in the future of KIRC research. In particular, we explore the potential role of CPT2 in KIRC through in vitro experiments. When we overexpressed CPT2 in 786-O and ACHN kidney cancer cell lines, the cell proliferation ability was significantly inhibited. Hereafter, we will continue to explore the potential role of these genes in KIRC. We believe that this model related to patient prognosis can help doctors choose more personalized treatment for KIRC patients in the future. After the grouping of this model, for patients in the low-risk group, clinicians can appropriately reduce the frequency of examinations and reduce the economic pressure on patients. For patients in the high-risk group, clinicians would be able to give more intensive treatments and strengthen follow-up and regular physical examination to monitor the development of the disease.

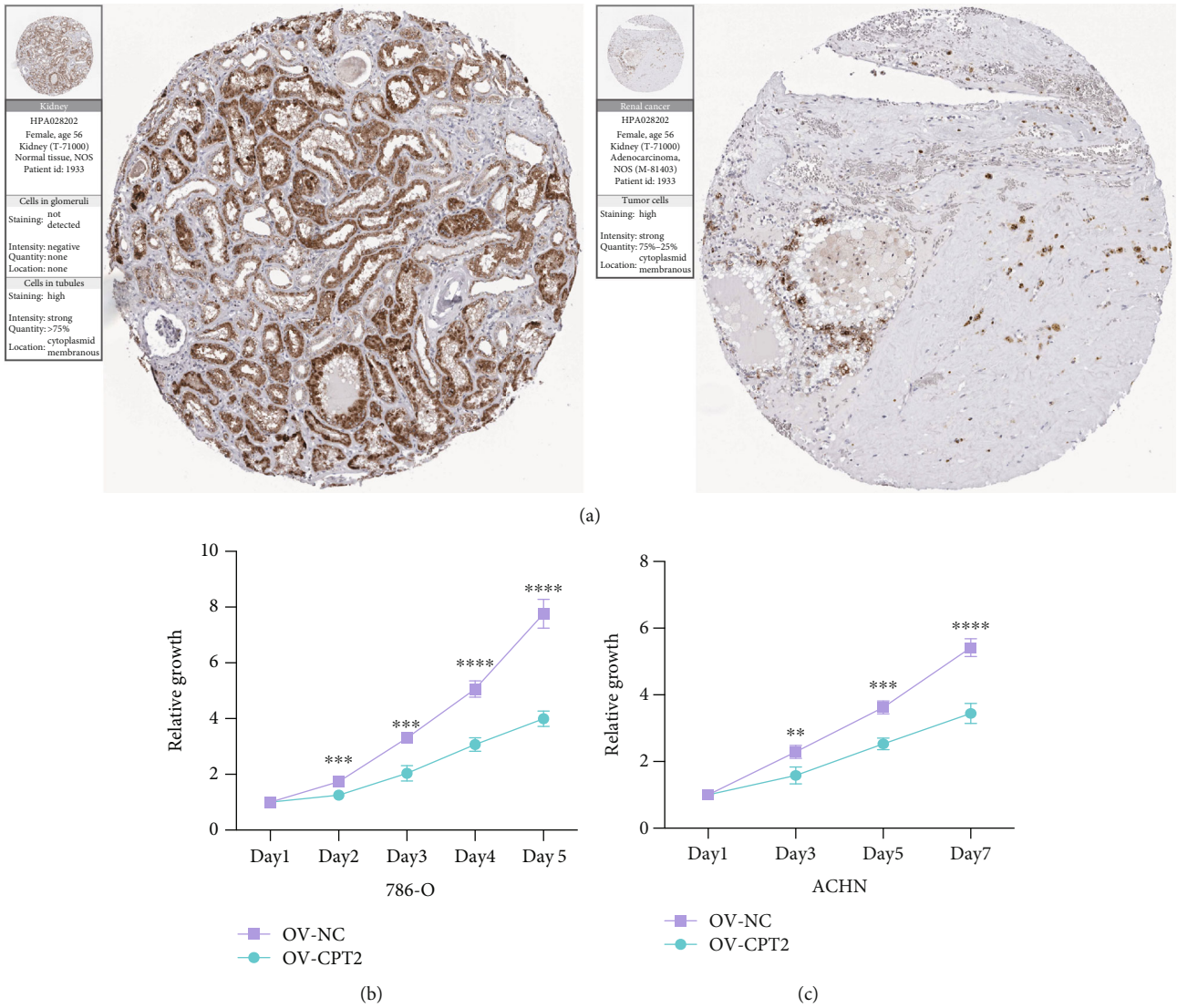

Figure 6: Experimental verification of CPT2. (a) Immunohistochemical images from the HPA database show CPT2 protein expression in normal kidney (N) and KIRC (T) tissues. (b, c) CCK8 assay results show the relative proliferation of OV-NC- and OV-CPT2-transfected 786-O and ACHN cell lines. The data are shown as mean ± S.D. $^{**}P < 0.01$; $^{***}P < 0.001$; $^{****}P < 0.0001$.

5. Conclusions

In this study, we used 13 genes related to the PPAR pathway to establish a new prognostic risk model in KIRC, which could accurately predict the five-year and ten-year survival rates of patients. However, it must be admitted that in this study, these thirteen target genes have not been thoroughly explored in KIRC. In the future, large-scale single-center or multicenter clinical validation of this risk model is needed. However, we believe that our research can provide valuable data for future scientific research and clinical practice.

Abbreviations

PPAR: Peroxisome proliferator-activated receptor
KIRC: Kidney renal clear cell carcinoma
GSEA: Gene set enrichment analysis
TCGA: The Cancer Genome Atlas
PPI: Protein-protein interaction
LASSO: Least absolute shrinkage and selection operator
RCC: Renal cell carcinoma
ccRCC: Clear cell renal cell carcinoma
VHL: Von Hippel-Lindau tumor suppressor
VEGF: Vascular endothelial growth factor
PDPK1: 3-Phosphoinositide dependent protein kinase 1
ACADM: Acyl-CoA dehydrogenase medium chain
SCP2: Sterol carrier protein 2
SLC27A2: Solute carrier family 27 member 2
EHHADH: Enoyl-CoA hydratase and 3-hydroxyacyl CoA dehydrogenase
CPT2: Carnitine palmitoyltransferase 2
SCD5: Stearoyl-CoA desaturase 5
SORBS1: Sorbin and SH3 domain containing 1
PLTP: Phospholipid transfer protein

FABP5: Fatty acid binding protein 5
PLIN1: Perilipin 1
PLIN4: Perilipin 4.

Data Availability

The data used to support the findings of this study are available from the corresponding author upon request.

Conflicts of Interest

The authors declare that they have no conflicts of interest.

Authors' Contributions

Yingkun Xu and Xiunan Li contributed equally to this study. Qinghua Xia, Guangzhen Wu, Yingkun Xu, and Xiunan Li designed the research methods and analyzed the data. Yuqing Han, Jianyi Li, and Zilong Wang participated in the data collection. Yingkun Xu conducted in vitro experiments. Chenglin Han, Xiao Yu, and Ningke Ruan drafted and revised the manuscript. All authors approved the version to be released and agreed to be responsible for all aspects of the work.

Acknowledgments

This work was supported by the National Natural Science Foundation of China (Grant No. 81672553). In addition, Yingkun Xu would like to thank Jiayi Li for her helpful guidance and suggestions for this research.

Supplementary Materials

Table S1: correlation value for coexpression analysis. Table S2: *P* value for coexpression analysis. *(Supplementary materials)*

References

[1] J. Ferlay, I. Soerjomataram, R. Dikshit et al., "Cancer incidence and mortality worldwide: sources, methods and major patterns in GLOBOCAN 2012," *International Journal of Cancer*, vol. 136, no. 5, pp. E359–E386, 2015.

[2] L. Kuthi, A. Jenei, A. Hajdu et al., "Prognostic factors for renal cell carcinoma subtypes diagnosed according to the 2016 WHO renal tumor classification: a study involving 928 patients," *Pathology Oncology Research*, vol. 23, no. 3, pp. 689–698, 2017.

[3] M. M. L. Baldewijns, I. J. H. van Vlodrop, L. J. Schouten, P. M. M. B. Soetekouw, A. P. de Bruïne, and M. van Engeland, "Genetics and epigenetics of renal cell cancer," *Biochimica et Biophysica Acta (BBA) - Reviews on Cancer*, vol. 1785, no. 2, pp. 133–155, 2008.

[4] C. Porta, L. Cosmai, B. C. Leibovich, T. Powles, M. Gallieni, and A. Bex, "The adjuvant treatment of kidney cancer: a multidisciplinary outlook," *Nature Reviews. Nephrology*, vol. 15, no. 7, pp. 423–433, 2019.

[5] S. Fernández-Pello, F. Hofmann, R. Tahbaz et al., "A systematic review and meta-analysis comparing the effectiveness and adverse effects of different systemic treatments for non-clear cell renal cell carcinoma," *European Urology*, vol. 71, no. 3, pp. 426–436, 2017.

[6] F. Massari, V. Di Nunno, L. Gatto et al., "Should CARMENA really change our attitude towards cytoreductive nephrectomy in metastatic renal cell carcinoma? A systematic review and meta-analysis evaluating cytoreductive nephrectomy in the era of targeted therapy," *Targeted Oncology*, vol. 13, no. 6, pp. 705–714, 2018.

[7] F. E. Vera-Badillo, A. J. Templeton, I. Duran et al., "Systemic therapy for non-clear cell renal cell carcinomas: a systematic review and meta-analysis," *European Urology*, vol. 67, no. 4, pp. 740–749, 2015.

[8] J. M. Peters and F. J. Gonzalez, "The evolution of carcinogenesis," *Toxicological Sciences*, vol. 165, no. 2, pp. 272–276, 2018.

[9] P. E. Porporato, N. Filigheddu, J. M. B.-S. Pedro, G. Kroemer, and L. Galluzzi, "Mitochondrial metabolism and cancer," *Cell Research*, vol. 28, no. 3, pp. 265–280, 2018.

[10] F. Hong, S. Pan, Y. Guo, P. Xu, and Y. Zhai, "PPARs as nuclear receptors for nutrient and energy metabolism," *Molecules*, vol. 24, no. 14, p. 2545, 2019.

[11] M. G. Borland, E. M. Kehres, C. Lee et al., "Inhibition of tumorigenesis by peroxisome proliferator-activated receptor (PPAR)-dependent cell cycle blocks in human skin carcinoma cells," *Toxicology*, vol. 404-405, pp. 25–32, 2018.

[12] J. M. Peters, J. E. Foreman, and F. J. Gonzalez, "Dissecting the role of peroxisome proliferator-activated receptor-β/δ (PPARβ/δ) in colon, breast, and lung carcinogenesis," *Cancer Metastasis Reviews*, vol. 30, no. 3-4, pp. 619–640, 2011.

[13] J. M. Peters, Y. M. Shah, and F. J. Gonzalez, "The role of peroxisome proliferator-activated receptors in carcinogenesis and chemoprevention," *Nature Reviews. Cancer*, vol. 12, no. 3, pp. 181–195, 2012.

[14] O. Abu Aboud, D. Donohoe, S. Bultman et al., "PPARα inhibition modulates multiple reprogrammed metabolic pathways in kidney cancer and attenuates tumor growth," *American Journal of Physiology. Cell Physiology*, vol. 308, no. 11, pp. C890–C898, 2015.

[15] P. R. Devchand, H. Keller, J. M. Peters, M. Vazquez, F. J. Gonzalez, and W. Wahli, "The PPARalpha-leukotriene B4 pathway to inflammation control," *Nature*, vol. 384, no. 6604, pp. 39–43, 1996.

[16] M. E. Poynter and R. A. Daynes, "Peroxisome proliferator-activated receptor alpha activation modulates cellular redox status, represses nuclear factor-kappaB signaling, and reduces inflammatory cytokine production in aging," *The Journal of Biological Chemistry*, vol. 273, no. 49, pp. 32833–32841, 1998.

[17] D. Leclerc, Y. Cao, L. Deng, L. G. Mikael, Q. Wu, and R. Rozen, "Differential gene expression and methylation in the retinoid/PPARA pathway and of tumor suppressors may modify intestinal tumorigenesis induced by low folate in mice," *Molecular Nutrition & Food Research*, vol. 57, no. 4, pp. 686–697, 2013.

[18] N. Shaw, M. Elholm, and N. Noy, "Retinoic acid is a high affinity selective ligand for the peroxisome proliferator-activated receptor beta/delta," *The Journal of Biological Chemistry*, vol. 278, no. 43, pp. 41589–41592, 2003.

[19] G. Skelhorne-Gross and C. J. B. Nicol, "The key to unlocking the chemotherapeutic potential of PPARγ ligands: having the right combination," *PPAR Research*, vol. 2012, Article ID 946943, 13 pages, 2012.

[20] J. Youssef and M. Badr, "Peroxisome proliferator-activated receptors and cancer: challenges and opportunities," *British Journal of Pharmacology*, vol. 164, no. 1, pp. 68–82, 2011.

[21] E. Saez, P. Tontonoz, M. C. Nelson et al., "Activators of the nuclear receptor PPARγ enhance colon polyp formation," *Nature Medicine*, vol. 4, no. 9, pp. 1058–1061, 1998.

[22] R. Govindarajan, L. Ratnasinghe, D. L. Simmons et al., "Thiazolidinediones and the risk of lung, prostate, and colon cancer in patients with diabetes," *Journal of Clinical Oncology*, vol. 25, no. 12, pp. 1476–1481, 2007.

[23] S. Fauconnet, I. Lascombe, E. Chabannes et al., "Differential regulation of vascular endothelial growth factor expression by peroxisome proliferator-activated receptors in bladder cancer cells," *The Journal of Biological Chemistry*, vol. 277, no. 26, pp. 23534–23543, 2002.

[24] M. Kostapanos, M. Elisaf, and D. Mikhailidis, "Pioglitazone and cancer: angel or demon?," *Current Pharmaceutical Design*, vol. 19, no. 27, pp. 4913–4929, 2013.

[25] A. Neumann, A. Weill, P. Ricordeau, J. P. Fagot, F. Alla, and H. Allemand, "Pioglitazone and risk of bladder cancer among diabetic patients in France: a population-based cohort study," *Diabetologia*, vol. 55, no. 7, pp. 1953–1962, 2012.

[26] D. Szklarczyk, A. L. Gable, D. Lyon et al., "STRING v11: protein-protein association networks with increased coverage, supporting functional discovery in genome-wide experimental datasets," *Nucleic Acids Research*, vol. 47, no. D1, pp. D607–d613, 2019.

[27] M. Uhlen, C. Zhang, S. Lee et al., "A pathology atlas of the human cancer transcriptome," *Science*, vol. 357, no. 6352, 2017.

[28] P. J. Thul, L. Åkesson, M. Wiking et al., "A subcellular map of the human proteome," *Science*, vol. 356, no. 6340, 2017.

[29] Y. Xu, G. Wu, X. Ma et al., "Identification of CPT1A as a prognostic biomarker and potential therapeutic target for kidney renal clear cell carcinoma and establishment of a risk signature of CPT1A-related genes," *International Journal of Genomics*, vol. 2020, Article ID 9493256, 2020.

[30] G. Wu, Q. Wang, Y. Xu et al., "Targeting the transcription factor receptor LXR to treat clear cell renal cell carcinoma: agonist or inverse agonist?," *Cell Death & Disease*, vol. 10, no. 6, p. 416, 2019.

[31] G. Pascual, A. L. Fong, S. Ogawa et al., "A SUMOylation-dependent pathway mediates transrepression of inflammatory response genes by PPAR-gamma," *Nature*, vol. 437, no. 7059, pp. 759–763, 2005.

[32] A. K. Reka, H. Kurapati, V. R. Narala et al., "Peroxisome proliferator-activated receptor-gamma activation inhibits tumor metastasis by antagonizing Smad3-mediated epithelial-mesenchymal transition," *Molecular Cancer Therapeutics*, vol. 9, no. 12, pp. 3221–3232, 2010.

[33] J. J. Lee, A. Drakaki, D. Iliopoulos, and K. Struhl, "MiR-27b targets PPARγ to inhibit growth, tumor progression and the inflammatory response in neuroblastoma cells," *Oncogene*, vol. 31, no. 33, pp. 3818–3825, 2012.

[34] M. R. Milone, B. Pucci, T. Colangelo et al., "Proteomic characterization of peroxisome proliferator-activated receptor-γ (PPARγ) overexpressing or silenced colorectal cancer cells unveils a novel protein network associated with an aggressive phenotype," *Molecular Oncology*, vol. 10, no. 8, pp. 1344–1362, 2016.

[35] A. Aimudula, H. Nasier, Y. Yang et al., "PPARα mediates sunitinib resistance via NF-κB activation in clear cell renal cell carcinoma," *International Journal of Clinical and Experimental Pathology*, vol. 11, no. 5, pp. 2389–2400, 2018.

[36] Y. Wu, T. Song, M. Liu et al., "PPARG negatively modulates Six2 in tumor formation of clear cell renal cell carcinoma," *DNA and Cell Biology*, vol. 38, no. 7, pp. 700–707, 2019.

[37] D. J. Sanchez, D. J. Steger, N. Skuli, A. Bansal, and M. C. Simon, "PPARγ is dispensable for clear cell renal cell carcinoma progression," *Molecular Metabolism*, vol. 14, pp. 139–149, 2018.

[38] B. Liang, J. Zhao, and X. Wang, "A three-microRNA signature as a diagnostic and prognostic marker in clear cell renal cancer: an in silico analysis," *PLoS One*, vol. 12, no. 6, 2017.

[39] T. Chen, W. Zheng, J. Chen et al., "Systematic analysis of survival-associated alternative splicing signatures in clear cell renal cell carcinoma," *Journal of Cellular Biochemistry*, vol. 121, no. 10, pp. 4074–4084, 2020.

[40] L. Xu, J. He, Q. Cai, M. Li, X. Pu, and Y. Guo, "An effective seven-CpG-based signature to predict survival in renal clear cell carcinoma by integrating DNA methylation and gene expression," *Life Sciences*, vol. 243, p. 117289, 2020.

[41] H. Liu, T. Ye, X. Yang et al., "A panel of four-lncRNA signature as a potential biomarker for predicting survival in clear cell renal cell carcinoma," *Journal of Cancer*, vol. 11, no. 14, pp. 4274–4283, 2020.

[42] N. Bhutiani, M. E. Egger, N. Ajkay, C. R. Scoggins, R. C. G. Martin II, and K. M. McMasters, "Multigene Signature Panels and Breast Cancer Therapy: Patterns of Use and Impact on Clinical Decision Making," *Journal of the American College of Surgeons*, vol. 226, no. 4, pp. 406–412.e1, 2018.

[43] S. Kopetz, J. Tabernero, R. Rosenberg et al., "Genomic classifier ColoPrint predicts recurrence in stage II colorectal cancer patients more accurately than clinical factors," *The Oncologist*, vol. 20, no. 2, pp. 127–133, 2015.

[44] S. Y. Wang, W. Dang, I. Richman, S. S. Mougalian, S. B. Evans, and C. P. Gross, "Cost-effectiveness analyses of the 21-gene assay in breast cancer: systematic review and critical appraisal," *Journal of Clinical Oncology*, vol. 36, no. 16, pp. 1619–1627, 2018.

[45] P. A. Gagliardi, L. di Blasio, and L. Primo, "PDK1: a signaling hub for cell migration and tumor invasion," *Biochimica et Biophysica Acta*, vol. 1856, no. 2, pp. 178–188, 2015.

[46] X. W. Ye, H. Yu, Y. K. Jin et al., "miR-138 inhibits proliferation by targeting 3-phosphoinositide-dependent protein kinase-1 in non-small cell lung cancer cells," *The Clinical Respiratory Journal*, vol. 9, no. 1, pp. 27–33, 2015.

[47] R. I. Feldman, J. M. Wu, M. A. Polokoff et al., "Novel small molecule inhibitors of 3-phosphoinositide-dependent kinase-1," *The Journal of Biological Chemistry*, vol. 280, no. 20, pp. 19867–19874, 2005.

[48] X. H. Li, Q. M. Gong, Y. Ling et al., "Inherent lipid metabolic dysfunction in glycogen storage disease IIIa," *Biochemical and Biophysical Research Communications*, vol. 455, no. 1-2, pp. 90–97, 2014.

[49] A. Gugliucci, "Fructose surges damage hepatic adenosylmonophosphate-dependent kinase and lead to increased lipogenesis and hepatic insulin resistance," *Medical Hypotheses*, vol. 93, pp. 87–92, 2016.

[50] M. H. Liang and J. G. Jiang, "Advancing oleaginous microorganisms to produce lipid via metabolic engineering

technology," *Progress in Lipid Research*, vol. 52, no. 4, pp. 395–408, 2013.

[51] Y. C. Lin, L. T. Lu, H. Y. Chen et al., "SCP phosphatases suppress renal cell carcinoma by stabilizing PML and inhibiting mTOR/HIF signaling," *Cancer Research*, vol. 74, no. 23, pp. 6935–6946, 2014.

[52] Y. Feng, S. Li, R. Zhang et al., "FOXM1 as a prognostic biomarker promotes endometrial cancer progression via transactivation of SLC27A2 expression," *International Journal of Clinical and Experimental Pathology*, vol. 11, no. 8, pp. 3846–3857, 2018.

[53] F. D. Chen, H. H. Chen, S. C. Ke, L. R. Zheng, and X. Y. Zheng, "SLC27A2 regulates miR-411 to affect chemo-resistance in ovarian cancer," *Neoplasma*, vol. 65, no. 6, pp. 915–924, 2018.

[54] G. Hoefler, M. Forstner, M. C. McGuinness et al., "cDNA cloning of the human peroxisomal enoyl-CoA hydratase: 3-hydroxyacyl-CoA dehydrogenase bifunctional enzyme and localization to chromosome 3q26.3-3q28: a free left Alu arm is inserted in the 3′ noncoding region," *Genomics*, vol. 19, no. 1, pp. 60–67, 1994.

[55] K. Suto, H. Kajihara-Kano, Y. Yokoyama et al., "Decreased expression of the peroxisomal bifunctional enzyme and carbonyl reductase in human hepatocellular carcinomas," *Journal of Cancer Research and Clinical Oncology*, vol. 125, no. 2, pp. 83–88, 1999.

[56] S. Cablé, J. M. Keller, S. Colin et al., "Peroxisomes in human colon carcinomas," *Virchows Archiv. B, Cell Pathology Including Molecular Pathology*, vol. 62, no. 1, pp. 221–226, 1992.

[57] M. Lin, D. Lv, Y. Zheng et al., "Downregulation of CPT2 promotes tumorigenesis and chemoresistance to cisplatin in hepatocellular carcinoma," *Oncotargets and Therapy*, vol. Volume 11, pp. 3101–3110, 2018.

[58] N. Fujiwara, H. Nakagawa, K. Enooku et al., "CPT2 downregulation adapts HCC to lipid-rich environment and promotes carcinogenesis via acylcarnitine accumulation in obesity," *Gut*, vol. 67, no. 8, pp. 1493–1504, 2018.

[59] Y. Z. Chen, J. Y. Xue, C. M. Chen et al., "PPAR signaling pathway may be an important predictor of breast cancer response to neoadjuvant chemotherapy," *Cancer Chemotherapy and Pharmacology*, vol. 70, no. 5, pp. 637–644, 2012.

[60] D. I. Sinner, G. J. Kim, G. C. Henderson, and R. A. Igal, "StearoylCoA desaturase-5: a novel regulator of neuronal cell proliferation and differentiation," *PLoS One*, vol. 7, no. 6, 2012.

[61] C. Gong, Y. Hu, M. Zhou et al., "Identification of specific modules and hub genes associated with the progression of gastric cancer," *Carcinogenesis*, vol. 40, no. 10, pp. 1269–1277, 2019.

[62] S. Vuletic, W. Dong, G. Wolfbauer, C. Tang, and J. J. Albers, "PLTP regulates STAT3 and NFκB in differentiated THP1 cells and human monocyte-derived macrophages," *Biochimica et Biophysica Acta*, vol. 1813, no. 10, pp. 1917–1924, 2011.

[63] R. Audo, V. Deckert, C. I. Daien et al., "PhosphoLipid transfer protein (PLTP) exerts a direct pro-inflammatory effect on rheumatoid arthritis (RA) fibroblasts-like-synoviocytes (FLS) independently of its lipid transfer activity," *PLoS One*, vol. 13, no. 3, p. e0193815, 2018.

[64] G. Wu, Z. Zhang, Q. Tang et al., "Study of FABP's interactome and detecting new molecular targets in clear cell renal cell carcinoma," *Journal of Cellular Physiology*, vol. 235, no. 4, pp. 3776–3789, 2019.

[65] Q. Lv, G. Wang, Y. Zhang et al., "FABP5 regulates the proliferation of clear cell renal cell carcinoma cells via the PI3K/AKT signaling pathway," *International Journal of Oncology*, vol. 54, no. 4, pp. 1221–1232, 2019.

[66] G. Wu, Y. Xu, Q. Wang et al., "FABP5 is correlated with poor prognosis and promotes tumour cell growth and metastasis in clear cell renal cell carcinoma," *European Journal of Pharmacology*, vol. 862, p. 172637, 2019.

[67] V. Vantaku, J. Dong, C. R. Ambati et al., "Multi-omics integration analysis robustly predicts high-grade patient survival and identifies CPT1B effect on fatty acid metabolism in bladder cancer," *Clinical Cancer Research*, vol. 25, no. 12, pp. 3689–3701, 2019.

[68] C. Zhou, M. Wang, L. Zhou et al., "Prognostic significance of PLIN1 expression in human breast cancer," *Oncotarget*, vol. 7, no. 34, pp. 54488–54502, 2016.

[69] G. Sultan, S. Zubair, I. A. Tayubi, H. U. Dahms, and I. H. Madar, "Towards the early detection of ductal carcinoma (a common type of breast cancer) using biomarkers linked to the PPAR(γ) signaling pathway," *Bioinformation*, vol. 15, no. 11, pp. 799–805, 2019.

[70] I. Sirois, A. Aguilar-Mahecha, J. Lafleur et al., "A unique morphological phenotype in chemoresistant triple-negative breast cancer reveals metabolic reprogramming and PLIN4 expression as a molecular vulnerability," *Molecular Cancer Research*, vol. 17, no. 12, pp. 2492–2507, 2019.

Hindawi
PPAR Research
Volume 2020, Article ID 3817573, 20 pages
https://doi.org/10.1155/2020/3817573

Research Article

Diet Modifies Pioglitazone's Influence on Hepatic PPARγ-Regulated Mitochondrial Gene Expression

Sakil Kulkarni,[1] Jiansheng Huang,[1] Eric Tycksen,[2] Paul F. Cliften,[2] and David A. Rudnick[1,3]

[1]*Department of Pediatrics, Washington University School of Medicine, St. Louis, MO 63110, USA*
[2]*Department of Genetics, Washington University School of Medicine, St. Louis, MO 63110, USA*
[3]*Department of Developmental Biology, Washington University School of Medicine, St. Louis, MO 63110, USA*

Correspondence should be addressed to David A. Rudnick; rudnick_d@wustl.edu

Received 22 May 2020; Revised 28 July 2020; Accepted 20 August 2020; Published 10 September 2020

Academic Editor: Fuquan Zhang

Pioglitazone (Pio) is a thiazolidinedione (TZD) insulin-sensitizing drug whose effects result predominantly from its modulation of the transcriptional activity of peroxisome proliferator-activated-receptor-gamma (PPARγ). Pio is used to treat human insulin-resistant diabetes and also frequently considered for treatment of nonalcoholic steatohepatitis (NASH). In both settings, Pio's beneficial effects are believed to result primarily from its actions on adipose PPARγ activity, which improves insulin sensitivity and reduces the delivery of fatty acids to the liver. Nevertheless, a recent clinical trial showed variable efficacy of Pio in human NASH. Hepatocytes also express PPARγ, and such expression increases with insulin resistance and in nonalcoholic fatty liver disease (NAFLD). Furthermore, mice that overexpress hepatocellular PPARγ and Pio-treated mice with extrahepatic PPARγ gene disruption develop features of NAFLD. Thus, Pio's direct impact on hepatocellular gene expression might also be a determinant of this drug's ultimate influence on insulin resistance and NAFLD. Previous studies have characterized Pio's PPARγ-dependent effects on hepatic expression of specific adipogenic, lipogenic, and other metabolic genes. However, such transcriptional regulation has not been comprehensively assessed. The studies reported here address that consideration by genome-wide comparisons of Pio's hepatic transcriptional effects in wildtype (WT) and liver-specific PPARγ-knockout (KO) mice given either control or high-fat (HFD) diets. The results identify a large set of hepatic genes for which Pio's liver PPARγ-dependent transcriptional effects are concordant with its effects on RXR-DNA binding in WT mice. These data also show that HFD modifies Pio's influence on a subset of such transcriptional regulation. Finally, our findings reveal a broader influence of Pio on PPARγ-dependent hepatic expression of nuclear genes encoding mitochondrial proteins than previously recognized. Taken together, these studies provide new insights about the tissue-specific mechanisms by which Pio affects hepatic gene expression and the broad scope of this drug's influence on such regulation.

1. Introduction

Pioglitazone (Pio) is a thiazolidinedione (TZD) agonist of the nuclear hormone receptor (NHR) peroxisome proliferator-activated receptor gamma (PPARγ). Pio-bound PPARγ forms a heterodimer with retinoid X receptor (RXR [1]), and the PPARγ-RXR complex interacts with specific peroxisome proliferator response elements (PPREs) in DNA to regulate metabolic and other gene expressions in adipose and other tissues [2]. Pio has beneficial effects on insulin sensitivity and nonalcoholic fatty liver disease (NAFLD) in experimental animal models [3–7], and this drug is approved for treatment of insulin-resistant diabetes in humans [8]. Pio's efficacy in human nonalcoholic steatohepatitis (NASH), which is strongly associated with insulin resistance, was recently investigated in the "**Pi**oglitazone versus **V**itamin **E** versus Placebo for the Treatment of Non-Diabetic Patients with **N**onalcoholic **S**teatohepatitis" (i.e. **PIVENS**) clinical trial [9]. The results showed favorable Pio-induced changes in NASH activity in some study subjects. However, most

Pio-treated PIVENS subjects did not exhibit benefit from that treatment. These observations implicate still-unknown genetic and/or environmental factors as modifiers of Pio's physiological effects in mice and humans. Other research has revealed tissue-specific effects of PPARγ, the canonical target of Pio, on NAFLD in experimental models. For example, hepatocellular PPARγ overexpression induces hepatic steatosis [10], while liver-specific PPARγ disruption prevents hepatic fat accumulation in mouse NAFLD models [11–13]. Conversely, muscle- [14] or adipocyte-specific PPARγ deletion promotes hepatic steatosis [15], which is consistent with the idea that PPARγ activity in adipose, and perhaps muscle, mediates much of Pio's efficacy towards NAFLD [16]. Other studies show that hepatic PPARγ expression, though lower than that of hepatic PPARα expression, is nevertheless significantly induced in experimental and human NAFLD [17–19]. Taken together, these considerations raise the interesting possibility that Pio's variable influence on human NAFLD in the PIVENS trial [9] could have resulted at least in part from the effects of genetic or environmental modifiers on hepatic PPARγ expression and/or transcriptional activity.

PPARγ-independent effects of Pio have also been implicated as candidate mediators of Pio's beneficial effects on hepatic steatosis in experimental models. For example, direct effects of this drug on the mitochondrial pyruvate carrier protein (MPC) were recently identified as a possible contributor to Pio's beneficial effects in NAFLD [20, 21]. Indeed, that consideration has stimulated new interest in developing PPARγ-sparing TZDs as novel pharmacological approaches to human NAFLD that avoid TZD-associated side effects. Other studies have identified beneficial effects of both Pio and PPARγ on mitochondrial function in experimental models of NAFLD [22] and other diseases [23]. Although Pio's PPARγ-dependent effects on hepatic expression of specific adipogenic and other genes have been investigated [10, 12, 13, 24], comprehensive assessments of such regulation in general and of hepatic mitochondrial gene expression in particular have not been reported. Moreover, whether genetic or environmental modifiers influence such control remains unknown. The studies reported here address these considerations by testing the hypothesis that diet alters Pio-induced, liver-PPARγ-dependent regulation of hepatic gene expression and comprehensively characterizing such regulation in mice. Our results provide new insights into the tissue-specific mechanisms by which Pio and hepatocellular PPARγ interact to influence hepatic gene expression and have implications for the variable efficacy Pio had in the PIVENS trial.

2. Experimental Methods

2.1. Mouse Husbandry. Liver-specific PPARγ knockout (KO) mice were generated by breeding PPARγ-loxP mice (The Jackson Laboratory, Bar Harbor, ME) to transgenic Alb-Cre (B6.Cg-Tg (Alb-Cre) 21Mgn/J, The Jackson Laboratory) mice as previously described [25]. Two-month-old male KO or control (i.e., wildtype (WT) C57BL6/J; The Jackson Laboratory) mice were given ad lib access to sterile, irradiated low-fat (S4031, BioServ, Flemington, NJ) or high-fat (S3282, BioServ; 60% kcal from fat) diets, with or without 0.01% (w/w) pioglitazone hydrochloride (Pio, Sigma-Aldrich, St. Louis, MO) for 3 months ($n = 4 - 5$ mice/experimental group). Body weight was measured weekly and body composition analyzed at the experimental endpoint by ECHO MRI spectroscopy [26]; after which, mice were euthanized for tissue harvest and analysis. Blood glucose, serum insulin and free fatty acid levels, and liver histology and triglyceride content were determined as previously described [25–27]. All experiments were approved by the Washington University Institutional Animal Care and Use Committee (IACUC), and all animals received humane care in accordance with institutional guidelines and criteria in the "Guide for the Care and Use of Laboratory Animals" (8th edition, 2011, https://grants.nih.gov/grants/olaw/guide-for-the-care-and-use-of-laboratory-animals.pdf).

2.2. Hepatic Transcriptomic Analyses (RNA-Seq and RT-qPCR). Total liver RNA was purified using the Trizol method (Invitrogen, Carlsbad, CA). Libraries were prepared by poly-A selection of 10 μg of liver RNA using Invitrogen mRNA Direct™ kits. mRNA was fragmented for cDNA synthesis, which was done using Invitrogen Superscript III and random hexamers. The cDNAs were end repaired, A-tailed, and ligated to standard Illumina adapters. Libraries were amplified with primers to incorporate a unique index into each sample. RNA-seq reads were aligned to the Ensembl release 76 GRCm38 assembly with STAR version 2.0.4b. Gene counts were derived from the number of uniquely aligned unambiguous reads by Subread:featureCount version 1.4.5.

All gene-level counts were then imported into R version 3.4.1, and TMM normalization size factors were calculated to adjust samples for differences in library size with the Bioconductor package EdgeR version 3.20.2. Genes expressed less than 1 count per million in less than 5 samples, and ribosomal genes were excluded from further analysis. The TMM size factors and the matrix of counts were then imported into the R/Bioconductor package Limma version 3.34.4 [28, 29], and weighted likelihoods based on the observed mean-variance relationship of every gene were then calculated for all samples with the voomWithQualityWeights function. Performance of the samples was then assessed with Spearman correlation matrix multidimensional scaling plots and principal component analysis. Gene performance was assessed with plots of residual standard deviation of every gene to their average log-count with a robustly fitted trend line of the residuals. Generalized linear models with robust dispersion estimates were then created to test for gene/transcript level differential expression. Differentially expressed genes and transcripts were then filtered for FDR adjusted p values of $q \leq 0.05$ [30, 31]. To enhance the biological interpretation of the large set of transcripts, the filtered gene lists were interrogated for overrepresentation of Hallmark gene sets using the hypergeometric tests available through the Broad Institute's Molecular Signature Database (http://software.broadinstitute.org/gsea/msigdb/annotate.jsp [32, 33],). Perturbations in expression across these gene sets versus the background gene signals were assessed with the R package Gage version 2.28.0.

Hepatic expression patterns of some of the genes identified as differentially expressed by RNA-Seq were confirmed using real-time semiquantitative RT-PCR (RT-qPCR) analyses as described previously [27] together with the oligonucleotide primers listed in Supplementary Table S1.

2.3. RXR Chromatin Immunoprecipitation (ChIP) with High Throughput DNA Sequencing (Seq). RXR ChIP-Seq was conducted using an approach analogous to the one previously employed for acetyl-histone ChIP-Seq [27, 34]. Briefly, frozen liver was minced, crosslinked in 1% formaldehyde, homogenized, and suspended in nuclear lysis buffer in the presence of protease inhibitors, then centrifuged to recover chromatin, which was sheared in a Bioruptor Sonicator (Diagenode, Denville, NJ) to generate uniform 100-500 base pair (bp) fragments. Equal quantities of chromatin (based on protein content) were immunoprecipitated using a ChIP-grade anti-RXR$\alpha/\beta/\gamma$ antibody (sc-774; Santa Cruz Biotechnology, Inc., Beverly, MA) previously validated and used in RXR ChIP-Seq studies of liver tissue [35, 36]. The studies reported here adhered to the guidelines and practices recommended for analyses and quality control of ChIP-Seq data by the Encyclopedia of DNA elements (i.e., ENCODE and modENCODE) consortia guidelines [37]. These include recommendations to validate the specificity of the ChIP target transcription factor antibody by immunoblot (Supplementary Figure S1) and to assess each replicate of immunoprecipitated chromatin for quality metrics including NSC, RSC, Qtag score, and Irreproducible Discovery Rate (IDR) data. As described in Supplementary Materials, assessment of those metrics here met ENCODE guidelines' criteria (as described in detail in the Supporting Information). Of note, the replicate livers studied here came from separate animals as opposed to the independent cell cultures, embryo pools, or tissue sampling that account for most substrates of the ENCODE experiments. Based on that, we anticipated the possibility of increased variability when considering experimental design, which prompted us to use liver samples from each of 5 mouse replicates per group, retain all replicates for these analyses, and apply the additional stringencies to data analysis described below.

Immunoprecipitated DNAs and corresponding input samples were submitted to the WU GTAC for blunt ending, adaptor ligation, size selection, and amplification according to established protocols and as previously described [27, 34]. Libraries were sequenced using the Illumina HiSeq-3000 as single 50 bp reads. Raw data were demultiplexed and aligned to the most recent mouse reference genome assembly (i.e., mm10) using Novoalign (Novocraft; Selangor, Malaysia). Sequence peaks were identified by comparing data from the anti-RXR antibody immunoprecipitated samples to corresponding inputs for each replicate using MACS2 [38]. Peaks were associated to genes using Peak Annotation and VISualization (PAVIS) software [39]. Significant differences in gene-associated peak sequence abundances between experimental groups were determined using DiffBind, an open source Bioconductor package that utilizes edgeR software for statistical analysis of replicated sequence count data [30, 31]. These analyses used a Benjamini and Hochberg false discovery rate (FDR) threshold of $q < 0.05$ [40, 41]. We also applied the following additional stringencies: (i) ≥2-fold change in RXR liver-DNA binding between experimental groups as defined by DiffBind and (ii) identification of the gene-associated RXR-bound peak by MACS in at least 3 (out of the 4-5) replicates in each experimental group with increased binding. Gene set overrepresentation analysis was conducted on genes differentially bound by RXR using the approach described for RNA-Seq data analyses.

Efforts to conduct PPARγ ChIP-Seq analyses on these liver samples were also attempted here, but those efforts were unsuccessful based on inability to identify a PPARγ antibody meeting the ENCODE guidelines when tested on mouse liver (as summarized above and described in detail in the Supporting Information; S. Kulkarni, J. Huang, and D.A. Rudnick, unpublished observations). Therefore, in order to assess the liver PPARγ-dependence of RXR liver DNA binding in the samples studied here, RXR-ChIP-Seq studies were conducted on livers from WT and liver-specific PPARγ KO mice and the result compared.

2.4. Venn Diagram Analyses and Binding and Expression Target Analysis (BETA). Interactivenn [42]) was used to determine and illustrate overlaps between genes identified as differentially expressed or differentially RXR-bound between groups. RXR ChIP-Seq and RNA-Seq datasets were also compared using "Binding and Expression Target Analysis" (BETA) software [43]. BETA is a publicly available software package that integrates ChIP- and RNA-Seq data to infer the function of a cis-acting regulator (in this case RXR-DNA binding as defined by ChIP-Seq data) on gene-specific patterns of expression (as defined by RNA-Seq data). Here, RXR-ChIP-Seq-defined peaks identified as differentially RXR-bound between groups ($q < 0.05$) were entered into the BETA algorithm (as a bed file using the format: chromosome number, chromosome start locus, and chromosome end locus). Differential gene expression data, extracted from the RNA-Seq data analysis, was provided to the software (as a tab-delimited text file using the format: gene ID, expression change, and FDR). The BETA algorithm assigned a rank and rank-product to each gene, with higher ranks and lower rank-products corresponding to genes whose change in expression is more likely to be regulated by the transcription factor-DNA binding event. Inferences about the effects of Pio, hepatic PPARγ expression, and HFD exposure on RXR-dependent liver gene expression were made based on comparisons between experimental groups.

2.5. Statistical Analysis. ChIP- and RNA-Seq datasets were analyzed as described above. All other data were analyzed using SigmaPlot 13.0 (Systat Software Inc., San Jose, CA). Numerical data comparisons between groups were made using unpaired two-tailed Student's t-test for pair-wise comparisons and ANOVA for multiple groups. Secondary post hoc comparisons were conducted using Holm-Sidak for normally distributed data or Tukey for data that was not normally distributed. Chi-squared analysis was used to compare rates and proportions between groups. Significance (alpha) was set at 0.05. Data are reported as mean ± standard error.

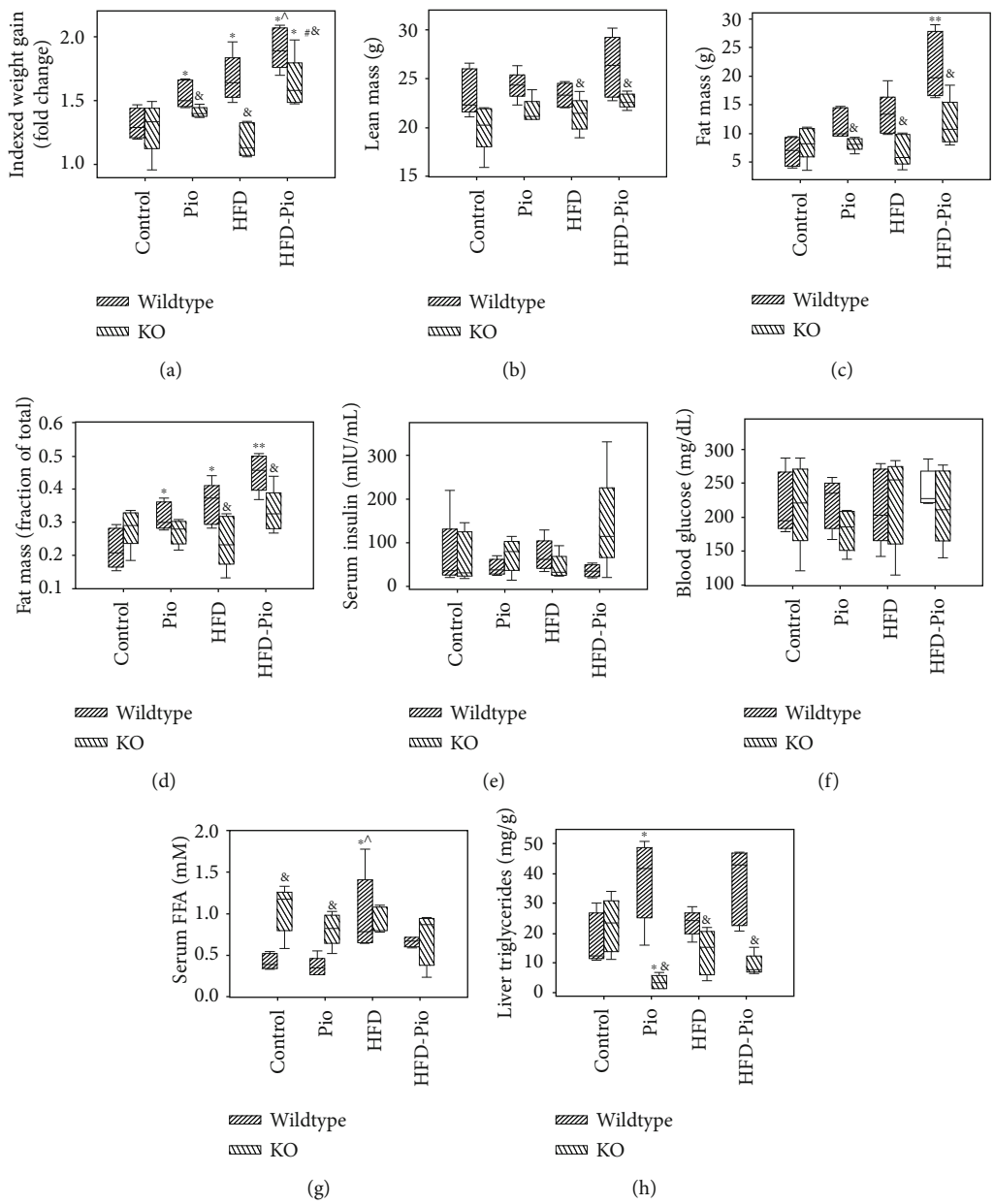

Figure 1: Effects of Pio on WT and PPARγ KO mice. (a) Weight (indexed to initial weight), (b) lean mass (g), (c) fat mass (g), (d) fat mass (expressed as fraction of total mass), (e) serum insulin (mIU/mL, nonfasting a.m.), (f) blood glucose (mg/dL, nonfasting a.m.), (g) serum free fatty acids (FFA) (mM, nonfasting a.m.), and (h) liver triglycerides (mg/g liver) in wildtype (WT) and liver-specific PPARγ knockout (KO) mice given a control or high-fat diet (HFD) unsupplemented or supplemented with Pioglitazone (Pio). $^{*}p < 0.05$ vs. corresponding control diet-treated group; $^{\wedge}p < 0.05$ vs. corresponding Pio-treated group; $^{**}p < 0.05$ vs. all other WT groups; $^{\#}p < 0.05$ vs. corresponding HFD-treated group; $^{\&}p < 0.05$ vs. corresponding WT group.

3. Results

3.1. Pio Has Distinct Effects on Mouse Metabolism in WT versus Liver-Specific PPARγ KO Mice Given Control versus HFD. Unsupplemented- or Pio-supplemented-control (i.e., "control" or "Pio") or high-fat (i.e., "HFD" or "HFD-Pio") diets were given to male WT and liver-specific PPARγ KO mice from age 2 to 5 months. Initial body weights were comparable between treatment groups (i.e., ±Pio, ±HFD) but significantly greater in 2-month-old WT versus age-matched KO mice (Supplementary Figure S2). By the experimental endpoint, 5-month-old WT mice exposed to Pio, HFD, or HFD-Pio showed significantly greater weight gain and body fat mass fractions compared to controls (Figures 1(a)–1(d)). In contrast, KO mice displayed only limited changes in weight and no change in percent body fat mass in response to either intervention. Consistent with those findings, lean mass, fat mass, and percent fat mass were also significantly higher in HFD and HFD-Pio-treated WT mice compared to the corresponding KOs. Nonfasting a.m. serum insulin and blood glucose levels were comparable across all experimental groups (Figures 1(e)–1(f)). HFD-exposed WT

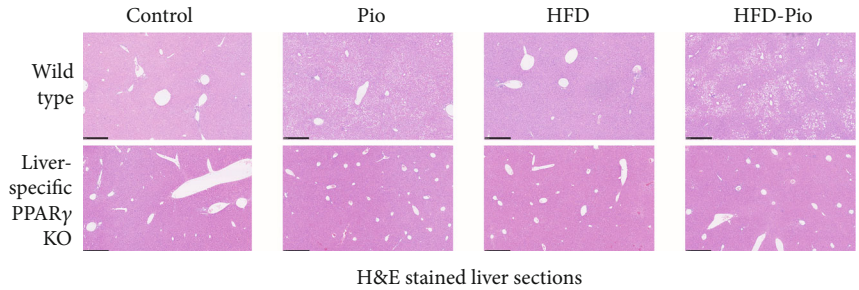

Figure 2: Effects of Pio on WT and KO mouse liver histology. H&E -stained liver sections from control diet (Control)-, Pio-, high-fat diet (HFD)-, or HFD and PIO (HFD-Pio)-treated mice. 500 micron bar shown in lower left corner.

mice displayed increased serum-free fatty acids (FFA's) compared to control and Pio-treated WT mice, while control and Pio-treated KO mice exhibited increased serum FFA's compared to the corresponding WT animals (Figure 1(g)). Finally, the effects of both Pio and diet on liver triglyceride content and hepatic steatosis varied depending on hepatocellular PPARγ expression: Pio increased liver fat content in WT mice on control diet but decreased these measures in the corresponding KO mice, and HFD-exposed KO mice displayed reduced liver triglycerides and less hepatic steatosis than the corresponding WT mice (Figures 1(h) and 2). Taken together, these data reveal distinct hepatic and systemic metabolic responses to Pio in the absence versus the presence of HFD and define the hepatocellular PPARγ dependence of those effects.

3.2. Diet Modifies Some of the Effects of Pio on Hepatic Gene Expression. Next, Pio's influence on genome-wide patterns of hepatic gene expression in WT mice on control or HFD was determined, with those results compared to corresponding analyses of the liver-specific PPARγ KO mice. First, to establish the validity of this approach, these transcriptomic data were first inspected for patterns of Pio-induced, PPARγ-dependent changes in hepatic expression of canonical adipogenic and lipogenic genes whose PPARγ-regulated hepatic expression has previously been reported [10, 12, 13, 24]. Consistent with such published data, the transcriptomic data reported here show Pio-induced hepatic expression of Caveolin 1 (*Cav1*), *Cd36*, Complement factor D (*Cfd*, also known as Adipsin), *Cidec* (also known as *Fsp27*), *Fabp4* (also known as *Ap2*), *Mogat1*, and *Plin4* (also known as *S3-12*) in WT but not KO mice on control diet (Figure 3(a)). Further analyses also showed that Pio induces *Cd36*, *Cfd*, *Cidec*, *Mogat1*, and *Plin4* but not *Cav1* or *Fabp4* in WT mice on the HFD. As for mice on the control diet, Pio also had no significant effects on expression of these genes in HFD-treated KO mice (Figure 3(b)). Finally, to further validate our transcriptomic data, the RNA-Seq based results depicted in Figure 3 were compared to RT-qPCR based analyses of differential expression between groups in these exemplar genes, with the results of the latter studies (Supplementary Figure S3) highly concordant with those of the former (Figure 3). These data are consistent with previously published analyses of PPARγ-dependent hepatic transcriptional effects, and they implicate diet as a specific modifier of those effects.

Next, these transcriptomic data were subjected to principle component analysis (PCA). The results showed excellent segregation of replicates of WT mice by exposure to drug (±Pio) and diet (±HFD) (Figure 4(a)). In contrast, the corresponding KO replicates showed poor separation (Figure 4(b)). Similarly, heat map analyses of Pio-induced changes in hepatic gene expression also showed more faithful segregation of the WT versus the KO experimental replicates (Figures 4(c) and 4(d)). Consistent with the exemplar gene expression data in Figure 3, Venn diagram analyses of patterns of overlap in these data identified subsets of genes whose Pio-induced hepatic expression is concordantly regulated in WT mice on control or HFD, and others whose Pio-induced regulation is altered by HFD (Figure 4(e)). This analysis also revealed a lack of concordance between the hepatic transcriptional effects of Pio in KO mice on control versus HFD and, furthermore, that Pio has no significant effects on hepatic gene expression in KO mice on HFD (Figure 4(f)). The results of the converse analyses, comparing the influence of diet on mice with or without Pio exposure, provide further support for the modifying influence of diet on Pio-induced changes in hepatic gene expression (Figures 4(g) and 4(h)). Taken together, these data reveal interactions between diet and hepatocellular PPARγ expression that influence Pio-induced changes in hepatic gene expression.

To further explore dietary influences on Pio-regulated changes in hepatic gene expression, those genes identified as differentially expressed in the studies summarized in Figure 4 were subject to gene set overrepresentation analysis using the Hallmark gene set database, on the Broad Institute platform (http://software.broadinstitute.org/gsea/msigdb/annotate.jsp [32, 33],), and the most stringent FDR threshold cutoff on that platform (i.e., $q < 1e^{-6}$). This evaluation identified significant enrichment of genes induced by Pio in livers from WT mice on the control diet for those associated with metabolic and other functional categories (Table 1(a)). The most highly enriched of those groupings, fatty acid metabolism, adipogenesis, and bile acid metabolism, were also identified as enriched for genes induced by Pio in WT mice on the HFD (Table 1(b)). However, this analysis also revealed distinct hepatic transcriptional effects of Pio in WT mice on

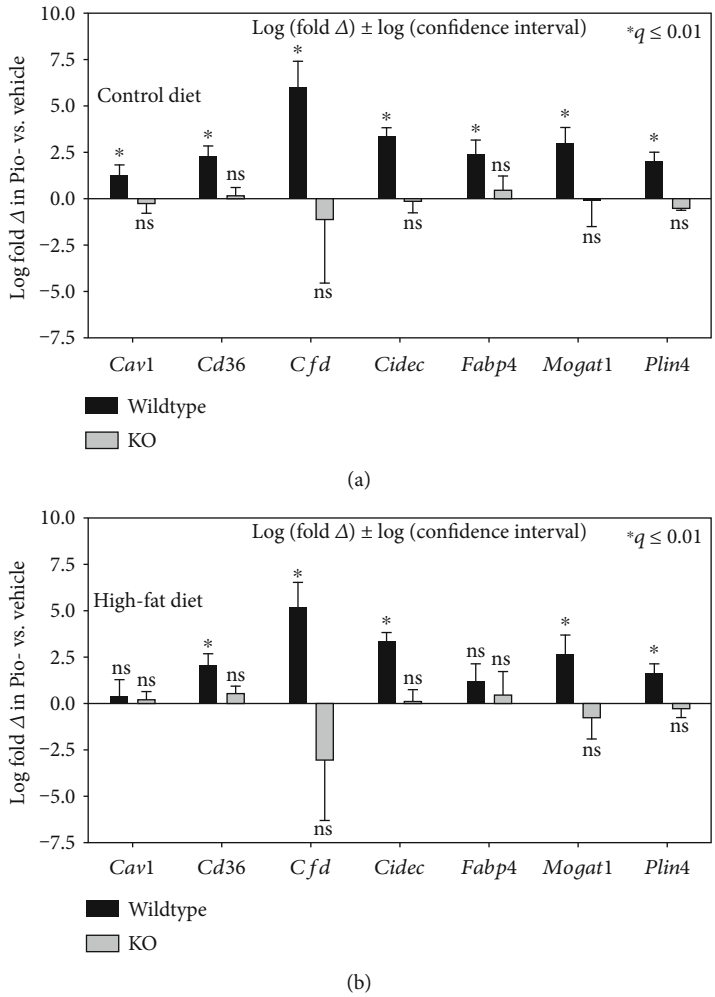

Figure 3: Effects of Pio on hepatic expression of exemplar genes. Summary of RNA-Seq data of exemplar genes whose expression is known to be regulated by PPARγ. $^*q \leq 0.01$; ns: no significant difference.

control versus HFD, including specific enrichment of genes associated with cholesterol homeostasis in livers from mice on the control but not the HFD diet, and of glycolysis in mice on HFD but not control diet (Table 1(a) and (b)). These transcriptomic data were also subjected to GAGE analysis for gene set level changes in expression, and the results of that independent assessment of these data are highly concordant with those of the gene set overrepresentation study (Supplementary Table S3). For example, the GAGE examination also identified enrichment of Pio-induced genes associated with fatty acid metabolism, adipogenesis, and bile acid metabolism in mice on either diet, but specific enrichment for cholesterol homeostasis genes in mice on the control diet and for glycolysis genes in mice on the HFD. Genes whose hepatic expression is suppressed by Pio in WT mice were similarly assessed and also showed marked differences between control and HFD-treated mice. For example, those suppressed by Pio in WT mice on control diets are enriched in many different categories, including UV response up and heme metabolism, while those suppressed by Pio in mice on HFD were not significantly enriched for any gene categories when analyzed in this way (Table 1C and D). As for Pio-induced genes, the results of GAGE-based investigation of these data are also quite concordant with gene set overrepresentation analyses (Supplementary Table S3). Similar hepatic transcriptomic investigations of liver-specific PPARγ KO mice, using gene set overrepresentation- and GAGE-based analyses, identified distinct dietary effects on patterns of Pio-induced and Pio-suppressed genes in these compared to WT mice (Table 2 vs. Table 1 and Supplementary Table S3). In this case, gene set overrepresentation analyses showed that Pio's suppressive effects on hepatic gene expression in KO mice on control diet and its inductive and suppressive effects in KO mice on HFD are virtually undetectable (Table 2B–D). Converse analyses, of the influence of diet in the absence or presence of Pio, showed a greater range of dietary influence in Pio-treated compared to untreated WT mice and markedly fewer effects of diet on the KO mice (Figures 4(g) and 4(h) and Supplementary Tables S4 and S5). Taken together, these data provide evidence for the modifying influence of diet on PPARγ-dependent, Pio-induced changes in hepatic gene expression.

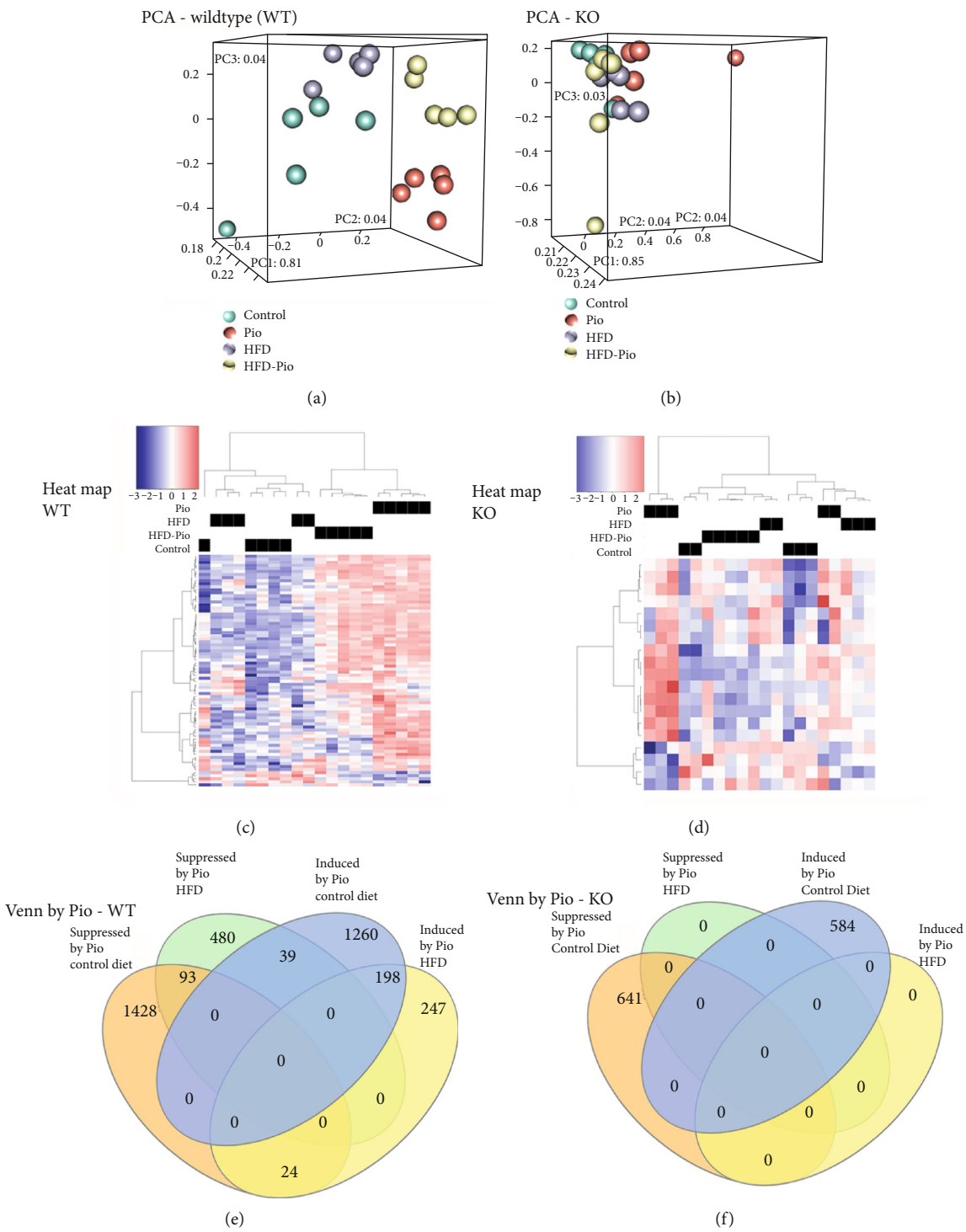

Figure 4: Continued.

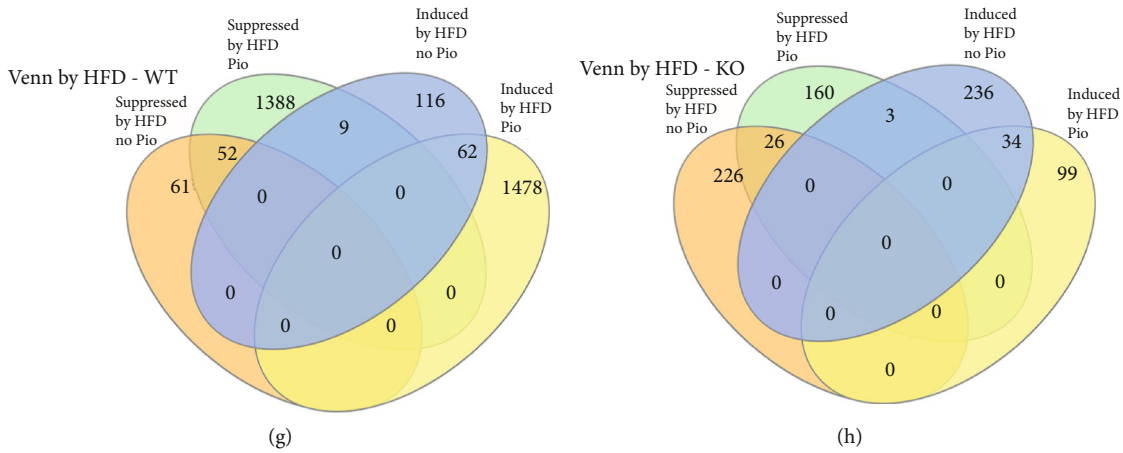

Figure 4: Effects of Pio on the hepatic transcriptome. (a, b) Principle component (PCA) and (c, d) heat map analyses of differentially expressed genes from RNA-Seq analyses of livers from (a, c) WT or (b, d) KO mice treated with control diet, Pio, HFD, or HFD and Pio. Heat map analyses are based on Pio-induced differences in gene expression. (e–h) Venn diagrams (generated using InteractiVenn [42]) depict overlap between differentially expressed genes by treatment group in WT (e, g) or KO (f, h) mice.

3.3. PPARγ-Dependent Effects of Pio and HFD on Liver RXR-DNA Binding Are Highly Concordant with Corresponding Effects on Hepatic Gene Expression. To further characterize Pio's direct effects on hepatic transcriptional regulation, the consequences of Pio and HFD on gene-specific RXR-binding to liver DNA in WT and KO mice were characterized and compared by RXR-chromatin-immunoprecipitation combined with next-generation DNA sequencing (ChIP-Seq). The results identified specific RXR-DNA binding sites in both untreated and Pio-treated WT mice on either a control or HFD. They also revealed Pio-induced differences in such binding at some of those sites. In most cases, Pio increased RXR-DNA binding, but sites whose RXR-DNA binding is suppressed by Pio were also identified (Figures 5(a)–5(c)). This analysis also showed that Pio has broader effects on gene-specific RXR-liver DNA binding in WT mice on the control versus the HFD, with most binding sites identified in HFD-treated mice also identified in mice on the control diet but many binding sites detected in mice on the control diet not detected in those on the HFD (Figure 5(d)). Thus, these data provide further evidence for the modifying influence of diet on Pio-induced hepatic transcriptional regulation, and they implicate diet-induced differences in Pio's direct effects on liver RXR-DNA binding as a contributing mechanism. More than half of the Pio-induced RXR-liver DNA binding sites detected in WT mice on either diet occurred within exons or introns of specific genes, with binding to $5'$ or $3'$ untranslated regions (UTRs), upstream, downstream, or other sites accounting for the rest of such binding (Figure 5(e)). While parallel analyses of the KO mice also identified RXR-liver DNA binding sites (Figure 5(f)), in this case, very few sites with significant (i.e., $q < 0.05$) Pio-induced changes in RXR binding were identified (Figure 5(g)). Furthermore, most of those sites showed Pio-inhibited binding (Figure 5(g)) and none withstood the additional stringencies of our analytical approach (Figure 5(h) and Experimental Methods). Further analyses of HFD effects on such regulation identified a small number of differentially bound genes in WT mice in the absence of Pio and none in WT mice in the presence of Pio or in KO mice with or without Pio (data not shown). Together, these data define Pio's PPARγ-dependent effects on induction of gene-specific RXR-liver DNA binding in mice on either diet. They also reveal that HFD exposure blunts the effects of Pio on such transcriptional regulation.

Next, gene set hypergeometric tests were performed on genes exhibiting Pio-induced RXR-liver DNA binding in WT mice fed either the control (Table 3A) or HFD (Table 3B). The results showed enrichment in many of the same categories identified by analyses of Pio-induced (Table 1A and B) or Pio-suppressed (Table 1C and D) hepatic gene expression. These observations imply that Pio-induced changes in RXR-liver DNA binding are transcription-inducing in some cases and transcription-suppressing in others. However, some categories enriched for genes whose expression is induced (i.e., in Table 1) were not similarly identified by these analyses of RXR-liver DNA binding (i.e., in Table 3A and B), including bile acid metabolism and cholesterol homeostasis. Presumably, this finding results from transcription-altering influences of Pio on hepatic gene expression (in Table 1A and B) that are independent of hepatocellular PPARγ expression, hepatic RXR activity, or both. For example, recently described direct effects of Pio on the mitochondrial pyruvate carrier protein activity [20, 21] might have indirect transcriptional consequences. Conversely, other categories identified as enriched for RXR-bound genes in Table 3A and B were not identified by the gene set analysis of RNA-Seq data in Table 1, including glycolysis and unfolded protein response, and the significance of RXR-binding to those gene sites with respect to transcriptional regulation is uncertain. Finally, these studies did not identify any categorical gene set enrichment amongst genes with Pio-mediated suppression of RXR-liver DNA

Table 1: Gene set analysis* on RNA-Seq data from WT Pio-treated vs. Pio-untreated mice on control or HFD (as designated).

Gene set name (# in Hallmark set)	Description	Overlap	q value
(a) Induced by Pio in WT mice on control diet			
FATTY_ACID_METABOLISM [158]	Genes encoding proteins involved in metabolism of fatty acids.	51	$4.84e^{-33}$
ADIPOGENESIS [200]	Genes upregulated during adipocyte differentiation (adipogenesis).	48	$6.52e^{-25}$
BILE_ACID_METABOLISM [112]	Genes involve in metabolism of bile acids and salts.	30	$3.36e^{-17}$
CHOLESTEROL_HOMEOSTASIS [74]	Genes involved in cholesterol homeostasis.	22	$7.81e^{-14}$
OXIDATIVE_PHOSPHORYLATION [200]	Genes encoding proteins involved in oxidative phosphorylation.	32	$9.78e^{-12}$
PEROXISOME [104]	Genes encoding components of peroxisome.	21	$7.38e^{-10}$
UV_RESPONSE_DN [144]	Genes down-regulated in response to ultraviolet (UV) radiation.	24	$1.98e^{-9}$
MYC_TARGETS_V1 [200]	A subgroup of genes regulated by MYC—version 1 (v1).	28	$3.84e^{-9}$
INTERFERON_GAMMA_RESPONSE [200]	Genes upregulated in response to IFNG (GeneID=3458).	26	$6.74e^{-8}$
(b) Induced by Pio in WT mice on HFD			
FATTY_ACID_METABOLISM [158]	Genes encoding proteins involved in metabolism of fatty acids.	32	$1.32e^{-28}$
OXIDATIVE_PHOSPHORYLATION [200]	Genes encoding proteins involved in oxidative phosphorylation.	33	$9.38e^{-27}$
ADIPOGENESIS [200]	Genes upregulated during adipocyte differentiation (adipogenesis).	32	$1.13e^{-25}$
PEROXISOME [104]	Genes encoding components of peroxisome.	20	$7.76e^{-18}$
BILE_ACID_METABOLISM [112]	Genes involve in metabolism of bile acids and salts.	14	$5.33e^{-10}$
GLYCOLYSIS [200]	Genes encoding proteins involved in glycolysis & gluconeogenesis.	14	$8.69e^{-7}$
(c) Suppressed by Pio in WT mice on control diet			
UV_RESPONSE_UP [158]	Genes upregulated in response to UV radiation.	35	$9.3e^{-16}$
HEME_METABOLISM [200]	Genes involved in metabolism of heme & erythroblast differentiation.	32	$1.43e^{-10}$
MTORC1_SIGNALING [200]	Genes upregulated through activation of mTORC1 complex.	28	$3.4e^{-8}$
P53_PATHWAY [200]	Genes involved in p53 pathways and networks.	28	$3.4e^{-8}$
APOPTOSIS [161]	Genes mediating apoptosis by activation of caspases.	24	$8.69e^{-8}$
HYPOXIA [200]	Genes upregulated in response to low oxygen levels.	27	$8.69e^{-8}$
DNA_REPAIR [150]	Genes involved in DNA repair.	23	$8.69e^{-8}$
XENOBIOTIC_METABOLISM [200]	Genes encoding proteins that process drugs & other xenobiotics.	26	$2.71e^{-7}$
UNFOLDED_PROTEIN_RESPONSE [113]	Genes upregulated during unfolded protein response.	19	$2.71e^{-7}$
MYC_TARGETS_V1 [200]	A subgroup of genes regulated by MYC - version 1 (v1).	25	$9.04e^{-7}$
(d) Suppressed by Pio in WT mice on HFD			
No overlaps found			

*Using the Broad Institute platform with the Hallmark gene sets platform to identify the top 10 categories with $p \leq 1e^{-6}$ (see text for details).

binding (Table 3C and D), nor did they demonstrate any Pio- or HFD-induced differences in such binding in the KO mice (Table 3E–H). When taken together, these data reveal a high overall degree of concordance between PPARγ-dependent and Pio-induced effects on RXR-liver DNA binding to and differential hepatic expression of specific genes, and they further implicate diet as a modifier of that regulation.

Table 2: Gene set analysis* on RNA-Seq data from Pio-treated vs. Pio-untreated KO mice on control or HFD (as designated).

Gene set name (# in Hallmark set)	Description	Overlap	q value
(a) Induced by Pio in KO mice on control diet			
CHOLESTEROL_HOMEOSTASIS [74]	Genes involved in cholesterol homeostasis.	20	$1.04e^{-18}$
ESTROGEN_RESPONSE_LATE [200]	Genes defining late response to estrogen.	22	$3.64e^{-12}$
TNFA_SIGNALING_VIA_NFKB [200]	Genes regulated by NF-κB in response to TNF (GeneID=7124).	21	$2.17e^{-11}$
MTORC1_SIGNALING [200]	Genes upregulated through activation of mTORC1 complex.	20	$1.38e^{-10}$
APOPTOSIS [161]	Genes mediating apoptosis by activation of caspases.	18	$1.83e^{-10}$
ESTROGEN_RESPONSE_EARLY [200]	Genes defining early response to estrogen.	19	$7.36e^{-10}$
NOTCH_SIGNALING [32]	Genes upregulated by activation of notch signaling.	8	$8.45e^{-8}$
HYPOXIA [200]	Genes upregulated in response to low oxygen levels (hypoxia).	16	$1.98e^{-7}$
UV_RESPONSE_UP [158]	Genes upregulated in response to ultraviolet (UV) radiation.	14	$3.57e^{-7}$
ADIPOGENESIS [200]	Genes upregulated during adipocyte differentiation (adipogenesis).	15	$9.91e^{-7}$
(b) Induced by Pio in KO mice on HFD			
No significantly differentially expressed genes			
(c) Suppressed by Pio in KO mice on control diet			
XENOBIOTIC_METABOLISM [200]	Genes encoding proteins that process drugs and xenobiotics.	24	$2.13e^{-13}$
(d) Suppressed by Pio in KO mice on HFD			
No significantly differentially expressed genes			

*Using the Broad Institute platform with the Hallmark gene set platform to identify the top 10 categories with $p \leq 1e^{-6}$ (see text for details).

3.4. Integrating Pio's Influences on Liver RXR-DNA Binding and Hepatic Transcription. Finally, to further characterize and clarify the impact of diet on Pio-induced, PPARγ-dependent hepatic transcriptional regulation, the RNA- and ChIP-Seq datasets generated in these studies were compared to each other using the "Binding and expression target analysis" (BETA [43],) algorithm. This analytical tool was developed to infer target gene regulation by specific transcription factors. The results here identified 760 genes bound by RXR and induced by Pio and 1066 RXR-bound genes suppressed by Pio in WT mice on control diet, and 420 induced and 531 suppressed RXR-bound gene targets of Pio in WT mice on HFD (Figure 6(a)). Most genes identified by this analysis as induced or suppressed by Pio in mice on the control diet were not similarly identified in mice on the HFD (Figure 6(a)). However, gene set over-representation analysis did demonstrate high concordance between the categorical terms identified as enriched for RXR-bound genes induced by Pio on control or HFD. Those categories include Oxidative phosphorylation, Fatty acid metabolism, and Myc targets (Table 4A and B). Further inspection of the specific Pio-regulated genes enriched in these sets revealed an abundance of nuclear genes encoding mitochondrial proteins involved in oxidative phosphorylation. Those genes include components of complexes I-IV, and the mitochondrial ATP synthase, as well as transporters, ion channels, enzymes involved in TCA cycle, and other outer membrane, intermembrane space, inner membrane, and matrix mitochondrial proteins (Figure 6(b)). Moreover, almost all of the specific mitochondrial protein-encoding genes identified in this way that were induced in mice on the control diet were not induced in mice on the HFD, and, conversely, most of those induced in HFD-treated mice were not similarly upregulated in mice on the control diet. Thus, this analysis also demonstrates that diet induces unique changes in Pio's specific transcriptional effects on nuclear genes encoding mitochondrial proteins. Gene set over-representation analysis on RXR-bound genes suppressed by Pio in WT mice was also conducted, with the results showing no overlap between functional categories enriched in suppressed genes from mice on control versus those on HFD. For example, genes associated with Unfolded protein response were enriched amongst those suppressed by Pio in WT mice on the control diet but not the HFD (Table 4C and D). These results provide further evidence for the modifying influence of diet on Pio's hepatic transcriptional effects. Finally, the differences in RXR liver DNA binding detected in the KO mice were insufficient to permit the corresponding BETA analysis on these data (Figure 5(g) and 5(h)).

4. Discussion

Previously published studies have reported PPARγ-dependent effects of TZDs on the hepatic expression of individual

Binding sites	
Group (WT)	# of RXR-DNA binding sites (mean ± SEM)
Control	5221 ± 2281
Pio	14576 ± 5602
HFD	1477 ± 231
HFD-Pio	12405 ± 4107

(a)

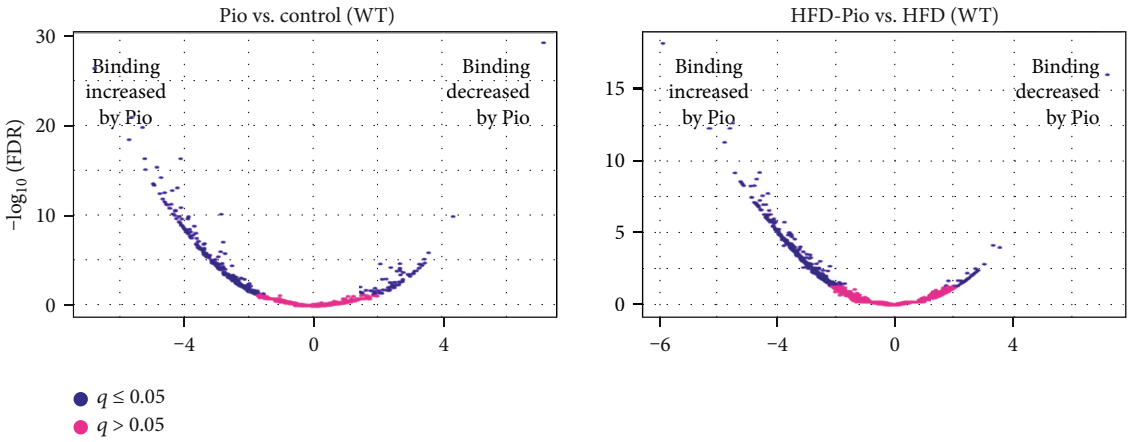

(b)

Differential binding	
Differential binding between groups: (WT)	Total (unique) sites
↑ in Pio vs. control	1377 (952)
↓ in Pio vs. control	37 (20)
↑ in HFD-Pio vs. HFD	748 (530)
↓ in HFD-Pio vs. HFD	54 (16)

(c)

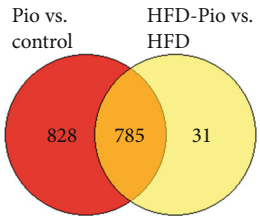

(d)

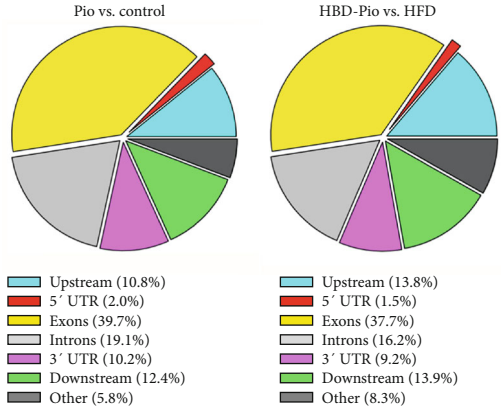

(e)

Binding sites	
Group (KO)	# of RXR-DNA binding sites (mean ± SEM)
Control	19481 ± 3380
Pio	25798 ± 1701
HFD	21464 ± 3537
HFD-Pio	23438 ± 965

(f)

Figure 5: Continued.

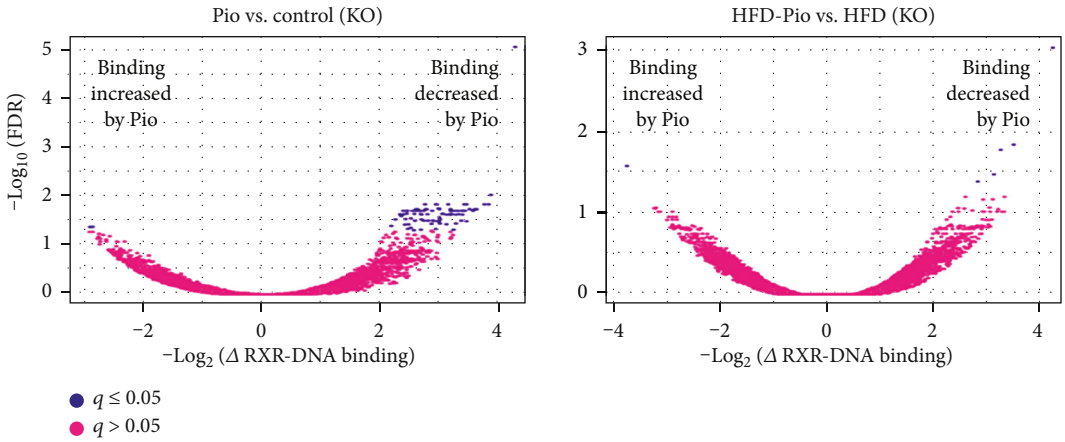

(g)

Differential binding	
Differential binding between groups: (KO)	Total (unique) sites
↑ in Pio vs. control	0
↓ in Pio vs. control	0
↑ in HFD-Pio vs. HFD	0
↓ in HFD-Pio vs. HFD	0

(h)

Figure 5: Effects of Pio on the hepatic RXR cistrome. (a) Total RXR-DNA binding sites (by group), (b) Volcano plots comparing differential RXR-DNA binding in replicate livers from Pio- versus Control- or HFD-Pio- versus HFD-treated groups of mice, and (c) Total (and unique) DNA sites with significantly different RXR-DNA binding (between groups), each defined as described in Experimental methods. (d) Venn diagram of overlap between sites of significant Pio-induced RXR-liver DNA binding in mice on control versus HFD. (e) Pie chart illustration of the locations of sites for genes summarized in (d) with respect to gene-specific transcription start sites in control versus HFD mice. (f–h) Results of corresponding RXR-liver DNA binding ChIP-Seq analyses of liver-specific PPARγ KO mice.

target genes of interest by comparing the hepatic expression of those specific genes in WT versus PPARγ-overexpressing or liver-specific PPARγ KO mice [10, 12, 13, 24]. Such studies, which were recently reviewed [44], show that hepatic PPARγ expression regulates the expression of adipogenic genes in the liver and also modulates extrahepatic lipid accumulation and insulin sensitivity. Nevertheless, the studies reported here are the first to comprehensively characterize such transcriptional regulation (by RNA-Seq), compare the results to genome-wide assessment of PPARγ-dependent, Pio-induced effects on liver RXR-DNA binding (with ChIP-Seq), and integrate those datasets (with BETA). The results show (i) Pio's liver-PPARγ-dependent hepatic transcriptional effects are highly concordant with its effects on liver RXR-DNA binding in WT mice on either diet. (ii) HFD modifies Pio's influence on such transcriptional regulation. (iii) Pio has a much broader influence on PPARγ-dependent hepatic expression of nuclear genes encoding mitochondrial proteins than has previously been reported. These data provide new insights into the molecular and cellular mechanisms by which Pio and hepatocellular PPARγ interact to influence hepatic gene expression. They also raise the possibility that diet is a modifier of Pio's efficacy in human NAFLD. Such efficacy was variable amongst subjects enrolled in the PIVENS trial [9]. Consistent with previously published work [10–13], our data also show that (i) hepatocellular PPARγ overexpression induces hepatic steatosis. (ii) Liver-specific PPARγ disruption protects mice from HFD-induced NAFLD. (iii) TZD administration (Pio here) stimulates hepatic fat accumulation in WT but not liver-specific PPARγ-KO mice. Other studies have also shown that extrahepatic tissue-specific (i.e. muscle- [14] or adipocyte- [15]) PPARγ deletion promotes NAFLD and that TZD-treatment exacerbates fatty liver disease in muscle-specific PPARγ KO mice [14]. Taken together, our data and these considerations are also consistent with the possibility that variable responses to Pio in human NAFLD might be determined, at least in part, by the balance between TZD effects on hepatic versus extrahepatic (i.e., adipose or perhaps skeletal muscle) PPARγ activity.

The studies here are the first to compare Pio-induced changes in the liver RXR cistrome and hepatic transcriptome with the hepatocellular PPARγ dependence of those changes. Nevertheless, similar analyses of other RXR-binding, metabolic-sensing nuclear hormone receptors (NHRs) have been reported. For example, the effects of the farnesoid X

Table 3: Gene set analysis* on RXR ChIP-Seq data from Pio-treated vs. Pio-untreated WT or KO mice on control or HFD (as designated).

Gene set name (# in Hallmark set)	Description	Overlap	q value
(a) Induced by Pio in WT mice on control diet			
OXIDATIVE_PHOSPHORYLATION [200]	Genes encoding proteins involved in oxidative phosphorylation.	48	$2.55e^{-35}$
MYC_TARGETS_V1 [200]	A subgroup of genes regulated by MYC - version 1 (v1).	40	$2.33e^{-26}$
ADIPOGENESIS [200]	Genes upregulated during adipocyte differentiation (adipogenesis).	31	$3.41e^{-17}$
ESTROGEN_RESPONSE_LATE [200]	Genes defining late response to estrogen.	24	$5.47e^{-11}$
FATTY_ACID_METABOLISM [158]	Genes encoding proteins involved in metabolism of fatty acids.	21	$1.34e^{-10}$
MTORC1_SIGNALING [200]	Genes upregulated through activation of mTORC1 complex.	23	$2.45e^{-10}$
GLYCOLYSIS [200]	Genes encoding proteins involved in glycolysis and gluconeogenesis.	21	$8.17e^{-9}$
UNFOLDED_PROTEIN_RESPONSE [113]	Genes upregulated during unfolded protein response.	16	$8.78e^{-9}$
ESTROGEN_RESPONSE_EARLY [200]	Genes defining early response to estrogen.	19	$2e^{-7}$
DNA_REPAIR [150]	Genes involved in DNA repair.	16	$4.31e^{-7}$
(b) Induced by Pio in WT mice on HFD			
OXIDATIVE_PHOSPHORYLATION [200]	Genes encoding proteins involved in oxidative phosphorylation.	31	$2.38e^{-24}$
MYC_TARGETS_V1 [200]	A subgroup of genes regulated by MYC—version 1 (v1).	25	$1.66e^{-17}$
ADIPOGENESIS [200]	Genes upregulated during adipocyte differentiation (adipogenesis).	20	$2.72e^{-12}$
ESTROGEN_RESPONSE_LATE [200]	Genes defining late response to estrogen.	15	$1.22e^{-7}$
(c, d) Suppressed by Pio in WT mice on control or HFD			
No overlaps found.			
(e, f, g, h) Induced or suppressed by Pio or HFD in KO mice in presence or absence of HFD or Pio			
No overlaps found.			

*Using the Broad Institute platform with the Hallmark gene set platform to identify the top 10 categories with $p \leq 1e^{-6}$ (see text for details).

receptor (FXR) agonist obeticholic acid on FXR-DNA binding and gene expression in human and mouse liver tissue were recently reported [45]. The availability of that published data permitted us to compare and contrast genes whose expression was significantly induced or suppressed by obeticholic acid in that study to those identified here as regulated by Pio in WT mouse liver. The results show distinct hepatic transcriptional effects of the FXR agonist (obeticholic acid) in that study versus those of the PPARγ agonist (Pio) studied here (Figure 7(a)). Another recent study reported the RXR-liver DNA binding effects of a liver X receptor (LXR) agonist (i.e., T0901317 [35]). We also compared those published data to our characterization of Pio-induced gene-specific RXR-liver DNA binding here. That analysis also shows very little overlap between the T0901317- and Pio-induced RXR-DNA binding signatures (Figure 7(b)). These results are consistent with the idea that specific pharmacological agonists of different metabolic-sensing NHRs (e.g., Pio/PPARγ, obeticholic acid/FXR, and T0901317/LXR) induce distinct effects on RXR-liver DNA binding and hepatic transcriptional regulation. That conclusion raises the possibility, also implicated by other studies [35, 46–48], that "cross-talk" in RXR-binding to different NHRs is an important determinant of NHR-ligand effects on gene expression patterns. These considerations are also consistent with the idea that drugs with distinct NHR-binding activities compete with each other and endogenous NHR ligands to exert unique effects on RXR-dependent transcriptional regulation. That concept, illustrated by the hypothetical model in Figure 7(c), raises the additional consideration that specific combinations of different NHR agonist drugs with additive beneficial (or, conversely, deleterious) effects on experimental (and perhaps human) NAFLD can be discovered using the approaches described here [49]. For example, obeticholic acid, like Pio, was also recently reported to have efficacy in human NAFLD [50]. Thus, future assessments of the combinatorial effects of Pio and obeticholic acid on transcriptional regulation and liver disease in experimental NAFLD models might inform consideration of new NHR-agonist combination intervention trials for this increasingly prevalent disease.

Pio has previously been reported to improve hepatic mitochondrial dysfunction in an in vivo NAFLD mouse model [22]. Although its effects on hepatic mitochondrial protein expression were not examined in that study, other

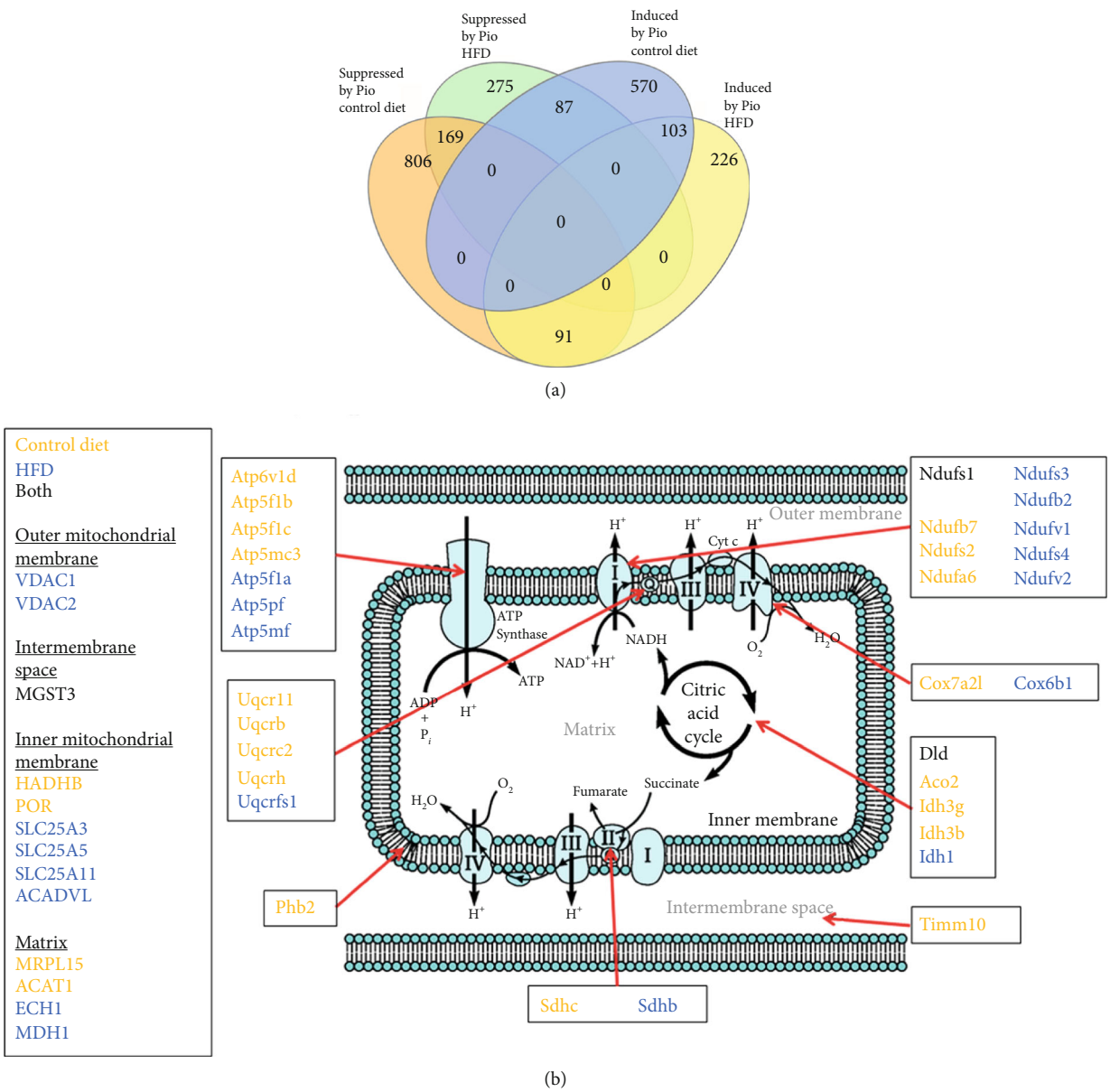

Figure 6: BETA Analyses of Pio's Effects on Mitochondrial Gene Expression - (a) Venn diagram analysis depicting genes identified by BETA as most likely to be regulated by Pio-induced effects on liver RXR-DNA binding in WT mice on control versus HFD. (Input RXR-liver DNA binding data from the KO mice was insufficient to execute BETA.) (b) Nuclear genes encoding mitochondrial proteins identified by BETA as likely to be Pio-induced by PPARγ-dependent effects on liver RXR-DNA binding (genes in orange were identified from analyses of mice on control diet; those in blue from analyses of mice on HFD; and those in black from analyses of mice on either diet). *The mitochondria illustration is adapted from an image freely available in the public domain at https://commons.wikimedia.org/wiki/File:Mitochondrial_electron_transport_chain%E2%80%94Etc4.svg.

investigations have shown that Pio stimulates mitochondrial biogenesis by upregulating specific PGC1α-regulated target gene expression in extrahepatic tissues [51–53]. Those observations, together with the data reported here showing that Pio broadly induces liver PPARγ-dependent RXR binding and hepatic expression of many nuclear genes encoding mitochondrial proteins (Figure 6(b)), implicate such regulation as a plausible mechanism by which Pio exerts its beneficial metabolic effects. However, older studies have paradoxically reported that Pio and other TZDs inhibit hepatocellular mitochondrial function in vitro [54–56]. Thus, further investigations are required.

One limitation of the studies reported here is that the HFD regimen employed here (60% of calories from fat) had relatively modest metabolic effects. Although hepatic steatosis was not significantly increased by this regimen, the HFD-fed mice studied here did gain more weight over the experimental timecourse and display higher adiposity and serum FFA levels at the experimental endpoint, compared to mice fed the control diet (Figures 1 and 2). Reports in

Table 4: Gene set analysis* on BETA data from WT Pio-treated vs. Pio-untreated mice on control or HFD (as designated).

Gene set name (# in Hallmark set)	Description	Overlap	q value
(a) Induced by Pio in WT mice on control diet			
OXIDATIVE_PHOSPHORYLATION [200]	Genes encoding proteins involved in oxidative phosphorylation.	28	$7.09e^{-16}$
FATTY_ACID_METABOLISM [158]	Genes encoding proteins involved in metabolism of fatty acids.	25	$9.9e^{-16}$
ADIPOGENESIS [200]	Genes upregulated during adipocyte differentiation (adipogenesis).	20	$5.16e^{-9}$
MYC_TARGETS_V1 [200]	A subgroup of genes regulated by MYC—version 1 (v1).	19	$2.54e^{-8}$
(b) Induced by Pio in WT mice on HFD			
OXIDATIVE_PHOSPHORYLATION [200]	Genes encoding proteins involved in oxidative phosphorylation.	23	$5.46e^{-16}$
MYC_TARGETS_V1 [200]	A subgroup of genes regulated by MYC - version 1 (v1).	15	$5.89e^{-8}$
FATTY_ACID_METABOLISM [158]	Genes encoding proteins involved in metabolism of fatty acids.	13	$1.52e^{-7}$
(c) Suppressed by Pio in WT mice on control diet			
UV_RESPONSE_UP [158]	Genes upregulated in response to ultraviolet (UV) radiation.	23	$1.49e^{-9}$
UNFOLDED_PROTEIN_RESPONSE [113]	Genes upregulated during unfolded protein response, a cellular stress response related to the endoplasmic reticulum.	17	$1.66e^{-7}$
E2F_TARGETS [200]	Genes encoding cell cycle related targets of E2F transcription factors.	21	$8.05e^{-7}$
P53_PATHWAY [200]	Genes involved in p53 pathways and networks.	21	$8.05e^{-7}$
TNFA_SIGNALING_VIA_NFKB [200]	Genes regulated by NF-kB in response to TNF (GeneID=7124).	21	$8.05e^{-7}$
(d) Suppressed by Pio in WT mice on HFD			
MYC_TARGETS_V1 [200]	A subgroup of genes regulated by MYC—version 1 (v1).	17	$4.45\ e^{-8}$

*Using the Broad Institute platform with the Hallmark gene set platform to identify the top 10 categories with $p \leq 1e^{-6}$ (see text for details).

the literature describing results with this model are consistent with the data reported here and also note the correlation between duration-of-HFD-exposure and development of steatosis. Despite this limitation, our data nevertheless demonstrate a PPARγ-dependent modifying influence of this diet on Pio-regulated changes in hepatic gene expression, including Pio's effects on mitochondrial gene expression (Figure 6(b)). Moreover, our data also indicate that the HFD regimen used here does not detectably alter liver RXR-DNA binding patterns, suggesting that the HFD effects on Pio-regulated hepatic gene expression reported here are either independent of such RXR-DNA binding or dependent on extrahepatic effects of HFD, Pio, or both (as additionally considered below). Future analyses comparing Pio's transcriptional effects here to those in mice given a "Western" or "methionine-choline deficient" diet, each of which induces more severe NAFLD phenotypes, might offer additional insights about these consideration. A second limitation is that only male mice were studied here. This strategy emerged from feasibility constraints while optimizing the experimental and analytical methodologies required for these experiments. Of note, a recent study reported sexually dimorphic RXR-liver DNA binding and hepatic expression of specific metabolic genes [36]. Thus, with the feasibility of the approach employed here now established, future investigations should investigate sex-specific effects on Pio-induced, PPARγ-dependent hepatic transcriptional regulation and the influence of diet on such control. The results could have important implication for future human clinical trials testing Pio or other NHR-binding drugs. A third caveat relates to the considerations that these studies were limited to examination of hepatic transcriptional regulation, despite well-known extra-hepatic PPARγ-dependent (and independent) transcriptional effects of Pio. Feasibility considerations also influenced this approach. Nevertheless, inclusion of assessments of liver RXR-DNA binding and analyses of liver-specific PPARγ KO mice, here, has novel implications for consideration of direct versus indirect hepatic effects of Pio. For example, our observation that Pio does not alter liver RXR-DNA binding in liver-specific PPARγ KO mice leads us to conclude not only that Pio-induced changes in RXR-liver DNA binding depend on hepatocellular PPARγ expression but also that Pio-induced hepatic transcriptional effects in KO mice result, at least in part, from regulation by extrahepatic signals. Nevertheless,

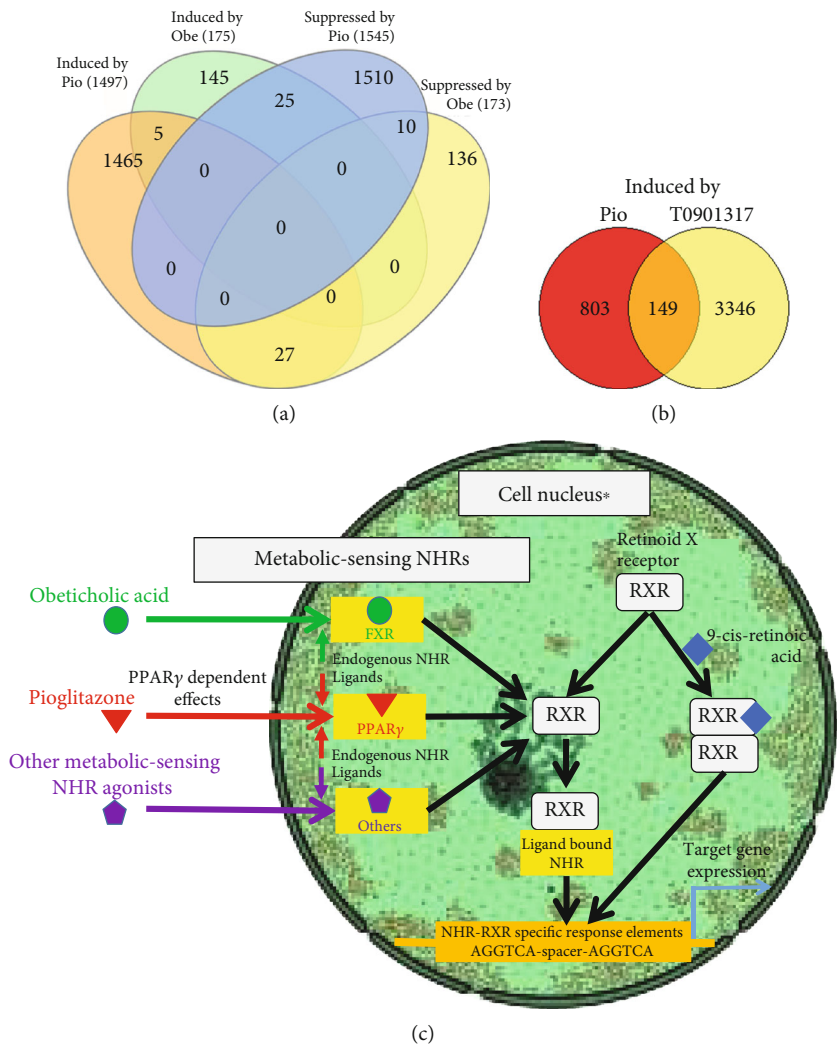

Figure 7: Distinct effects of Pio vs other NHR agonists. (a, b) Venn diagrams depicting (a) distinct effects of PIO (reported here) versus obeticholic acid (Obe, reported in [45]) on the hepatic transcriptome in mice and (b) PIO (reported here) versus the LXRα agonist T0901317 (reported in [35]) on the liver RXR cistrome. (c) Hypothetical model illustrating how different NHR-binding drugs might exert unique effects on transcriptional regulation by competing for RXR-binding, with different NHR-RXR heterodimers displaying distinct affinities for specific NHR-RXR DNA response elements based on spacer length and other factors (e.g., RXR-ligand binding by 9-cis-retinoic acid). RXR homo-dimerization also affects transcription. *The cell nucleus illustration is adapted from vectors from http://www.servier.com and licensed under the Creative Commons Attributions Unported license.

future studies could query relationships between and the tissue-specific dependence of Pio's hepatic and extrahepatic transcriptional effects by similar analyses of muscle and adipose collected from the liver-specific PPARγ KO mice studied here and of mice with extra-hepatic PPARγ disruption. Hepatic mitochondrial activity could also be assessed to evaluate the relationship between mitochondrial gene transcriptional regulation and function in these models.

In conclusion, these analyses define Pio's direct and indirect effects on hepatic transcriptional regulation and implicate diet as a modifier of those effects. They also show that Pio broadly induces liver PPARγ-dependent hepatic expression of nuclear genes encoding mitochondrial proteins and that diet also impacts that regulation. Of note, only c.a. half of the subjects in the PIVENS trial showed drug-induced improvements in NAFLD [9]. Our data raise the provocative possibility that dietary effects on Pio-induced, liver PPARγ-dependent hepatic expression of nuclear genes encoding mitochondrial proteins might correlate with or even mediate the variable efficacy of Pio in that trial. This consideration is important because of the current epidemic of NAFLD together with the paucity of FDA-approved drugs for treatment of that condition. Indeed, based on those circumstances, the American Association for the Study of Liver Disease (AASLD) and the European Association for the Study of the Liver (EASL) have recommended that Pio be considered in patients with biopsy-proven NASH taking into account the risks [57]. Finally, mitochondrial gene expression and function are also known to be dysregulated in other

human diseases [58–60]. Thus, the data reported here might ultimately have broader relevance for future efforts to develop NHR-based therapies for human diseases.

Abbreviations

ChIP-Seq: Chromatin immunoprecipitation with next generation sequencing;
ENCODE: Encyclopedia of DNA elements
FXR: Farnesoid X receptor
GSEA: Gene set enrichment analysis
HFD: High-fat diet
KO: Knockout
LXR: Liver X receptor
NAFLD: Nonalcoholic fatty liver disease
NHR: Nuclear hormone receptor
ns: Not significant
PCA: Principle component analysis
PIO: Pioglitazone
PIVENS: Pioglitazone versus Vitamin E versus Placebo for the Treatment of Non-Diabetic Patients with Nonalcoholic Steatohepatitis
PPAR: Peroxisome proliferator receptor
PPRE: Peroxisome proliferator receptor response element
RNA-Seq: RNA sequencing with next generation sequencing
RXR: Retinoid X receptor
TZD: Thiazolidinedione
UPR: Unfolded protein response
UTR: Untranslated region
WT: Wildtype.

Data Availability

The ChIP- and RNA-Seq data used to support the findings of the studies reported here have been deposited in NCBI's Gene Expression Omnibus (GEO [34]) and will be made accessible to the public as GEO series records GSE137820 (for ChIP-Seq data) and GSE140607 (for RNA-Seq data) at the time this manuscript is accepted for publication. In addition, excel spreadsheets summarizing the results of the RNA-Seq, RXR-ChIP, and BETA data analyses (i.e., for RNA-Seq, lists of differentially expressed genes with fold change, confidence interval, p and q value; for ChIP-Seq, lists of differentially RXR-bound genes, with fold difference, q value, and genomic site of binding; for BETA, gene name, rank, and rank product) are provided in Supplementary Table S2.

Disclosure

The content reported here is solely the responsibility of the authors. Funding was provided by the NASPGHAN Foundation for Children's Digestive Health & Nutrition to DAR; an unrestricted donation from Karsyn's Kause Foundation to DAR; the Washington University School of Medicine Department of Pediatrics to (DAR); the WUSM Digestive Disease Research Core Center (DDRCC) facilities (supported by NIH-NIDDK P30-DK52574); and the WUSM Genome Technology Access Center (GTAC) in the Department of Genetics. The GTAC is partially supported by an NCI Cancer Center Support Grant (P30CA91842) to the Siteman Cancer Center and by an ICTS/CTSA Grant (UL1TR000448) from the National Center for Research Resources (NCRR), a component of the National Institutes of Health (NIH), and NIH Roadmap for Medical Research.

Conflicts of Interest

The authors declare that they have no conflicts of interest.

Acknowledgments

The authors are grateful to Andrew Schriefer for assisting with preliminary analyses of the ChIP-Seq data reported here and to Brian Finck and Phil Tarr for critical review of this manuscript.

Supplementary Materials

Supplementary Figure S1: immunoblot analysis of the anti-RXR$\alpha/\beta/\gamma$ (Santa Cruz sc-774) antibody that was used for the ChIP-Seq studies reported here. The predominant detectable band in all liver samples (i.e., from control, Pio-treated, HFD-treated, and HFD-Pio-treated mice) is ~53 kDa band, which is the molecular weight of RXR, and accounts for >50% of the total detected signal in each lane (average 81% across all samples, as assessed using Odyssey Infrared Imaging System Application Software Version 3.0.21, Licor Biosciences), which is consistent with the ENCODE and modENCODE guidelines [37, 61]. Supplementary Figure S2: the left panel shows initial body weights (in grams) of WT and KO mice (as designated) that were subsequently assigned to the indicated experimental groups (no significant differences between groups). The right panel shows a summary of initial body weights in all WT versus all KO mice ($p < 0.05$). Supplementary Figure S3: summary of RT-qPCR based analyses of exemplar genes whose RNA-Seq based patterns of expression are depicted in Figure 3. Supplementary Table S1: gene-specific oligonucleotide primers for RT-qPCR. Supplementary Table S2: RNA-Seq, ChIP-Seq, and BETA Analyses Results—see excel Table S2. This excel spreadsheet contains (A) List of Experimental Groups, (B) a merged summary of all RNA-Seq differential expression analyses, summaries of differentially RXR-bound peaks identified by ChIP-Seq analyses of liver samples from wildtype (C) Pio vs. control or (D) HFD-Pio-treated vs. HFD-treated mice, and (E) summary lists from BETA analyses of RNA- and ChIP-Seq data from comparisons of Pio vs. control and HFD-Pio vs. HFD (including rank, Gene name, and rank product). Supplementary Table S3: GAGE results—see excel Table S3: this excel spreadsheet contains GAGE gene set expression perturbation test results for all comparisons between groups conducted by Limma. Log 2 fold changes of all genes within specific gene sets were compared to all those outside those sets using Student's t-tests. Results are reported as mean log 2 fold-change, p value, and Benjamini-Hochberg FDR adjusted p value. Supplementary

Table S4: gene set analysis on RNA-Seq data from HFD vs. control diet-treated WT mice: these tables were generated using the Broad Institute platform with the Hallmark gene set platform to identify the top 10 categories with $p \leq 1e^{-6}$ (see text for additional details). Supplementary Table S5: gene set analysis* on RNA-Seq data from HFD vs. control diet-treated KO mice: these tables were generated using the Broad Institute platform with the Hallmark gene set platform to identify the top 10 categories with $p \leq 1e^{-6}$ (see text for additional details). *(Supplementary Materials)*

References

[1] F. Gilardi and B. Desvergne, "RXRs: collegial partners," *Sub-Cellular Biochemistry*, vol. 70, pp. 75–102, 2014.

[2] G. P. Ables, "Update on Ppar and nonalcoholic fatty liver disease," *PPAR Research*, vol. 2012, Article ID 912351, 5 pages, 2012.

[3] K. Kawaguchi, I. Sakaida, M. Tsuchiya, K. Omori, T. Takami, and K. Okita, "Pioglitazone prevents hepatic steatosis, fibrosis, and enzyme-altered lesions in rat liver cirrhosis induced by a choline-deficient L-amino acid-defined diet," *Biochemical and Biophysical Research Communications*, vol. 315, no. 1, pp. 187–195, 2004.

[4] A. Da Silva Morais, V. Lebrun, J. Abarca-Quinones et al., "Prevention of steatohepatitis by pioglitazone: implication of adiponectin-dependent inhibition of SREBP-1c and inflammation," *Journal of Hepatology*, vol. 50, no. 3, pp. 489–500, 2009.

[5] P. D. Hockings, K. K. Changani, N. Saeed et al., "Rapid reversal of hepatic steatosis, and reduction of muscle triglyceride, by rosiglitazone: MRI/S studies in Zucker fatty rats," *Diabetes, Obesity and Metabolism*, vol. 5, no. 4, pp. 234–243, 2003.

[6] S. J. Yang, J. M. Choi, S. W. Chae et al., "Activation of peroxisome proliferator-activated receptor gamma by rosiglitazone increases sirt6 expression and ameliorates hepatic steatosis in rats," *PLoS One*, vol. 6, no. 2, article e17057, 2011.

[7] I. A. Leclercq, V. A. Lebrun, P. Starkel, and Y. J. Horsmans, "Intrahepatic insulin resistance in a murine model of steatohepatitis: effect of PPARgamma agonist pioglitazone," *Laboratory Investigation*, vol. 87, no. 1, pp. 56–65, 2007.

[8] F. Alam, M. A. Islam, M. Mohamed et al., "Efficacy and safety of pioglitazone monotherapy in type 2 diabetes mellitus: a systematic review and meta-analysis of randomised controlled trials," *Scientific Reports*, vol. 9, no. 1, p. 5389, 2019.

[9] A. J. Sanyal, N. Chalasani, K. V. Kowdley et al., "Pioglitazone, vitamin E, or placebo for nonalcoholic steatohepatitis," *New England Journal of Medicine*, vol. 362, no. 18, pp. 1675–1685, 2010.

[10] S. Yu, K. Matsusue, P. Kashireddy et al., "Adipocyte-specific gene expression and adipogenic steatosis in the mouse liver due to peroxisome proliferator-activated receptor gamma1 (PPARgamma1) overexpression," *Journal of Biological Chemistry*, vol. 278, no. 1, pp. 498–505, 2003.

[11] E. Moran-Salvador, M. Lopez-Parra, V. Garcia-Alonso et al., "Role for PPARγ in obesity-induced hepatic steatosis as determined by hepatocyte- and macrophage-specific conditional knockouts," *The FASEB Journal*, vol. 25, no. 8, pp. 2538–2550, 2011.

[12] K. Matsusue, M. Haluzik, G. Lambert et al., "Liver-specific disruption of PPARgamma in leptin-deficient mice improves fatty liver but aggravates diabetic phenotypes," *Journal of Clinical Investigation*, vol. 111, no. 5, pp. 737–747, 2003.

[13] O. Gavrilova, M. Haluzik, K. Matsusue et al., "Liver peroxisome proliferator-activated receptor gamma contributes to hepatic steatosis, triglyceride clearance, and regulation of body fat mass," *Journal of Biological Chemistry*, vol. 278, no. 36, pp. 34268–34276, 2003.

[14] A. L. Hevener, W. He, Y. Barak et al., "Muscle-specific Pparg deletion causes insulin resistance," *Nature Medicine*, vol. 9, no. 12, pp. 1491–1497, 2003.

[15] W. He, Y. Barak, A. Hevener et al., "Adipose-specific peroxisome proliferator-activated receptor gamma knockout causes insulin resistance in fat and liver but not in muscle," *Proceedings of the National Academy of Sciences of the United States of America*, vol. 100, no. 26, pp. 15712–15717, 2011.

[16] M. Stumvoll and H. U. Haring, "Glitazones: clinical effects and molecular mechanisms," *Annals of Medicine*, vol. 34, no. 3, pp. 217–224, 2009.

[17] X. Pan, P. Wang, J. Luo et al., "Adipogenic changes of hepatocytes in a high-fat diet-induced fatty liver mice model and non-alcoholic fatty liver disease patients," *Endocrine*, vol. 48, no. 3, pp. 834–847, 2015.

[18] P. Pettinelli and L. A. Videla, "Up-regulation of PPAR-gamma mRNA expression in the liver of obese patients: an additional reinforcing lipogenic mechanism to SREBP-1c induction," *The Journal of Clinical Endocrinology and Metabolism*, vol. 96, no. 5, pp. 1424–1430, 2011.

[19] J. Skat-Rordam, D. Hojland Ipsen, J. Lykkesfeldt, and P. Tveden-Nyborg, "A role of peroxisome proliferator-activated receptor γ in non-alcoholic fatty liver disease," *Basic & Clinical Pharmacology & Toxicology*, vol. 124, no. 5, pp. 528–537, 2019.

[20] K. S. McCommis and B. N. Finck, "Treating hepatic steatosis and fibrosis by modulating mitochondrial pyruvate metabolism," *Cellular and Molecular Gastroenterology and Hepatology*, vol. 7, no. 2, pp. 275–284, 2019.

[21] K. H. H. Liss and B. N. Finck, "PPARs and nonalcoholic fatty liver disease," *Biochimie*, vol. 136, pp. 65–74, 2017.

[22] S. Kalavalapalli, F. Bril, J. P. Koelmel et al., "Pioglitazone improves hepatic mitochondrial function in a mouse model of nonalcoholic steatohepatitis," *American Journal of Physiology. Endocrinology and Metabolism*, vol. 315, no. 2, pp. E163–E173, 2018.

[23] J. C. Corona and M. R. Duchen, "PPARγ as a therapeutic target to rescue mitochondrial function in neurological disease," *Free Radical Biology & Medicine*, vol. 100, pp. 153–163, 2016.

[24] Y. J. Lee, E. H. Ko, J. E. Kim et al., "Nuclear receptor PPARγ-regulated monoacylglycerol O-acyltransferase 1 (MGAT1) expression is responsible for the lipid accumulation in diet-induced hepatic steatosis," *Proceedings of the National Academy of Sciences of the United States of America*, vol. 109, no. 34, pp. 13656–13661, 2012.

[25] V. Gazit, J. Huang, A. Weymann, and D. A. Rudnick, "Analysis of the role of hepatic PPARγ expression during mouse liver regeneration," *Hepatology*, vol. 56, no. 4, pp. 1489–1498, 2012.

[26] V. Gazit, A. Weymann, E. Hartman et al., "Liver regeneration is impaired in lipodystrophic fatty liver dystrophy mice," *Hepatology*, vol. 52, no. 6, pp. 2109–2117, 2010.

[27] J. Huang, A. E. Schriefer, P. F. Cliften et al., "Postponing the hypoglycemic response to partial hepatectomy delays mouse

liver regeneration," *The American Journal of Pathology*, vol. 186, no. 3, pp. 587–599, 2016.

[28] C. W. Law, M. Alhamdoosh, S. Su, G. K. Smyth, and M. E. Ritchie, "RNA-seq analysis is easy as 1-2-3 with limma, Glimma and edgeR," *F1000Research*, vol. 5, article 1408, 2016.

[29] M. E. Ritchie, B. Phipson, D. Wu et al., "Limma powers differential expression analyses for RNA-sequencing and microarray studies," *Nucleic Acids Research*, vol. 43, no. 7, article e47, 2015.

[30] M. D. Robinson, D. J. McCarthy, and G. K. Smyth, "edgeR: a bioconductor package for differential expression analysis of digital gene expression data," *Bioinformatics*, vol. 26, no. 1, pp. 139-140, 2009.

[31] C. S. Ross-Innes, R. Stark, A. E. Teschendorff et al., "Differential oestrogen receptor binding is associated with clinical outcome in breast cancer," *Nature*, vol. 481, no. 7381, pp. 389–393, 2012.

[32] A. Subramanian, P. Tamayo, V. K. Mootha et al., "Gene set enrichment analysis: a knowledge-based approach for interpreting genome-wide expression profiles," *Proceedings of the National Academy of Sciences of the United States of America*, vol. 102, no. 43, pp. 15545–15550, 2005.

[33] V. K. Mootha, C. M. Lindgren, K. F. Eriksson et al., "PGC-1alpha-responsive genes involved in oxidative phosphorylation are coordinately downregulated in human diabetes," *Nature Genetics*, vol. 34, no. 3, pp. 267–273, 2003.

[34] J. Huang, A. E. Schriefer, W. Yang, P. F. Cliften, and D. A. Rudnick, "Identification of an epigenetic signature of early mouse liver regeneration that is disrupted by Zn-HDAC inhibition," *Epigenetics*, vol. 9, no. 11, pp. 1521–1531, 2014.

[35] M. Boergesen, T. A. Pedersen, B. Gross et al., "Genome-wide profiling of liver X receptor, retinoid X receptor, and peroxisome proliferator-activated receptor α in mouse liver reveals extensive sharing of binding sites," *Molecular and Cellular Biology*, vol. 32, no. 4, pp. 852–867, 2012.

[36] A. Kosters, D. Sun, H. Wu et al., "Sexually dimorphic genome-wide binding of retinoid X receptor alpha (RXRα) determines male-female differences in the expression of hepatic lipid processing genes in mice," *PLoS One*, vol. 8, no. 8, article e71538, 2013.

[37] S. G. Landt, G. K. Marinov, A. Kundaje et al., "ChIP-seq guidelines and practices of the ENCODE and modENCODE consortia," *Genome Research*, vol. 22, no. 9, pp. 1813–1831, 2012.

[38] Y. Zhang, T. Liu, C. A. Meyer et al., "Model-based analysis of ChIP-Seq (MACS)," *Genome Biology*, vol. 9, no. 9, article R137, 2008.

[39] W. Huang, R. Loganantharaj, B. Schroeder, D. Fargo, and L. Li, "PAVIS: a tool for peak annotation and visualization," *Bioinformatics*, vol. 29, no. 23, pp. 3097–3099, 2013.

[40] Y. Benjamini and Y. Hochberg, "Controlling the false discovery rate: a practical and powerful approach to multiple testing," *Journal of the Royal Statistical Society: Series B (Methodological)*, vol. 57, no. 1, pp. 289–300, 1995.

[41] Y. Benjamini, D. Drai, G. Elmer, N. Kafkafi, and I. Golani, "Controlling the false discovery rate in behavior genetics research," *Behavioural Brain Research*, vol. 125, no. 1-2, pp. 279–284, 2001.

[42] H. Heberle, G. V. Meirelles, F. R. da Silva, G. P. Telles, and R. Minghim, "InteractiVenn: a web-based tool for the analysis of sets through Venn diagrams," *BMC Bioinformatics*, vol. 16, no. 1, p. 169, 2015.

[43] S. Wang, H. Sun, J. Ma et al., "Target analysis by integration of transcriptome and ChIP-seq data with BETA," *Nature Protocols*, vol. 8, no. 12, pp. 2502–2515, 2013.

[44] Y. Wang, T. Nakajima, F. J. Gonzalez, and N. Tanaka, "PPARs as metabolic regulators in the liver: lessons from liver-specific PPAR-null mice," *International Journal of Molecular Sciences*, vol. 21, no. 6, article 2061, 2020.

[45] N. Ijssennagger, A. W. F. Janssen, A. Milona et al., "Gene expression profiling in human precision cut liver slices in response to the FXR agonist obeticholic acid," *Journal of Hepatology*, vol. 64, no. 5, pp. 1158–1166, 2016.

[46] P. Chambon, "A decade of molecular biology of retinoic acid receptors," *The FASEB Journal*, vol. 10, no. 9, pp. 940–954, 1996.

[47] T. Yoshikawa, T. Ide, H. Shimano et al., "Cross-talk between peroxisome proliferator-activated receptor (PPAR) alpha and liver X receptor (LXR) in nutritional regulation of fatty acid metabolism. I. PPARs suppress sterol regulatory element binding protein-1c promoter through inhibition of LXR signaling," *Molecular Endocrinology*, vol. 17, no. 7, pp. 1240–1254, 2003.

[48] T. Ide, H. Shimano, T. Yoshikawa et al., "Cross-talk between peroxisome proliferator-activated receptor (PPAR) alpha and liver X receptor (LXR) in nutritional regulation of fatty acid metabolism. II. LXRs suppress lipid degradation gene promoters through inhibition of PPAR signaling," *Molecular Endocrinology*, vol. 17, no. 7, pp. 1255–1267, 2003.

[49] M. C. Cave, H. B. Clair, J. E. Hardesty et al., "Nuclear receptors and nonalcoholic fatty liver disease," *Biochimica et Biophysica Acta*, vol. 1859, no. 9, pp. 1083–1099, 2016.

[50] B. A. Neuschwander-Tetri, R. Loomba, A. J. Sanyal et al., "Farnesoid X nuclear receptor ligand obeticholic acid for non-cirrhotic, non-alcoholic steatohepatitis (FLINT): a multicentre, randomised, placebo-controlled trial," *The Lancet*, vol. 385, no. 9972, pp. 956–965, 2015.

[51] I. Pagel-Langenickel, J. Bao, J. J. Joseph et al., "PGC-1alpha integrates insulin signaling, mitochondrial regulation, and bioenergetic function in skeletal muscle," *The Journal of Biological Chemistry*, vol. 283, no. 33, pp. 22464–22472, 2008.

[52] Z. Arany, "PGC-1 coactivators and skeletal muscle adaptations in health and disease," *Current Opinion in Genetics & Development*, vol. 18, no. 5, pp. 426–434, 2008.

[53] I. Bogacka, H. Xie, G. A. Bray, and S. R. Smith, "Pioglitazone induces mitochondrial biogenesis in human subcutaneous adipose tissue in vivo," *Diabetes*, vol. 54, no. 5, pp. 1392–1399, 2005.

[54] I. García-Ruiz, P. Solís-Muñoz, D. Fernández-Moreira, T. Muñoz-Yagüe, and J. A. Solís-Herruzo, "Pioglitazone leads to an inactivation and disassembly of complex I of the mitochondrial respiratory chain," *BMC Biology*, vol. 11, no. 1, p. 88, 2013.

[55] M. N. Sanz, C. Sanchez-Martin, D. Detaille et al., "Acute mitochondrial actions of glitazones on the liver: a crucial parameter for their antidiabetic properties," *Cellular Physiology and Biochemistry*, vol. 28, no. 5, pp. 899–910, 2011.

[56] D. Hu, C. Q. Wu, Z. J. Li et al., "Characterizing the mechanism of thiazolidinedione-induced hepatotoxicity: an in vitro model in mitochondria," *Toxicology and Applied Pharmacology*, vol. 284, no. 2, pp. 134–141, 2015.

[57] B. A. Neuschwander-Tetri, "Pharmacologic management of nonalcoholic steatohepatitis," *Gastroenterology & Hepatology*, vol. 14, no. 10, pp. 582–589, 2018.

[58] B. Ding, Y. Xi, M. Gao et al., "Gene expression profiles of entorhinal cortex in Alzheimer's disease," *American Journal of Alzheimer's Disease and Other Dementias*, vol. 29, no. 6, pp. 526–532, 2014.

[59] D. Vacirca, F. Delunardo, P. Matarrese et al., "Autoantibodies to the adenosine triphosphate synthase play a pathogenetic role in Alzheimer's disease," *Neurobiology of Aging*, vol. 33, no. 4, pp. 753–766, 2012.

[60] M. W. Dodson and M. Guo, "Pink1, Parkin, DJ-1 and mitochondrial dysfunction in Parkinson's disease," *Current Opinion in Neurobiology*, vol. 17, no. 3, pp. 331–337, 2007.

[61] G. K. Marinov, A. Kundaje, P. J. Park, and B. J. Wold, "Large-scale quality analysis of published ChIP-seq data," *G3: Genes, Genomes, Genetics*, vol. 4, no. 2, pp. 209–223, 2014.

Hindawi
PPAR Research
Volume 2020, Article ID 3608315, 16 pages
https://doi.org/10.1155/2020/3608315

Review Article

The Emerging Role of PPAR Beta/Delta in Tumor Angiogenesis

Siyue Du, Nicole Wagner, and Kay-Dietrich Wagner

Université Côte d'Azur, CNRS, INSERM, iBV, 06107 Nice, France

Correspondence should be addressed to Siyue Du; sdu@unice.fr

Nicole Wagner and Kay-Dietrich Wagner contributed equally to this work.

Received 28 May 2020; Accepted 24 July 2020; Published 13 August 2020

Academic Editor: Anastasia Nesterova

PPARs are ligand-activated transcriptional factors that belong to the nuclear receptor superfamily. Among them, PPAR alpha and PPAR gamma are prone to exert an antiangiogenic effect, whereas PPAR beta/delta has an opposite effect in physiological and pathological conditions. Angiogenesis has been known as a hallmark of cancer, and our recent works also demonstrate that vascular-specific PPAR beta/delta overexpression promotes tumor angiogenesis and progression in vivo. In this review, we will mainly focus on the role of PPAR beta/delta in tumor angiogenesis linked to the tumor microenvironment to further facilitate tumor progression and metastasis. Moreover, the crosstalk between PPAR beta/delta and its downstream key signal molecules involved in tumor angiogenesis will also be discussed, and the network of interplay between them will further be established in the review.

1. Introduction

Peroxisome proliferator-activated receptors (PPARs) as ligand-activated transcription factors belong to the steroid receptor superfamily, which includes three isoforms, PPAR alpha, PPAR beta/delta, and PPAR gamma [1]. PPARs form heterodimers with retinoic X receptors and regulate the expression of various genes upon ligand binding. PPARs also interact with corepressors or coactivators to modulate the transcription of its downstream target genes. PPARs as important transcriptional regulators have been suggested to be involved in lipid metabolism and multiple cellular functions. For instance, PPAR alpha also functions in fatty acid beta-oxidation and vascular inflammation [2]. PPAR gamma acts as a regulator in adipocyte differentiation and type 2 diabetes [3]. PPAR beta/delta is a key player in cardiac energy production, angiogenesis, and particularly in cancer progression [4].

PPAR alpha and PPAR gamma exert predominantly an antiangiogenic effect [5–10], but there still exist conflicting studies showing opposite results [11, 12]. On the contrary, PPAR beta/delta produces more obviously proangiogenic effects [13–18]. In this review, we will focus on the promoting role of PPAR beta/delta in angiogenesis, especially in tumor angiogenesis. The network of interplay between PPAR beta/-delta and its various downstream signal molecules, and also between those key molecules, will be further discussed and established. Remarkably, diverse important signal molecules involved in tumor angiogenesis and progression, and cancer cell metabolism have been identified as direct PPAR beta/-delta target genes.

2. Angiogenesis

Angiogenesis is the physiological process through which a new capillary network forms from the preexisting vasculature [19, 20], whereas vasculogenesis denotes de novo blood vessel formation mostly during embryogenesis in which endothelial progenitor cells (EPC) migrate to sites of vascularization, then differentiate into endothelial cells (EC), and coalesce into the initial vascular plexus [21, 22]. Besides the interaction between proangiogenic factors and antiangiogenic factors, angiogenesis is also a multiple step biological process during which a variety of molecules cooperate including cell adhesion molecules, matrix metalloproteinases

(MMPs), extracellular matrix (ECM), and basement membrane components.

Angiogenesis is a physiological and vital process in development and growth. An imbalance of proangiogenic and antiangiogenic factors causes angiogenesis in pathological conditions such as diabetic retinopathy and tumor growth. Thus, when the imbalance comes to a point at which angiogenesis is triggered by tumor cells, then an "angiogenic switch" of tumor cells is turned on; during tumor progression, the "angiogenic switch" is often activated and remains on [23–25]. Inducing angiogenesis is known as a hallmark of cancer [26], and angiogenesis is also a fundamental step by which most benign tumors transition into malignant ones.

2.1. Tumor Angiogenesis. Tumor needs to sprout new vessels and further develop a vascular network in order to supply nutrients and oxygen, remove waste products, support a continually high proliferative rate, and ultimately expand neoplastic growth [23, 27]. Hence, angiogenesis is essential for helping sustain tumor growth and facilitate tumor progression. Besides being a requirement for angiogenesis, an abnormal vasculature also helps to promote tumor progression and metastasis. The tumor vascular wall is imperfect and prone to leakage, so it is much easier for tumor cells to directly penetrate into the blood vessels or lymphatic vessels and then proliferate at another distant site to form metastasis [28].

Due to intensive abnormal neovascularization in tumor tissues, most malignant tumors grow rapidly and acquire the ability to spread to adjacent and distant organs, which makes them more malignant and even life threatening. Therefore, angiogenesis indeed plays an important role in tumor progression and metastasis, and to intervene with this process would obviously prevent tumor development and spread. Thus, this has been regarded as a critical target for antitumor therapy.

3. PPAR Alpha and Angiogenesis

It was reported firstly that a selective PPAR alpha agonist WY14643 did not show any effect on angiogenesis or EC proliferation [29]. But some subsequent studies showed that the activation of PPAR alpha inhibited angiogenesis in vitro by using fenofibrate, a clinically used PPAR alpha agonist [30]. Moreover, fenofibrate suppressed EC proliferation, migration, and tube formation through inhibition of protein kinase B (Akt) and disruption of the cytoskeleton [31]. Furthermore, PPAR alpha activation was shown to inhibit vascular endothelial growth factor- (VEGF-) induced EC migration and basic fibroblast growth factor- (bFGF/FGF2-) induced corneal angiogenesis in vitro and in vivo [5]. Especially, in vivo, reduced tumor growth and microvessel numbers were observed in mice implanted with melanoma, Lewis lung carcinoma (LLC), fibrosarcoma, and glioblastoma due to a systemic treatment of PPAR alpha ligand, and the antiangiogenic state induced through activation of PPAR alpha with elevated thrombospondin-1 (TSP1) and endostatin expression [5].

However, in that same year, it was demonstrated in another observation that activation of PPAR alpha stimulated neovascularization in vivo with increased phosphorylation of endothelial nitric oxide synthase (eNOS) and Akt via a VEGF-dependent manner [32]. Furthermore, Zhang and Ward also suggested that PPAR alpha activation induced proangiogenic responses in human ocular cells [33]. In another study, it was shown that a new PPAR alpha agonist (R)-K-13675 had no effect on angiogenesis [34]. Recently, PPAR alpha activation is further shown to have antineovascularization effects with downregulation of VEGF and angiopoietin expression in a rat alkali burn model [35].

In summary, the role of PPAR alpha in angiogenesis is still controversial. Some observations showed that ligand activation of PPAR alpha had antiangiogenic effects mediated either through upregulation of antiangiogenic factors such as TSP1 and endostatin, or downregulation of proangiogenic factors including VEGF, FGF2, AKT, and angiopoietins. Others also reported opposite results showing a proangiogenic role upon PPAR alpha activation. Thus, the specific molecular mechanism is still unclear and needs to be further studied.

4. PPAR Gamma and Angiogenesis

Ligand activation of PPAR gamma was previously shown to inhibit human umbilical vein endothelial cell (HUVEC) tube formation in collagen gels [36] and VEGF-induced choroidal neovascularization in vitro and in vivo [37]. Another study also demonstrated that EC apoptosis was induced through treatment with the PPAR gamma ligand 15d-PGJ2 [38]. Furthermore, rosiglitazone, a potent PPAR gamma agonist, was shown to inhibit primary tumor growth and metastasis through both direct and indirect antiangiogenic effects in vitro, and bFGF-induced corneal neovascularization in vivo [8]. Moreover, a similar observation also displayed the inhibition of VEGF-induced angiogenesis in a chick chorioallantonic membrane model [39]. In a mouse model with ischemia-induced retinopathy, pioglitazone, a PPAR gamma agonist, also showed a protective effect against pathological neoangiogenesis through upregulation of anti-inflammatory adipokine adiponectin [40]. Additionally, the PPAR gamma antagonist GW9662 was shown to reverse Omega-3 polyunsaturated fatty acid-induced reduction of E-Selectin, angiopoietin-2, vascular cell adhesion molecule-1, and intracellular adhesion molecule-1 [41], implicating an antiangiogenic potential of PPAR gamma itself. However, opposite results also showed that pioglitazone enhanced neovascularization and inhibited apoptosis of EPC in vitro and in vivo via a Phosphoinositide-3-Kinase- (PI3K-) dependent manner [42].

Nadra et al. observed that PPAR gamma-null embryos displayed a vascular structural defect at E9.5. Moreover, disorganized placental layers and an altered placental microvasculature were observed in pregnant wild-type mice treated with the PPAR gamma agonist rosiglitazone, as well as reduced expression of proangiogenic factors including VEGF, proliferin, and platelet-endothelial cell adhesion molecule-1 (PECAM1/CD31) [43], suggesting a crucial role of PPAR gamma in placental vascular development. The

major antiangiogenic properties on PPAR gamma activation were also reviewed here [44].

Notably, in most cancers, the canonical Wnt/beta-catenin pathway is upregulated, while on the contrary, PPAR gamma is downregulated. Interestingly, in numerous tissues, the activation of PPAR gamma inhibits the beta-catenin pathway, whereas the stimulation of the canonical Wnt/beta-catenin signal cascade also inactivates PPAR gamma [45], implicating a negative regulatory role of PPAR gamma in carcinogenesis where tumor angiogenesis might be a fundamental step.

In summary, PPAR gamma predominantly displays an antiangiogenic effect that may be mediated through the inhibition of VEGF or bFGF-induced neovascularization and reduction of the expression level of some proangiogenic factors.

5. PPAR Beta/Delta and Angiogenesis

Unlike PPAR alpha and PPAR gamma, on the contrary, many studies have explicitly shown the proangiogenic effects of PPAR beta/delta on physiological and pathological angiogenesis. The first evidence provided in a study is that activation of PPAR beta/delta with GW501516, a highly selective PPAR beta/delta agonist, induces HUVEC proliferation and an increased expression of VEGF and its receptor VEGFR1 (FLT1) [46]. Besides inducing EC proliferation, PPAR beta/delta activation by its ligand prostacyclin (PGI2) also stimulates upregulation of 14-3-3 alpha expression, an antiapoptotic and anti-inflammatory protein, which thereby protects ECs from H_2O_2-induced apoptosis and oxidant injury [47]. Moreover, a subsequent study further provides evidence that activation of PPAR beta/delta with GW501516 induces angiogenesis during which VEGF release is considered as a major trigger factor [48], firstly suggesting the promotion for angiogenesis upon PPAR beta/delta activation.

Müller-Brüsselbach et al. show that PPAR beta/delta -/- mice implanted with LLC and B16 melanoma exhibit diminished blood flow and immature microvascular structures compared with wild-type mice. Moreover, reexpression of PPAR beta/delta into the matrigel-invading cells triggers microvessel maturation and restores normal vascularization [17], indicating a crucial role of PPAR beta/delta in tumor vascularization. Additionally, another study also observed reduced levels of calcium intracellular channel protein 4 (CLIC4), but it observed enhanced expression of cellular retinol binding protein 1 (CRBP1) in migrating ECs from PPAR beta/delta-null mice [49], both of which play a role in tumor vascularization [50, 51]. It was reported that PPAR beta/delta was required for placentation [52], and most of the PPAR beta/delta-null mutant embryos died at E9.5 to E10.5 due to abnormal cell-to-cell communication at the placental-decidual interface [53]. However, in these studies [52–54], a defect in angiogenesis was not observed during normal development in PPAR beta/delta-knockout mice.

Some observations also show the important role of PPAR beta/delta in physiological angiogenesis. For instance, skeletal muscle-specific PPAR beta/delta overexpression leads to an increase in the number of oxidative muscle fibers and running endurance in adult mice [55–57]. Moreover, PPAR beta/delta activation promotes a rapid muscle remodeling via a calcineurin-dependent manner, and induces muscle angiogenesis in highly selective PPAR beta/delta agonist GW0742-treated animals [58]. Furthermore, in the heart, pharmacological PPAR beta/delta stimulation with GW0742 induces rapid cardiac growth and cardiac angiogenesis through direct transcriptional activation of calcineurin [15]. Interestingly, the same cardiac phenotype was also observed after treatment with the PPAR beta/delta agonist GW501516, implicating a response specificity for PPAR beta/delta stimulation [15]. Calcineurin activation further leads to the stimulation of nuclear factor-activated T cell c3 (NFATc3) and an enhanced expression of hypoxia inducible factor 1 alpha (HIF-1alpha) and cyclin-dependent kinase 9 (CDK9) [15]. Overall, the remodeling in skeletal muscle and heart is perfectly the same as the phenotype observed with exercise, and both of them are mediated through activation of calcineurin.

PPAR beta/delta may act as a key regulator in mediating pathological angiogenesis. For instance, PPAR beta/delta was shown to regulate retinal angiogenesis in vitro and in vivo, and its inhibition reduced preretinal neovascularization possibly via an Angiopoietin-like protein 4- (Angptl4-) dependent manner [59], implicating the potential of PPAR beta/delta in modulating pathological ocular angiogenesis. Recently, an observation reported that PPAR beta/delta knockdown in both retinal pigment epithelial and choroidal endothelial cells caused an antiangiogenic phenotype, and PPAR beta/delta promoted laser-induced choroidal neovascular (CNV) lesions in PPAR beta/delta +/+ mice [60]. Moreover, pharmacological inhibition of PPAR beta/delta with the antagonist GSK0660 also resulted in a significantly decreased CNV lesion size in vivo, suggesting a functional role of PPAR beta/delta in the development of CNV lesions [60]. This indicates that PPAR beta/delta has an important association with pathological angiogenesis.

Angiotensin II (Ang II), the biologically active peptide of the renin-angiotensin system (RAS), is a major blood pressure and cardiovascular homeostasis regulator and is also recognized as a potent mitogen. Angiotensin-converting enzyme inhibitors were introduced approximately 30 years ago as antihypertensive agents and have since become a successful therapeutic approach for high blood pressure, congestive heart failure, and postmyocardial infarction. In experimental systems, the antitumor effects of diverse ACE inhibitors show that these inhibit cell proliferation and possess antiangiogenic, antimetastatic, and anti-inflammatory effects [61–63]. It has been shown recently that activation of PPAR beta/delta inhibits Ang II-stimulated protein synthesis in a concentration-dependent manner and suppresses Ang II-induced generation of reactive oxygen species (ROS) in vascular smooth muscle cells [64]. PPAR beta/delta was further shown to inhibit Ang II-mediated atherosclerosis [65]. However, it is not clear until now if PPAR beta/delta activation can be considered as an ACE inhibitor-mimicking approach as it is for example the case for PPAR gamma activators [66].

Furthermore, the relevance of this hypothetical PPAR beta/delta feature might be limited for tumor angiogenesis where vascular smooth muscle hypertrophy and atherosclerosis do not contribute to the major pathology.

Besides inducing angiogenesis, it has been demonstrated that PPAR beta/delta directly acts on early EPC through activation of the AKT pathway and induces an enhanced vasculogenesis [67]. Similarly, the PPAR beta/delta-mediated provasculogenic effects are also observed on late EPC [68]. He et al. showed that PPAR beta/delta activation with GW501516 induced EPC proliferation and tube formation, whereas EPC treated with an inhibitor of cyclooxygenase (COX) or PGI2 synthase, or with PPAR beta/delta-specific siRNA also displayed an opposite effect [68]. Furthermore, it has been demonstrated that PPAR beta/delta induces angiogenesis and skeletal muscle regeneration through matrix metalloproteinase- (MMP-) 9-mediated insulin-like growth factor-1 paracrine networks upon EPC activation [69]. Han et al. also observed that PPAR beta/delta activation promoted a rapid wound healing with enhanced angiogenesis in a mouse model with skin punch wound [69]. Overall, in addition to EC, PPAR beta/delta is also a key regulator of EPC, or even may act as an initiator of activation of EPC to further induce vasculogenesis.

6. PPAR Beta/Delta and Tumor Angiogenesis Linked to Tumor Microenvironment

PPAR beta/delta expression is often upregulated and promotes cancer progression in many major human cancers such as colon, lung, breast, and gastric cancers [70–73], which suggests a crucial role of PPAR beta/delta in cancer cells even though there exist some conflicting studies indicating that the functional role of PPAR beta/delta in tumorigenesis or carcinogenesis still remains highly controversial [74–77] and dependent on specific tumor or cancer cell types. Thus, here we discuss the promotion of PPAR beta/delta in tumor progression through facilitating tumor angiogenesis.

PPAR beta/delta has been suggested as a critical "hub node" transcriptional factor which governs a tumor "angiogenic switch" [13, 78–80]. In the transcriptional network analysis, it was reported that tumor growth and tumor angiogenesis were markedly inhibited in PPAR beta/delta-null mice in comparison with wild-type mice [13]. Moreover, the elevated PPAR beta/delta expression level was also considered to be highly correlated to pathologically advanced tumor stage and increased cancer risk for recurrence and distant metastasis in patients with pancreatic cancer [13], indicating the crucial association of PPAR beta/delta with tumor angiogenesis, progression, and cancer invasiveness.

PPAR beta/delta may indirectly facilitate tumor angiogenesis and progression through its function on the tumor microenvironment (TME) where tumor angiogenesis is fostered. Moreover, a tumor also releases some extracellular signals to closely communicate and constantly collaborate with TME to facilitate tumor angiogenesis, in order to further enable tumor growth and progression. For instance, it was shown that colon cancer cells with PPAR beta/delta knockout failed to stimulate EC vascularization in response to hypoxic stress, whereas wild-type cells exposed to hypoxia were able to induce angiogenesis [81, 82], suggesting that PPAR beta/-delta is required for the promotion of angiogenesis in hypoxic stress-mediated TME. Moreover, in the TME, tumor-infiltrating myeloid cells are considered as the most important cells for fostering tumor angiogenesis among the multiple different kinds of stromal cells [82]. Besides stimulating tumor angiogenesis, tumor myeloid cells also support tumor growth by suppressing tumor immunity and promoting tumor metastasis to distinct sites [83]. Interestingly, it has been demonstrated that PPAR beta/delta activation in tumor-infiltrating myeloid cells stimulates cancer cell invasion and facilitates tumor angiogenesis via an Interleukin 10- (IL10-) dependent manner [84]. Moreover, impaired tumor growth and angiogenesis were observed in PPAR beta/delta KO BMT mice due to PPAR beta/delta deficiency in tumor myeloid cells [84], suggesting that PPAR beta/delta plays a key role in tumor angiogenesis and progression in tumor myeloid cells of TME.

Furthermore, the endoplasmic reticulum (ER), an essential organelle involved in many cellular functions, is implicated in TME. In cancer, stressors like hypoxia, nutrient deprivation, and acidosis disrupt ER function and lead to accumulation of unfolded proteins in ER, a condition known as ER stress. Cells adapt to ER stress by activating an integrated signal transduction pathway called the unfolded protein response (UPR). UPR represents a survival response by the cells to restore ER homeostasis and has both survival and cell death effects. The mechanisms that determine cell fate during ER stress are not well understood. For instance, short exposure to ER stress initially increases AKT signaling, but long-term ER stress suppresses AKT signaling [85]. PPAR beta/delta activation has been shown to reduce endoplasmic reticulum (ER) stress-associated inflammation in skeletal muscle through an AMPK-dependent mechanism [86] and to reduce inflammation in response to chronic ER stress in cardiac cells [87]. Furthermore, it has been nicely shown that PPAR beta/delta can repress RAS-oncogene-induced ER stress to promote senescence in tumors [88] This is mediated through the decrease of p-AKT activity promoting cellular senescence through upregulation of p53 and p27 expression [89]. It would be interesting to investigate the direct effects of PPAR beta/delta on senescence of tumor endothelial cells in an in vivo setting. We recently showed that senescent endothelial cells are indispensable for a healthy lifespan and that removal of senescent endothelium disrupts vascular function leading to diminished vessel densities and fibrotic lesions [90]. If PPAR beta/delta mediates senescence of tumor endothelium thereby protecting vessel integrity, this might explain the enhanced tumor growth and vascularization upon PPAR beta/delta activation observed by us and others [13, 16, 77].

Most recently, Zuo et al. demonstrated that PPAR beta/delta in cancer cells regulates tumor angiogenesis in vivo and in vitro by promoting the secretion of proangiogenic factors including VEGF and Interleukin 8 (IL8) [18]. Most importantly, in our recent works, it has been shown that conditional inducible vascular endothelium-specific PPAR beta/delta overexpression in vivo leads to

enhanced tumor angiogenesis, tumor growth, and metastasis formation, further indicating a vascular EC-specific PPAR beta/delta action mechanism in tumor progression, independent of some controversial observations of PPAR beta/delta in specific tumor or cancer cell types [16]. Wagner et al. also firstly reported the mouse model in which rapid induction of cardiac angiogenesis and cardiac hypertrophy were observed [91, 92].

6.1. Crosstalk between PPAR Beta/Delta and Signal Molecules. PPAR beta/delta activation or overexpression may upregulate the expression of its various downstream signal molecules involved in tumor angiogenesis including proangiogenic factors (such as VEGF, PDGF, and FGF), proinvasive matrix-degrading enzymes (such as MMP9), proinflammatory mediators (such as COX2), and cytokines and chemokines (such as IL1 and CXCL8), even some of which have been further identified as PPAR beta/delta direct target genes. Besides a leading role of PPAR beta/delta among the signal molecules, PPAR beta/delta may function in TME linked to diverse kinds of cells through direct or indirect modulation of its downstream molecules.

6.1.1. Interplay between PPAR Beta/Delta and Inflammatory Angiogenesis. Inflammatory angiogenesis is a crucial process in tumor progression. For instance, the proinflammatory mediator cyclooxygenase-2 (COX2) is considered as a key regulator of angiogenesis and tumor growth through multiple downstream proangiogenic mechanisms such as production of VEGF and induction of MMPs. Moreover, selective inhibition of COX2 has also been shown to suppress angiogenesis in vivo and in vitro [93]. It is well known that VEGFA plays a critical role in both angiogenesis and vasculogenesis [94], and it leads the directional migration of tip cells and stalk cell proliferation in microtubule branches [95, 96]. It has also been demonstrated that MMP9 triggers the "angiogenic switch" during carcinogenesis and enhances the availability of VEGF to its receptors [97]. Furthermore, it has been reported that inflammatory cell MMP9 initiates the onset of tumor neovascularization during which there exists functional links between VEGF and MMPs including MMP9 [98]. LEPTIN is shown to mediate angiogenesis in vivo and in vitro through induction of EC proliferation and expression of MMP2 and MMP9 [99], and to further promote EC differentiation and directional migration through enhancement of COX2 activity [100]. LEPTIN could also induce angiogenesis via transactivation of VEGFR in ECs [101]. Additionally, besides inducing angiogenesis, PPAR beta/delta also functions in chronic inflammation-facilitating tumorigenesis through induction of COX2 and its product prostaglandin E2 (PGE2) in vivo [102, 103]. Interestingly, COX2, VEGF, MMP9, and LEPTIN have been identified as PPAR beta/delta target genes via a direct transcriptional activation mechanism in hepatocellular carcinoma cells [104], colorectal cancer cells [105, 106], EPCs [67, 69], and liposarcoma cells [107], respectively.

In TME, tumor-infiltrating inflammatory cells also help to induce and sustain tumor angiogenesis, and further to facilitate tissue invasion and tumor metastatic spread by releasing some signal molecules such as proinvasive MMP9 and inflammatory chemokines [108–110]. Chemotaxis is also a crucial process for inducing angiogenesis in tumors, either directly by attracting ECs towards tumor cells to form new vessels, or indirectly by mediating immune inflammatory cells to infiltrate, eventually promoting tumor angiogenesis [111]. Chemotaxis of tumor cells and stromal cells in TME is also required for tumor dissemination during tumor progression and metastasis [110, 111].

CXC chemokines such as CXCL8 (encoding IL8) and CXCL5 are also involved in COX2-associated angiogenesis to contribute to non-small-cell lung cancer progression [111, 112]. It is further shown that IL8 directly regulates angiogenesis via recruitment of neutrophils [112], which further drives VEGF activation [113]. Moreover, IL8-responding neutrophils are considered as the major source of angiogenesis-inducing MMP9 [98, 114]. Chemokine C-C motif ligand 2 (CCL2), in addition to the promotion of angiogenesis [115, 116], also enhances tumor metastasis [117]. Furthermore, myeloid monocytic cells such as myeloid-derived suppressor cells (MDSCs), tumor-associated macrophages (TAMs), and dendritic cells are recruited to the tumor site mainly by CCL2 and produce many proangiogenic factors such as VEGF, CXCL8, platelet-derived growth factor (PDGF), and transforming growth factor beta (TGF beta) [118–120]. In fact, both TGF beta and hypoxia are potent inducers of VEGF expression in tumor cells and collaborate with TME to provide the foundation of tumor angiogenesis and cancer cell invasion [121]. Importantly, IL8 has been reported as a key target gene of PPAR beta/delta to promote angiogenesis in vivo and in vitro [18], and CCL2 expression is also significantly upregulated upon vascular PPAR beta/-delta overexpression in vivo [16].

COX2 also mediates IL1 beta-induced angiogenesis in vitro and in vivo [122, 123]. IL1 beta supports neovascularization through the regulation of the expression of VEGF and its receptor VEGFR2 (FLK1/KDR) on ECs [124]. IL1 acts as an upstream proinflammatory mediator that initiates and disseminates the inflammatory state by inducing a local interactive network and increasing adhesion molecule expression on ECs and leukocytes, which facilitates tumor-associated angiogenesis [125]. In TME, inflammatory IL1 beta recruits myeloid cells from bone marrow and activates them to produce proangiogenic factors such as VEGF; VEGF further activates ECs and myeloid cells, promoting tumor invasiveness and fostering tumor angiogenesis [125]. In addition, IL6 also stimulates angiogenesis and vasculogenesis [126, 127]. However, Gopinathan et al. observed an IL6-induced newly forming vascular structure with defective pericyte (PC) coverage ex vivo [128], thus facilitating cancer cell infiltration and tumor metastasis through vascular leakage. Interestingly, IL1 and IL6 expression levels are significantly upregulated in the PPAR beta/delta overexpression mouse model reported recently [16].

In summary, PPAR beta/delta seems to act as a key leader in inflammatory mediator-driven tumor angiogenesis linked to TME in which many proinflammatory mediators, chemokines, and proangiogenic factors closely communicate with

each other, and also associate with tumor-infiltrating myeloid cells such as neutrophils, TAMs, and MDSCs.

6.1.2. Other Key PPAR Beta/Delta-Mediated Proangiogenic Factors. It has been demonstrated that Wilms' tumor suppressor WT1 is a major regulator of tumor neovascularization and tumor progression [129]. E26 avian leukemia oncogene 1 (ETS1) also plays a key role in regulating vascular development and haemopoiesis, particularly in angiogenesis [130]. In addition, ETS1 promotes cancer cell invasion through upregulation of MMPs [131]. Consistent with this, silencing of ETS1 in highly invasive breast cancer cells also reduces the expression of MMP9 and MMP1 [132].

ETS1 also acts as a key regulator of MMPs such as MMP1, MMP3, and MMP9 in human cancer-associated fibroblasts (CAFs) [133, 134]. CAFs support tumor growth by secreting growth factors such as VEGF, FGF, PDGF, and chemokines to stimulate angiogenesis and thereby promote cancer cell invasion and metastasis formation [135, 136]. CAFs, as metastatic tumor stroma, are a crucial component in tumor progression through the remodeling of the ECM structure, thus helping a tumor to acquire an aggressive phenotype [136, 137]. PPAR beta/delta in CAFs also exhibits a protumorigenic effect. It was reported that ablation of PPAR beta/delta in CAFs attenuated tumor growth by altering the redox balance in TME [138], suggesting that PPAR beta/delta in CAFs is also an important player in tumor development. ETS1 induces the expression of VEGF, VEGFR1, and VEGFR2 in ECs [139–141]. In turn, VEGF is also a major inducer of ETS1 in ECs through the activation of either the PI3K/AKT pathway or the MEK/ERK/1/2 signal cascade [142, 143]. WT1 is also reported to regulate tumor angiogenesis via direct transactivation of ETS1 [144].

SRY-related HMG-box 18 (SOX18) has also been reported previously to induce angiogenesis during tissue repair and wound healing [145] and cancer progression [146]. And most recently, it was further shown that specific EC-derived endovascular progenitors initiated a vasculogenic process and differentiated into more mature endothelial phenotypes within the core of the growing tumors through reactivation of SOX18 [147]. Interestingly, these important proangiogenic molecules including WT1, ETS1, and SOX18 are also significantly upregulated in the vascular PPAR beta/delta overexpression model in vivo [16]. And, WT1 is also identified as a target gene of PPAR beta/delta in melanoma cells [148].

6.1.3. PPAR Beta/Delta May Facilitate Cancer Progression at Diverse Cellular Levels in TME. PPAR beta/delta activation is shown to induce colonic cancer stem cell (CSC) expansion and to promote the liver metastasis of colorectal cancer in vivo via direct transactivation of the Nanog gene [149]. NANOG as a key transcriptional factor governs the self-renewal and pluripotency of stem cells [150], and cancer cells expressing NANOG also often exhibit stem cell properties [151]. Protooncogene c-KIT/CD117 is known as the mast/-stem cell factor receptor and receptor tyrosine kinase, and its activation in CSCs may regulate the stemness to control tumor progression and drug resistance to tyrosine kinase inhibitors. Moreover, c-KIT has been identified as a potential marker of the cancer stem-like cells [152]. In addition, c-KIT not only functions on ECs [153, 154] but also belongs to the tumor angiogenesis-promoting molecule [155–158]. Studies also suggested that activation of c-KIT enhances the expression of VEGF that can be suppressed by imatinib, an inhibitor of c-KIT in gastrointestinal stromal tumor cells, which thereby has an impact on tumor angiogenesis [159, 160]. c-KIT is also involved in pathological ocular neovascularization [161] and is regulated transcriptionally by WT1 [129] and PPAR beta/delta [16].

PDGFB and its receptor PDGFR beta, also known as angiogenic factors, are suggested to enhance angiogenesis and vasculogenesis via their function in ECs [162–164] and EPCs [165], and to regulate vascular permeability and vessel maturation through recruitment of pericytes (PCs) [166, 167] and smooth muscle cells (SMCs) [168] in newly forming vessels. Moreover, PDGFB and PDGFR beta also interact with other proangiogenic factors such as FGF2 [169, 170], VEGFA, and its receptor VEGFR2 [163]. Furthermore, PDGFB and PDGFR beta may also affect cancer growth and progression by directly acting on TME. Besides the crosstalk with CAFs [171–173], PDGFR beta in stromal fibroblasts may mediate PDGFB-induced TAM recruitment [174], thus implicating a role of PDGFR beta in tumor stroma to facilitate tumor progression. Most recently, it was further shown that specific targeting of PDGFR beta kinase activity in TME inhibited cancer growth and vascularization in cancers with high PDGFB expression such as LLC [175]. Therefore, this indicates the diverse role of PDGFB and PDGFR beta in facilitating tumor angiogenesis and progression at different cellular levels in TME. PDGFR beta is demonstrated as a target of telomeric repeat binding factor 2 (TRF2) that is further activated transcriptionally by WT1 [176]. PDGFB and PDGFR beta have further been identified as critical targets of PPAR beta/delta via a direct transactivation mechanism in vivo [16].

In conclusion, a variety of key signal molecules involved in tumor angiogenesis and tumor progression and metastasis have either been identified as PPAR beta/delta direct targets or largely upregulated in the vascular PPAR beta/delta overexpression model in vivo reported recently [16]. Thus, PPAR beta/delta activation seems to give rise to a highly angiogenic phenotype, and even plays a "hallmark" role in promoting tumor angiogenesis and progression. Interestingly, it appears that there could also exist a widely interactive network between the downstream protumor-angiogenic molecules as described above. Therefore, the crosstalk network is established between PPAR beta/delta and the various signal molecules, and also between those molecules (Figure 1(a)).

Moreover, in addition to cancer cells, PPAR beta/delta may also produce pleiotropic effects in TME by modulating downstream key molecules to act on ECs, EPCs, PCs, SMCs, CSCs, CAFs, and tumor-infiltrating inflammatory cells, indirectly facilitating tumor angiogenesis and further promoting cancer development (Figure 1(b)).

6.2. Other PPAR Beta/Delta Target Genes. PPAR beta/delta regulates the transcription of target genes via a direct

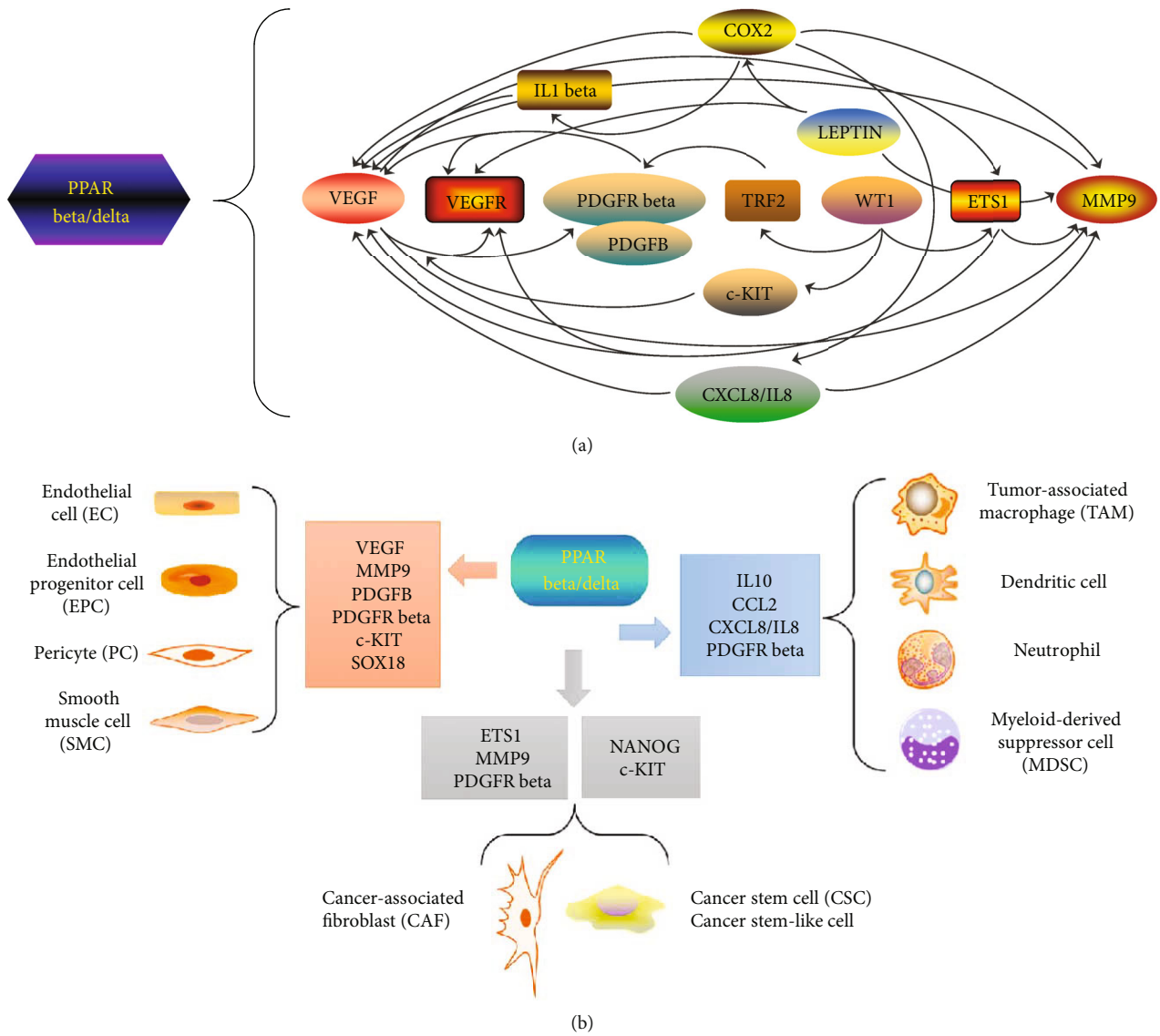

Figure 1: The "hallmark" role of PPAR beta/delta in tumor angiogenesis and progression. (a) Interplay between PPAR beta/delta and downstream key signal molecules. In the signal network of proangiogenic molecules, COX2 promotes the secretion of VEGF and MMPs including MMP9; COX2 infiltration also mediates IL1 beta-induced angiogenesis, which further activates VEGF; COX2 also contributes to cancer progression through the enhancement of the angiogenic chemokine CXCL8 (IL8) expression. IL8 drives VEGF activation and induces MMP9 expression. LEPTIN induces MMP9 expression, enhances COX2 activity, or transactivates VEGFR to facilitate angiogenesis. WT1 transactivates ETS1, TRF2, and c-KIT. ETS1 further upregulates the MMP9, VEGF, and VEGFR expression. In turn, VEGF is also a major inducer of ETS1. TRF2 transactivates PDGFR beta, and c-KIT may affect angiogenesis through the promotion of VEGF production. There exists a crosstalk between VEGF and MMP9 and between VEGF, VEGFR, and PDGFB and PDGFR beta. Oval shape: they represent those molecules that have been identified as direct target genes of PPAR beta/delta; rectangle shape: they represent those molecules that are significantly upregulated upon PPAR beta/delta overexpression. (b) Function of PPAR beta/delta at diverse cellular levels in TME. In TME, multiple distinct cells communicate and collaborate to enable tumor growth and progression. These cells include cancer cells, CSCs, ECs, EPCs, PCs, SMCs, CAFs, and tumor-infiltrating inflammatory cells. PPAR beta/delta can directly function on ECs and EPCs, or directly take action on them by regulating downstream signal molecules such as VEGF, MMP9, PDGFB, PDGFR beta, and SOX18. PDGFB and PDGFR beta regulate vascular permeability and maturation through the recruitment of PCs and SMCs. c-KIT also functions on ECs, c-KIT, and NANOG and may regulate the stemness to control cancer progression. ETS1 regulates MMP9 expression in CAFs; the crosstalk between CAFs and PDGFR beta also exists. PPAR beta/delta may act on tumor-infiltrating myeloid cells through the modulation of the IL10, IL8, CCL2, and PDGFR beta expression. As mentioned above, PPAR beta/delta stimulates cancer cell invasion and facilitates tumor angiogenesis in an IL10-dependent manner in tumor-infiltrating myeloid cells. IL8 can directly regulate angiogenesis via the recruitment of neutrophils. CCL2 is also a major regulator of recruitment of the myeloid monocytic cells such as MDSCs, TAMs, and dendritic cells. Also, PDGFR beta in stromal fibroblasts may mediate PDGFB-induced TAM recruitment. Among these molecules, SOX18, IL10, CCL2, and ETS1 are overexpressed upon PPAR beta/delta activation, and the others have been reported as direct targets of PPAR beta/delta.

Table 1: List of target genes of PPAR beta/delta.

PPAR beta/delta target genes	Cellular biological function	References (for target genes)
Calcineurin A	Induction of cardiac vascularization, cardiac growth, and skeletal muscle remodeling [47, 48]	[15]
COX2	An inflammatory angiogenic mediator and a key regulator of tumor angiogenesis [93, 122, 123]	[104]
VEGF	A key regulator of vasculogenesis and angiogenesis [74, 75, 76]	[105, 106]
MMP9	A proinvasive matrix-degrading enzyme and a key regulator of tumor angiogenesis and metastasis [77, 78]	[69]
LEPTIN	Regulation of endothelial cell behavior and angiogenesis [79, 80, 81]	[107]
IL8	A key angiogenic chemokine, a proinflammatory mediator, and a key regulator of tumor angiogenesis and progression [98, 111, 112, 114]	[18]
WT1	An important regulator of tumor angiogenesis and progression [129]	[148]
NANOG	Regulation of self-renewal of cancer stem cells or cancer stem-like cells [149–151]	[149]
c-KIT	A potential marker of cancer stem-like cells [152]; promotion of tumor angiogenesis [155–158] and pathological ocular neovascularization [161]	[16]
PDGFB	A key regulator of angiogenesis and vasculogenesis [162–165] and vascular permeability and maturation [166–168]	[16]
PDGFR beta	A key regulator of angiogenesis and vasculogenesis [162–165], vascular permeability and maturation [166–168], and tumor progression [174, 175]	[16]
ANGPTL4	Promotion of angiogenesis, tumor progression, and metastasis [178–182]	[183, 184]
PDK4	Regulation of EMT and cell metabolism, and cancer progression [185–188]	[189]
FABP4	Regulation of glucose and lipid metabolism; cell proliferation and apoptosis [190, 191]	[192]
CDKN1C	A prognostic factor for many types of cancer; regulation of angiogenesis and cancer hallmarks [193]	[17, 46]
SRC	Promotion of angiogenesis, cancer invasion, and tumor progression [194]	[194]
EDG2	Enhancement of endothelial cell differentiation and vasculogenesis [195]	[195]
FOXO1	Involvement of physiological, pathological, and developmental angiogenesis [196–198]	[199]
GLUT1	Promotion of cancer cell metabolism and tumor growth [200, 201]	[202]
SLC1-A5	Promotion of cancer cell metabolism and tumor progression [203, 204]	[202]

PPRE-dependent transactivation mechanism. The peroxisome proliferator response element (PPRE) comprises a direct repeat (DR) of AGGTCA separated by one nucleotide (DR1) as AGGTCA (N) AGGTCA [177]. But currently, it was shown that only PPAR alpha binds to this sequence; whether ligand activation has an impact on PPARs binding to DNA response elements is still controversial [4]. A variety of genes have been identified as direct targets of PPAR beta/-delta and are known to be involved in various cellular biological processes such as fatty acid oxidation, cell survival, inflammation, angiogenesis, cancer cell metabolism, and tumor progression. Direct target genes of PPAR beta/delta identified to date already include Calcineurin A, COX2, VEGF, MMP9, LEPTIN, IL8, WT1, NANOG, c-KIT, PDGFB, PDGFRB, ANGPTL4, PDK4, FABP4, CDKN1C, SRC, EDG2, FOXO1, GLUT1, and SLC1-A5 (Table 1).

As mentioned above, most of these PPAR beta/delta target genes have been suggested to be involved in tumor angiogenesis and progression. ANGPTL4 is a well-known target gene of PPAR beta/delta [183, 184], and it promotes angiogenesis [178, 179], cancer cell invasion [180], and tumor progression and metastasis [181, 182]. Pyruvate dehydrogenase kinase 4 (PDK4) may promote cancer progression by regulating epithelial-mesenchymal transition (EMT) [185, 186] and cancer cell metabolism [186–188]. Fatty acid binding protein 4 (FABP4) may affect cell proliferation and apoptosis by regulating glucose and lipid metabolism [190, 191]. Both PDK4 and FABP4 are the established targets of PPAR beta/delta respectively [189, 192].

Cyclin-dependent kinase inhibitor 1C (CDKN1C) gene, which encodes the cell cycle inhibitor $p57^{KIP2}$, has been suggested to be involved in the regulation of several cancer hallmarks such as inducing angiogenesis, and it has been tested as a prognostic factor for various cancers [17, 193], as well as a target of PPAR beta/delta [17]. Oncogene SRC has been reported to be a direct PPAR beta/delta target, and its tyrosine kinase activity triggers the EGFR/ERK1/2 signal cascade, which promotes the development of ultraviolet radiation-induced skin cancer [194]. Endothelial differentiation gene 2 (EDG2) is also transactivated directly by PPAR beta/delta in late EPCs and leads to enhanced vasculogenesis [195]. Forkhead box protein O1 (FOXO1) is required for EC proliferation and vascular growth [196, 198], and directly regulates VEGFA expression during wound healing [197]. In addition to the physiological angiogenesis, FOXO1 is suggested to be involved in developmental and pathological angiogenesis

[198], which is also activated transcriptionally by PPAR beta/delta [199].

Finally, glucose transporter 1 (GLUT1/SLC2A1), as a member of the GLUT family, is widely expressed in many types of cancer cells and plays a key role in glucose uptake for cancer cell metabolism to enable tumor cell growth and proliferation [200, 201]. Neutral amino acid transporter B (SLC1-A5) is an important glutamine transporter in the regulation of essential amino acid influx [203]; and importantly, depletion of SLC1-A5 is demonstrated to abolish tumor progression [204]. Both GLUT1 and SLC1-A5 have been suggested to facilitate tumor progression and are transactivated directly by PPAR beta/delta [202].

For further information, PPARbeta/delta-related signaling pathways are covered by KEGG (Kyoto Encyclopedia of Genes and Genomes) (PATHWAY: map 03320), by the REACTOME pathway database (R-HSA-446176), and by the Protein-Protein Interaction Networks Functional Enrichment Analysis in STRING functional protein association network database (https://string-db.org/cgi/network.pl?taskId=OUdxEiHw19dW).

7. Conclusion

PPAR alpha and PPAR gamma seem to have an antiangiogenic role, but there are still conflicting observations. Unlike them, PPAR beta/delta exerts proangiogenic effects. Especially, there exists an intensive crosstalk between PPAR beta/delta and various signal molecules including the identified target genes, and also between those molecules. PPAR beta/delta plays a leading role in the network of interplay by directly and indirectly modulating the downstream proinflammatory or protumorigenic angiogenic molecules which further act on multiple different cell types in TME, thus indicating a potent "hallmark" role of PPAR beta/delta in tumor angiogenesis, cancer progression, and metastasis.

Conflicts of Interest

The authors declare no conflict of interest.

Authors' Contributions

S.D. conceived the idea. S.D., N.W., and K.-D.W. searched the literature and wrote the manuscript. S.D. performed the schematic visualization. Nicole Wagner and Kay-Dietrich Wagner contributed equally to this work.

Acknowledgments

This research was funded by a grant from the China Scholarship Council (CSC) (S.D.), the Fondation ARC pour la Recherche sur le Cancer, grant number n_PJA 20161204650 (N.W.), Gemluc (N.W.), Plan Cancer INSERM, and Fondation pour la Recherche Médicale (K.-D.W.).

References

[1] L. A. Moraes, L. Piqueras, and D. Bishop-Bailey, "Peroxisome proliferator-activated receptors and inflammation," *Pharmacology & Therapeutics*, vol. 110, no. 3, pp. 371–385, 2006.

[2] D. H. van Raalte, M. Li, P. H. Pritchard, and K. M. Wasan, "Peroxisome proliferator-activated receptor (PPAR)-: a pharmacological target with a promising future," *Pharmaceutical Research*, vol. 21, no. 9, pp. 1531–1538, 2004.

[3] M. Ahmadian, J. M. Suh, N. Hah et al., "PPARγ signaling and metabolism: the good, the bad and the future," *Nature Medicine*, vol. 19, no. 5, pp. 557–566, 2013.

[4] K. D. Wagner and N. Wagner, "Peroxisome proliferator-activated receptor beta/delta (PPARβ/δ) acts as regulator of metabolism linked to multiple cellular functions," *Pharmacology & Therapeutics*, vol. 125, no. 3, pp. 423–435, 2010.

[5] D. Panigrahy, A. Kaipainen, S. Huang et al., "PPARalpha agonist fenofibrate suppresses tumor growth through direct and indirect angiogenesis inhibition," in *Proceedings of the National Academy of Sciences*, vol. 105no. 3, pp. 985–990, 2008.

[6] Y. Yokoyama, B. Xin, T. Shigeto et al., "Clofibric acid, a peroxisome proliferator-activated receptor alpha ligand, inhibits growth of human ovarian cancer," *Molecular Cancer Therapeutics*, vol. 6, no. 4, pp. 1379–1386, 2007.

[7] A. Pozzi and J. H. Capdevila, "PPAR Ligands as Antitumorigenic and Antiangiogenic Agents," *PPAR Research*, vol. 2008, Article ID 906542, 8 pages, 2008.

[8] D. Panigrahy, S. Singer, L. Q. Shen et al., "PPARgamma ligands inhibit primary tumor growth and metastasis by inhibiting angiogenesis," *Journal of Clinical Investigation*, vol. 110, no. 7, pp. 923–932, 2002.

[9] V. G. Keshamouni, D. A. Arenberg, R. C. Reddy, M. J. Newstead, S. Anthwal, and T. J. Standiford, "PPAR-γ Activation Inhibits Angiogenesis by Blocking ELR+CXC Chemokine Production in Non-small Cell Lung Cancer," *Neoplasia*, vol. 7, no. 3, pp. 294–301, 2005.

[10] J. A. Copland, L. A. Marlow, S. Kurakata et al., "Novel high-affinity PPAR _γ_ agonist alone and in combination with paclitaxel inhibits human anaplastic thyroid carcinoma tumor growth via $p21^{WAF1/CIP1}$," *Oncogene*, vol. 25, no. 16, pp. 2304–2317, 2006.

[11] A. Kaipainen, M. W. Kieran, S. Huang et al., "PPARalpha deficiency in inflammatory cells suppresses tumor growth," *PLoS ONE*, vol. 2, no. 2, article e260, 2007.

[12] L. Tian, J. Zhou, M. C. Casimiro et al., "Activating peroxisome proliferator-activated receptor gamma mutant promotes tumor growth in vivo by enhancing angiogenesis," *Cancer Research*, vol. 69, no. 24, pp. 9236–9244, 2009.

[13] A. Abdollahi, C. Schwager, J. Kleeff et al., "Transcriptional network governing the angiogenic switch in human pancreatic cancer," in *Proceedings of the National Academy of Sciences*, vol. 104no. 31, pp. 12890–12895, 2007.

[14] M. Yoshinaga, Y. Kitamura, T. Chaen et al., "The simultaneous expression of peroxisome proliferator-activated receptor delta and cyclooxygenase-2 may enhance angiogenesis and tumor venous invasion in tissues of colorectal cancers," *Digestive Diseases and Sciences*, vol. 54, no. 5, pp. 1108–1114, 2009.

[15] N. Wagner, C. Jehl-Piétri, P. Lopez et al., "Peroxisome proliferator-activated receptor beta stimulation induces rapid

cardiac growth and angiogenesis via direct activation of calcineurin," *Cardiovascular Research*, vol. 83, no. 1, pp. 61–71, 2009.

[16] K. D. Wagner, S. Du, L. Martin, N. Leccia, J. F. Michiels, and N. Wagner, "Vascular PPARβ/δ promotes tumor angiogenesis and progression," *Cells*, vol. 8, no. 12, p. 1623, 2019.

[17] S. Müller-Brüsselbach, M. Kömhoff, M. Rieck et al., "Deregulation of tumor angiogenesis and blockade of tumor growth in PPARbeta-deficient mice," *The EMBO Journal*, vol. 26, no. 15, pp. 3686–3698, 2007.

[18] X. Zuo, W. Xu, M. Xu et al., "Metastasis regulation by PPARD expression in cancer cells," *JCI Insight*, vol. 2, no. 1, article e91419, 2017.

[19] P. Carmeliet, "VEGF as a Key Mediator of Angiogenesis in Cancer," *Oncology*, vol. 69, no. 3, Suppl 3, pp. 4–10, 2005.

[20] P. Carmeliet and R. K. Jain, "Molecular mechanisms and clinical applications of angiogenesis," *Nature*, vol. 473, no. 7347, pp. 298–307, 2011.

[21] P. Carmeliet, "Angiogenesis in health and disease," *Nature Medicine*, vol. 9, no. 6, pp. 653–660, 2003.

[22] W. Risau and I. Flamme, "Vasculogenesis," *Annual Review of Cell and Developmental Biology*, vol. 11, no. 1, pp. 73–91, 1995.

[23] D. Hanahan and J. Folkman, "Patterns and emerging mechanisms of the angiogenic switch during tumorigenesis," *Cell*, vol. 86, no. 3, pp. 353–364, 1996.

[24] G. Bergers and L. E. Benjamin, "Tumorigenesis and the angiogenic switch," *Nature Reviews Cancer*, vol. 3, no. 6, pp. 401–410, 2003.

[25] V. Baeriswyl and G. Christofori, "The angiogenic switch in carcinogenesis," *Seminars in Cancer Biology*, vol. 19, no. 5, pp. 329–337, 2009.

[26] D. Hanahan and R. A. Weinberg, "Hallmarks of cancer: the next generation," *Cell*, vol. 144, no. 5, pp. 646–674, 2011.

[27] S. R. McDougall, A. R. A. Anderson, and M. A. J. Chaplain, "Mathematical modelling of dynamic adaptive tumour-induced angiogenesis: clinical implications and therapeutic targeting strategies," *Journal of Theoretical Biology*, vol. 241, no. 3, pp. 564–589, 2006.

[28] L. M. Sherwood, E. E. Parris, and J. Folkman, "Tumor angiogenesis: therapeutic implications," *New England Journal of Medicine*, vol. 285, no. 21, pp. 1182–1186, 1971.

[29] N. Marx, G. K. Sukhova, T. Collins, P. Libby, and J. Plutzky, "PPARalpha activators inhibit cytokine-induced vascular cell adhesion molecule-1 expression in human endothelial cells," *Circulation*, vol. 99, no. 24, pp. 3125–3131, 1999.

[30] J.-V. Pille, J. Varet, L. Vincent et al., "Fenofibrate inhibits angiogenesis in vitro and in vivo," *Cellular and Molecular Life Sciences (CMLS)*, vol. 60, no. 4, pp. 810–819, 2003.

[31] J. Varet, S. K. Douglas, L. Gilmartin et al., "VEGF in the lung: a role for novel isoforms," *American Journal of Physiology-Lung Cellular and Molecular Physiology*, vol. 298, no. 6, pp. L768–L774, 2010.

[32] F. Biscetti, E. Gaetani, A. Flex et al., "Selective activation of peroxisome proliferator-activated receptor (PPAR) alpha and PPAR gamma induces neoangiogenesis through a vascular endothelial growth factor-dependent mechanism," *Diabetes*, vol. 57, no. 5, pp. 1394–1404, 2008.

[33] J. Z. Zhang and K. W. Ward, "WY-14 643, a selective PPAR{-alpha} agonist, induces proinflammatory and proangiogenic responses in human ocular cells," *International Journal of Toxicology*, vol. 29, no. 5, pp. 496–504, 2010.

[34] K. Kitajima, S. Miura, Y. Mastuo, Y. Uehara, and K. Saku, "Newly developed PPAR-α agonist (R)-K-13675 inhibits the secretion of inflammatory markers without affecting cell proliferation or tube formation," *Atherosclerosis*, vol. 203, no. 1, pp. 75–81, 2009.

[35] T. Arima, M. Uchiyama, Y. Nakano et al., "Peroxisome proliferator-activated receptor alpha agonist suppresses neovascularization by reducing both vascular endothelial growth factor and angiopoietin-2 in corneal alkali burn," *Scientific Reports*, vol. 7, no. 1, p. 17763, 2017.

[36] X. Xin, S. Yang, J. Kowalski, and M. E. Gerritsen, "Peroxisome proliferator-activated receptor gamma ligands are potent inhibitors of angiogenesis in vitro and in vivo," *Journal of Biological Chemistry*, vol. 274, no. 13, pp. 9116–9121, 1999.

[37] T. Murata, S. He, M. Hangai et al., "Peroxisome proliferator-activated receptor-gamma ligands inhibit choroidal neovascularization," *Investigative Ophthalmology & Visual Science*, vol. 41, no. 8, pp. 2309–2317, 2000.

[38] D. Bishop-Bailey and T. Hla, "Endothelial cell apoptosis induced by the peroxisome proliferator-activated receptor (PPAR) ligand 15-deoxy-delta 12, 14-prostaglandin J2," *Journal of Biological Chemistry*, vol. 274, no. 24, pp. 17042–17048, 1999.

[39] A. Aljada, L. O'Connor, Y.-Y. Fu, and S. A. Mousa, "PPAR gamma ligands, rosiglitazone and pioglitazone, inhibit bFGF- and VEGF-mediated angiogenesis," *Angiogenesis*, vol. 11, no. 4, pp. 361–367, 2008.

[40] A. Higuchi, K. Ohashi, R. Shibata, S. Sono-Romanelli, K. Walsh, and N. Ouchi, "Thiazolidinediones reduce pathological neovascularization in ischemic retina via an adiponectin-dependent mechanism," *Arteriosclerosis, Thrombosis, and Vascular Biology*, vol. 30, no. 1, pp. 46–53, 2010.

[41] A. Stahl, P. Sapieha, K. M. Connor et al., "Short communication: PPAR gamma mediates a direct antiangiogenic effect of omega 3-PUFAs in proliferative retinopathy," *Circulation Research*, vol. 107, no. 4, pp. 495–500, 2010.

[42] C. Gensch, Y. P. Clever, C. Werner, M. Hanhoun, M. Böhm, and U. Laufs, "The PPAR-γ agonist pioglitazone increases neoangiogenesis and prevents apoptosis of endothelial progenitor cells," *Atherosclerosis*, vol. 192, no. 1, pp. 67–74, 2007.

[43] K. Nadra, L. Quignodon, C. Sardella et al., "PPARγ in placental angiogenesis," *Endocrinology*, vol. 151, no. 10, pp. 4969–4981, 2010.

[44] J. Kotlinowski and A. Jozkowicz, "PPAR gamma and angiogenesis: endothelial cells perspective," *Journal of Diabetes Research*, vol. 2016, Article ID 8492353, 11 pages, 2016.

[45] Y. Lecarpentier, V. Claes, A. Vallée, and J. L. Hébert, "Thermodynamics in cancers: opposing interactions between PPAR gamma and the canonical WNT/beta-catenin pathway," *Clinical and Translational Medicine*, vol. 6, no. 1, p. 14, 2017.

[46] R. L. Stephen, M. C. U. Gustafsson, M. Jarvis et al., "Activation of peroxisome proliferator-activated receptor delta stimulates the proliferation of human breast and prostate cancer cell lines," *Cancer Research*, vol. 64, no. 9, pp. 3162–3170, 2004.

[47] J. Y. Liou, S. Lee, D. Ghelani, N. Matijevic-Aleksic, and K. K. Wu, "Protection of endothelial survival by peroxisome

proliferator-activated Receptor-δ mediated 14-3-3 upregulation," *Arteriosclerosis, Thrombosis, and Vascular Biology*, vol. 26, no. 7, pp. 1481–1487, 2006.

[48] L. Piqueras, A. R. Reynolds, K. M. Hodivala-Dilke et al., "Activation of PPARβ/δ induces endothelial cell proliferation and angiogenesis," *Arteriosclerosis, Thrombosis, and Vascular Biology*, vol. 27, no. 1, pp. 63–69, 2007.

[49] J. Adamkiewicz, K. Kaddatz, M. Rieck, B. Wilke, S. Müller-Brüsselbach, and R. Müller, "Proteomic profile of mouse fibroblasts with a targeted disruption of the peroxisome proliferator activated receptor-beta/delta gene," *Proteomics*, vol. 7, no. 8, pp. 1208–1216, 2007.

[50] S. Bohman, T. Matsumoto, K. Suh et al., "Proteomic analysis of vascular endothelial growth factor-induced endothelial cell differentiation reveals a role for chloride intracellular channel 4 (CLIC4) in tubular morphogenesis," *Journal of Biological Chemistry*, vol. 280, no. 51, pp. 42397–42404, 2005.

[51] Y. S. Kuppumbatti, B. Rexer, S. Nakajo, K. Nakaya, and R. Mira-y-Lopez, "CRBP suppresses breast cancer cell survival and anchorage-independent growth," *Oncogene*, vol. 20, no. 50, pp. 7413–7419, 2001.

[52] Y. Barak, D. Liao, W. He et al., "Effects of peroxisome proliferator-activated receptor delta on placentation, adiposity, and colorectal cancer," in *Proceedings of the National Academy of Sciences*, vol. 99no. 1, pp. 303–308, 2002.

[53] K. Nadra, S. I. Anghel, E. Joye et al., "Differentiation of Trophoblast Giant Cells and Their Metabolic Functions Are Dependent on Peroxisome Proliferator-Activated Receptor β/δ," *Molecular and Cellular Biology*, vol. 26, no. 8, pp. 3266–3281, 2006.

[54] F. Wieser, L. Waite, C. Depoix, and R. N. Taylor, "PPAR action in human placental development and pregnancy and its complications," *PPAR Research*, vol. 2008, Article ID 527048, 14 pages, 2008.

[55] S. Luquet, J. Lopez-Soriano, D. Holst et al., "Peroxisome proliferator-activated receptor δ controls muscle development and oxydative capability," *The FASEB Journal*, vol. 17, no. 15, pp. 2299–2301, 2003.

[56] Y. X. Wang, C. L. Zhang, R. T. Yu et al., "Regulation of muscle fiber type and running endurance by PPARdelta," *PLoS Biology*, vol. 2, no. 10, article e294, 2004.

[57] V. A. Narkar, M. Downes, R. T. Yu et al., "AMPK and PPARδ Agonists Are Exercise Mimetics," *Cell*, vol. 134, no. 3, pp. 405–415, 2008.

[58] C. Gaudel, C. Schwartz, C. Giordano, N. A. Abumrad, and P. A. Grimaldi, "Pharmacological activation of PPARbeta promotes rapid and calcineurin-dependent fiber remodeling and angiogenesis in mouse skeletal muscle," *American Journal of Physiology-Endocrinology and Metabolism*, vol. 295, no. 2, pp. E297–E304, 2008.

[59] M. E. Capozzi, G. W. McCollum, S. R. Savage, and J. S. Penn, "Peroxisome proliferator-activated receptor-β/δ regulates angiogenic cell behaviors and oxygen-induced retinopathy," *Investigative Opthalmology & Visual Science*, vol. 54, no. 6, pp. 4197–4207, 2013.

[60] M. Choudhary, J.-d. Ding, X. Qi et al., "PPARβ/δ selectively regulates phenotypic features of age-related macular degeneration," *Aging*, vol. 8, no. 9, pp. 1952–1978, 2016.

[61] R. Yasumatsu, T. Nakashima, M. Masuda et al., "Effects of the angiotensin-I converting enzyme inhibitor perindopril on tumor growth and angiogenesis in head and neck squamous cell carcinoma cells," *Journal of Cancer Research and Clinical Oncology*, vol. 130, no. 10, pp. 567–573, 2004.

[62] O. V. Volpert, W. F. Ward, M. W. Lingen et al., "Captopril inhibits angiogenesis and slows the growth of experimental tumors in rats," *Journal of Clinical Investigation*, vol. 98, no. 3, pp. 671–679, 1996.

[63] A. Dueñas-González, P. García-López, L. Herrera, J. Medina-Franco, A. González-Fierro, and M. Candelaria, "The prince and the pauper. A tale of anticancer targeted agents," *Molecular Cancer*, vol. 7, no. 1, p. 82, 2008.

[64] E. S. Kang, J. S. Hwang, W. J. Lee et al., "Ligand-activated PPARδ inhibits angiotensin II-stimulated hypertrophy of vascular smooth muscle cells by targeting ROS," *PLOS ONE*, vol. 14, no. 1, p. e0210482, 2019.

[65] Y. Takata, J. Liu, F. Yin et al., "PPARdelta-mediated antiinflammatory mechanisms inhibit angiotensin II-accelerated atherosclerosis," in *Proceedings of the National Academy of Sciences*, vol. 105no. 11, pp. 4277–4282, 2008.

[66] A. Vallée, B. L. Lévy, and J. Blacher, "Interplay between the renin-angiotensin system, the canonical WNT/β-catenin pathway and PPARγ in hypertension," *Current Hypertension Reports*, vol. 20, no. 7, 2018.

[67] J. K. Han, H. S. Lee, H. M. Yang et al., "Peroxisome proliferator-activated receptor-delta agonist enhances vasculogenesis by regulating endothelial progenitor cells through genomic and nongenomic activations of the phosphatidylinositol 3-kinase/Akt pathway," *Circulation*, vol. 118, no. 10, pp. 1021–1033, 2008.

[68] T. He, T. Lu, L. V. d'Uscio, C. F. Lam, H. C. Lee, and Z. S. Katusic, "Angiogenic function of prostacyclin biosynthesis in human endothelial progenitor cells," *Circulation Research*, vol. 103, no. 1, pp. 80–88, 2008.

[69] J. K. Han, H. L. Kim, K. H. Jeon et al., "Peroxisome proliferator-activated receptor-δ activates endothelial progenitor cells to induce angio-myogenesis through matrix metallo-proteinase-9-mediated insulin-like growth factor-1 paracrine networks," *European Heart Journal*, vol. 34, no. 23, pp. 1755–1765, 2013.

[70] R. A. Gupta, J. Tan, W. F. Krause et al., "Prostacyclin-mediated activation of peroxisome proliferator-activated receptor delta in colorectal cancer," in *Proceedings of the National Academy of Sciences*, vol. 97no. 24, pp. 13275–13280, 2000.

[71] T. V. Pedchenko, A. L. Gonzalez, D. Wang, R. N. DuBois, and P. P. Massion, "Peroxisome proliferator-activated receptor beta/delta expression and activation in lung cancer," *American Journal of Respiratory Cell and Molecular Biology*, vol. 39, no. 6, pp. 689–696, 2008.

[72] H. Yuan, J. Lu, J. Xiao et al., "PPARδ induces estrogen receptor-positive mammary neoplasia through an inflammatory and metabolic phenotype linked to mTOR activation," *Cancer Research*, vol. 73, no. 14, pp. 4349–4361, 2013.

[73] X. Zuo, Y. Deguchi, W. Xu et al., "PPARD and interferon gamma promote transformation of gastric progenitor cells and tumorigenesis in mice," *Gastroenterology*, vol. 157, no. 1, pp. 163–178, 2019.

[74] J. M. Peters, J. E. Foreman, and F. J. Gonzalez, "Dissecting the role of peroxisome proliferator-activated receptor-β/δ (PPARβ/δ) in colon, breast, and lung carcinogenesis," *Cancer and Metastasis Reviews*, vol. 30, no. 3-4, pp. 619–640, 2011.

[75] J. M. Peters, Y. M. Shah, and F. J. Gonzalez, "The role of peroxisome proliferator-activated receptors in carcinogenesis and chemoprevention," *Nature Reviews Cancer*, vol. 12, no. 3, pp. 181–195, 2012.

[76] J. M. Peters, F. J. Gonzalez, and R. Müller, "Establishing the role of PPARβ/δ in carcinogenesis," *Trends in Endocrinology & Metabolism*, vol. 26, no. 11, pp. 595–607, 2015.

[77] N. Wagner and K. D. Wagner, "PPAR beta/delta and the hallmarks of cancer," *Cells*, vol. 9, no. 5, p. 1133, 2020.

[78] D. Bishop-Bailey and K. E. Swales, "The role of PPARs in the endothelium: implications for cancer therapy," *PPAR Research*, vol. 2008, Article ID 904251, 12 pages, 2008.

[79] D. Bishop-Bailey, "A Role for PPAR β / δ in Ocular Angiogenesis," *PPAR Research*, vol. 2008, Article ID 825970, 6 pages, 2008.

[80] D. Bishop-Bailey, "PPARs and angiogenesis," *Biochemical Society Transactions*, vol. 39, no. 6, pp. 1601–1605, 2011.

[81] E. Jeong, J. E. Koo, S. H. Yeon, M. K. Kwak, D. H. Hwang, and J. Y. Lee, "PPARδ deficiency disrupts hypoxia-mediated tumorigenic potential of colon cancer cells," *Molecular Carcinogenesis*, vol. 53, no. 11, pp. 926–937, 2014.

[82] J. Condeelis and J. W. Pollard, "Macrophages: obligate partners for tumor cell migration, invasion, and metastasis," *Cell*, vol. 124, no. 2, pp. 263–266, 2006.

[83] M. C. Schmid and J. A. Varner, "Myeloid cells in the tumor microenvironment: modulation of tumor angiogenesis and tumor inflammation," *Journal of Oncology*, vol. 2010, Article ID 201026, 10 pages, 2010.

[84] J. Park, S. E. Lee, J. Hur et al., "M-CSF from cancer cells induces fatty acid synthase and PPARβ/δ activation in tumor myeloid cells, leading to tumor progression," *Cell Reports*, vol. 10, no. 9, pp. 1614–1625, 2015.

[85] Y. C. Tsai and A. M. Weissman, "The unfolded protein response, degradation from endoplasmic reticulum and cancer," *Genes Cancer*, vol. 1, no. 7, pp. 764–778, 2010.

[86] L. Salvadó, E. Barroso, A. M. Gómez-Foix et al., "PPARβ/δ prevents endoplasmic reticulum stress-associated inflammation and insulin resistance in skeletal muscle cells through an AMPK-dependent mechanism," *Diabetologia*, vol. 57, no. 10, pp. 2126–2135, 2014.

[87] X. Palomer, E. Capdevila-Busquets, G. Botteri et al., "PPARβ/δ attenuates palmitate-induced endoplasmic reticulum stress and induces autophagic markers in human cardiac cells," *International Journal of Cardiology*, vol. 174, no. 1, pp. 110–118, 2014.

[88] B. Zhu, C. H. Ferry, L. K. Markell et al., "The nuclear receptor peroxisome proliferator-activated receptor-β/δ (PPARβ/δ) promotes oncogene-induced cellular senescence through repression of endoplasmic reticulum stress," *Journal of Biological Chemistry*, vol. 289, no. 29, pp. 20102–20119, 2014.

[89] B. Zhu, C. H. Ferry, N. Blazanin et al., "PPARβ/δ promotes HRAS-induced senescence and tumor suppression by potentiating p-ERK and repressing p-AKT signaling," *Oncogene*, vol. 33, no. 46, pp. 5348–5359, 2014.

[90] L. Grosse, N. Wagner, A. Emelyanov et al., "Defined p16^{High} Senescent Cell Types Are Indispensable for Mouse Healthspan," *Cell Metabolism*, vol. 32, no. 1, pp. 87–99.e6, 2020.

[91] K. D. Wagner, A. Vukolic, D. Baudouy, J. F. Michiels, and N. Wagner, "Erratum to "Inducible conditional vascular-specific overexpression of peroxisome proliferator-activated receptor beta/delta leads to rapid cardiac hypertrophy"," *PPAR Research*, vol. 2018, Article ID 5480829, 4 pages, 2018.

[92] K. D. Wagner, A. Vukolic, D. Baudouy, J. F. Michiels, and N. Wagner, "Inducible conditional vascular-specific overexpression of peroxisome proliferator-activated receptor beta/-delta leads to rapid cardiac hypertrophy," *PPAR Research*, vol. 2016, Article ID 7631085, 12 pages, 2016.

[93] S. Gately and W. W. Li, "Multiple roles of COX-2 in tumor angiogenesis: a target for antiangiogenic therapy," *Seminars in Oncology*, vol. 31, 2 Suppl 7, pp. 2–11, 2004.

[94] J. A. Nagy, A. M. Dvorak, and H. F. Dvorak, "VEGF-A and the induction of pathological angiogenesis," *Annual Review of Pathology: Mechanisms of Disease*, vol. 2, no. 1, pp. 251–275, 2007.

[95] H. Gerhardt, M. Golding, M. Fruttiger et al., "VEGF guides angiogenic sprouting utilizing endothelial tip cell filopodia," *Journal of Cell Biology*, vol. 161, no. 6, pp. 1163–1177, 2003.

[96] M. Hellström, L. K. Phng, and H. Gerhardt, "VEGF and Notch Signaling," *Cell Adhesion & Migration*, vol. 1, no. 3, pp. 133–136, 2014.

[97] G. Bergers, R. Brekken, G. McMahon et al., "Matrix metalloproteinase-9 triggers the angiogenic switch during carcinogenesis," *Nature Cell Biology*, vol. 2, no. 10, pp. 737–744, 2000.

[98] E. I. Deryugina and J. P. Quigley, "Tumor angiogenesis: MMP-mediated induction of intravasation- and metastasis-sustaining neovasculature," *Matrix Biology*, vol. 44-46, pp. 94–112, 2015.

[99] H.-Y. Park, H. M. Kwon, H. J. Lim et al., "Potential role of leptin in angiogenesis: leptin induces endothelial cell proliferation and expression of matrix metalloproteinases in vivo and in vitro," *Experimental & Molecular Medicine*, vol. 33, no. 2, pp. 95–102, 2001.

[100] E. Garonna, K. M. Botham, G. M. Birdsey, A. M. Randi, R. R. Gonzalez-Perez, and C. P. D. Wheeler-Jones, "Vascular endothelial growth factor receptor-2 couples cyclo-oxygenase-2 with pro-angiogenic actions of leptin on human endothelial cells," *PLoS ONE*, vol. 6, no. 4, p. e18823, 2011.

[101] V. Lanier, C. Gillespie, M. Leffers et al., "Leptin-induced transphosphorylation of vascular endothelial growth factor receptor increases Notch and stimulates endothelial cell angiogenic transformation," *The International Journal of Biochemistry & Cell Biology*, vol. 79, pp. 139–150, 2016.

[102] D. Wang, L. Fu, W. Ning et al., "Peroxisome proliferator-activated receptor δ promotes colonic inflammation and tumor growth," in *Proceedings of the National Academy of Sciences*, vol. 111no. 19, pp. 7084–7089, 2014.

[103] D. Wang and R. N. DuBois, "Therapeutic potential of peroxisome proliferator-activated receptors in chronic inflammation and colorectal cancer," *Gastroenterology Clinics of North America*, vol. 39, no. 3, pp. 697–707, 2010.

[104] B. Glinghammar, J. Skogsberg, A. Hamsten, and E. Ehrenborg, "PPARδ activation induces COX-2 gene expression and cell proliferation in human hepatocellular carcinoma cells," *Biochemical and Biophysical Research Communications*, vol. 308, no. 2, pp. 361–368, 2003.

[105] D. Wang, H. Wang, Y. Guo et al., "Crosstalk between peroxisome proliferator-activated receptor delta and VEGF stimulates cancer progression," in *Proceedings of the*

National Academy of Sciences, vol. 103no. 50, pp. 19069–19074, 2006.

[106] X. Zuo, Z. Peng, M. J. Moussalli et al., "Targeted genetic disruption of peroxisome proliferator-activated receptor-delta and colonic tumorigenesis," *JNCI: Journal of the National Cancer Institute*, vol. 101, no. 10, pp. 762–767, 2009.

[107] K. D. Wagner, M. Benchetrit, L. Bianchini, J. F. Michiels, and N. Wagner, "Peroxisome proliferator-activated receptor β/δ (PPARβ/δ) is highly expressed in liposarcoma and promotes migration and proliferation," *The Journal of Pathology*, vol. 224, no. 4, pp. 575–588, 2011.

[108] B. Z. Qian and J. W. Pollard, "Macrophage diversity enhances tumor progression and metastasis," *Cell*, vol. 141, no. 1, pp. 39–51, 2010.

[109] S. B. Coffelt, A. O. Tal, A. Scholz et al., "Angiopoietin-2 regulates gene expression in TIE2-expressing monocytes and augments their inherent proangiogenic functions," *Cancer Research*, vol. 70, no. 13, pp. 5270–5280, 2010.

[110] E. T. Roussos, J. S. Condeelis, and A. Patsialou, "Chemotaxis in cancer," *Nature Reviews Cancer*, vol. 11, no. 8, pp. 573–587, 2011.

[111] M. Põld, L. X. Zhu, S. Sharma et al., "Cyclooxygenase-2-dependent expression of angiogenic CXC chemokines ENA-78/CXC ligand (CXCL) 5 and interleukin-8/CXCL8 in human non-small cell lung cancer," *Cancer Research*, vol. 64, no. 5, pp. 1853–1860, 2004.

[112] S. Tazzyman, C. E. Lewis, and C. Murdoch, "Neutrophils: key mediators of tumour angiogenesis," *International Journal of Experimental Pathology*, vol. 90, no. 3, pp. 222–231, 2009.

[113] H. Nozawa, C. Chiu, and D. Hanahan, "Infiltrating neutrophils mediate the initial angiogenic switch in a mouse model of multistage carcinogenesis," in *Proceedings of the National Academy of Sciences*, vol. 103no. 33, pp. 12493–12498, 2006.

[114] E. I. Deryugina, E. Zajac, A. Juncker-Jensen, T. A. Kupriyanova, L. Welter, and J. P. Quigley, "Tissue-Infiltrating Neutrophils Constitute the Major _In Vivo_ Source of Angiogenesis-Inducing MMP-9 in the Tumor Microenvironment," *Neoplasia*, vol. 16, no. 10, pp. 771–788, 2014.

[115] S. M. Stamatovic, R. F. Keep, M. Mostarica-Stojkovic, and A. V. Andjelkovic, "CCL2 regulates angiogenesis via activation of Ets-1 transcription factor," *The Journal of Immunology*, vol. 177, no. 4, pp. 2651–2661, 2006.

[116] J. Ehling, M. Bartneck, X. Wei et al., "CCL2-dependent infiltrating macrophages promote angiogenesis in progressive liver fibrosis," *Gut*, vol. 63, no. 12, pp. 1960–1971, 2014.

[117] M. Roblek, D. Protsyuk, P. F. Becker et al., "CCL2 is a vascular permeability factor inducing CCR2-dependent endothelial retraction during lung metastasis," *Molecular Cancer Research*, vol. 17, no. 3, pp. 783–793, 2019.

[118] J. A. Joyce and J. W. Pollard, "Microenvironmental regulation of metastasis," *Nature Reviews Cancer*, vol. 9, no. 4, pp. 239–252, 2009.

[119] S. Danese and A. Mantovani, "Inflammatory bowel disease and intestinal cancer: a paradigm of the Yin-Yang interplay between inflammation and cancer," *Oncogene*, vol. 29, no. 23, pp. 3313–3323, 2010.

[120] M. Erreni, A. Mantovani, and P. Allavena, "Tumor-associated macrophages (TAM) and inflammation in colorectal cancer," *Cancer Microenviron*, vol. 4, no. 2, pp. 141–154, 2011.

[121] G. Breier, S. Blum, J. Peli et al., "Transforming growth factor-beta and Ras regulate the VEGF/VEGF-receptor system during tumor angiogenesis," *International Journal of Cancer*, vol. 97, no. 2, pp. 142–148, 2002.

[122] T. Kuwano, S. Nakao, H. Yamamoto et al., "Cyclooxygenase 2 is a key enzyme for inflammatory cytokine-induced angiogenesis," *The FASEB Journal*, vol. 18, no. 2, pp. 300–310, 2003.

[123] S. Nakao, T. Kuwano, C. Tsutsumi-Miyahara et al., "Infiltration of COX-2-expressing macrophages is a prerequisite for IL-1 beta-induced neovascularization and tumor growth," *Journal of Clinical Investigation*, vol. 115, no. 11, pp. 2979–2991, 2005.

[124] K. Amano, M. Okigaki, Y. Adachi et al., "Mechanism for IL-1β-mediated neovascularization unmasked by IL-1β knockout mice," *Journal of Molecular and Cellular Cardiology*, vol. 36, no. 4, pp. 469–480, 2004.

[125] E. Voronov, Y. Carmi, and R. N. Apte, "The role IL-1 in tumor-mediated angiogenesis," *Frontiers in Physiology*, vol. 5, 2014.

[126] Y. Fan, J. Ye, F. Shen et al., "Interleukin-6 stimulates circulating blood-derived endothelial progenitor cell Angiogenesisin vitro," *Journal of Cerebral Blood Flow & Metabolism*, vol. 28, no. 1, pp. 90–98, 2007.

[127] M. B. Nilsson, R. R. Langley, and I. J. Fidler, "Interleukin-6, secreted by human ovarian carcinoma cells, is a potent proangiogenic cytokine," *Cancer Research*, vol. 65, no. 23, pp. 10794–10800, 2005.

[128] G. Gopinathan, C. Milagre, O. M. T. Pearce et al., "Interleukin-6 stimulates defective angiogenesis," *Cancer Research*, vol. 75, no. 15, pp. 3098–3107, 2015.

[129] K. D. Wagner, J. Cherfils-Vicini, N. Hosen et al., "The Wilms' tumour suppressor Wt1 is a major regulator of tumour angiogenesis and progression," *Nature Communications*, vol. 5, no. 1, 2014.

[130] P. Oettgen, "Regulation of vascular inflammation and remodeling by ETS factors," *Circulation Research*, vol. 99, no. 11, pp. 1159–1166, 2006.

[131] S. Singh, J. Barrett, K. Sakata, R. G. Tozer, and G. Singh, "ETS Proteins and MMPs: Partners in Invasion and Metastasis," *Current Drug Targets*, vol. 3, no. 5, pp. 359–367, 2002.

[132] M. Vetter, S. G. Blumenthal, R. K. Lindemann et al., "Ets1 is an effector of protein kinase C _α_ in cancer cells," *Oncogene*, vol. 24, no. 4, pp. 650–661, 2005.

[133] Y. Nakamura, S. Esnault, T. Maeda, E. A. B. Kelly, J. S. Malter, and N. N. Jarjour, "Ets-1 Regulates TNF-α-Induced Matrix Metalloproteinase-9 and Tenascin Expression in Primary Bronchial Fibroblasts," *The Journal of Immunology*, vol. 172, no. 3, pp. 1945–1952, 2004.

[134] N. Wernert, "Identification of ETS-1 target genes in human fibroblasts," *International Journal of Oncology*, 2011.

[135] N. Erez, M. Truitt, P. Olson, S. T. Arron, and D. Hanahan, "Cancer-Associated Fibroblasts Are Activated in Incipient Neoplasia to Orchestrate Tumor-Promoting Inflammation in an NF-κB-Dependent Manner," *Cancer Cell*, vol. 17, no. 2, pp. 135–147, 2010.

[136] E. Giannoni, F. Bianchini, L. Masieri et al., "Reciprocal activation of prostate cancer cells and cancer-associated fibroblasts stimulates epithelial-mesenchymal transition and cancer stemness," *Cancer Research*, vol. 70, no. 17, pp. 6945–6956, 2010.

[137] R. Kalluri, "The biology and function of fibroblasts in cancer," *Nature Reviews Cancer*, vol. 16, no. 9, pp. 582–598, 2016.

[138] E. H. P. Tan, M. K. Sng, I. S. B. How et al., "ROS release by _PPAR_ β/δ-null fibroblasts reduces tumor load through epithelial antioxidant response," *Oncogene*, vol. 37, no. 15, pp. 2067–2078, 2018.

[139] N. Hashiya, N. Jo, M. Aoki et al., "In vivo evidence of angiogenesis induced by transcription factor Ets-1: Ets-1 is located upstream of angiogenesis cascade," *Circulation*, vol. 109, no. 24, pp. 3035–3041, 2004.

[140] D. Dutta, S. Ray, J. L. Vivian, and S. Paul, "Activation of the VEGFR1 chromatin domain: an angiogenic signal-ETS1/HIF-2alpha regulatory axis," *Journal of Biological Chemistry*, vol. 283, no. 37, pp. 25404–25413, 2008.

[141] G. Elvert, A. Kappel, R. Heidenreich et al., "Cooperative interaction of hypoxia-inducible factor-2alpha (HIF-2alpha) and Ets-1 in the transcriptional activation of vascular endothelial growth factor receptor-2 (Flk-1)," *J Biol Chem*, vol. 278, no. 9, pp. 7520–7530, 2003.

[142] D. Watanabe, H. Takagi, K. Suzuma et al., "Transcription factor Ets-1 mediates ischemia- and vascular endothelial growth factor-dependent retinal neovascularization," *The American Journal of Pathology*, vol. 164, no. 5, pp. 1827–1835, 2004.

[143] K. R. Lavenburg, J. Ivey, T. Hsu, and R. C. Muise-Helmericks, "Coordinated functions of Akt/PKB and ETS1 in tubule formation," *The FASEB Journal*, vol. 17, no. 15, pp. 2278–2280, 2003.

[144] N. Wagner, J. F. Michiels, A. Schedl, and K. D. Wagner, "The Wilms' tumour suppressor WT1 is involved in endothelial cell proliferation and migration: expression in tumour vessels _in vivo_," *Oncogene*, vol. 27, no. 26, pp. 3662–3672, 2008.

[145] I. A. Darby, T. Bisucci, S. Raghoenath, J. Olsson, G. E. O. Muscat, and P. Koopman, "_Sox18_ Is Transiently Expressed during Angiogenesis in Granulation Tissue of Skin Wounds with an Identical Expression Pattern to _Flk-1_ mRNA," *Laboratory Investigation*, vol. 81, no. 7, pp. 937–943, 2001.

[146] T. Duong, S. T. Proulx, P. Luciani et al., "Genetic ablation of SOX18 function suppresses tumor lymphangiogenesis and metastasis of melanoma in mice," *Cancer Research*, vol. 72, no. 12, pp. 3105–3114, 2012.

[147] P. Donovan, J. Patel, J. Dight et al., "Endovascular progenitors infiltrate melanomas and differentiate towards a variety of vascular beds promoting tumor metastasis," *Nature Communications*, vol. 10, no. 1, p. 18, 2019.

[148] J. F. Michiels, C. Perrin, N. Leccia, D. Massi, P. Grimaldi, and N. Wagner, "PPARbeta activation inhibits melanoma cell proliferation involving repression of the Wilms' tumour suppressor WT1," *Pflügers Archiv - European Journal of Physiology*, vol. 459, no. 5, pp. 689–703, 2010.

[149] D. Wang, L. Fu, J. Wei, Y. Xiong, and R. N. DuBois, "PPARδ mediates the effect of dietary fat in promoting colorectal cancer metastasis," *Cancer Research*, vol. 79, no. 17, pp. 4480–4490, 2019.

[150] J. Yu, M. A. Vodyanik, K. Smuga-Otto et al., "Induced pluripotent stem cell lines derived from human somatic cells," *Science*, vol. 318, no. 5858, pp. 1917–1920, 2007.

[151] J. Shan, J. Shen, L. Liu et al., "Nanog regulates self-renewal of cancer stem cells through the insulin-like growth factor pathway in human hepatocellular carcinoma," *Hepatology*, vol. 56, no. 3, pp. 1004–1014, 2012.

[152] B. Foster, D. Zaidi, T. Young, M. Mobley, and B. Kerr, "CD117/c-kit in Cancer Stem Cell-Mediated Progression and Therapeutic Resistance," *Biomedicines*, vol. 6, no. 1, p. 31, 2018.

[153] V. C. Broudy, N. L. Kovach, L. G. Bennett, N. Lin, F. W. Jacobsen, and P. G. Kidd, "Human umbilical vein endothelial cells display high-affinity c-kit receptors and produce a soluble form of the c-kit receptor," *Blood*, vol. 83, no. 8, pp. 2145–2152, 1994.

[154] J. Matsui, T. Wakabayashi, M. Asada, K. Yoshimatsu, and M. Okada, "Stem cell factor/c-kit signaling promotes the survival, migration, and capillary tube formation of human umbilical vein endothelial cells," *Journal of Biological Chemistry*, vol. 279, no. 18, pp. 18600–18607, 2004.

[155] H. Sihto, O. Tynninen, R. Bützow, U. Saarialho-Kere, and H. Joensuu, "Endothelial cell KIT expression in human tumours," *The Journal of Pathology*, vol. 211, no. 4, pp. 481–488, 2007.

[156] M. Puputti, O. Tynninen, P. Pernilä et al., "Expression of KIT receptor tyrosine kinase in endothelial cells of juvenile brain tumors," *Brain Pathology*, vol. 20, no. 4, pp. 763–770, 2010.

[157] S. Fang, J. Wei, N. Pentinmikko, H. Leinonen, and P. Salven, "Generation of functional blood vessels from a single c-kit+ adult vascular endothelial stem cell," *PLoS Biology*, vol. 10, no. 10, p. e1001407, 2012.

[158] S. Qin, A. Li, M. Yi, S. Yu, M. Zhang, and K. Wu, "Recent advances on anti-angiogenesis receptor tyrosine kinase inhibitors in cancer therapy," *Journal of Hematology & Oncology*, vol. 12, no. 1, p. 27, 2019.

[159] T. Jin, H. Nakatani, T. Taguchi et al., "STI571 (Glivec) suppresses the expression of vascular endothelial growth factor in the gastrointestinal stromal tumor cell line, GIST-T1," *World Journal of Gastroenterology*, vol. 12, no. 5, pp. 703–708, 2006.

[160] J. Litz and G. W. Krystal, "Imatinib inhibits c-Kit-induced hypoxia-inducible factor-1alpha activity and vascular endothelial growth factor expression in small cell lung cancer cells," *Molecular Cancer Therapeutics*, vol. 5, no. 6, pp. 1415–1422, 2006.

[161] K. L. Kim, S. Seo, J. T. Kim et al., "SCF (stem cell factor) and cKIT modulate pathological ocular neovascularization," *Arteriosclerosis, Thrombosis, and Vascular Biology*, vol. 39, no. 10, pp. 2120–2131, 2019.

[162] M. Bjarnegård, M. Enge, J. Norlin et al., "Endothelium-specific ablation of PDGFB leads to pericyte loss and glomerular, cardiac and placental abnormalities," *Development*, vol. 131, no. 8, pp. 1847–1857, 2004.

[163] P. U. Magnusson, C. Looman, A. Ahgren, Y. Wu, L. Claesson-Welsh, and R. L. Heuchel, "Platelet-derived growth factor Receptor-β constitutive activity promotes angiogenesis in vivo and in vitro," *Arteriosclerosis, Thrombosis, and Vascular Biology*, vol. 27, no. 10, pp. 2142–2149, 2007.

[164] M. W. von Ballmoos, Z. Yang, J. Völzmann, I. Baumgartner, C. Kalka, and S. Di Santo, "Endothelial Progenitor Cells Induce a Phenotype Shift in Differentiated Endothelial Cells towards PDGF/PDGFRβ Axis-Mediated Angiogenesis," *PLoS ONE*, vol. 5, no. 11, p. e14107, 2010.

[165] H. Wang, Y. Yin, W. Li et al., "Over-expression of PDGFR-β promotes PDGF-induced proliferation, migration, and angiogenesis of EPCs through PI3K/Akt signaling pathway," *PLoS ONE*, vol. 7, no. 2, p. e30503, 2012.

[166] P. Lindahl, B. R. Johansson, P. Levéen, and C. Betsholtz, "Pericyte loss and microaneurysm formation in PDGF-B-deficient mice," *Science*, vol. 277, no. 5323, pp. 242–245, 1997.

[167] M. Hellström, M. Kalén, P. Lindahl, A. Abramsson, and C. Betsholtz, "Role of PDGF-B and PDGFR-beta in recruitment of vascular smooth muscle cells and pericytes during embryonic blood vessel formation in the mouse," *Development*, vol. 126, no. 14, pp. 3047–3055, 1999.

[168] Y. Wang, Y. Jin, M. A. Mäe et al., "Smooth muscle cell recruitment to lymphatic vessels requires PDGFB and impacts vessel size but not identity," *Development*, vol. 144, no. 19, pp. 3590–3601, 2017.

[169] L. J. Nissen, R. Cao, E. M. Hedlund et al., "Angiogenic factors FGF2 and PDGF-BB synergistically promote murine tumor neovascularization and metastasis," *Journal of Clinical Investigation*, vol. 117, no. 10, pp. 2766–2777, 2007.

[170] J. Zhang, R. Cao, Y. Zhang, T. Jia, Y. Cao, and E. Wahlberg, "Differential roles of PDGFR-alpha and PDGFR-beta in angiogenesis and vessel stability," *The FASEB Journal*, vol. 23, no. 1, pp. 153–163, 2008.

[171] C. Gialeli, D. Nikitovic, D. Kletsas, A. Theocharis, G. Tzanakakis, and N. Karamanos, "PDGF/PDGFR signaling and targeting in cancer growth and progression: focus on tumor microenvironment and cancer-associated fibroblasts," *Current Pharmaceutical Design*, vol. 20, no. 17, pp. 2843–2848, 2014.

[172] S. Rizvi, J. C. Mertens, S. F. Bronk et al., "Platelet-derived growth factor primes cancer-associated fibroblasts for apoptosis," *Journal of Biological Chemistry*, vol. 289, no. 33, pp. 22835–22849, 2014.

[173] T. Y. Chu, J. T. Yang, T. H. Huang, and H. W. Liu, "Crosstalk with cancer-associated fibroblasts increases the growth and radiation survival of cervical cancer cells," *Radiation Research*, vol. 181, no. 5, pp. 540–547, 2014.

[174] Y. Yang, P. Andersson, K. Hosaka et al., "The PDGF-BB-SOX7 axis-modulated IL-33 in pericytes and stromal cells promotes metastasis through tumour-associated macrophages," *Nature Communications*, vol. 7, no. 1, 2016.

[175] M. Tsioumpekou, S. I. Cunha, H. Ma et al., "Specific targeting of PDGFRβ in the stroma inhibits growth and angiogenesis in tumors with high PDGF-BB expression," *Theranostics*, vol. 10, no. 3, pp. 1122–1135, 2020.

[176] M. El Maï, K.-D. Wagner, J.-F. Michiels et al., "The Telomeric Protein TRF2 Regulates Angiogenesis by Binding and Activating the PDGFRβ Promoter," *Cell Reports*, vol. 9, no. 3, pp. 1047–1060, 2014.

[177] C. N. A. Palmer, M.-H. Hsu, K. J. Griffin, and E. F. Johnson, "Novel sequence determinants in peroxisome proliferator signaling," *Journal of Biological Chemistry*, vol. 270, no. 27, pp. 16114–16121, 1995.

[178] O. Gealekman, A. Burkart, M. Chouinard, S. M. Nicoloro, J. Straubhaar, and S. Corvera, "Enhanced angiogenesis in obesity and in response to PPARgamma activators through adipocyte VEGF and ANGPTL4 production," *American Journal of Physiology-Endocrinology and Metabolism*, vol. 295, no. 5, pp. E1056–E1064, 2008.

[179] S. Le Jan, C. Amy, A. Cazes et al., "Angiopoietin-like 4 is a proangiogenic factor produced during ischemia and in conventional renal cell carcinoma," *The American Journal of Pathology*, vol. 162, no. 5, pp. 1521–1528, 2003.

[180] T. Adhikary, D. T. Brandt, K. Kaddatz et al., "Inverse PPARβ/δ agonists suppress oncogenic signaling to the _ANGPTL4_ gene and inhibit cancer cell invasion," *Oncogene*, vol. 32, no. 44, pp. 5241–5252, 2013.

[181] M. J. Tan, Z. Teo, M. K. Sng, P. Zhu, and N. S. Tan, "Emerging roles of angiopoietin-like 4 in human cancer," *Molecular Cancer Research*, vol. 10, no. 6, pp. 677–688, 2012.

[182] S. Mandard, F. Zandbergen, E. van Straten et al., "The fasting-induced adipose factor/angiopoietin-like protein 4 is physically associated with lipoproteins and governs plasma lipid levels and adiposity," *Journal of Biological Chemistry*, vol. 281, no. 2, pp. 934–944, 2006.

[183] H. Staiger, C. Haas, J. Machann et al., "Muscle-derived angiopoietin-like protein 4 is induced by fatty acids via peroxisome proliferator-activated receptor (PPAR)-delta and is of metabolic relevance in humans," *Diabetes*, vol. 58, no. 3, pp. 579–589, 2009.

[184] T. Inoue, T. Kohro, T. Tanaka et al., "Cross-enhancement of ANGPTL4 transcription by HIF1 alpha and PPAR beta/delta is the result of the conformational proximity of two response elements," *Genome Biology*, vol. 15, no. 4, p. R63, 2014.

[185] Y. Sun, A. Daemen, G. Hatzivassiliou et al., "Metabolic and transcriptional profiling reveals pyruvate dehydrogenase kinase 4 as a mediator of epithelial-mesenchymal transition and drug resistance in tumor cells," *Cancer & Metabolism*, vol. 2, no. 1, p. 20, 2014.

[186] J. A. Menendez and R. Lupu, "Fatty acid synthase and the lipogenic phenotype in cancer pathogenesis," *Nature Reviews Cancer*, vol. 7, no. 10, pp. 763–777, 2007.

[187] N. Zaidi, L. Lupien, N. B. Kuemmerle, W. B. Kinlaw, J. V. Swinnen, and K. Smans, "Lipogenesis and lipolysis: the pathways exploited by the cancer cells to acquire fatty acids," *Progress in Lipid Research*, vol. 52, no. 4, pp. 585–589, 2013.

[188] M. R. Guda, S. Asuthkar, C. M. Labak et al., "Targeting PDK4 inhibits breast cancer metabolism," *American Journal of Cancer Research*, vol. 8, no. 9, pp. 1725–1738, 2018.

[189] T. Degenhardt, A. Saramäki, M. Malinen et al., "Three Members of the Human Pyruvate Dehydrogenase Kinase Gene Family Are Direct Targets of the Peroxisome Proliferator-activated Receptor β/δ," *Journal of Molecular Biology*, vol. 372, no. 2, pp. 341–355, 2007.

[190] C. Wolfrum, "Lipid sensing and lipid sensors," *Cellular and Molecular Life Sciences*, vol. 64, no. 19-20, pp. 2465–2476, 2007.

[191] M. L. De Santis, R. Hammamieh, R. Das, and M. Jett, "Adipocyte-fatty acid binding protein induces apoptosis in DU145 prostate cancer cells," *Journal of Experimental Therapeutics and Oncology*, vol. 4, no. 2, pp. 91–100, 2004.

[192] J. Shin, B. Li, M. E. Davis, Y. Suh, and K. Lee, "Comparative analysis of fatty acid-binding protein 4 promoters: conservation of peroxisome proliferator-activated receptor binding sites1," *Journal of Animal Science*, vol. 87, no. 12, pp. 3923–3934, 2009.

[193] E. Kavanagh and B. Joseph, "The hallmarks of CDKN1C (p57, KIP2) in cancer," *Biochimica et Biophysica Acta*, vol. 1816, no. 1, pp. 50–56, 2011.

[194] A. Montagner, M. B. Delgado, C. Tallichet-Blanc et al., "Src is activated by the nuclear receptor peroxisome proliferator-activated receptor β/δ in ultraviolet radiation-induced skin cancer," *EMBO Molecular Medicine*, vol. 6, no. 1, pp. 80–98, 2013.

[195] J. K. Han, B. K. Kim, J. Y. Won et al., "Interaction between platelets and endothelial progenitor cells via LPA-Edg-2 axis is augmented by PPAR-δ activation," *Journal of Molecular and Cellular Cardiology*, vol. 97, pp. 266–277, 2016.

[196] K. Wilhelm, K. Happel, G. Eelen et al., "FOXO1 couples metabolic activity and growth state in the vascular endothelium," *Nature*, vol. 529, no. 7585, pp. 216–220, 2016.

[197] H. H. Jeon, Q. Yu, Y. Lu et al., "FOXO1 regulates VEGFA expression and promotes angiogenesis in healing wounds," *The Journal of Pathology*, vol. 245, no. 3, pp. 258–264, 2018.

[198] Y. H. Kim, J. Choi, M. J. Yang et al., "A MST1-FOXO1 cascade establishes endothelial tip cell polarity and facilitates sprouting angiogenesis," *Nature Communications*, vol. 10, no. 1, p. 838, 2019.

[199] Z. Nahlé, M. Hsieh, T. Pietka et al., "CD36-dependent regulation of muscle FoxO1 and PDK4 in the PPARδ/β-mediated adaptation to metabolic stress," *Journal of Biological Chemistry*, vol. 283, no. 21, pp. 14317–14326, 2008.

[200] F.-Q. Zhao and A. Keating, "Functional properties and genomics of glucose transporters," *Current Genomics*, vol. 8, no. 2, pp. 113–128, 2007.

[201] C. D. Young, A. S. Lewis, M. C. Rudolph et al., "Modulation of glucose transporter 1 (GLUT1) expression levels alters mouse mammary tumor cell growth in vitro and in vivo," *PLoS ONE*, vol. 6, no. 8, p. e23205, 2011.

[202] W. Zhang, Y. Xu, Q. Xu, H. Shi, J. Shi, and Y. Hou, "PPARδ promotes tumor progression via activation of Glut 1 and SLC1-A5 transcription," *Carcinogenesis*, vol. 38, no. 7, pp. 748–755, 2017.

[203] P. Nicklin, P. Bergman, B. Zhang et al., "Bidirectional transport of amino acids regulates mTOR and autophagy," *Cell*, vol. 136, no. 3, pp. 521–534, 2009.

[204] Y. J. Jeon, S. Khelifa, B. Ratnikov et al., "Regulation of glutamine carrier proteins by RNF5 determines breast cancer response to ER stress-inducing chemotherapies," *Cancer Cell*, vol. 27, no. 3, pp. 354–369, 2015.

Hindawi
PPAR Research
Volume 2020, Article ID 3480412, 6 pages
https://doi.org/10.1155/2020/3480412

Research Article

PPARD May Play a Protective Role against the Development of Schizophrenia

Xinrong Li,[1,2] **Sha Liu**,[1,2] **Karan Kapoor**,[3] **and Yong Xu**[1,2]

[1]*Shanxi Key Laboratory of Artificial Intelligence Assisted Diagnosis and Treatment for Mental Disorder, First Hospital of Shanxi Medical University, Taiyuan, China*
[2]*Department of Psychiatry, First Hospital/First Clinical Medical College of Shanxi Medical University, Taiyuan, China*
[3]*NIH Center for Macromolecular Modeling and Bioinformatics, Beckman Institute for Advanced Science and Technology, University of Illinois at Urbana-Champaign, Urbana, IL 61801, USA*

Correspondence should be addressed to Yong Xu; xuyongsmu@vip.163.com

Received 28 February 2020; Accepted 29 May 2020; Published 7 August 2020

Guest Editor: Anastasia Nesterova

PPARD has been suggested to contribute to the etiology of schizophrenia (SCZ) with the underlying mechanisms largely unknown. Here, we first collected and analyzed the PPARD expression profile from three groups: (1) 18 healthy control (HC) subjects, (2) 14 clinical high-risk (CHR) patients, and (3) 19 early onset of SCZ (EOS) patients. After that, we conducted a systematical pathway analysis to explore the potential mechanisms involved in PPARD exerting influence on the pathological development of SCZ. Compared to the HC group, the expression of PPARD was slightly decreased in the EOS group (LFC = −0.34; $p = 0.23$) and increased in the CHR group (LFC = 0.65; $p = 0.20$). However, there was a significant difference between the EOS group and the CHR group (LFC = −0.99; $p = 0.015$), reflecting the amount of variation in PPARD expression before and after the onset of SCZ. Pathway analysis suggested that overexpression of PPARD may regulate ten proteins or molecules to inhibit the pathological development of SCZ, including the deactivation of eight SCZ promoters and stimulation of two SCZ inhibitors. Our results support the association between PPARD and SCZ. The pathways identified may help in the understanding of the potential mechanisms by which PPARD contributes to the etiology of SCZ.

1. Introduction

Schizophrenia (SCZ) is a common and often disabling mental illness characterized not only by a varied group of clinical symptoms [1], but wide-ranging deficits in neurocognitive and neurophysiological functions [2, 3]. The prodromal period is thought to have a high risk of clinical symptoms and precedes illness onset by 1 to 6 years [4, 5]. Subjects with these characteristics are called clinical high-risk (CHR) patients, with about one-third developing SCZ and two-third recovering to normal [4, 5] (PMID: 8782291; PMID: 1571314). Early-onset SCZ (EOS), defined as SCZ with onset before the 21st birthday, shows worse psychosocial disability and poor prognosis [6]. As a neurodevelopment disease [7], SCZ in childhood tends to have a higher possibility of abnormal neural development [8].

PPARD is a nuclear hormone receptor that governs a variety of biological processes [9]. This gene has been suggested to play roles in the development of several chronic diseases, including diabetes, obesity, atherosclerosis, and cancer [10]. Several studies have suggested that PPARG may contribute to the etiology of SCZ [11–13]. For instance, Sun et al.'s study showed that the PPARD polymorphism rs2076169 had an allelic association with SCZ ($X2 = 13.62$, $p = 0.0002$) in a trio study using a transmission disequilibrium test [11]. Maekawa et al. identified a significantly downregulated expression of PPARD ($p < 0.05$) in individuals with SCZ compared with the control subjects [12]. Dzana et al. also discovered linkages between the genetic variants of multiple genes including PPARD and the increased waist circumference in SCZ patients ($p < 0.037$) [13]. However, the underlying mechanism regarding the PPARD-SCZ association is largely unknown.

To explore the relationship between PPARD and SCZ, we studied the expression changes of PPARD in both CHR and EOS groups and compared that to the healthy control (HC) group. CHR is a special state of SCZ before its onset. We hypothesized that the changes in PPARD expression in the CHR group could lead to the regulation of genes not observed in the SCZ group. After that, we conducted a systematic bioinformatics analysis and identified multiple pathways through which PPARD could exert influence on SCZ. Our study provides novel evidence for the association between PPARD and SCZ and adds new insights into the understanding of the roles of PPARD in the etiology of SCZ.

2. Materials and Methods

2.1. Subject Recruitment for Expression Profile Collection. All participants were unrelated Han Chinese recruited from the north of China and under the age of 18 years. EOS patients were diagnosed by 2 associate doctors according to the Diagnostic and Statistical Manual of Mental Disorders: Fourth Edition (DSM-IV) and the Chinese version of the Modified Structured Clinical Interview for DSM-IV, patient version (SCID-I/P). The total score of PANSS was ≥60, and IQ score was ≥70. Exclusions included patients with organic disease of heart, liver, and kidney; all kinds of immune diseases, brain injury, or brain congenital malformation; a tumor of brain and epilepsy; mental retardation, along with anyone taking antipsychotic drugs, antimanic drugs, antidepressants, or mood stabilizers. In addition, we excluded serious excitement or impulsion patients. CHR patients were assessed with the Structured Interview of Prodromal Syndromes (SIPS) [14]. The exclusion criteria of this group were the same as the EOS group. The healthy controls (HC) were selected by matching the age and sex with never having taken any drugs in the latest one month. Exclusion criteria included (1) meeting the standards of inclusion or exclusion term of patients, (2) having the family history of any spirit or nervous system disease, (3) having head injury or newborn related disease, (4) having hyperpyretic convulsion before, and (5) being an adopted child or living in a single-parent family.

All teenage participants' informed consent was signed by their parents. The study was conducted under the protocols approved by the First Hospital of Shanxi Medical University (Ethical Code: 2019-Y01).

2.2. RNA Extraction and Quantity Control. Total RNA was extracted from all of the samples which had been snap-frozen using TRIzol reagent (Invitrogen, Carlsbad, CA, U.S.) according to the manufacturer's previous protocol [15]. Total RNA from each sample was quantified by the NanoDrop ND-1000, and RNA integrity was assessed by standard denaturing agarose gel electrophoresis.

2.3. RNA Labeling and Microarray Hybridization. The RNA labeling and microarray hybridization followed the routine process described as follows [16]. The Arraystar Human LncRNA Array v2.0 is designed for researchers who are interested in profiling both lncRNAs and protein-coding RNAs in the human genome. Sample labeling and array hybridization were performed according to the Agilent One-Color Microarray-Based Gene Expression Analysis protocol (Agilent Technology) with minor modifications. Briefly, mRNA was purified from total RNA after removal of rRNA (mRNA-ONLY™ Eukaryotic mRNA Isolation Kit, Epicentre). Then, each sample was amplified and transcribed into fluorescent cRNA along the entire length of the transcripts without $3'$ bias utilizing a random priming method. The labeled cRNAs were purified by the RNeasy Mini Kit (Qiagen). The concentration and specific activity of the labeled cRNAs (pmol Cy3/μg cRNA) were measured by NanoDrop ND-1000. 1 μg of each labeled cRNA was fragmented by adding 11 μl 10x Blocking Agent and 2.2 μl of 25x Fragmentation Buffer and then heating the mixture at 60°C for 30 min. Finally, 55 μl 2x GE Hybridization buffer was added to dilute the labeled cRNA. 100 μl of hybridization solution was dispensed into the gasket slide and assembled on the RNA expression microarray slide. The slides were incubated for 17 hours at 65°C in an Agilent Hybridization Oven. The hybridized arrays were washed, fixed, and scanned using the Agilent DNA Microarray Scanner (part number G2505C). The microarray work was performed by KangChen Bio-tech (Shanghai).

2.4. Bioinformatics Analysis. To gain a better understanding of the gene expression resulting from different groups of subjects and explore possible roles of PPARD in the etiology of SCZ, we conducted a literature-based pathway analysis to identify the possible molecular pathways connecting PPARD and SCZ. Specifically, by using the tool Pathway studio (version 12.3; http://www.pathwaystudio.com), we identified genes and small molecules that are downstream targets of PPARD and upstream regulators of SCZ with polarity. Then, we constructed the PPARD-driven functional pathways with polarity and direction.

3. Results

3.1. Demographics. The three groups of subjects were comparable in age and gender. In all, we recruited 19 EOS patients (8 males and 11 females, aged 14.79 ± 1.90 years), 14 CHR patients (9 males and 5 females, aged 16.14 ± 1.41 years), and 18 HC (9 males and 9 females, aged 15.67 ± 2.40 years). The demographic information for all participants is provided in Table 1.

3.2. Expression Variation of PPARD in Different Groups. Compared with the HC group, PPARD presented increased expression levels in the CHR group (LFC = 0.65) and decreased expression levels in the EOS group (LFC = −0.34), as shown in Figure 1(a). The changes were milder in terms of the statistical p value (p value = 0.23 and 0.20 for EOS vs HC and CHR vs HC, respectively). However, the difference between EOS and CHR group showed statistical significance (p value = 0.015; LFC = −0.99). The downregulation of PPARD in the EOS group was consistent with previous study results (PubMed 28872641); however, the increased

Table 1: Demographics and clinical characteristics for all participants.

	EOS patients	CHR patients	HC	F/x^2	p value
n	19	14	18		
Age (years)	14.79 ± 1.90	16.14 ± 1.41	15.67 ± 2.40	2.012	0.145
Gender (M/F)	8/11	9/5	9/9	1.598	0.450
PANSS total scores	62.17 ± 13.32				

Note: PANSS; Positive and Negative Syndrome Scale.

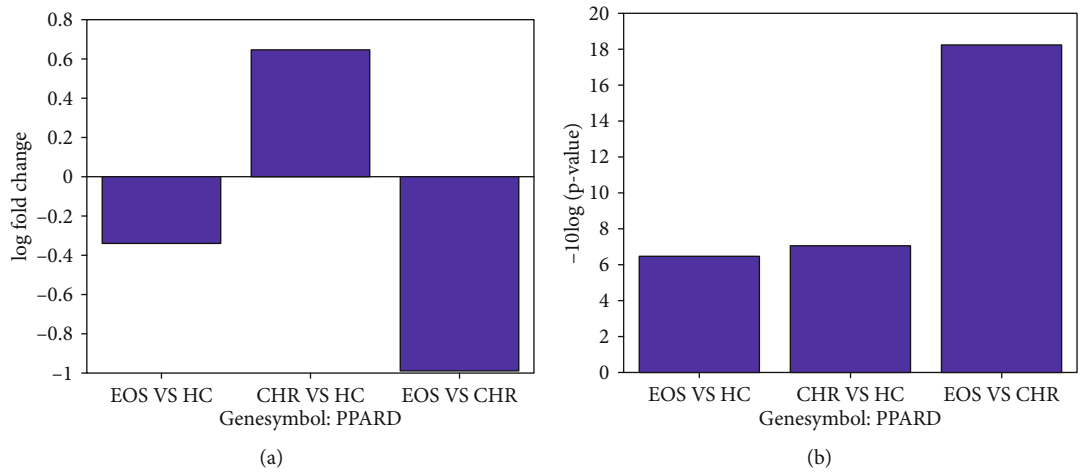

Figure 1: PPARD expression comparison among three different groups: healthy control (HC) group, clinical high-risk (CHR) group, and early-onset schizophrenia (EOS) group. (a) The -10 ∗ log10 transferred p values in different comparisons; (b) the log fold change of PPARD expression for different comparisons.

PPARD expression levels in the CHR groups were not reported before. Usually, there are about two-third of the CHR subjects who do not develop SCZ (PMID: 8782291; PMID: 1571314). Thus, our results indicated that increased PPARD expression might play a protective role against the development of SCZ, with the underlying mechanism explored using subsequent pathway analysis.

3.3. Genetic Pathways Driven by PPARD. To understand the possible roles that PPARD could exert on the pathologic development of SCZ, we constructed a literature-based genetic pathway connecting PPARD and SCZ, as shown in Figure 2. Our results showed that PPARD deactivates four promoters of SCZ, including CNR1, AGTR1, ACAN, and IL1B. Moreover, one SCZ inhibitor could also get activated by PPARD. These results may partially explain the mechanism regarding the roles of PPARD in the etiology of SCZ. Each relation within Figure 2 was supported by one or more scientific references (Supplementary Material: Ref 4 Figure 2). The corresponding sentences where a relationship has been identified were reviewed to confirm the confidence of the identified relation.

3.4. Molecule Pathways Driven by PPARD. Besides the genetic pathway, we also identified multiple molecules influencing the pathologic development of SCZ and regulated by PPARG, as shown in Figure 3. Specifically, PPARG promotes the secretion of glutathione, which is an inhibitor of SCZ. Moreover, PPARD suppresses four molecules that could promote the development of SCZ, including superoxide, ROS, glutamate, and fatty acid. These results may further explain the underlying mechanism in which increased expression of PPARD could protect against the development of SCZ. Each relation within Figure 3 was supported by one or more scientific references (Supplementary Material: Ref 4 Figure 3). The corresponding sentences where a relationship has been identified were reviewed to confirm the confidence of the identified relation.

4. Discussion

Previous studies have suggested that PPARD may contribute to the etiology of SCZ. However, the underlying mechanism is largely unknown [11, 12]. To better understand the role of PPARD, we tested the expression variation of PPARD in both CHR and EOS groups and compared it to the HC group. We hypothesize that PPARD expression changes in the CHR group may reflect the activities of genes during the development of SCZ but before its onset. Our results showed that the EOS group presented decreased expression levels compared to healthy controls, which was consistent with a previous study [12]. However, we observed increased PPARD expression in the CHR group compared to both HC and EOS groups. The opposite change between CHR and EOS groups may reflect the PPARD variation before and after the onset of SCZ.

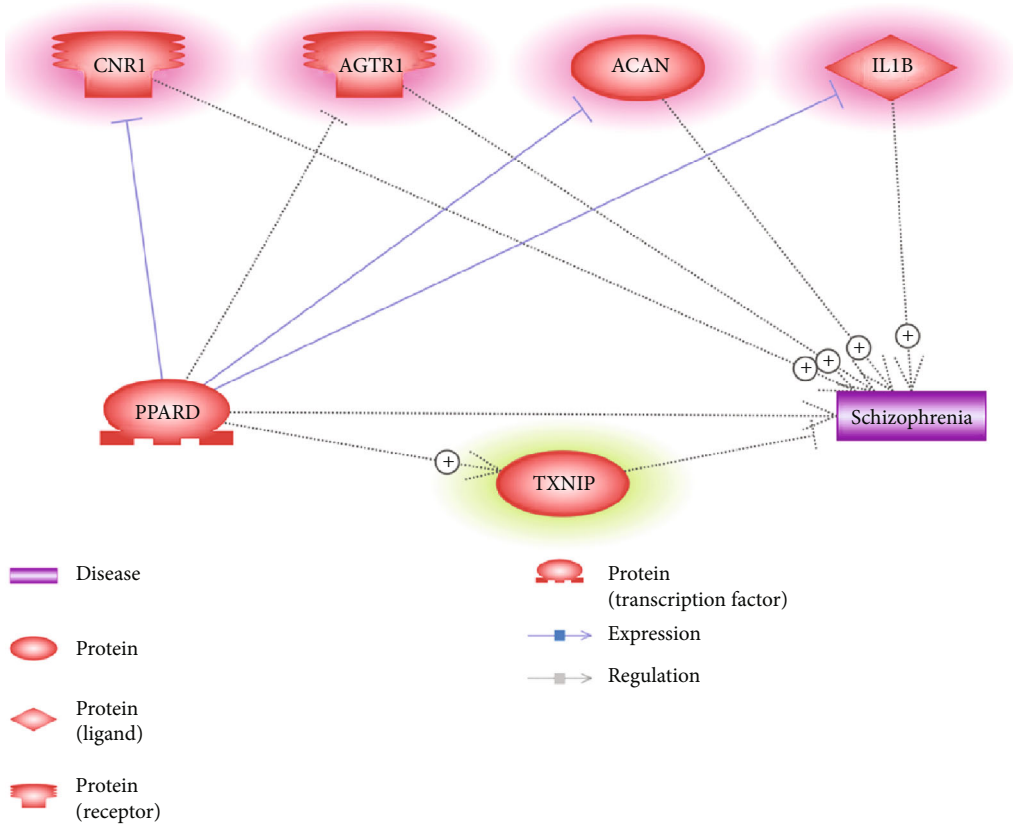

Figure 2: PPARD driven genetic pathways inhibiting schizophrenia. The genes highlighted in red are schizophrenia promoters; green denoting schizophrenia inhibitors.

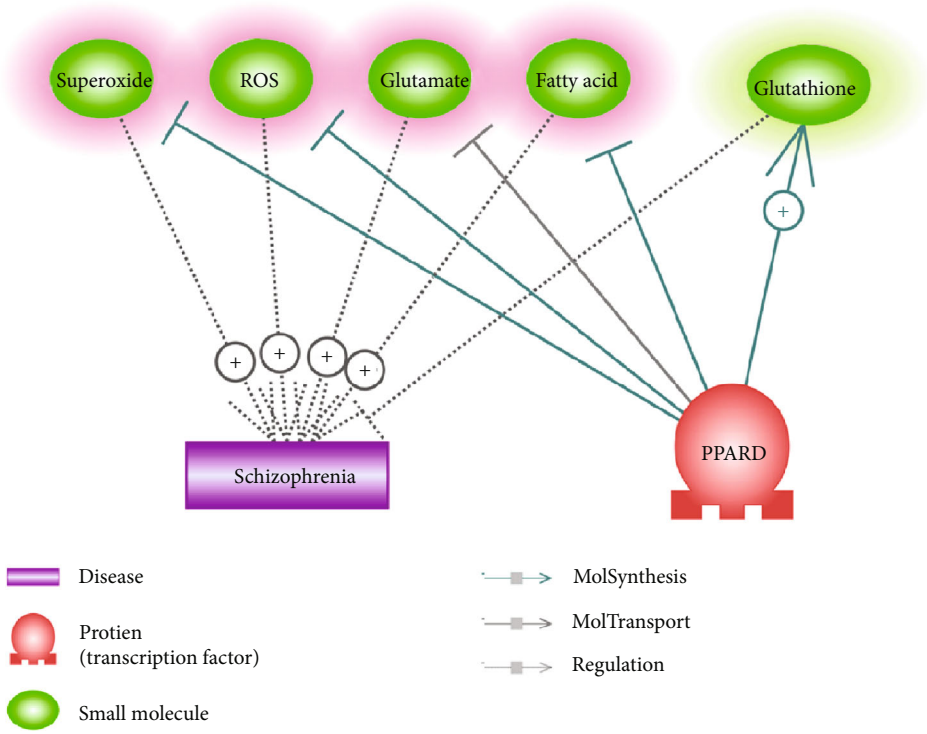

Figure 3: PPARD driven genetic pathways inhibiting schizophrenia. The molecules highlighted in red are schizophrenia promoters; green denoting schizophrenia inhibitors.

Pathway analysis showed that increased expression of PPARD might drive proteins and small molecules to protect against the pathologic development of SCZ, as shown in Figures 2 and 3. These pathways suggested that increased expression of PPARD could inhibit SCZ promoters and activate SCZ inhibitors, consequently influencing the pathophysiology of SCZ. For instance, PPARD has been shown to inhibit CB1 receptor expression (CNR1), which contributes to the pathophysiology of SCZ [17]. PPARD also reduces the upregulation of angiotensin II type 1 receptor (AGTR1) [18], the antagonists of which have been reported to improve clinical symptoms in SCZ patients [19]. In addition, PPARD activation promotes the degradation of aggrecan (ACAN) and attenuates gene expression of IL1B [20, 21]. Both ACAN and IL1B were suggested to contribute to the increased risk of SCZ [22, 23]. Moreover, SCZ patients have been shown to present decreased expression of tumor suppressor gene TXNIP, a thioredoxin-binding protein that is a member of the alpha arrestin protein family [24]. Ratneswaran et al. showed that PPARD could upregulate the expression of TXNIP [25]. These results support the association between PPARD and SCZ and also suggest the possible mechanisms of the protective roles of PPARD in the pathologic development of SCZ.

Our study also shows that PPARD may inhibit the generation and release of four molecules that play important roles in the pathophysiology of SCZ, including superoxide, oxygen free radicals (ROS), glutamate, and fatty acid (Figure 3). Moreover, it has been shown that agonists of PPARD could promote glutathione synthesis [26], with the deficit of glutathione impairing neurotransmission and cerebral connectivity that lead to clinical symptoms of SCZ [27]. These molecule pathways add more support for the mechanisms involved in the PPARD-SCZ association.

To our knowledge, no previous study has explored the PPARD expression variations between CHR patients and the EOS group, which provide new vision of the activity of PPARD in the case of SCZ. This study also has some limitations. Firstly, larger datasets could be collected to validate the expression levels of PPARD in CHR and EOS patients. Secondly, a follow-up study should be conducted to identify the expression of PPARD throughout the clinical high-risk stage to the recovery or disease stage of SCZ. Due to the limitation of supporting sources, this work has been left for future studies.

5. Conclusion

Our results confirmed decreased expression of PPARD in the case of SCZ and revealed increased expression in the clinical high-risk group. Pathway analysis suggested that the overexpression of PPARD in the high-risk group may contribute to the protection of a subject from developing SCZ.

Data Availability

The data of this study are available from the corresponding author upon reasonable request.

Conflicts of Interest

All the authors declare no conflict of interest.

Acknowledgments

This work was supported by the National Key Research and Development Program of China (2016YFC1307004), the National Natural Science Foundation of China (81971601 and 81701326), the Support Program of the Youth Sanjin Scholars, the 136 Medical Rejuvenation Project of Shanxi Province, and the Multidisciplinary Team for Cognitive Impairment of Shanxi Science and Technology Innovation Training Team (201705D131027) and Youth Science, Technology Research Fund of Shanxi (201801D221418), and Scientific Research Project of Shanxi Health Commission (201601034).

Supplementary Materials

| Reference for Figure 2 and reference for Figure 3. *(Supplementary Materials)*

References

[1] C. A. Tamminga and H. H. Holcomb, "Phenotype of schizophrenia: a review and formulation," *Molecular Psychiatry*, vol. 10, no. 1, pp. 27–39, 2005.

[2] J. van Os, G. Kenis, and B. P. F. Rutten, "The environment and schizophrenia," *Nature*, vol. 468, no. 7321, pp. 203–212, 2010.

[3] B. I. Turetsky, M. E. Calkins, G. A. Light, A. Olincy, A. D. Radant, and N. R. Swerdlow, "Neurophysiological endophenotypes of schizophrenia: the viability of selected candidate measures," *Schizophrenia Bulletin*, vol. 33, no. 1, pp. 69–94, 2007.

[4] A. R. Yung and P. D. McGorry, "The prodromal phase of first-episode psychosis: past and current conceptualizations," *Schizophrenia Bulletin*, vol. 22, no. 2, pp. 353–370, 1996.

[5] H. Häfner, A. Riecher-Rössler, M. Hambrecht et al., "IRAOS: an instrument for the assessment of onset and early course of schizophrenia," *Schizophrenia Research*, vol. 6, no. 3, pp. 209–223, 1992.

[6] L. Clemmensen, D. L. Vernal, and H. C. Steinhausen, "A systematic review of the long-term outcome of early onset schizophrenia," *BMC Psychiatry*, vol. 12, no. 1, 2012.

[7] J. L. Rapoport, J. N. Giedd, and N. Gogtay, "Neurodevelopmental model of schizophrenia: update 2012," *Molecular Psychiatry*, vol. 17, no. 12, pp. 1228–1238, 2012.

[8] N. Gogtay, "Cortical brain development in schizophrenia: insights from neuroimaging studies in childhood-onset schizophrenia," *Schizophrenia Bulletin*, vol. 34, no. 1, pp. 30–36, 2007.

[9] J. Berger and D. E. Moller, "The mechanisms of action of PPARs," *Annual Review of Medicine*, vol. 53, no. 1, pp. 409–435, 2002.

[10] J. N. Feige, L. Gelman, L. Michalik, B. Desvergne, and W. Wahli, "From molecular action to physiological outputs: peroxisome proliferator-activated receptors are nuclear receptors at the crossroads of key cellular functions," *Progress in Lipid Research*, vol. 45, no. 2, pp. 120–159, 2006.

[11] S. L. Sun, G. Z. Ju, Y. Liu et al., "281 – association of polymorphism of PPARD gene with schizophrenia in Chinese Han population," *Schizophrenia Research*, vol. 98, p. 149, 2008.

[12] M. Maekawa, A. Watanabe, Y. Iwayama et al., "Polyunsaturated fatty acid deficiency during neurodevelopment in mice models the prodromal state of schizophrenia through epigenetic changes in nuclear receptor genes," *Translational Psychiatry*, vol. 7, no. 9, p. e1229, 2017.

[13] D. S. Hukic, U. Ösby, E. Olsson et al., "Genetic variants of increased waist circumference in psychosis," *Psychiatric Genetics*, vol. 27, no. 6, pp. 210–218, 2017.

[14] T. J. Miller, T. H. McGlashan, S. W. Woods et al., "Symptom assessment in schizophrenic prodromal states," *The Psychiatric Quarterly*, vol. 70, no. 4, pp. 273–287, 1999.

[15] Y. Xu, F. Li, B. Zhang et al., "MicroRNAs and target site screening reveals a pre-microRNA-30e variant associated with schizophrenia," *Schizophrenia Research*, vol. 119, no. 1-3, pp. 219–227, 2010.

[16] Y. Lou, H. Jiang, Z. Cui, X. Wang, L. Wang, and Y. Han, "Gene microarray analysis of lncRNA and mRNA expression profiles in patients with high-grade ovarian serous cancer," *International Journal of Molecular Medicine*, vol. 42, no. 1, pp. 91–104, 2018.

[17] A. Seillier, A. A. Martinez, and A. Giuffrida, "Phencyclidine-induced social withdrawal results from deficient stimulation of cannabinoid CB_1 receptors: implications for schizophrenia," *Neuropsychopharmacology*, vol. 38, no. 9, pp. 1816–1824, 2013.

[18] M. Romero, R. Jimenez, M. Toral et al., "Vascular and central activation of peroxisome proliferator-activated receptor-β attenuates angiotensin II-induced hypertension: role of RGS-5," *The Journal of Pharmacology and Experimental Therapeutics*, vol. 358, no. 1, pp. 151–163, 2016.

[19] S. Mohite, S. M. de Campos-Carli, N. P. Rocha et al., "Lower circulating levels of angiotensin-converting enzyme (ACE) in patients with schizophrenia," *Schizophrenia Research*, vol. 202, pp. 50–54, 2018.

[20] A. Ratneswaran, E. A. LeBlanc, E. Walser et al., "Peroxisome Proliferator–Activated Receptor δ Promotes the Progression of Posttraumatic Osteoarthritis in a Mouse Model," *Arthritis & Rhematology*, vol. 67, no. 2, pp. 454–464, 2015.

[21] C. Wang, G. Zhou, and Z. Zeng, "Effects of peroxisome proliferator-activated receptor-β/δ on sepsis induced acute lung injury," *Chinese Medical Journal*, vol. 127, no. 11, pp. 2129–2137, 2014.

[22] H. Pantazopoulos, M. Markota, F. Jaquet et al., "Aggrecan and chondroitin-6-sulfate abnormalities in schizophrenia and bipolar disorder: a postmortem study on the amygdala," *Translational Psychiatry*, vol. 5, no. 1, p. e496, 2015.

[23] M. Yoshida, K. Shiroiwa, K. Mouri et al., "Haplotypes in the expression quantitative trait locus of interleukin-1β gene are associated with schizophrenia," *Schizophrenia Research*, vol. 140, no. 1-3, pp. 185–191, 2012.

[24] Y. Su, W. Ding, M. Xing, D. Qi, Z. Li, and D. Cui, "The interaction of TXNIP and AFq1 genes increases the susceptibility of schizophrenia," *Molecular Neurobiology*, vol. 54, no. 6, pp. 4806–4812, 2017.

[25] A. Ratneswaran, M. M.-G. Sun, H. Dupuis, C. Sawyez, N. Borradaile, and F. Beier, "Nuclear receptors regulate lipid metabolism and oxidative stress markers in chondrocytes," *Journal of Molecular Medicine (Berlin, Germany)*, vol. 95, no. 4, pp. 431–444, 2017.

[26] E. Esposito, I. Paterniti, R. Meli, P. Bramanti, and S. Cuzzocrea, "GW0742, a high-affinity PPAR-δ agonist, mediates protection in an organotypic model of spinal cord damage," *Spine*, vol. 37, no. 2, pp. E73–E78, 2012.

[27] V. Castagné, M. Cuénod, and K. Q. Do, "An animal model with relevance to schizophrenia: sex-dependent cognitive deficits in osteogenic disorder-Shionogi rats induced by glutathione synthesis and dopamine uptake inhibition during development," *Neuroscience*, vol. 123, no. 4, pp. 821–834, 2004.

Hindawi
PPAR Research
Volume 2020, Article ID 9657380, 21 pages
https://doi.org/10.1155/2020/9657380

Review Article

The PPAR Ω Pocket: Renewed Opportunities for Drug Development

Åsmund Kaupang and Trond Vidar Hansen

Section for Pharmaceutical Chemistry, Department of Pharmacy, University of Oslo, 0316 Oslo, Norway

Correspondence should be addressed to Åsmund Kaupang; asmund.kaupang@farmasi.uio.no

Received 29 January 2020; Accepted 13 May 2020; Published 1 July 2020

Guest Editor: Hongbao Cao

The past decade of PPARγ research has dramatically improved our understanding of the structural and mechanistic bases for the diverging physiological effects of different classes of PPARγ ligands. The discoveries that lie at the heart of these developments have enabled the design of a new class of PPARγ ligands, capable of isolating central therapeutic effects of PPARγ modulation, while displaying markedly lower toxicities than previous generations of PPARγ ligands. This review examines the emerging framework around the design of these ligands and seeks to unite its principles with the development of new classes of ligands for PPARα and PPARβ/δ. The focus is on the relationships between the binding modes of ligands, their influence on PPAR posttranslational modifications, and gene expression patterns. Specifically, we encourage the design and study of ligands that primarily bind to the Ω pockets of PPARα and PPARβ/δ. In support of this development, we highlight already reported ligands that if studied in the context of this new framework may further our understanding of the gene programs regulated by PPARα and PPARβ/δ. Moreover, recently developed pharmacological tools that can be utilized in the search for ligands with new binding modes are also presented.

1. Introduction

The peroxisome proliferator-activated receptors (PPARs) are members of a class of transcription factors whose regulation of gene transcription is modulated by ligand binding—a class also known as nuclear receptors. The three PPAR subtypes described thus far, PPARα, PPARβ/δ, and PPARγ (NR1C1, NR1C2, and NR1C3, respectively) [1], are multidomain proteins that each consist of a highly mobile N-terminal domain (domains A/B), a DNA-binding domain (DBD, domain C), a hinge region (domain D), and a C-terminal ligand-binding domain (LBD, domains E/F). Of these, the N-terminal and the C-terminal domains, respectively, contain the ligand-independent activation function 1 (AF-1) and ligand-dependent activation function 2 (AF-2) (Figure 1(a)) [2, 3]. The PPARs are primarily described as acting through heterodimeric complexes with the retinoic X receptors (RXRs) [4]. Upon binding to DNA, each DBD of the PPAR:RXR heterodimer typically interacts with its own half-site of a peroxisome proliferator response element (PPRE) in the promoter or enhancer region of a target gene, e.g., a repeated consensus sequence separated by a single nucleotide—a direct repeat 1 (DR1) element (Figure 1(b)) [5–7]. The PPAR:RXR heterodimer is characterized as *permissive*, in the sense that the binding of ligands in the ligand-binding pocket (LBP) of either receptor can activate transcription. Thus, while the binding of 9-*cis*-retinoic acid (Figure S1) or other RXR agonists to the RXR LBP can positively regulate target genes, the binding of an agonist to the PPAR LBP appears to exert a stronger and dominant role in the activation of the PPAR:RXR heterodimer. Coherently, the binding of agonists to both receptors can synergistically activate transcription [8–11].

In the canonical mechanism, the introduction of an agonist in the PPAR LBP leads to the release of a corepressor protein complex bound to the apo-PPAR:RXR heterodimer through platform proteins such as nuclear receptor corepressor (NCoR), silencing mediator for retinoid and thyroid

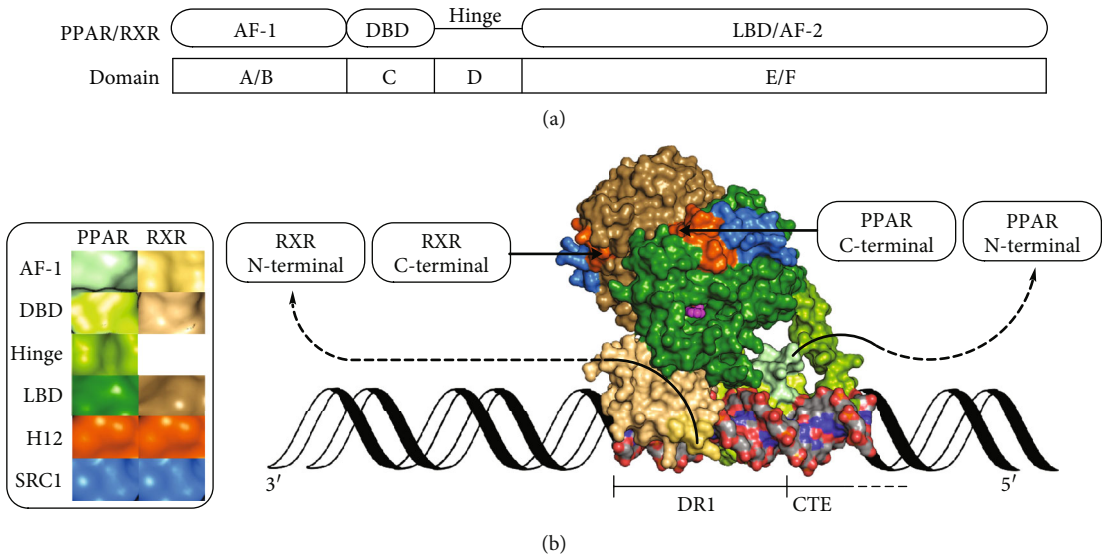

Figure 1: Structural overview of the PPAR/RXR heterodimer. AF-1: ligand-independent activation function 1; DBD: DNA-binding domain; LBD: ligand-binding domain; AF-2: activation function 2; H12: helix 12; SRC1: steroid receptor coactivator 1; DR1: direct repeat 1; CTE: carboxy-terminal extension. (a) Schematic overview of the domains in PPAR/RXR. (b) A molecular surface representation of the structure of the PPARγ:RXRα heterodimer bound to rosiglitazone (magenta spheres), 9-*cis*-retinoic acid (not visible), two peptides derived from SRC1, and a DNA fragment. The DNA fragment is shown as a molecular surface (C, grey; O, red; N, blue; P, orange), extended with a cartoon representation (black). The structural data was taken from PDB ID: 3DZY [12] and presented with PyMOL (ver. 1.8.4.0) [13, 14].

hormone receptors (SMRT) or SMRT and histone deacetylase-associated protein (SHARP), that either contain or interact with histone deacetylases (HDACs) [15–18]. The holo-PPAR:RXR complex subsequently recruits coactivator proteins such as CREB-binding protein (CBP), steroid receptor coactivator 1–3 (SRC1–3), mediator complex subunit 1 (MED1, TRAP220, or DRIP205), or PPARγ coactivator 1α (PGC-1α), which in turn recruit other nuclear proteins leading to a coactivator complex that usually displays histone acetylase (HAT) activity. The switch from the action of HDACs to that of HATs increases histone acetylation and leads to the remodelling of chromatin required for the assembly of the functional, multiprotein transcription complex [19–22]. Subsequent transcription of PPAR target genes completes the process known as transactivation. Interestingly, the binding of a PPAR agonist can also lead to the recruitment of certain corepressor proteins, such as receptor-interacting protein 140 (RIP140) [23, 24] or TNFAIP3-interacting protein 1 (TNIP1) [25], that contain receptor-interacting domains (RIDs) similar to those found in coactivator proteins [26].

In contrast to the PPRE-mediated regulation of target gene expression by the PPAR:RXR heterodimer, a holo-PPAR monomer can also interact directly with other transcription factors and attenuate the expression of their target genes—a mechanism called transrepression [27–33]. This fundamentally different mechanism of transcriptional regulation has been shown to be involved in, e.g., the anti-inflammatory effects of PPAR activation [31, 32, 34–36].

The proteins produced upon the expression of PPAR target genes hold key roles in the regulation of lipid and glucose metabolism [37–39]. Consequently, the PPARs have attracted significant attention as possible points of pharmacological intervention in human metabolic diseases. Through the last decades, several members of classical agonist families such as the fibrates (PPARα), the glitazones (PPARγ), and the glitazars (PPARα/γ) have been approved for the treatment of metabolic diseases in humans. However, many of these drugs have since been withdrawn from the market due to the serious side effects that accompanied their clinical use (e.g., carcinogenesis in various tissues, myocardial infarction, loss of bone density, and weight gain) [40–51]. Albeit efficacious at improving selected metabolic parameters in patients, the relative failure of PPAR classical agonists to represent safe treatment options may have caused researchers both in academia and in the industry to abandon further ligand development targeting the PPARs.

Nevertheless, results from the last decade, particularly from the study of the effects of partial and nonagonistic ligands on PPARγ, suggest that the side effects caused by classical agonists and some of the desired, beneficial effects of PPARγ ligation are of separate mechanistic origins. Together, these results form a basis for a new ligand design paradigm, a key concept of which relates to how ligand binding can modulate the occurrence of posttranslational modifications (PTMs) of PPARγ, which in turn lead to particular patterns of gene expression. This and related concepts from the history of PPARγ ligand development are reviewed initially. We then venture to apply these concepts to historic and future ligand development in PPARα and PPARβ/δ by highlighting results and ligands that merit renewed attention and further study as

tools that can potentially reveal hereto unknown transcriptional profiles of therapeutic relevance.

2. PPAR Structure

In addition to the large body of atomic resolution data existing in the public domain on the structures of both apo- and holo forms of the LBDs of the PPARs (domains E/F), our understanding of the structures of the C and D domains, as well as the quaternary organization of domains C–F, is improving [7, 12, 52, 53]. Less is however known about the structural dispositions of the highly mobile N-terminal A/B domains and the AF-1 [54]. Nonetheless, the ability of the AF-1 to induce transcription independently of the AF-2 and of ligand binding has been demonstrated [55–57]. The sequences of the A/B domains also vary significantly between the PPAR subtypes and between the observed splice variants (isoforms) of each subtype [58–61]. Coherently, the AF-1 region has been demonstrated to influence the selectivity with which each PPAR subtype regulates the expression of its target genes [3], but also the degree of transcriptional activation induced by ligand binding [62].

The structure of the PPAR LBD comprises a sandwich of helices 1–12 (H1–H12), 3-4 β strands (β1–β4), and several prominent loops, with the overall fold being similar to that of other nuclear receptors (NRs) in the steroid hormone receptor superfamily. For the standard PPAR helix numbering scheme, see Uppenberg et al. [63]. The main cavity of the LBD is larger than in other NRs (~1300 Å^3 [64, 65]) and wraps around the central H3. On either side of H3, the cavity is capped either by the Ω loop (the H2′-H3 loop) or by the H12 and the H11–H12 loop. The subcavities on either side of H3 extend along its axis and are additionally limited by the H1-H2 loop, the β sheet region, H2′, H5, and H6, on the one side, and by H5, H7, and H11, on the other side. Taking cues from the nomenclature employed by Waku et al. [66], these two subcavities of the PPAR LBP will be referred to as the Ω pocket and the AF-2 pocket, respectively (Figure 2). Comparing with more recent literature on PPARγ, these cavities roughly align with the regions referred to as the alternate- or allosteric binding site and the orthosteric binding site, respectively [67, 68]. Overall, the LBPs of the PPARs can be regarded as T- or Y-shaped and they have consequently been divided into three arms [69]; arm I reaches into the AF-2 pocket, while arms II and III largely constitute the Ω pocket. The residue numbers given in this text refer to the UNIPROT canonical isoforms for each of the known human PPARs: hPPARα1 (Q07869-1), hPPARβ/δ1 (Q03181-1), and hPPARγ2 (P37231-1) [1]. For comparison with earlier literature using, e.g., hPPARγ1 numbering, these residue numbers are given in parentheses were applicable.

On H3, at the interface between the Ω pocket and the AF-2 pocket, the PPARs host a region of conserved cysteine residues. The cysteine that is conserved across all three PPARs (hPPARα: Cys276, hPPARβ/δ: Cys249, and hPPARγ2(γ1): Cys313(285)) is located behind H3 and points into the narrow neck between the Ω pocket and the AF-2 pocket (Figure 2) [1, 70]. While this cysteine is demonstrably nucleophilic in PPARβ/δ [71–75] and PPARγ [66, 67, 71, 76–84], the eventual nucleophilicity of the corresponding Cys276 in PPARα appears to be surpassed by its neighbour Cys275 [76], which is located on the side of H3 that faces the Ω pocket. On the solvent-exposed side of H3, PPARα and PPARβ/δ contain additional cysteines (Cys278 and Cys251, respectively), the reactivities of which have not been established (Figure 2).

3. Classical PPAR Agonism, Antagonism, and beyond

Structurally, the dissociation of a corepressor protein complex and association with a coactivator protein complex appears to be related to the formation of a tighter groove between H3, H4, and H12, suited for the binding of the RIDs of a given coactivator protein, but that is unable to accommodate the slightly longer RIDs of typical corepressor proteins [64, 85–88]. As the outer surface of H12 is central to the binding of coactivator proteins, many of the known PPAR ligands have either been observed to, or have indeed been designed to, stabilize H12 through interactions with a conserved hydrogen bonding network in the AF-2 pocket, involving conserved tyrosine and histidine residues on H5, H11, and H12 [89].

Access to the AF-2 pocket through the binding of the head groups of classical agonistic ligands has also opened for the development of ligands that display H12-mediated antagonism [90]. These ligands destabilize H12 through perturbation of the AF-2 pocket hydrogen bonding network or by introducing sterically demanding moieties in the AF-2 pocket [86, 90–96]. In PPARγ, interactions with other nearby residues, such as Phe310(282) and Phe391(363), have also been implicated in the mode of action of this class of antagonistic ligands [97, 98]. Based on the observed conformations and folding states of H12 in the few available X-ray crystallographic structures of complexes with such ligands, they appear to disrupt the stable docking of H12 onto the core of the LBD and thus the formation or stabilization of the coactivator-binding groove [85, 88, 99]. In the Phe310/Phe391-interacting class of PPARγ antagonistic ligands, more subtle interactions or alternative binding modes may be involved, which in turn affect the conformational populations of H12 [97, 98].

Some of the reported antagonistic ligands display inverse agonism in that they cause the PPAR-mediated transcription to fall below basal levels in a given model system or assay [91, 94, 95, 97, 103]. In similarity to other reported PPAR inverse agonists [104–106], the observed subbasal transcription levels are likely reflected in the tendency of such ligands to strengthen the interactions of the PPARs with corepressor proteins, such as NCoR and SMRT, compared to those of the apo-PPARs [85, 88, 93, 103–106].

Considering LBD conformational dynamics, ligand binding leads to changes in the conformational populations of the LBD, as observed by nuclear magnetic resonance (NMR) spectroscopy [68, 86, 87, 97, 107–111], hydrogen-deuterium exchange coupled to mass spectrometry (HDX-MS) [68, 97,

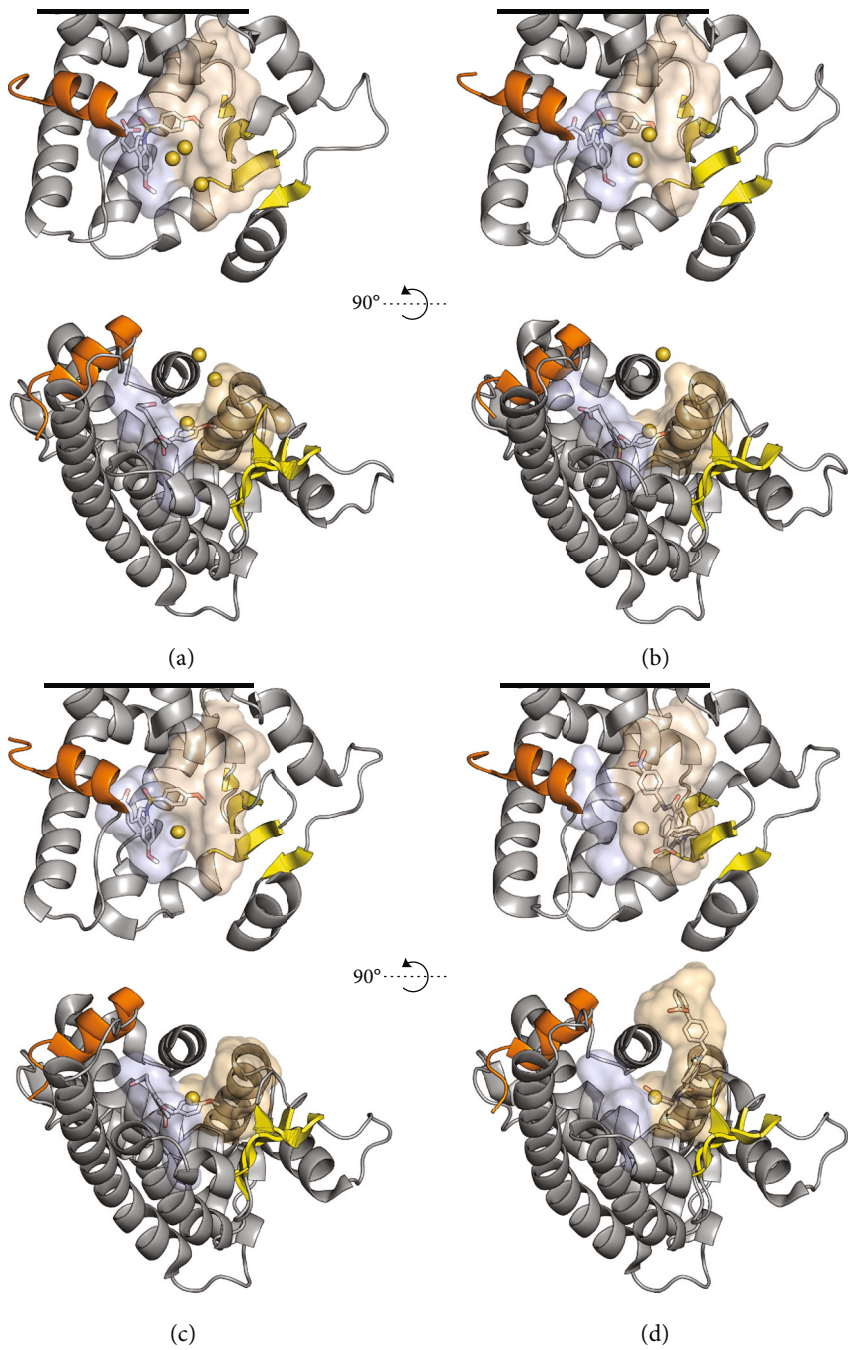

Figure 2: An overview of the shapes of the PPARα (a), PPARβ/δ (b), and PPARγ (c, d) LBPs and the subcavities referred to as the AF-2 pocket (light blue) and the Ω pocket (beige), lined by helix 12 (orange) and β1–β4 (yellow), respectively. For clarity, the N-terminal half of H3 and the Ω loop are hidden in the front views (top). Also, the visualizations of the LBDs have been truncated (black lines) in order to maximize the visibility of the LBP. Similarly, H2$'$, the Ω loop, and the N-terminal half of H3 are hidden in the top view (bottom). The sulfur atoms of the centrally located cysteines are shown as gold spheres, at 50% of their van der Waals radii. (a–c) PPARα, PPARβ/δ, and PPARγ in their respective complexes with indeglitazar (Figure S1) predominantly bound to the AF-2 pocket (PDB ID: 3ET1, 3ET2, and 3ET3, respectively) [100]. (d) PPARγ in complex with SR1664 (Figure S1) bound to the Ω pocket (PDB ID: 5DWL) [101]. The LBP surfaces were mapped with a 1.4 Å probe using HOLLOW [102], and the resulting population of probes was truncated at the solvent interface of the Ω pocket. The structures and surfaces were visualized in PyMOL (ver. 1.8.4.0) [13, 14].

101, 107, 112–117], and molecular dynamics (MD) simulations [86, 87, 96, 118, 119]. In PPARγ, analyses of such structural ensembles have demonstrated that the large conformational diversity observed in apo-PPARγ, in particular that of H12, is strongly reduced upon interaction with classical agonists. In contrast, upon treatment with less potent agonists, partial- and nonagonists, H12 still populates several minima [87, 107]. Coherently, high H-D exchange

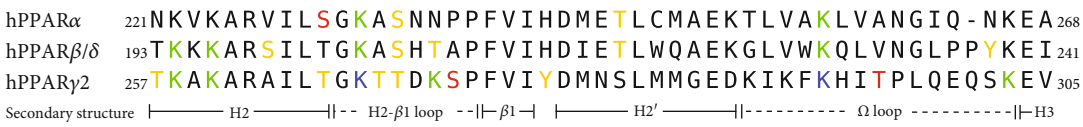

Figure 3: Sequence alignment of the H2-H3 region of the human PPARs, annotated with experimentally observed Ser/Thr/Tyr phosphorylations (red) and Lys acetylations (blue) [152] and with the same PTMs predicted using the tools [147–151] listed in Section 4 (orange and green, respectively). Notably, the employed tools also identified the experimentally observed PTMs.

rates have been observed for H12 in PPARγ treated with an inverse agonist, compared to those of H12 in apo-PPARγ [97]. Notably, the motions of the Ω loop in holo-PPAR complexes have also been suggested to affect the conformational populations of H12 [78, 118, 119].

During the last decade, evidence has accumulated on the toxicity of clinically employed PPARα and PPARγ classical agonists, such as certain fibrates [40, 41], glitazones [42–46], and glitazars [47–51], as well as that of a PPARβ/δ classical agonist in rodents [120, 121]. Combined with the knowledge of their common capacity for stabilization of H12, the frequently observed undesirable effects of these ligands could be interpreted as signs of a mechanism-based toxicity. Furthermore, as findings from the study of PPARγ demonstrate that classical agonism is not required to attain therapeutically relevant transcriptional outcomes (see Section 5), recent ligand development targeting PPARγ has aimed at avoiding ligands that strongly stabilize H12 [97, 122–127]. And while such nonclassical ligands for PPARγ are becoming numerous (Section 5.3), there is a scarcity of similar ligands for PPARα and PPARβ/δ (see Sections 6.1 and 7.1).

To amend this, the accumulated experience with the functional effects of ligand interaction with H12, delineated above, may serve as a guide for the future design of partial- and nonagonistic PPAR ligands. Ideally, these ligands should not cause a supraphysiological stabilization of H12, but may rather seek to achieve therapeutically relevant effects, e.g., by influencing PPAR posttranslational modifications (PTMs) (Section 4).

4. PPAR Posttranslational Modifications

Ligand binding is far from the only event that affects the activity and physiological roles of the PPARs during their lifetime. The PPARs are observed to be subject to a number of covalent modifications that are common to the nuclear environment and that, as such, are also found on other transcription factors and on histone proteins [128, 129]. So far, the PTMs observed in the PPARs include O-phosphorylation, O-GlcNAcylation, *N*-acetylation, *N*-SUMOylation, and *N*-ubiquitination [130–133]. The investigation of how each of these PTMs modulates protein function is among other things complicated by the effect one PTM can have on another. This encompasses the possibility of a direct competition between PTMs like O-phosphorylation and O-GlcNAcylation of the same serine, threonine, or tyrosine residue [134], as well as between PTMs such as *N*-acetylation, *N*-SUMOylation, and *N*-ubiquitination, which may compete for lysine residues [135–139]. PTMs can also operate in positive- or negative synergy, as in the case of phosphorylation-dependent SUMOylations [140–142] or as observed in the crosstalk between PTMs occurring on lysine or arginine residues, and the phosphorylation of nearby serine or threonine residues [143].

The PTMs that occur in the N-terminal domains of the PPARs can affect both their ligand-independent and their ligand-dependent regulation of gene expression [130–133]. However, while data exist on the influence of some of these PPAR PTMs on the degree of transactivation induced by ligand binding, less is known about the degree to which ligand binding affects the propensity of each of the PPARs towards undergoing such PTMs. From a medicinal chemistry perspective, this question may be of particular interest for PTMs occurring in the LBD, as the magnitude of the influence of ligand binding on the conformational populations of the LBD and thus on the propensity of the LBD to undergo a certain PTM could be larger than for distant regions, such as the N-terminal domain. On the other hand, conformational changes in the LBD may also lead to altered interdomain contacts that in turn can mask or unveil distant PTM sites. Thus, a modulation of the transcriptional outcome by PTMs that occur in the LBD may either be mediated by differential coregulator recruitment [116, 144, 145] or by altered interdomain contacts between the PPAR LBD, the PPAR:RXR DBDs [11, 146], or their N-termini. Additionally, such changes in the conformational populations of the PPARs may influence the promoter binding of PPAR:RXR-heterodimers [7, 12, 118] or the transrepressive activity of PPAR monomers [28–30].

Most of the knowledge on PPAR PTMs stems from studies of PPARγ and PPARα, while less is known about PTMs occurring in PPARβ/δ [130–132]. Interestingly, a large number of consensus PTM sites can be found in the primary sequences of all three PPARs using PTM consensus site mapping algorithms such as GPS-PAIL [147] (*N*-acetylation), PhosphoNET [148], PhosphoMotif Finder [149], or NetPhos [150, 151] (*O*-phosphorylation) (Figure 3). Meanwhile, databases of experimental PTM data, such as PhosphoSitePlus [152], contain records of several PTMs (not limited to phosphorylation), some of which occur in the PPAR LBDs. Among these, some ligand-sensitive PTMs occurring in the PPAR LBDs have been identified and studied experimentally, such as the phosphorylation of PPARγ Ser273, the acetylation of PPARγ Lys268/Lys293, and the phosphorylation of PPARα Ser179/Ser230 (Figure 3 and Sections 5.1, 5.2, and 6, respectively). Guided by data obtained from studies of these PTMs, their therapeutic relevance and the mode of action of the ligands that influence their occurrence are discussed in the following sections.

5. New Directions in PPARγ Pharmacology Guided by Relationships between Ligand Binding and PTMs

Among the beneficial effects of PPARγ activation by classical agonists, such as the thiazolidinediones (TZDs) used in the treatment of type II diabetes mellitus (T2DM) and other morbidities associated with obesity, two important axes have been recognized: firstly, improved insulin sensitivity and glucose tolerance, and secondly, increased energy expenditure in white adipose tissue [153, 154]. While historically the structural and mechanistic bases for each of these effects have been unclear, the discoveries and studies of the PTMs introduced above have greatly improved our understanding of their separate origins.

5.1. Posttranslational Phosphorylation of Ser273(245) in the PPARγ LBD. In 2010, following the identification of a consensus site for phosphorylation by cyclin-dependent kinase 5 (Cdk5) in PPARγ, Choi et al. demonstrated that Cdk5 indeed phosphorylates Ser273 and that this PTM was associated with insulin resistance in obese mice and humans [116]. The authors could also show that tumor necrosis factor (TNFα) induced this phosphorylation, indicating a link between this PTM and the inflammatory state of the obese mice. Using a nonphosphorylatable Ser273Ala mutant, Choi et al. further demonstrated that Ser273 phosphorylation was linked to a reduction in the expression of a subset of PPARγ target genes, including genes linked to insulin sensitivity such as adipsin and adiponectin [116]. The importance of this discovery was amplified by two concurrent findings: firstly, ligand binding decreased phosphorylation at Ser273 and secondly, the ability of a ligand to inhibit Ser273 phosphorylation did not correlate with its ability to induce adipogenesis or transcription in PPARγ reporter gene assays [116, 122]. These results were also in line with observations made previously by other workers, who had developed PPARγ ligands that were poor inducers of transcription of PPARγ reporter constructs, yet displayed potent insulin-sensitizing activity in isolated rodent cells and *in vivo* [155–161].

Choi et al. later demonstrated that a selective interaction of PPARγ phosphorylated at Ser273 (pSer273-PPARγ) with the coregulator protein thyroid hormone receptor-associated protein 3 (Thrap3) underlies the diabetogenic gene dysregulation [162]. In contrast, dephosphorylated PPARγ appears to interact with the coactivator SRC3 [116, 144]. The same group further demonstrated that in the absence of Cdk5, extracellular signal-regulated kinase (ERK) can directly phosphorylate Ser273 in PPARγ and that this phosphorylation is similarly inhibited by PPARγ ligands. In this work, Banks et al. also revealed Thr296 as a novel site of Cdk5 phosphorylation in PPARγ (Figure 3) [163].

Taken together, the above-described findings strongly suggested that an important part of the antidiabetic effects of PPARγ ligands was not linked to their potency as classical agonists but rather to their inhibition of Ser273 phosphorylation [116]. Against the background of the potentially life-threatening side effects observed in the clinical use of PPARγ classical agonists such as the glitazones [42–46], that in comparison strongly stabilize H12 [114, 115], these findings launched a new era for PPARγ-targeting pharmacotherapeutics for the treatment of metabolic disease, in which the focus has shifted towards the development of potent inhibitors of Ser273 phosphorylation, that display little or no classical agonism [123, 127, 164–166].

The discoveries described above were complimented by results from Li et al., who demonstrated that the interaction of Cdk5 with PPARγ was enhanced by interaction of PPARγ with the corepressor protein NCoR [144]. This effect was also observed in adipocyte-specific NCoR knockout mice, in that they displayed decreased levels of pSer273-PPARγ [144]. Together, these findings suggest that an inhibition of PPARγ association with NCoR may be a necessary aspect of the antidiabetic mode of action of PPARγ ligands (see also Section 5.2). Interestingly, Guo et al. recently demonstrated that for optimal repression of PPARγ, but not of PPARα and PPARβ/δ, both NCoR and SMRT make use of the corepressor complex component G protein pathway suppressor 2 (GPS-2) [167].

5.2. Posttranslational Acetylation of Lysine Residues in the PPARγ LBD. The interaction of PPARγ with NCoR has also been central to the study of another ligand-sensitive PTM, namely, the acetylation of Lys268 (Lys238, mPPARγ1) [145, 168] and Lys293 [145], which are located in the H2-β1 loop, close to Ser273, and in the Ω loop, respectively (Figure 3). Qiang et al. demonstrated that acetylation of both these lysine residues promoted PPARγ binding to NCoR and that this interaction was further strengthened in the presence of the HAT-containing coactivator protein CBP [145]. Using Lys-Gln mutants to mimic lysine acetylation, the authors also found that the acetylation of Lys293, but that not of Lys268, was linked to Ser273 phosphorylation [145]. These results thus paralleled the previous demonstration by Li et al. of the enhanced interaction of Cdk5 with NCoR-bound PPARγ [144].

Intriguingly, treatment of PPARγ with rosiglitazone, which inhibits Ser273 phosphorylation, also leads to deacetylation of Lys268 and Lys293 (among other lysines [168]) by the nicotinamide adenine dinucleotide- (NAD^+-) dependent deacetylase Sirtuin 1 (SirT1) [145, 169, 170]. The SirT1-mediated deacetylation of PPARγ was first shown by Han et al., who also demonstrated that PPARγ overexpression or troglitazone (Figure S1) treatment could downregulate SirT1 through the binding of an inhibitory PPARγ/SirT1 complex on the *SIRT1* promoter [171]. Nonetheless, Qiang et al. further demonstrated that the SirT1-mediated deacetylation of Lys293 in particular promoted the interaction of PPARγ with the coregulator PR domain zinc finger protein 16 (Prdm16) [145], which in turn upregulated a thermogenic, brown adipose tissue- (BAT-) related gene program in white adipose tissue (WAT) [145, 172, 173]. In further support of a link between the inhibition of phosphorylation of Ser273 and the deacetylation of Lys293, Wang et al. recently demonstrated that treatment of 3T3-L1-derived adipocytes with the Cdk-inhibitor roscovitine

(Figure S1) promoted the dissociation of PPARγ from NCoR, its association with SirT1 and Prdm16, and the subsequent expression of BAT-related genes such as uncoupling protein 1 (*Ucp1*) [174]. Similar results were obtained with a nonphosphorylatable PPARγ Ser273Ala mutant [174]. In contrast, Qiang et al. observed that while both a Ser273Ala mutant and a nonacetylatable Lys268Arg/Lys293Arg double mutant could induce adiponectin in differentiated Swiss 3T3 cells, only the Lys268Arg/Lys293Arg double mutant caused an upregulation of *Ucp1* compared to wild-type PPARγ [145]. Indeed, the interplay between PPARγ acetylation and the phosphorylation status of Ser273 appears to be complex; Mayoral et al. observed that a short-term high-fat diet (HFD) led to increased PPARγ acetylation and Ser273 phosphorylation in adipocyte-specific SirT1 knockout (ATKO) mice. However, although a chronic HFD (15 weeks) led to a further increase in PPARγ acetylation, it was accompanied by a decrease in Ser273 phosphorylation. Consistently, the ATKO mice displayed a concomitant increase in the expression of an insulin-sensitizing gene set and were thus better protected against the negative metabolic effects of the HFD, compared to wild-type mice [175].

As mentioned above, treatment of PPARγ with rosiglitazone, which binds to both the AF-2 pocket and the Ω pocket, leads to deacetylation of Lys268 and Lys293 [145, 169, 170]. However, despite the proximity of Lys268 and Lys293 to a ligand binding in the Ω pocket, Ohno et al. demonstrated that several partial and nonagonistic PPARγ ligands, which bind to the Ω pocket and inhibit Ser273 phosphorylation [116], had practically no effect on the upregulation of the brown adipocyte marker *Ucp1* in mice, compared to rosiglitazone [173]. In contrast, the partial agonist telmisartan (Figure S1) [176, 177], which also inhibits Ser273 phosphorylation [178], has been shown to moderately upregulate *Ucp1* [179, 180]. Additionally, although its binding mode in the PPARγ LBP is not known, the partial agonist natural product formonetin (Figure S1) [181] displayed the same ability [182]. In summary, these results indicate that the structural mechanisms through which PPARγ ligands can influence the acetylation status of Lys268/Lys293 and the upregulation of BAT-related genes in WAT, is in need of further study [183, 184].

5.3. Effects of Interaction Patterns and Binding Stoichiometries in the PPARγ LBP on Ser273 Phosphorylation and Transactivation. Given that various classical agonists, partial and nonagonists of PPARγ can all be efficacious as, e.g., insulin sensitizers, the observed toxicity of classical agonists in clinical use has emphasized a need to examine the interactions of each of these ligand classes with the PPARγ LBP, in order to establish which interaction patterns are likely to be conducive to desirable effects, such as the inhibition of Ser273 phosphorylation. In this vein, data from techniques such as X-ray crystallography and HDX-MS have demonstrated that a general theme among PPARγ ligands that are capable of inhibiting Ser273 phosphorylation is their binding to the Ω pocket, where they interact with the β-sheet region, H2$'$, the Ω loop, or H3 [101, 114, 185]. Through analysis of the binding mode of the 2-aminopyridine tail of rosiglitazone (Figure S1) in the Ω pocket, and subsequent ligand design, Bae et al. showed that interaction with a region between H3, residues 312-313 (284-285), and the β3-β4 loop, residues 368-370 (340-342), was conducive to the inhibition of Ser273 phosphorylation [101]. Notably, this region partially overlaps with the probe clusters P4 and P3, identified in a solvent mapping of the PPARγ LBP performed by Sheu et al., a study which also revealed several other possible sites of ligand interaction in the Ω pocket [186]. Consistently, a varied set of ligands of synthetic origin display the general interaction pattern outlined above and inhibit Ser273 phosphorylation, such as MRL24 [116], BVT.13 [116], nTZDpa [116], Mbx-102 [116], GQ-16 [115], F12016 [187], and imatinib [112] (Figure S1). Additionally, a range of natural products of diverse origins [188] bind to the PPARγ Ω pocket, some of which have been demonstrated to inhibit Ser273 phosphorylation, e.g., ionomycin [189], pseudoginsenoside F11 [190], amorfrutin 1 [191], and chelerythrine [192] (Figure S1).

The design of ligands for the PPARγ Ω pocket is complicated among other things by the potential of the PPARγ LBP to harbour more than one ligand simultaneously. Thus, although the binding of a single ligand to the PPARγ Ω pocket was observed crystallographically already in the early days of PPAR research [193], multiple ligands have since been observed to occupy the LBP in complexes with ligand : receptor stoichiometries of 2 : 1 [10, 66, 80, 194–198] and 3 : 1 [66, 199]. Additionally, Shang et al. recently identified electron densities in data from PPARγ cocrystals previously thought to be stoichiometric complexes, corresponding to cocrystallized nonanoic acid ligands [200]. Such passenger fatty acids, likely derived from the bacteria in which the PPAR proteins are expressed, have also been observed in PPARβ/δ cocrystals [201, 202].

As metabolic sensors, the PPARs are moderately to strongly activated by medium chain fatty acids (MCFAs) [199, 203], long-chain mono- and polyunsaturated fatty acids (MUFAs/PUFAs) and some of their metabolites [65, 204–209], as well as by oxo- and nitro-fatty acids [76–78, 80–82]. The members of the latter two ligand groups bind covalently to the central cysteine residue, Cys313(285) of the PPARγ LBP. In PPARγ reporter gene assays, the degree of transactivation by both MCFAs and MUFAs peak at certain chain lengths [199, 203], possibly reflecting the ligand : receptor binding geometries and -stoichiometries available to a given fatty acid. Furthermore, the simultaneous binding of 15-oxoeicosatetraenoic acid (15-oxoETE, Figure S2) and the serotonin metabolite 5-methoxyindole acetate (MIA, Figure S2) has been observed in the crystal phase. Notably, the maximum transcriptional activity induced by a combination of 15-oxoETE (10 μM) and MIA (100 μM) in a PPARγ reporter gene assay was roughly twice that induced by rosiglitazone (1 μM), while either 15-oxoETE or MIA alone, at the same concentrations, only induced about half the activity of rosiglitazone [66].

In parallel, while treatment of PPARγ with nonanoic acid or docosahexaenoic acid (DHA) (Figure S1) inhibited Ser273

phosphorylation [199], treatment with a mixture of oleic and palmitic acid (Figure S1) [116], with palmitic acid alone [210] or with eicosapentaenoic acid (EPA, Figure S1) [211], appeared to promote this PTM. Interestingly, in the latter study, DHA induced a higher expression of adiponectin at 100 μM than at 200 μM [211].

Considering ligands of synthetic origin, the ligand BVT.13 [159, 212] (Figure S2) was observed to bind to PPARγ in a 1 : 1 stoichiometry in the crystal phase, primarily interacting with H3 and not with H12 [12, 114, 159]. And while HDX-MS experiments did not indicate that BVT.13 treatment stabilized H12 significantly compared to apo-PPARγ [114], the transcriptional response to BVT.13 was 60-80% of that of rosiglitazone, in PPARγ reporter gene assays [114, 159]. BVT.13 is also an inhibitor of Ser273 phosphorylation [116]. In contrast, 10 μM of the ligand GW0072 (Figure S2), which also appears to bind exclusively to the Ω pocket, displayed a maximum transcriptional activation of 20% of that induced by rosiglitazone (1 μM, 100%) in a PPARγ reporter gene assay. While data on the ability of GW0072 to inhibit phosphorylation of Ser273 is not available, GW0072 caused dissociation of NCoR from PPARγ [193]. However, it is noteworthy that GW0072 (10 μM) did not induce the expression of neither adipsin nor fatty acid-binding protein 4 (FABP4/aP2) in 10T1/2 cells after up to 6 days, while rosiglitazone (1 μM) strongly upregulated both after 6 days [193].

Examples of negative cooperativity from the binding of multiple ligands of synthetic origin have also been reported. The ligand T2384 (Figure S2) displayed biphasic response curves in coregulator recruitment assays, with reduced recruitment of the coactivator MED1 (DRIP205) and increased recruitment of the corepressor NCoR at higher concentrations [197]. A similar biphasic coregulator recruitment pattern was also observed for the partial agonist telmisartan [176].

The phenomenon of multiple ligation of the PPARγ Ω pocket at higher ligand concentrations is paralleled by the binding of a single ligand in multiple conformations, as observed in the case of, e.g., SR1664 (Figure S1) [97, 101]. In the crystal phase, SR1664 was first shown to bind in a conformation similar to that of classical agonists, in which its interactions with Phe310(282) appeared to prevent it from functioning as an agonist [97, 98]. Bae et al. later demonstrated that SR1664 also binds to the Ω pocket (Figure 2(d)) and that this binding mode is likely of greater importance for its inhibition of Ser273 phosphorylation [101].

Taken together, these results paint a complex picture in which the binding of multiple molecules of the same or of different ligands is possible and may result in either positive or negative cooperativity in terms of transactivation. The collective efforts described above also illustrate that while inhibition of Ser273 phosphorylation likely requires interactions with regions of the PPARγ Ω pocket, a single consensus pharmacophore for the design of nonagonistic inhibitors of Ser273 phosphorylation has yet to be firmly established.

5.4. Clinical Applications of pSer273 Inhibitors. Interestingly, metabolic disease was not the only condition that could potentially be remediated by partial or nonagonistic PPARγ ligands. In a microarray analysis of the genes regulated by the murine, nonphosphorylatable Ser273Ala PPARγ mutant, Choi et al. revealed that two genes involved in myelination, neuroblast differentiation-associated protein AHNAK (*Ahnak*/desmoyokin) [213] and myelin proteolipid protein (*Plp1)* [214], were also positively regulated [116]. PPARγ has been found in high concentrations in the cerebrospinal fluid of multiple sclerosis (MS) patients [215] and has been suggested to play a role in neuroprotection and remyelination [216, 217]. Although the cluster containing *Ahnak* and *Plp1* was not as strongly upregulated by PPARγ ligands as by the Ser273Ala mutant [116], these findings suggested that inhibitors of PPARγ Ser273 phosphorylation may also be useful in the treatment of inflammation-related neurodegenerative diseases.

This dual therapeutic potential is exemplified in the account of the PPARγ partial agonist CHS-131 (formerly INT131, T0903131, T131, and AMG131, Figure S2) [156, 218, 219]. While CHS-131 (1–10 mg/day) displayed promising results in clinical trials oriented towards the treatment of metabolic diseases (NCT00952445 [220] and NCT00631007 [221]), it was later repurposed for the treatment of relapsing-remitting MS (RRMS) [222]. In 2016, upon completion of a 6-month phase IIb trial in patients with treatment-naïve RRMS, Coherus BioSciences Inc. reported that CHS131 decreased cumulative contrast-enhancing (CE) and T2 lesions, as well as cortical volume loss in the treatment group (NCT02638038) [223, 224]. In the former, metabolism-oriented trials, dose-dependent, yet less severe side effects were observed [220], comparing CHS131 to the PPARγ classical agonist pioglitazone (Figure S2) on parameters such as hemodilution and edema. No bone demineralization was observed with CHS-131, although the study was not powered to statistically evaluate this effect against that of pioglitazone [221]. In the RRMS trial, no serious side effects were noted at the employed effective dose (3 mg/day) [223, 224]. On the background of the gene expression data for rosiglitazone versus that of the weak partial agonist MRL24, reported by Choi et al. [116], these clinical observations can also be interpreted to provide support for the notion that the observed side effects of PPARγ classical agonists stem from the broader gene set they induce.

In the context of this review, the apparent clinical efficacy and safety of CHS-131 are of particular interest since, as a PPARγ ligand, CHS-131 may be characterized as a partial classical agonist based on its observed activation of transcription in various PPARγ reporter gene assays (15-40% of the effect of rosiglitazone) [218, 219, 156]. This could suggest that more completely nonagonistic ligands may display even better safety profiles. Indeed, two studies report that structural modifications to CHS-131 can produce ligands with substantially lower transactivation capacities, without sacrificing affinity for PPARγ [218, 225].

Finally, as suggested by a recent study, a future clinical application of nontoxic inhibitors of PPARγ Ser273 phosphorylation may also include their use as adjuvants to chemotherapy, in cases in which increased levels of

pSer273-PPARγ, resulting from DNA damage by cytotoxic agents, leads to reduced sensitivity to the chemotherapy [226].

6. Relationships between PTMs and Ligand Binding in PPARα

The available data on relationships between PTMs in the PPARα C-terminal domains (D–F) and ligand binding are limited, but include two reports describing the protein kinase C- (PKC-) mediated phosphorylation of PPARα and its effects on the propensity for ligand binding to confer either transactivation (PPRE-mediated transcription of target genes) or transrepression [227, 228]. Prompted by an earlier result linking the expression of PPARα to that of PKC in rat liver [229], Blanquart et al. demonstrated that the phosphorylation of PPARα at Ser179 and/or Ser230 by PKC increased both basal and ligand-induced transcription of target genes such as carnitine palmitoyltransferase 1 (*CPT1)* and *PPARA* in a human liver cancer cell line [227]. Conversely, pharmacological inhibition of PKC or the use of a nonphosphorylatable, Ser179Ala/Ser230Ala double mutant, reduced the ability of PPARα classical agonists like WY14643 (pirinixic acid) and GW7647 (Figure S3) to induce the expression of these target genes and increased both the basal and the ligand-induced PPARα-mediated transrepression of the basal expression of fibrinogen beta chain (FGB) [230, 231] in HepG2 cells [227]. Similarly, Paumelle et al. could demonstrate that PKC inhibition or use of the PPARα double mutant attenuated the lipopolysaccharide-(LPS-) induced expression of the proinflammatory nuclear factor NF-kappa-B (NFκB) target gene inducible nitric oxide synthase (iNOS) in murine macrophages. The transrepression of LPS-induced iNOS expression was also observed upon treatment of PPARα with the agonist GW9578 (Figure S3) and the 3-hydroxy-3-methyl-glutaryl-coenzyme A (HMG-CoA) reductase inhibitor simvastatin (Figure S3). The authors further demonstrated that while the transrepression of iNOS expression was dependent on PPARα for both these ligands, pretreatment of murine macrophages or neutrophils with simvastatin also interfered with the ability of LPS-induced, immunoprecipitated PKCα to phosphorylate a generic target like histone H1 in an *in vitro* assay [228]. Nonetheless, taken together with the stronger transrepressive effect observed upon upstream inhibition of PPARα phosphorylation using PKC inhibitors, the transrepressive effects of PPARα treatment with WY14643, GW7647, or GW9578 alone, compared to DMSO controls, may indicate that ligand binding itself, at least in part, reduces the propensity for PPARα to be phosphorylated by PKC.

Structurally, PPARα Ser179 is located in the hinge region, close to the PPARα DBDs, while Ser230 is located in the H2-β1 loop, in similarity to the Cdk5 phosphorylation target Ser273 in PPARγ (Figure 3). Thus, the results described above could indicate that the H2-β1 loop is a region of general interest for ligand-sensitive PTMs in the PPAR LBDs.

Interestingly, in a later, independent study by Roy et al., it was confirmed that simvastatin is also a PPARα ligand ($EC_{50} = 4.26\,\mu$M) [232]. In this study, the authors also performed molecular docking of the simvastatin δ-lactone to the PPARα LBP and found that it bound to the Ω pocket, where it interacted with Leu331 and Tyr334 of β3. Subsequently, site-directed mutagenesis of these residues (Leu331-Met, Tyr334Asp) and evaluation in a PPARα reporter gene assay revealed that simvastatin was unable to activate transcription through the Leu331Met/Tyr334Asp mutant. Notably, similar results were obtained for mevastatin and its 6-hydroxylated, ring-opened analogue pravastatin (Figure S3) [232]. However, the propensity of statin δ-lactones to be converted to their 3,5-dihydroxy acids (Figure S3) through hydrolysis or metabolism [233–236] raises the question of whether the observed effects of PPARα treatment with statins stem from the binding of the intact δ-lactones, the 3,5-dihydroxy acids, or both.

Nevertheless, Roy et al. demonstrated that treatment of murine astrocytes with simvastatin led to an upregulation of neurotrophin 3 (NT-3) and brain-derived neurotrophic factor (BDNF) which was dependent on cAMP response element-binding protein (CREB), whose expression is in turn regulated by PPARα [232]. The transcriptional regulation of CREB by PPARα appears to play a central role in hippocampal neuron plasticity and spatial memory consolidation in mice [237]. These results suggest a potential for PPARα-targeting ligands that regulate CREB expression in the treatment of neurodegenerative diseases such as Alzheimer's disease [238, 239].

In summary, additional studies are needed to elucidate whether both of the discussed PKC phosphorylation sites in PPARα are involved in the observed effects, to what degree their phosphorylation is sensitive to ligand binding and what the binding modes of such ligands are. Taken together, however, these results illustrate that a refinement of our understanding of the interplay between ligand binding modes, PTMs, and their combined physiological effects may be instrumental towards harnessing the therapeutic potentials of PPARα ligands that do not necessarily share the transcriptional profiles of classical agonists.

6.1. PPARα Ligands with Alternative Binding Modes. So far, few ligands have been reported to display alternative binding modes in the PPARα LBP. In the crystal phase, Bernardes et al. observed that while one molecule of WY14643 bound in a conformation akin to other PPARα classical agonists, a second molecule bound to a novel site under the Ω loop (Figure 4). This binding mode strongly stabilized the Ω loop, as observed both in the crystal phase and with MD simulations [119]. Of particular interest in the context of the studies on the possible PKC-mediated phosphorylation of PPARα Ser230 described above, MD simulations also demonstrated that the binding of the second molecule of WY14643 stabilized the Ser230-containing H2-β1 loop (Figure 3) [119].

Finally, during the development of the Ω pocket-binding PPARγ ligand BVT.13 [159, 212], described in Section 5.3, three additional ligands, BVT.762, BVT.763, and Compound 5d (Figure S3), also displayed binding to PPARα ($K_i = 25\,\mu$M, $20\,\mu$M, and $19\,\mu$M, respectively) and induced transcription in a PPARα reporter gene assay

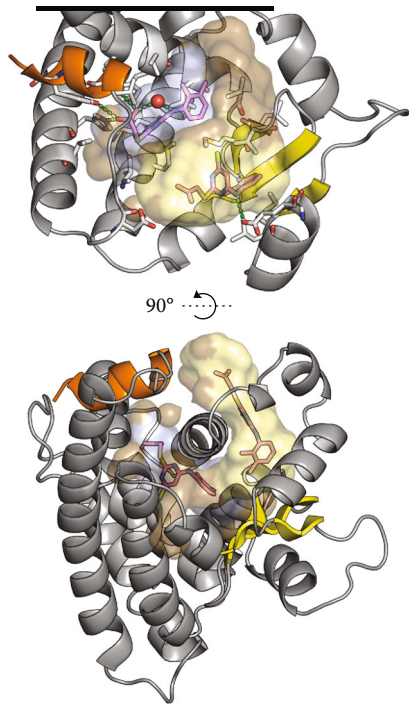

Figure 4: PPARα in complex with two molecules of WY14643 (shown with magenta carbons) taken from PDB ID: 4BCR [119]. H12 is shown in orange, and β1-β4 are shown in yellow. To illustrate ligand-pocket interactions, the inner surface of the binding pocket is shown in brown with surface areas ≤ 3.7 Å from the ligand binding primarily in the AF-2 pocket highlighted in light blue. Similarly, the contact surfaces of the ligand binding in the Ω pocket and under the Ω loop are shown in pale yellow. Top: residues ≤ 5.0 Å from the ligands are shown with grey carbons. Plausible hydrogen bonds are indicated with green dashes. The side chain oxygen of Ser280 is shown as a red sphere at 50% of its van der Waals radius. For clarity, the Ω loop and the N-terminal half of H3 (residues 252-284) are hidden. Also, the visualization of the LBD has been truncated (black line) in order to maximize the visibility of the LBP. Bottom: a perpendicular view to the LBP illustrating the distance between the WY14643 binding sites. The Ω loop is shown in a cartoon representation with two notable helical segments, indicating its stabilization by the binding of the second molecule of WY14643 [119]. The LBP surfaces were mapped with a 1.4 Å probe using HOLLOW [102], and the resulting population of probes was truncated at the solvent interface of the Ω pocket. The structures and surfaces were visualized in PyMOL (ver. 1.8.4.0) [13, 14].

with $EC_{50} = 5\,\mu M$, $3.8\,\mu M$, and $2.5\,\mu M$, respectively [212]. Although no data is available on their binding modes in the PPARα LBP or their influence on PPARα PTMs, the binding of BVT.13 to the PPARγ Ω pocket suggests that these ligand structures may be of interest in the development of ligands for the PPARα Ω pocket.

7. PPARβ/δ PTMs and Ligands with Nonclassical Binding Modes

To the best of our knowledge, the only records to date of experimentally determined PTM-like modifications of the PPARβ/δ LBD are contained within a curated entry in the PhosphoSitePlus database. This entry denotes the immunohistochemical- and mass spectrometrical detection of PPARβ/δ apparently phosphorylated at Thr252, Thr253, and Thr256 on H3 by ribosomal protein S6 kinase alpha-3 (RPS6KA3), also known as p90 ribosomal S6 kinase 2 (RSK2) [240]. Consequently, no further details exist on the function or ligand sensitivity of these PTMs. Structurally, the partially buried localization of Thr252, Thr253, and Thr256 raises the question of whether they are indeed plausible PTM sites. It is noteworthy, however, that RSK2 has been reported to interact with an overlapping region in the human estrogen receptor α (hERα, residues 326-394, including H1, the H1-H3 loop, H3, H4, and H5) [241].

7.1. PPARβ/δ Ligands with Alternative Binding Modes. In studies of PPARβ/δ, ligands that display binding modes other than those of classical agonists have also been described. Shearer et al. reported a series of potently binding partial agonists, some of which were intriguingly poor inducers of transcription. Compound 34, Compound 13, and Compound 14 (Figure S4) displaced a radioligand with $IC_{50} = 13$ nM, 3 nM, and 10 nM, respectively. In a cell-based reporter gene assay, Compound 34 and Compound 13 displayed an $EC_{50} = 0.2\,\mu M$ and an $EC_{50} = 1.3\,\mu M$, with 29% and 37% maximal activation, respectively. The transcriptional activation observed with Compound 14, on the other hand, was below the sensitivity threshold of the reporter gene assay (~20%). In comparison, the classical agonist GW501516 (Figure S4) displayed an $IC_{50} = 5$ nM and an $EC_{50} = 3$ nM (98% maximal activation) in the same assays. In a crystal structure of PPARβ/δ in complex with the original high-throughput screening (HTS) hit, GW9371 (Figure S4, $EC_{50} = 1.3\,\mu M$, 61% maximal activation), the ligand bound around H3, with its tetrahydroisoquinoline moiety protruding into the AF-2 pocket [242]. In contrast to the polar interactions common to the carboxylic acid head groups of classical agonists such as GW0742 (Figure S1), the distal aryl ring in GW9371 appears to display primarily hydrophobic interactions with the surrounding residues, among them Tyr437 of H12 (Figures 5(a) and 5(b)). Compound 13 and Compound 14 are structural analogues of GW9371 in which the hydrogen in the 5-position of its tetrahydroisoquinoline ring (Figure 5(b), teal sphere) has been substituted with a formic acid or a 2-oxyacetic acid, respectively (see Figure S4). While, as the authors suggest, the introduction of these substituents may have affected the membrane permeability of the resulting ligands [242], it is also possible that the diminished agonistic activities of Compound 13 and Compound 14 compared to GW9371 owe to the bulkiness of their AF-2 pocket-binding moieties, which may cause them to display H12-mediated antagonism (see Section 3).

Keil et al. described a series of ligands that interacted with H12 to a lesser degree than the GW series described above, binding in a U-shaped conformation around Cys249 (e.g., Compound 6, Figure 5(c) and Figure S4). From the extensive structure-activity relationships in all three PPARs established by the authors, a relevant ligand in this context was Compound 11j (Figure S4), which displayed

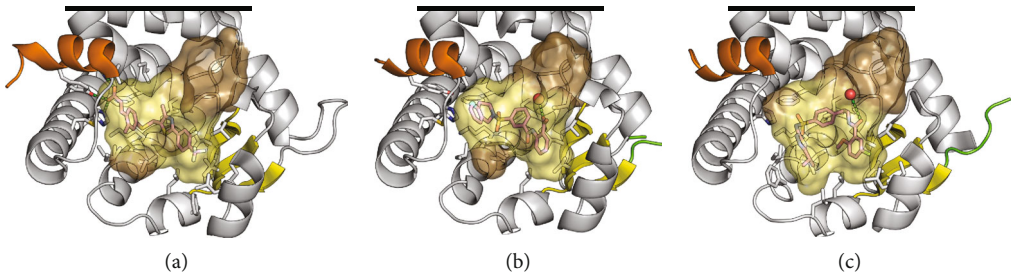

Figure 5: The LBP of PPARβ/δ in complex with ligands (shown with magenta carbons). To illustrate ligand-pocket interactions, the inner surface of the binding pocket is shown in brown with surface areas ≤ 3.7 Å from the ligand highlighted in pale yellow. Residues ≤ 5.0 Å from the ligand are shown with grey carbons. Plausible hydrogen bonds are shown with green dashes. H12 is shown in orange, and β1-β4 are shown in yellow. The unresolved termini of the H2–β1 loop are shown in light green. For clarity, the Ω loop and the N-terminal half of H3 (residues 224–257) are hidden. Also, the visualizations of the LBD have been truncated (black lines) in order to maximize the visibility of the LBP. (a) Classical agonist, GW0742 (PDB ID: 3TKM) [245]. (b) Partial agonist GW9371 (PDB ID: 3DY6) [242]. The side chain oxygen of Thr252 is shown as a red sphere at 50% of its van der Waals radius. (c) Compound 6 (PDB ID: 2XYX) [243]. The LBP surfaces were mapped with a 1.4 Å probe using HOLLOW [102], and the resulting population of probes was truncated at the solvent interface of the Ω pocket. The structures and surfaces were visualized in PyMOL (ver. 1.8.4.0) [13, 14].

an EC_{50} = 120 nM with 22% activation of a PPARβ/δ reporter gene assay (100% was set as the maximum achievable activation by GW501516). Importantly, Compound 11j also displayed a high selectivity for PPARβ/δ over the other PPARs [243].

In a genome-wide analyses of the transcriptional regulation by PPARβ/δ in myofibroblasts treated with a classical agonist such as GW501516 or L-165,041 (Figure S4), or with *PPARD* siRNA, Adhikary et al. demonstrated distinct modes of transcriptional response among PPARβ/δ target genes, including their individual ligand inducibilities [244]. If applied to nonclassical ligands such as Compound 14 (above) or Compound 11j, analyses in the same vein could reveal distinct regulatory patterns of therapeutic relevance. In summary, Compound 14 and Compound 11j represent valuable pharmacological tools to compare the transcriptional effects of weak partial agonists to those of classical agonists that actively stabilize PPARβ/δ H12.

8. Pharmacological Tools and Recent Advances in the Development of Ligands for the PPAR Ω Pockets

8.1. PPARγ. It has been observed that while treatment of PPARγ with ligands that bind covalently to the central cysteine residue, Cys313(285), such as GW9662 [71] or T0070709 [83] (Figure S2), limits the access to the AF-2 pocket (i.e., antagonizes the action of classical agonists), it does not inhibit the subsequent binding of an additional ligand in the Ω pocket [68, 101]. This phenomenon aligns with the numerous previous observations of the capacity of the PPARγ LBP to house multiple ligands simultaneously, as discussed in Section 5.3. Consequently, pharmacological and physiological (re)interpretations of the effects of treatment of PPARγ with this class of antagonists should reflect the possibility of interference from ligands that bind to the Ω pocket of the covalently modified receptor [68]. The notion that such interference could be pharmacologically relevant is substantiated by the observation that, in similarity to the synergistic activation observed upon simultaneous binding of multiple MCFAs [199, 203], the binding of a second ligand to PPARγ treated with GW9662 produced a stronger response in a PPARγ reporter gene assay than that observed with the ligand alone [246]. The classical PPARγ agonist MRL20 (Figure S2) has also been demonstrated to retain its ability to activate PPARγ after treatment with GW9662 or T0070907 by binding to the Ω pocket in a pose that was markedly different [68] from its crystallographically observed pose in untreated PPARγ (PDB ID: 2Q59) [114]. Thus, to address the "single-sided" antagonism of GW9662 and T0070907, Brust et al. recently designed analogues of these ligands, with bulkier groups protruding into the Ω pocket, blocking the binding of MRL20 [67].

On the other hand, the persistent ligand binding ability of the Ω pocket in PPARγ treated with GW9662 or T0070907 also opened up the possibility to use the covalently modified protein as a model in which to screen for new Ω pocket binders. Indeed, Ohtera et al. developed a method to screen a natural product extract library for the ability of the tested fractions to cooperatively activate transcription in a PPARγ reporter gene assay, upon cotreatment with GW9662 [246]. This allowed the authors to identify a methoxyphenylcinnamic ester ligand and further combine its structure with that of GW9662 to produce a hybrid partial agonist, Compound 5 (Figure S2), that bound covalently to Cys313(285) and likely occupied the Ω pocket (supported by molecular modelling) [246]. The ability of Compound 5 to inhibit PPARγ Ser273 phosphorylation was not investigated. In a later study, Bae et al. prepared a series of analogues of GW9662 which were shown by X-ray crystallography to bind covalently to Cys313(285), as well as to occupy the Ω pocket [101]. These ligands were designed to place an aryl moiety in a specific region between H3, β3, and β4 (see Section 5.3). The most promising of the resulting ligands, SB1405 and SB1453 (Figure S2), were shown to be potent inhibitors of Ser273 phosphorylation and practically devoid of classical agonism [101]. These results suggest that the covalent PPARγ partial agonist, L-764406 (Figure S2),

reported by Elbrecht et al. in 1999 [84], may also be capable of inhibiting Ser273 phosphorylation. During their studies, Bae et al. also prepared the *N*-methyl analogue of GW9662, SB1404 (Figure S2) [101], which given its marginal occupation of the Ω pocket may prove interesting in the context of screening campaigns similar to that of Ohtera et al. described above [246]. In the design of kinase inhibitors [247, 248], Serafimova et al. and Miller et al. took advantage of the reversibility of the 1,4-addition of thiolates to highly activated electrophiles, such as acrylonitriles [249]. Using this strategy, Kim et al. recently prepared and tuned a series of reversibly covalent and selective inhibitors of PPARγ Ser273 phosphorylation [250]. In a recent report by Jang et al., the crystal structure of PPARγ in complex with the most promising of the resulting ligands, SB1495 (Figure S2), demonstrated that SB1495 bound primarily to Ω pocket, where it stabilized the β-sheet region, H2$'$, and the Ω loop [251]. Given its covalent, reversible mode of action, ligands such as SB1495 may thus pave the way for more clinically efficacious, yet nontoxic inhibitors of PPARγ Ser273 phosphorylation.

8.2. PPARα and PPARβ/δ. GW9662, which targets Cys313(285) in PPARγ, has been reported to also covalently modify PPARα and PPARβ/δ [71]. In PPARα, Cys275 appears to be more reactive than its neighbour Cys276 [76], which corresponds to Cys313(285) in PPARγ. The side chain of Cys275 also points more directly into the Ω pocket than that of Cys276. Regardless of their position, both these cysteine residues may be favourably utilized in the design of electrophilic ligands for the PPARα Ω pocket.

In the field of PPARβ/δ, on the other hand, several members of the 5-trifluoromethyl-2-sulfonylpyridine class of covalent antagonists, such as GSK3787 [72], CC618 [73], and Compound 37 [74] (Figure S4) have been reported. While these ligands differed in their selectivity for PPARβ/δ versus the other PPAR subtypes and in their rate of reaction with Cys249 [74], treatment of PPARβ/δ with either of these ligands resulted in the formation of a Cys249 5-trifluoromethyl-2-pyridyl thioether [75]. Although the aryl moiety appended to PPARβ/δ Cys249 is less bulky than the moieties appended to PPARγ Cys313 by treatment with GW9662, T0070907, or SB1404, this modification still inhibited activation of PPARβ/δ by classical agonists whose head groups bind to the AF-2 pocket, such as GW501516 or GW0742 (Figure S4) [72–74, 252]. Treatment of PPARβ/δ with CC618 or GSK3787 alone did not induce transcription in reporter gene assays [72, 252] nor did treatment with GSK3787 cause the recruitment of the coactivator MED1 (TRAP220) in a TR-FRET-based assay [252]. In a similar assay, treatment with GSK3787 did however result in a moderate, but statistically significant dissociation from the corepressors NCoR and SMRT compared to apo-PPARβ/δ [252]. Whether PPARβ/δ covalently modified at Cys249 is still capable of binding additional ligands in its Ω pocket has yet to be investigated. More importantly, the transcriptional effects of this type of multiple ligation are also unknown. Thus, for the identification of ligands that bind to the PPARβ/δ Ω pocket, other screening methodologies than that of Ohtera et al. [246] described in the previous section may require consideration.

To that end, recent studies of PPARγ have highlighted that ^{19}F NMR represents a powerful technique to study the binding of fluorine-containing ligands to both the AF-2 pocket and the Ω pocket [68, 107]. Chrisman et al. also demonstrated that the effects of the binding of several classes of nonfluorinated ligands on the conformational dynamics of PPARγ could be characterized with ^{19}F NMR, after covalent modification of mutagenetically introduced cysteine residues in H3 and H12 with a trifluoroacetone probe [87]. Thus, in the context of screening for ligands that bind to the Ω pocket of PPARβ/δ treated with the 5-trifluoromethyl-2-sulfonylpyridine class of covalently modifying ligands, the relative proximity of the Cys249 5-trifluoromethyl-2-pyridylthioether to a ligand binding in the Ω pocket suggests that a ^{19}F NMR-based assay may be viable.

9. Conclusions

Herein, we have described discoveries and collective efforts from recent years that have promoted a more nuanced understanding of the pharmacology of PPARγ—an understanding that has already had important ramifications for both PPARγ-targeting therapy and further drug development. These achievements have occurred within a framework that integrates the study of ligand binding, PTMs, protein-protein interactions, and their combined effects on transcription. Collectively, the results obtained within this framework have signalled a shift in interest, away from classical PPARγ agonists that induce supraphysiological levels of unselective transcriptional activation, to the development of nonagonistic- and other noncanonical ligands that more selectively influence gene expression patterns by modulating the occurrence of PTMs. A common theme among many of these new ligands is their binding to the PPARγ Ω pocket. We have ventured to show that the application of these emerging principles to the study of PPARα and PPARβ/δ can potentially provide new insights, e.g., through the identification of ligand-sensitive PTMs and the study of their effects on gene expression patterns, but also through the application of known ligands with alternative binding modes in new assay contexts. The data generated by such efforts would lay the foundation for the development of new generations of drugs targeting PPARα and PPARβ/δ.

Conflicts of Interest

The authors declare that there is no conflict of interest regarding the publication of this paper.

Acknowledgments

We would like to thank current and past coworkers for fruitful collaborations and experimental and methodological efforts. The Norwegian Research Council is gratefully acknowledged for generously funding T.V.H through KOSK

(197708), KOSK II (207053), BIOTEK2021 (224811), and FRIPRO-FRINATEK (230470).

Supplementary Materials

The chemical structures of the ligands described in the contexts of PPARγ, PPARα, and PPARβ/δ are depicted in their order of appearance in Figures S1–S4 in the Supplementary Material. *(Supplementary Materials)*

References

[1] The UniProt Consortium, "UniProt: a hub for protein information," *Nucleic Acids Research*, vol. 43, no. D1, pp. D204–D212, 2015.

[2] H. E. Xu and Y. Li, "Ligand-dependent and -independent regulation of PPARγ and orphan nuclear receptors," *Science Signaling*, vol. 1, no. 48, article pe52, 2008.

[3] S. Hummasti and P. Tontonoz, "The peroxisome proliferator-activated receptor N-terminal domain controls isotype-selective gene expression and adipogenesis," *Molecular Endocrinology*, vol. 20, no. 6, pp. 1261–1275, 2006.

[4] R. M. Evans and D. J. Mangelsdorf, "Nuclear receptors, RXR, and the big bang," *Cell*, vol. 157, no. 1, pp. 255–266, 2014.

[5] C. Juge-Aubry, A. Pernin, T. Favez et al., "DNA binding properties of peroxisome proliferator-activated receptor subtypes on various natural peroxisome proliferator response elements: importance of the 5′-flanking region," *Journal of Biological Chemistry*, vol. 272, no. 40, pp. 25252–25259, 1997.

[6] D. G. Lemay and D. H. Hwang, "Genome-wide identification of peroxisome proliferator response elements using integrated computational genomics," *The Journal of Lipid Research*, vol. 47, no. 7, pp. 1583–1587, 2006.

[7] F. Rastinejad, V. Ollendorff, and I. Polikarpov, "Nuclear receptor full-length architectures: confronting myth and illusion with high resolution," *Trends in Biochemical Sciences*, vol. 40, no. 1, pp. 16–24, 2015.

[8] S. A. Kliewer, K. Umesono, D. J. Noonan, R. A. Heyman, and R. M. Evans, "Convergence of 9-*cis* retinoic acid and peroxisome proliferator signalling pathways through heterodimer formation of their receptors," *Nature*, vol. 358, no. 6389, pp. 771–774, 1992.

[9] T. Venäläinen, F. Molnár, C. Oostenbrink, C. Carlberg, and M. Peräkylä, "Molecular mechanism of allosteric communication in the human PPARα-RXRα heterodimer," *Proteins*, vol. 78, no. 4, pp. 873–887, 2010.

[10] H. Zhang, X. Xu, L. Chen et al., "Molecular determinants of magnolol targeting both RXRα and PPARγ," *PLoS One*, vol. 6, no. 11, article e28253, 2011.

[11] D. J. Kojetin, E. Matta-Camacho, T. S. Hughes et al., "Structural mechanism for signal transduction in RXR nuclear receptor heterodimers," *Nature Communications*, vol. 6, no. 1, article 8013, 2015.

[12] V. Chandra, P. Huang, Y. Hamuro et al., "Structure of the intact PPAR-γ-RXR-α nuclear receptor complex on DNA," *Nature*, vol. 456, no. 7220, pp. 350–356, 2008.

[13] L. L. C. Schrödinger, *The PyMOL Molecular Graphics System, Version 1.8*, 2015.

[14] W. L. Delano, "PyMOL: An Open-Source Molecular Graphics Tool," *CCP4 Newsletter On Protein Crystallography*, vol. 40, pp. 82–92, 2002.

[15] P. Dowell, J. E. Ishmael, D. Avram, V. J. Peterson, D. J. Nevrivy, and M. Leid, "Identification of nuclear receptor corepressor as a peroxisome proliferator-activated receptor α interacting protein," *Journal of Biological Chemistry*, vol. 274, no. 22, pp. 15901–15907, 1999.

[16] A.-M. Krogsdam, C. A. F. Nielsen, S. Neve et al., "Nuclear receptor corepressor-dependent repression of peroxisome-proliferator-activated receptor δ-mediated transactivation," *Biochemical Journal*, vol. 363, no. 1, pp. 157–165, 2002.

[17] H.-P. Guan, "Corepressors selectively control the transcriptional activity of PPARγ in adipocytes," *Genes & Development*, vol. 19, no. 4, pp. 453–461, 2005.

[18] M. L. Privalsky, "The role of corepressors in transcriptional regulation by nuclear hormone receptors," *Annual Review of Physiology*, vol. 66, no. 1, pp. 315–360, 2004.

[19] B. Desvergne and W. Wahli, "Peroxisome proliferator-activated receptors: nuclear control of metabolism," *Endocrine Reviews*, vol. 20, no. 5, pp. 649–688, 1999.

[20] C. K. Glass and M. G. Rosenfeld, "The coregulator exchange in transcriptional functions of nuclear receptors," *Genes & Development*, vol. 14, no. 2, pp. 121–141, 2000.

[21] V. Perissi and M. G. Rosenfeld, "Controlling nuclear receptors: the circular logic of cofactor cycles," *Nature Reviews Molecular Cell Biology*, vol. 6, no. 7, pp. 542–554, 2005.

[22] N. Viswakarma, Y. Jia, L. Bai et al., "Coactivators in PPAR-regulated gene expression," *PPAR Research*, vol. 2010, Article ID 250126, 21 pages, 2010.

[23] E. Treuter, T. Albrektsen, L. Johansson, J. Leers, and J.-Å. Gustafsson, "A regulatory role for RIP140 in nuclear receptor activation," *Molecular Endocrinology*, vol. 12, no. 6, pp. 864–881, 1998.

[24] P. Augereau, E. Badia, P. Balaguer et al., "Negative regulation of hormone signaling by RIP140," *The Journal of Steroid Biochemistry and Molecular Biology*, vol. 102, no. 1-5, pp. 51–59, 2006.

[25] A. M. Flores, I. Gurevich, C. Zhang, V. P. Ramirez, T. R. Devens, and B. J. Aneskievich, "TNIP1 is a corepressor of agonist-bound PPARs," *Archives of Biochemistry and Biophysics*, vol. 516, no. 1, pp. 58–66, 2011.

[26] I. Gurevich, A. M. Flores, and B. J. Aneskievich, "Corepressors of agonist-bound nuclear receptors," *Toxicology and Applied Pharmacology*, vol. 223, no. 3, pp. 288–298, 2007.

[27] G. S. Harmon, M. T. Lam, and C. K. Glass, "PPARs and lipid ligands in inflammation and metabolism," *Chemical Reviews*, vol. 111, no. 10, pp. 6321–6340, 2011.

[28] G. Pascual, A. L. Fong, S. Ogawa et al., "A SUMOylation-dependent pathway mediates transrepression of inflammatory response genes by PPAR-γ," *Nature*, vol. 437, no. 7059, pp. 759–763, 2005.

[29] S. Ghisletti, W. Huang, S. Ogawa et al., "Parallel SUMOylation-dependent pathways mediate gene- and signal-specific transrepression by LXRs and PPARγ," *Molecular Cell*, vol. 25, no. 1, pp. 57–70, 2007.

[30] C. Jennewein, A.-M. Kuhn, M. V. Schmidt et al., "Sumoylation of peroxisome proliferator-activated receptor γ by apoptotic cells prevents lipopolysaccharide-induced NCoR removal from KB binding sites mediating transrepression of proinflammatory cytokines," *The Journal of Immunology*, vol. 181, no. 8, pp. 5646–5652, 2008.

[31] M. Pawlak, E. Baugé, W. Bourguet et al., "The transrepressive activity of peroxisome proliferator-activated receptor alpha is

necessary and sufficient to prevent liver fibrosis in mice," *Hepatology*, vol. 60, no. 5, pp. 1593–1606, 2014.

[32] N. Perez-Diaz and L. Mackenzie, "Linking induction and transrepression of PPARβ/δ with cellular function," *Annual Research & Review in Biology*, vol. 6, no. 4, pp. 253–263, 2015.

[33] M. Ricote and C. Glass, "PPARs and molecular mechanisms of transrepression," *Biochimica et Biophysica Acta (BBA) - Molecular and Cell Biology of Lipids*, vol. 1771, no. 8, pp. 926–935, 2007.

[34] C.-H. Lee, A. Chawla, N. Urbiztondo, D. Liao, W. A. Boisvert, and R. M. Evans, "Transcriptional repression of atherogenic inflammation: modulation by PPAR," *Science*, vol. 302, no. 5644, pp. 453–457, 2003.

[35] G. Pascual and C. K. Glass, "Nuclear receptors versus inflammation: mechanisms of transrepression," *Trends in Endocrinology & Metabolism*, vol. 17, no. 8, pp. 321–327, 2006.

[36] S. J. Bensinger and P. Tontonoz, "Integration of metabolism and inflammation by lipid-activated nuclear receptors," *Nature*, vol. 454, no. 7203, pp. 470–477, 2008.

[37] S. Kersten, "Integrated physiology and systems biology of PPARα," *Molecular Metabolism*, vol. 3, no. 4, pp. 354–371, 2014.

[38] E. Ehrenborg and A. Krook, "Regulation of skeletal muscle physiology and metabolism by peroxisome proliferator-activated receptor δ," *Pharmacological Reviews*, vol. 61, no. 3, pp. 373–393, 2009.

[39] E. D. Rosen and B. M. Spiegelman, "Adipocytes as regulators of energy balance and glucose homeostasis," *Nature*, vol. 444, no. 7121, pp. 847–853, 2006.

[40] M. F. Oliver, J. A. Heady, J. N. Morris, and J. Cooper, "WHO cooperative trial on primary prevention of ischaemic heart disease with clofibrate to lower serum cholesterol: final mortality follow-up: report of the committee of principal investigators: report of the Committee of Principal Investigators," *The Lancet*, vol. 324, no. 8403, pp. 600–604, 1984.

[41] B. Qu, Q.-T. Li, K. P. Wong, T. M. C. Tan, and B. Halliwell, "Mechanism of clofibrate hepatotoxicity: mitochondrial damage and oxidative stress in hepatocytes," *Free Radical Biology and Medicine*, vol. 31, no. 5, pp. 659–669, 2001.

[42] S. E. Nissen and K. Wolski, "Effect of rosiglitazone on the risk of myocardial infarction and death from cardiovascular causes," *The New England Journal of Medicine*, vol. 356, no. 24, pp. 2457–2471, 2007.

[43] D. M. Nathan, "Rosiglitazone and cardiotoxicity — weighing the evidence," *The New England Journal of Medicine*, vol. 357, no. 1, pp. 64–66, 2007.

[44] M. Komajda, J. J. V. McMurray, H. Beck-Nielsen et al., "Heart failure events with rosiglitazone in type 2 diabetes: data from the RECORD clinical trial," *European Heart Journal*, vol. 31, no. 7, pp. 824–831, 2010.

[45] M. Ferwana, B. Firwana, R. Hasan et al., "Pioglitazone and risk of bladder cancer: a meta-analysis of controlled studies," *Diabetic Medicine*, vol. 30, no. 9, pp. 1026–1032, 2013.

[46] J. D. Lewis, L. A. Habel, C. P. Quesenberry et al., "Pioglitazone use and risk of bladder cancer and other common cancers in persons with diabetes," *JAMA*, vol. 314, no. 3, pp. 265–277, 2015.

[47] S. E. Nissen, K. Wolski, and E. J. Topol, "Effect of muraglitazar on death and major adverse cardiovascular events in patients with type 2 diabetes mellitus," *JAMA*, vol. 294, no. 20, pp. 2581–2586, 2005.

[48] G. G. Long, V. L. Reynolds, L. W. Dochterman, and T. E. Ryan, "Neoplastic and non-neoplastic changes in F-344 rats treated with naveglitazar, a γ-dominant PPAR α/γ agonist," *Toxicologic Pathology*, vol. 37, no. 6, pp. 741–753, 2009.

[49] M. B. Oleksiewicz, J. Southgate, L. Iversen, and F. L. Egerod, "Rat urinary bladder carcinogenesis by dual-acting PPAR$\alpha+\gamma$ agonists," *PPAR Research*, vol. 2008, Article ID 103167, 14 pages, 2008.

[50] H. Hellmold, H. Zhang, U. Andersson et al., "Tesaglitazar, a PPARα/γ agonist, induces interstitial mesenchymal cell DNA synthesis and fibrosarcomas in subcutaneous tissues in rats," *Toxicological Sciences*, vol. 98, no. 1, pp. 63–74, 2007.

[51] F. L. Egerod, H. S. Nielsen, L. Iversen, I. Thorup, T. Storgaard, and M. B. Oleksiewicz, "Biomarkers for early effects of carcinogenic dual-acting PPAR agonists in rat urinary bladder urothelium *in vivo*," *Biomarkers*, vol. 10, no. 4, pp. 295–309, 2008.

[52] C. Helsen and F. Claessens, "Looking at nuclear receptors from a new angle," *Molecular and Cellular Endocrinology*, vol. 382, no. 1, pp. 97–106, 2014.

[53] A. Bernardes, F. A. H. Batista, M. de Oliveira Neto et al., "Low-resolution molecular models reveal the oligomeric state of the PPAR and the conformational organization of its domains in solution," *PLoS One*, vol. 7, no. 2, article e31852, 2012.

[54] A. Bugge and S. Mandrup, "Molecular mechanisms and genome-wide aspects of PPAR subtype specific transactivation," *PPAR Research*, vol. 2010, Article ID 169506, 12 pages, 2010.

[55] A. Werman, A. Hollenberg, G. Solanes, C. Bjørbæk, A. J. Vidal-Puig, and J. S. Flier, "Ligand-independent activation domain in the N terminus of peroxisome proliferator-activated receptor γ (PPARγ)," *Journal of Biological Chemistry*, vol. 272, no. 32, pp. 20230–20235, 1997.

[56] L. Gelman, G. Zhou, L. Fajas, E. Raspé, J.-C. Fruchart, and J. Auwerx, "P300 interacts with the N- and C-terminal part of PPARγ2 in a ligand-independent and -dependent manner, *respectively*," *Journal of Biological Chemistry*, vol. 274, no. 12, pp. 7681–7688, 1999.

[57] R. Hi, S. Osada, N. Yumoto, and T. Osumi, "Characterization of the amino-terminal activation domain of peroxisome proliferator-activated receptor α," *Journal of Biological Chemistry*, vol. 274, no. 49, pp. 35152–35158, 1999.

[58] M. Aprile, M. R. Ambrosio, V. D'Esposito et al., "*PPARG* in human adipogenesis: differential contribution of canonical transcripts and dominant negative isoforms," *PPAR Research*, vol. 2014, Article ID 537865, 11 pages, 2014.

[59] J. C. Hanselman, M. V. Vartanian, B. P. Koester et al., "Expression of the MRNA encoding truncated PPAR alpha does not correlate with hepatic insensitivity to peroxisome proliferators," *Molecular and Cellular Biochemistry*, vol. 217, no. 1/2, pp. 91–97, 2001.

[60] K. Lundell, P. Thulin, A. Hamsten, and E. Ehrenborg, "Alternative splicing of human peroxisome proliferator-activated receptor delta (PPARdelta):effects on translation efficiency and *trans*-activation ability," *BMC Molecular Biology*, vol. 8, no. 1, p. 70, 2007.

[61] Y. Chen, A. R. Jimenez, and J. D. Medh, "Identification and regulation of novel PPAR-γ splice variants in human THP-1 macrophages," *Biochimica et Biophysica Acta (BBA) - Gene Structure and Expression*, vol. 1759, no. 1-2, pp. 32–43, 2006.

[62] P. M. Barger, A. C. Browning, A. N. Garner, and D. P. Kelly, "P38 mitogen-activated protein kinase activates peroxisome proliferator-activated receptor α," *Journal of Biological Chemistry*, vol. 276, no. 48, pp. 44495–44501, 2001.

[63] J. Uppenberg, C. Svensson, M. Jaki, G. Bertilsson, L. Jendeberg, and A. Berkenstam, "Crystal structure of the ligand binding domain of the human nuclear receptor PPARγ," *Journal of Biological Chemistry*, vol. 273, no. 47, pp. 31108–31112, 1998.

[64] R. T. Nolte, G. B. Wisely, S. Westin et al., "Ligand binding and co-activator assembly of the peroxisome proliferator- activated receptor-γ," *Nature*, vol. 395, no. 6698, pp. 137–143, 1998.

[65] H. E. Xu, M. H. Lambert, V. G. Montana et al., "Molecular recognition of fatty acids by peroxisome proliferator–activated receptors," *Molecular Cell*, vol. 3, no. 3, pp. 397–403, 1999.

[66] T. Waku, T. Shiraki, T. Oyama, K. Maebara, R. Nakamori, and K. Morikawa, "The nuclear receptor PPARγ individually responds to serotonin- and fatty acid-metabolites," *The EMBO Journal*, vol. 29, no. 19, pp. 3395–3407, 2010.

[67] R. Brust, H. Lin, J. Fuhrmann, A. Asteian, T. M. Kamenecka, and D. J. Kojetin, "Modification of the orthosteric PPARγ covalent antagonist scaffold yields an improved dual-site allosteric inhibitor," *ACS Chemical Biology*, vol. 12, no. 4, pp. 969–978, 2017.

[68] T. S. Hughes, P. K. Giri, I. M. S. de Vera et al., "An alternate binding site for PPARγ ligands," *Nature Communications*, vol. 5, no. 1, article 3571, 2014.

[69] V. Zoete, A. Grosdidier, and O. Michielin, "Peroxisome proliferator-activated receptor structures: ligand specificity, molecular switch and interactions with regulators," *Biochimica et Biophysica Acta (BBA) - Molecular and Cell Biology of Lipids*, vol. 1771, no. 8, pp. 915–925, 2007.

[70] H. M. Berman, J. Westbrook, Z. Feng et al., "The protein data bank," *Nucleic Acids Research*, vol. 28, no. 1, pp. 235–242, 2000.

[71] L. M. Leesnitzer, D. J. Parks, R. K. Bledsoe et al., "Functional consequences of cysteine modification in the ligand binding sites of peroxisome proliferator activated receptors by GW9662," *Biochemistry*, vol. 41, no. 21, pp. 6640–6650, 2002.

[72] B. G. Shearer, R. W. Wiethe, A. Ashe et al., "Identification and characterization of 4-chloro-*N*-2-5-trifluoromethyl-2-pyridylsulfonylethylbenzamide GSK3787, a selective and irreversible peroxisome proliferator-activated receptor δ PPARδ antagonist," *Journal of Medicinal Chemistry*, vol. 53, no. 4, pp. 1857–1861, 2010.

[73] Å. Kaupang, S. M. Paulsen, C. C. Steindal et al., "Synthesis, biological evaluation and molecular modeling studies of the PPARβ/δ antagonist CC618," *European Journal of Medicinal Chemistry*, vol. 94, pp. 229–236, 2015.

[74] Å. Kaupang, E. T. Kase, C. X. T. Vo, M. Amundsen, A. Vik, and T. V. Hansen, "Synthesis of 5-trifluoromethyl-2-sulfonylpyridine PPARβ/δ antagonists: effects on the affinity and selectivity towards PPARβ/δ," *Bioorganic & Medicinal Chemistry*, vol. 24, no. 2, pp. 247–260, 2016.

[75] Å. Kaupang, S. Hildonen, T. G. Halvorsen, M. Mortén, A. Vik, and T. V. Hansen, "Involvement of covalent interactions in the mode of action of PPARβ/δ antagonists," *RSC Advances*, vol. 5, no. 93, pp. 76483–76490, 2015.

[76] D. Egawa, T. Itoh, Y. Akiyama, T. Saito, and K. Yamamoto, "17-OxoDHA is a PPARα/γ dual covalent modifier and agonist," *ACS Chemical Biology*, vol. 11, no. 9, pp. 2447–2455, 2016.

[77] D. Egawa, T. Itoh, and K. Yamamoto, "Characterization of covalent bond formation between PPARγ and oxo-fatty acids," *Bioconjugate Chemistry*, vol. 26, no. 4, pp. 690–698, 2015.

[78] T. Waku, T. Shiraki, T. Oyama et al., "Structural insight into PPARγ activation through covalent modification with endogenous fatty acids," *Journal of Molecular Biology*, vol. 385, no. 1, pp. 188–199, 2009.

[79] T. Waku, T. Shiraki, T. Oyama, and K. Morikawa, "Atomic structure of mutant PPARγ LBD complexed with 15d-PGJ2: novel modulation mechanism of PPARγ/RXRα function by covalently bound ligands," *FEBS Letters*, vol. 583, no. 2, pp. 320–324, 2009.

[80] T. Itoh, L. Fairall, K. Amin et al., "Structural basis for the activation of PPARγ by oxidized fatty acids," *Nature Structural & Molecular Biology*, vol. 15, no. 9, pp. 924–931, 2008.

[81] F. J. Schopfer, M. P. Cole, A. L. Groeger et al., "Covalent peroxisome proliferator-activated receptor γ adduction by nitro-fatty acids," *Journal of Biological Chemistry*, vol. 285, no. 16, pp. 12321–12333, 2010.

[82] Y. Li, J. Zhang, F. J. Schopfer et al., "Molecular recognition of nitrated fatty acids by PPARγ," *Nature Structural & Molecular Biology*, vol. 15, no. 8, pp. 865–867, 2008.

[83] G. Lee, F. Elwood, J. McNally et al., "T0070907, a selective ligand for peroxisome proliferator-activated receptor γ, functions as an antagonist of biochemical and cellular activities," *Journal of Biological Chemistry*, vol. 277, no. 22, pp. 19649–19657, 2002.

[84] A. Elbrecht, Y. Chen, A. Adams et al., "L-764406 is a partial agonist of human peroxisome proliferator-activated receptor γ," *Journal of Biological Chemistry*, vol. 274, no. 12, pp. 7913–7922, 1999.

[85] H. E. Xu, T. B. Stanley, V. G. Montana et al., "Structural basis for antagonist-mediated recruitment of nuclear co- repressors by PPARα," *Nature*, vol. 415, no. 6873, pp. 813–817, 2002.

[86] M. R. B. Batista and L. Martínez, "Conformational diversity of the helix 12 of the ligand binding domain of PPARγ and functional implications," *The Journal of Physical Chemistry B*, vol. 119, no. 50, pp. 15418–15429, 2015.

[87] I. M. Chrisman, M. D. Nemetchek, I. M. S. de Vera et al., "Defining a conformational ensemble that directs activation of PPARγ," *Nature Communications*, vol. 9, no. 1, article 1794, 2018.

[88] R. L. Frkic, A. C. Marshall, A.-L. Blayo et al., "PPARγ in complex with an antagonist and inverse agonist: a tumble and trap mechanism of the activation helix," *iScience*, vol. 5, pp. 69–79, 2018.

[89] H. E. Xu, M. H. Lambert, V. G. Montana et al., "Structural determinants of ligand binding selectivity between the peroxisome proliferator-activated receptors," *Proceedings of the National Academy of Sciences of the United States of America*, vol. 98, no. 24, pp. 13919–13924, 2001.

[90] Y. Hashimoto and H. Miyachi, "Nuclear receptor antagonists designed based on the helix-folding inhibition hypothesis," *Bioorganic & Medicinal Chemistry*, vol. 13, no. 17, pp. 5080–5093, 2005.

[91] R. P. Trump, J. E. Cobb, B. G. Shearer et al., "Co-crystal structure guided array synthesis of PPARγ inverse agonists," *Bioorganic & Medicinal Chemistry Letters*, vol. 17, no. 14, pp. 3916–3920, 2007.

[92] J. Kasuga, S. Ishida, D. Yamasaki et al., "Novel biphenylcarboxylic acid peroxisome proliferator-activated receptor (PPAR) δ selective antagonists," *Bioorganic & Medicinal Chemistry Letters*, vol. 19, no. 23, pp. 6595–6599, 2009.

[93] M. Ohashi, K. Gamo, Y. Tanaka et al., "Structural design and synthesis of arylalkynyl amide-type peroxisome proliferator-activated receptor γ (PPARγ)-selective antagonists based on the helix12-folding inhibition hypothesis," *European Journal of Medicinal Chemistry*, vol. 90, pp. 53–67, 2015.

[94] A. Ammazzalorso, A. D'Angelo, A. Giancristofaro et al., "Fibrate-derived *N*-(methylsulfonyl)amides with antagonistic properties on PPARα," *European Journal of Medicinal Chemistry*, vol. 58, pp. 317–322, 2012.

[95] A. Ammazzalorso, A. Giancristofaro, A. D'Angelo et al., "Benzothiazole-based *N*-(phenylsulfonyl)amides as a novel family of PPARα antagonists," *Bioorganic & Medicinal Chemistry Letters*, vol. 21, no. 16, pp. 4869–4872, 2011.

[96] F. Fratev, I. Tsakovska, M. Al Sharif, E. Mihaylova, and I. Pajeva, "Structural and dynamical insight into PPARγ antagonism: *in silico* study of the ligand-receptor interactions of non-covalent antagonists," *International Journal of Molecular Sciences*, vol. 16, no. 12, pp. 15405–15424, 2015.

[97] D. P. Marciano, D. S. Kuruvilla, S. V. Boregowda et al., "Pharmacological repression of PPARγ promotes osteogenesis," *Nature Communications*, vol. 6, no. 1, article 7443, 2015.

[98] G. Brusotti, R. Montanari, D. Capelli et al., "Betulinic acid is a PPARγ antagonist that improves glucose uptake, promotes osteogenesis and inhibits adipogenesis," *Scientific Reports*, vol. 7, no. 1, article 5777, 2017.

[99] I. Pettersson, S. Ebdrup, M. Havranek et al., "Design of a partial PPARδ agonist," *Bioorganic & Medicinal Chemistry Letters*, vol. 17, no. 16, pp. 4625–4629, 2007.

[100] D. R. Artis, J. J. Lin, C. Zhang et al., "Scaffold-based discovery of indeglitazar, a PPAR pan-active anti-diabetic agent," *Proceedings of the National Academy of Sciences of the United States of America*, vol. 106, no. 1, pp. 262–267, 2009.

[101] H. Bae, J. Y. Jang, S.-S. Choi et al., "Mechanistic elucidation guided by covalent inhibitors for the development of anti-diabetic PPARγ ligands," *Chemical Science*, vol. 7, no. 8, pp. 5523–5529, 2016.

[102] B. K. Ho and F. Gruswitz, "HOLLOW: generating accurate representations of channel and interior surfaces in molecular structures," *BMC Structural Biology*, vol. 8, no. 1, p. 49, 2008.

[103] S. Lieber, F. Scheer, W. Meissner et al., "(Z)-2-(2-Bromophenyl)-3-{[4-(1-methyl-piperazine)amino]phenyl}acrylonitrile (DG172): an orally bioavailable PPARβ/δ-selective ligand with inverse agonistic properties," *Journal of Medicinal Chemistry*, vol. 55, no. 6, pp. 2858–2868, 2012.

[104] P. M. Toth, S. Lieber, F. M. Scheer et al., "Design and synthesis of highly active peroxisome proliferator-activated receptor (PPAR) β/δ inverse agonists with prolonged cellular activity," *ChemMedChem*, vol. 11, no. 5, pp. 488–496, 2016.

[105] P. M. Toth, S. Naruhn, V. F. S. Pape et al., "Development of improved PPARβ/δ inhibitors," *ChemMedChem*, vol. 7, no. 1, pp. 159–170, 2012.

[106] S. Naruhn, P. M. Toth, T. Adhikary et al., "High-affinity peroxisome proliferator-activated receptor β/δ-specific ligands with pure antagonistic or inverse agonistic properties," *Molecular Pharmacology*, vol. 80, no. 5, pp. 828–838, 2011.

[107] T. S. Hughes, M. J. Chalmers, S. Novick et al., "Ligand and receptor dynamics contribute to the mechanism of graded PPARγ agonism," *Structure*, vol. 20, no. 1, pp. 139–150, 2012.

[108] J. Lu, M. Chen, S. E. Stanley, and E. Li, "Effect of heterodimer partner RXRα on PPARγ activation function-2 helix in solution," *Biochemical and Biophysical Research Communications*, vol. 365, no. 1, pp. 42–46, 2008.

[109] R. Hartl, *Berechnung Der NMR-Struktur Der PPARgamma-LBD Und Hochdruck-NMR-Messungen an HPr I14A*, University of Regensburg, Germany, 2008.

[110] H. Riepl, R. Hartl, M. Bauer et al., "Sequential backbone assignment of peroxisome proliferator-activated receptor-γ ligand binding domain," *Journal of Biomolecular NMR*, vol. 32, no. 3, p. 259, 2005.

[111] B. A. Johnson, E. M. Wilson, Y. Li, D. E. Moller, R. G. Smith, and G. Zhou, "Ligand-induced stabilization of PPARγ monitored by NMR spectroscopy: implications for nuclear receptor activation," *Journal of Molecular Biology*, vol. 298, no. 2, pp. 187–194, 2000.

[112] S.-S. Choi, E.-S. Kim, J.-E. Jung et al., "PPARγ antagonist Gleevec improves insulin sensitivity and promotes the browning of white adipose tissue," *Diabetes*, vol. 65, no. 4, pp. 829–839, 2016.

[113] D. P. Marciano, D. S. Kuruvilla, B. D. Pascal, and P. R. Griffin, "Identification of bexarotene as a PPARγ antagonist with HDX," *PPAR Research*, vol. 2015, Article ID 254560, 6 pages, 2015.

[114] J. B. Bruning, M. J. Chalmers, S. Prasad et al., "Partial agonists activate PPARγ using a helix 12 independent mechanism," *Structure*, vol. 15, no. 10, pp. 1258–1271, 2007.

[115] A. A. Amato, S. Rajagopalan, J. Z. Lin et al., "GQ-16, a novel peroxisome proliferator-activated receptor γ (PPARγ) ligand, promotes insulin sensitization without weight gain," *Journal of Biological Chemistry*, vol. 287, no. 33, pp. 28169–28179, 2012.

[116] J. H. Choi, A. S. Banks, J. L. Estall et al., "Anti-diabetic drugs inhibit obesity-linked phosphorylation of PPARγ by Cdk5," *Nature*, vol. 466, no. 7305, pp. 451–456, 2010.

[117] Y. Hamuro, S. J. Coales, J. A. Morrow et al., "Hydrogen/deuterium-exchange (H/D-ex) of PPARγ LBD in the presence of various modulators," *Protein Science*, vol. 15, no. 8, pp. 1883–1892, 2006.

[118] J. A. Lemkul, S. N. Lewis, J. Bassaganya-Riera, and D. R. Bevan, "Phosphorylation of PPARγ affects the collective motions of the PPARγ-RXRα-DNA complex," *PLoS One*, vol. 10, no. 5, article e0123984, 2015.

[119] A. Bernardes, P. C. T. Souza, J. R. C. Muniz et al., "Molecular mechanism of peroxisome proliferator-activated receptor α activation by WY14643: a new mode of ligand recognition and receptor stabilization," *Journal of Molecular Biology*, vol. 425, no. 16, pp. 2878–2893, 2013.

[120] L. E. Geiger, W. S. Dunsford, D. J. Lewis, C. Brennan, K. C. Liu, and S. J. Newsholme, "Rat carcinogenicity study with GW501516, a PPAR delta agonist," in *The Toxicologist: Supplement to Toxicological Sciences*, vol. 108, no. 1, 2009Society of Toxicology, 2009, Abstract no. 895.

[121] S. J. Newsholme, W. S. Dunsford, T. Brodie, C. Brennan, M. Brown, and L. E. Geiger, "Mouse carcinogenicity study with GW501516, a PPAR delta agonist," in *The Toxicologist:*

Supplement to Toxicological Sciences, vol. 108, no. 1, 2009Society of Toxicology, 2009, Abstract no. 896.

[122] J. H. Choi, A. S. Banks, T. M. Kamenecka et al., "Antidiabetic actions of a non-agonist PPARγ ligand blocking Cdk5-mediated phosphorylation," *Nature*, vol. 477, no. 7365, pp. 477–481, 2011.

[123] S.-S. Choi, J. Park, and J. H. Choi, "Revisiting PPARγ as a target for the treatment of metabolic disorders," *BMB Reports*, vol. 47, no. 11, pp. 599–608, 2014.

[124] W. Yi, J. Shi, G. Zhao et al., "Identification of a novel selective PPARγ ligand with a unique binding mode and improved therapeutic profile *in vitro*," *Scientific Reports*, vol. 7, no. 1, article 41487, 2017.

[125] T. Shinozuka, T. Tsukada, K. Fujii et al., "Discovery of DS-6930, a potent selective PPARγ modulator. Part I: lead identification," *Bioorganic & Medicinal Chemistry*, vol. 26, no. 18, pp. 5079–5098, 2018.

[126] T. Shinozuka, T. Tsukada, K. Fujii et al., "Discovery of DS-6930, a potent selective PPARγ modulator. Part II: lead optimization," *Bioorganic & Medicinal Chemistry*, vol. 26, no. 18, pp. 5099–5117, 2018.

[127] L. Porskjær Christensen and R. Bahij El-Houri, "Development of an in vitro screening platform for the identification of partial PPARγ agonists as a source for antidiabetic lead compounds," *Molecules*, vol. 23, no. 10, article 2431, 2018.

[128] J.-S. Lee, E. Smith, and A. Shilatifard, "The language of histone crosstalk," *Cell*, vol. 142, no. 5, pp. 682–685, 2010.

[129] A. Sadakierska-Chudy and M. Filip, "A comprehensive view of the epigenetic landscape. Part II: histone post-translational modification, nucleosome level, and chromatin regulation by NcRNAs," *Neurotoxicity Research*, vol. 27, no. 2, pp. 172–197, 2015.

[130] R. Brunmeir and F. Xu, "Functional regulation of PPARs through post-translational modifications," *International Journal of Molecular Sciences*, vol. 19, no. 6, article 1738, 2018.

[131] M. Anbalagan, B. Huderson, L. Murphy, and B. G. Rowan, "Post-translational modifications of nuclear receptors and human disease," *Nuclear Receptor Signaling*, vol. 10, no. 1, 2018.

[132] W. Berrabah, P. Aumercier, P. Lefebvre, and B. Staels, "Control of nuclear receptor activities in metabolism by post-translational modifications," *FEBS Letters*, vol. 585, no. 11, pp. 1640–1650, 2011.

[133] T.-H. Kim, M.-Y. Kim, S.-H. Jo, J.-M. Park, and Y.-H. Ahn, "Modulation of the transcriptional activity of peroxisome proliferator-activated receptor gamma by protein-protein interactions and post-translational modifications," *Yonsei Medical Journal*, vol. 54, no. 3, pp. 545–559, 2013.

[134] S. A. M. Laarsevan der, A. C. Leney, and A. J. R. Heck, "Crosstalk between phosphorylation and O-GlcNAcylation: friend or foe," *The FEBS Journal*, vol. 285, no. 17, pp. 3152–3167, 2018.

[135] H. Xu, J. Zhou, S. Lin, W. Deng, Y. Zhang, and Y. Xue, "PLMD: an updated data resource of protein lysine modifications," *Journal of Genetics and Genomics*, vol. 44, no. 5, pp. 243–250, 2017.

[136] Z. Liu, Y. Wang, T. Gao et al., "CPLM: a database of protein lysine modifications," *Nucleic Acids Research*, vol. 42, no. D1, pp. D531–D536, 2013.

[137] Z. Liu, J. Cao, X. Gao et al., "CPLA 1.0: an integrated database of protein lysine acetylation," *Nucleic Acids Research*, vol. 39, Supplement_1, pp. D1029–D1034, 2011.

[138] E. S. Johnson, "Protein modification by SUMO," *Annual Review of Biochemistry*, vol. 73, no. 1, pp. 355–382, 2004.

[139] S. Ross, J. L. Best, L. I. Zon, and G. Gill, "SUMO-1 modification represses Sp3 transcriptional activation and modulates its subnuclear localization," *Molecular Cell*, vol. 10, no. 4, pp. 831–842, 2002.

[140] I. A. Hendriks, D. Lyon, C. Young, L. J. Jensen, A. C. O. Vertegaal, and M. L. Nielsen, "Site-specific mapping of the human SUMO proteome reveals co-modification with phosphorylation," *Nature Structural & Molecular Biology*, vol. 24, no. 3, pp. 325–336, 2017.

[141] S. H. Yang, A. Galanis, J. Witty, and A. D. Sharrocks, "An extended consensus motif enhances the specificity of substrate modification by SUMO," *The EMBO Journal*, vol. 25, no. 21, pp. 5083–5093, 2006.

[142] V. Hietakangas, J. Anckar, H. A. Blomster et al., "PDSM, a motif for phosphorylation-dependent SUMO modification," *Proceedings of the National Academy of Sciences of the United States of America*, vol. 103, no. 1, pp. 45–50, 2006.

[143] H. L. Rust and P. R. Thompson, "Kinase consensus sequences: a breeding ground for crosstalk," *ACS Chemical Biology*, vol. 6, no. 9, pp. 881–892, 2011.

[144] P. Li, W. Fan, J. Xu et al., "Adipocyte NCoR knockout decreases PPARγ phosphorylation and enhances PPARγ activity and insulin sensitivity," *Cell*, vol. 147, no. 4, pp. 815–826, 2011.

[145] L. Qiang, L. Wang, N. Kon et al., "Brown remodeling of white adipose tissue by SirT1-dependent deacetylation of Pparγ," *Cell*, vol. 150, no. 3, pp. 620–632, 2012.

[146] C. G. Ricci, R. L. Silveira, I. Rivalta, V. S. Batista, and M. S. Skaf, "Allosteric pathways in the PPARγ-RXRα nuclear receptor complex," *Scientific Reports*, vol. 6, no. 1, article 19940, 2016.

[147] W. Deng, C. Wang, Y. Zhang et al., "GPS-PAIL: prediction of lysine acetyltransferase-specific modification sites from protein sequences," *Scientific Reports*, vol. 6, no. 1, article 39787, 2016.

[148] "Kinexus | PhosphoNET," July 2018, http://www.phosphonet.ca/.

[149] R. Amanchy, B. Periaswamy, S. Mathivanan, R. Reddy, S. G. Tattikota, and A. Pandey, "A curated compendium of phosphorylation motifs," *Nature Biotechnology*, vol. 25, no. 3, pp. 285-286, 2007.

[150] N. Blom, T. Sicheritz-Pontén, R. Gupta, S. Gammeltoft, and S. Brunak, "Prediction of post-translational glycosylation and phosphorylation of proteins from the amino acid sequence," *Proteomics*, vol. 4, no. 6, pp. 1633–1649, 2004.

[151] N. Blom, S. Gammeltoft, and S. Brunak, "Sequence and structure-based prediction of eukaryotic protein phosphorylation sites," *Journal of Molecular Biology*, vol. 294, no. 5, pp. 1351–1362, 1999.

[152] P. V. Hornbeck, B. Zhang, B. Murray, J. M. Kornhauser, V. Latham, and E. Skrzypek, "PhosphoSitePlus, 2014: mutations, PTMs and recalibrations," *Nucleic Acids Research*, vol. 43, no. D1, pp. D512–D520, 2015.

[153] A. M. Sharma and B. Staels, "Peroxisome proliferator-activated receptor γ and adipose tissue—understanding obesity-related changes in regulation of lipid and glucose

metabolism," *The Journal of Clinical Endocrinology & Metabolism*, vol. 92, no. 2, pp. 386–395, 2007.

[154] J. Nedergaard and B. Cannon, "The browning of white adipose tissue: some burning issues," *Cell Metabolism*, vol. 20, no. 3, pp. 396–407, 2014.

[155] F. M. Gregoire, F. Zhang, H. J. Clarke et al., "MBX-102/JNJ39659100, a novel peroxisome proliferator-activated receptor-ligand with weak transactivation activity retains antidiabetic properties in the absence of weight gain and edema," *Molecular Endocrinology*, vol. 23, no. 7, pp. 975–988, 2009.

[156] L. S. Higgins and C. S. Mantzoros, "The development of INT131 as a selective PPAR γ modulator: approach to a safer insulin sensitizer," *PPAR Research*, vol. 2008, Article ID 936906, 9 pages, 2008.

[157] T. Allen, F. Zhang, S. A. Moodie et al., "Halofenate is a selective peroxisome proliferator–activated receptor γ modulator with antidiabetic activity," *Diabetes*, vol. 55, no. 9, pp. 2523–2533, 2006.

[158] J. J. Acton III, R. M. Black, A. B. Jones et al., "Benzoyl 2-methyl indoles as selective PPARγ modulators," *Bioorganic & Medicinal Chemistry Letters*, vol. 15, no. 2, pp. 357–362, 2005.

[159] T. Östberg, S. Svensson, G. Selén et al., "A new class of peroxisome proliferator-activated receptor agonists with a novel binding epitope shows antidiabetic effects," *Journal of Biological Chemistry*, vol. 279, no. 39, pp. 41124–41130, 2004.

[160] J. P. Berger, A. E. Petro, K. L. Macnaul et al., "Distinct properties and advantages of a novel peroxisome proliferator-activated protein γ selective modulator," *Molecular Endocrinology*, vol. 17, no. 4, pp. 662–676, 2003.

[161] S. Rocchi, F. Picard, J. Vamecq et al., "A unique PPARγ ligand with potent insulin-sensitizing yet weak adipogenic activity," *Molecular Cell*, vol. 8, no. 4, pp. 737–747, 2001.

[162] J. H. Choi, S.-S. Choi, E. S. Kim et al., "Thrap3 docks on phosphoserine 273 of PPARγ and controls diabetic gene programming," *Genes & Development*, vol. 28, no. 21, pp. 2361–2369, 2014.

[163] A. S. Banks, F. E. McAllister, J. P. G. Camporez et al., "An ERK/Cdk5 axis controls the diabetogenic actions of PPARγ," *Nature*, vol. 517, no. 7534, pp. 391–395, 2015.

[164] Z. E. Floyd and J. M. Stephens, "Controlling a master switch of adipocyte development and insulin sensitivity: covalent modifications of PPARγ," *Biochimica et Biophysica Acta (BBA) - Molecular Basis of Disease*, vol. 1822, no. 7, pp. 1090–1095, 2012.

[165] A. W. Norris and C. D. Sigmund, "A second chance for a PPARγ targeted therapy?," *Circulation Research*, vol. 110, no. 1, pp. 8–11, 2012.

[166] M. Ahmadian, J. M. Suh, N. Hah et al., "PPARγ signaling and metabolism: the good, the bad and the future," *Nature Medicine*, vol. 19, no. 5, pp. 557–566, 2013.

[167] C. Guo, Y. Li, C.-H. Gow et al., "The optimal corepressor function of nuclear receptor corepressor (NCoR) for peroxisome proliferator-activated receptor γ requires G protein pathway suppressor 2," *Journal of Biological Chemistry*, vol. 290, no. 6, pp. 3666–3679, 2015.

[168] L. Tian, C. Wang, F. K. Hagen et al., "Acetylation-defective mutants of PPARγ are associated with decreased lipid synthesis in breast cancer cells," *Oncotarget*, vol. 5, no. 17, pp. 7303–7315, 2014.

[169] H. Wang, L. Qiang, and S. R. Farmer, "Identification of a domain within peroxisome proliferator-activated receptor γ regulating expression of a group of genes containing fibroblast growth factor 21 that are selectively repressed by SIRT1 in adipocytes," *Molecular and Cellular Biology*, vol. 28, no. 1, pp. 188–200, 2008.

[170] M. J. Kraakman, Q. Liu, J. Postigo-Fernandez et al., "PPARγ deacetylation dissociates thiazolidinedione's metabolic benefits from its adverse effects," *Journal of Clinical Investigation*, vol. 128, no. 6, pp. 2600–2612, 2018.

[171] L. Han, R. Zhou, J. Niu, M. A. McNutt, P. Wang, and T. Tong, "SIRT1 is regulated by a PPARγ–SIRT1 negative feedback loop associated with senescence," *Nucleic Acids Research*, vol. 38, no. 21, pp. 7458–7471, 2010.

[172] P. Seale, H. M. Conroe, J. Estall et al., "Prdm16 determines the thermogenic program of subcutaneous white adipose tissue in mice," *Journal of Clinical Investigation*, vol. 121, no. 1, pp. 96–105, 2011.

[173] H. Ohno, K. Shinoda, B. M. Spiegelman, and S. Kajimura, "PPARγ agonists induce a white-to-brown fat conversion through stabilization of PRDM16 protein," *Cell Metabolism*, vol. 15, no. 3, pp. 395–404, 2012.

[174] H. Wang, L. Liu, J. Z. Lin, T. R. Aprahamian, and S. R. Farmer, "Browning of white adipose tissue with roscovitine induces a distinct population of UCP1$^+$ adipocytes," *Cell Metabolism*, vol. 24, no. 6, pp. 835–847, 2016.

[175] R. Mayoral, O. Osborn, J. McNelis et al., "Adipocyte SIRT1 knockout promotes PPARγ activity, adipogenesis and insulin sensitivity in chronic-HFD and obesity," *Molecular Metabolism*, vol. 4, no. 5, pp. 378–391, 2015.

[176] T. Tagami, H. Yamamoto, K. Moriyama et al., "A selective peroxisome proliferator-activated receptor-γ modulator, telmisartan, binds to the receptor in a different fashion from thiazolidinediones," *Endocrinology*, vol. 150, no. 2, pp. 862–870, 2009.

[177] Y. Amano, T. Yamaguchi, K. Ohno et al., "Structural basis for telmisartan-mediated partial activation of PPAR gamma," *Hypertension Research*, vol. 35, no. 7, pp. 715–719, 2012.

[178] T. Fang, Y. Di, G. Li et al., "Effects of telmisartan on TNFα induced PPARγ phosphorylation and insulin resistance in adipocytes," *Biochemical and Biophysical Research Communications*, vol. 503, no. 4, pp. 3044–3049, 2018.

[179] K. Araki, T. Masaki, I. Katsuragi, K. Tanaka, T. Kakuma, and H. Yoshimatsu, "Telmisartan prevents obesity and increases the expression of uncoupling protein 1 in diet-induced obese mice," *Hypertension*, vol. 48, no. 1, pp. 51–57, 2006.

[180] V. Kolli, L. A. Stechschulte, A. R. Dowling, S. Rahman, P. J. Czernik, and B. Lecka-Czernik, "Partial agonist, telmisartan, maintains PPARγ serine 112 phosphorylation, and does not affect osteoblast differentiation and bone mass," *PLoS One*, vol. 9, no. 5, article e96323, 2014.

[181] P. Shen, M. H. Liu, T. Y. Ng, Y. H. Chan, and E. L. Yong, "Differential effects of isoflavones, from *Astragalus membranaceus* and *Pueraria thomsonii*, on the activation of PPARα, PPARγ, and adipocyte differentiation in vitro," *The Journal of Nutrition*, vol. 136, no. 4, pp. 899–905, 2006.

[182] T. Nie, S. Zhao, L. Mao et al., "The natural compound, formononetin, extracted from *Astragalus membranaceus* increases adipocyte thermogenesis by modulating PPARγ activity," *British Journal of Pharmacology*, vol. 175, no. 9, pp. 1439–1450, 2018.

[183] F. Zhang, B. E. Lavan, and F. M. Gregoire, "Selective modulators of PPAR-γ activity: molecular aspects related to obesity and side-effects," *PPAR Research*, vol. 2007, Article ID 32696, 7 pages, 2007.

[184] D. Lasar, M. Rosenwald, E. Kiehlmann et al., "Peroxisome proliferator activated receptor gamma controls mature brown adipocyte inducibility through glycerol kinase," *Cell Reports*, vol. 22, no. 3, pp. 760–773, 2018.

[185] A. J. Kroker and J. B. Bruning, "Review of the structural and dynamic mechanisms of PPARγ partial agonism," *PPAR Research*, vol. 2015, Article ID 816856, 15 pages, 2015.

[186] S.-H. Sheu, T. Kaya, D. J. Waxman, and S. Vajda, "Exploring the binding site structure of the PPARγ ligand-binding domain by computational solvent mapping," *Biochemistry*, vol. 44, no. 4, pp. 1193–1209, 2005.

[187] C. Liu, T. Feng, N. Zhu et al., "Identification of a novel selective agonist of PPARγ with no promotion of adipogenesis and less inhibition of osteoblastogenesis," *Scientific Reports*, vol. 5, no. 1, article 12185, 2015.

[188] L. Wang, B. Waltenberger, E.-M. Pferschy-Wenzig et al., "Natural product agonists of peroxisome proliferator-activated receptor gamma (PPARγ): a review," *Biochemical Pharmacology*, vol. 92, no. 1, pp. 73–89, 2014.

[189] W. Zheng, X. Feng, L. Qiu et al., "Identification of the antibiotic ionomycin as an unexpected peroxisome proliferator-activated receptor γ (PPARγ) ligand with a unique binding mode and effective glucose-lowering activity in a mouse model of diabetes," *Diabetologia*, vol. 56, no. 2, pp. 401–411, 2013.

[190] G. Wu, J. Yi, L. Liu, P. Wang, Z. Zhang, and Z. Li, "Pseudoginsenoside F11, a novel partial PPARγ agonist, promotes adiponectin oligomerization and secretion in 3T3-L1 adipocytes," *PPAR Research*, vol. 2013, Article ID 701017, 8 pages, 2013.

[191] J. C. de Groot, C. Weidner, J. Krausze et al., "Structural characterization of amorfrutins bound to the peroxisome proliferator-activated receptor γ," *Journal of Medicinal Chemistry*, vol. 56, no. 4, pp. 1535–1543, 2013.

[192] W. Zheng, L. Qiu, R. Wang et al., "Selective targeting of PPARγ by the natural product chelerythrine with a unique binding mode and improved antidiabetic potency," *Scientific Reports*, vol. 5, no. 1, article 12222, 2015.

[193] J. L. Oberfield, J. L. Collins, C. P. Holmes et al., "A peroxisome proliferator-activated receptor γ ligand inhibits adipocyte differentiation," *Proceedings of the National Academy of Sciences of the United States of America*, vol. 96, no. 11, pp. 6102–6106, 1999.

[194] A. C. Puhl, F. A. Milton, A. Cvoro et al., "Mechanisms of peroxisome proliferator activated receptor γ regulation by non-steroidal anti-inflammatory drugs," *Nuclear Receptor Signaling*, vol. 13, no. 1, 2018.

[195] A. Laghezza, G. Pochetti, A. Lavecchia et al., "New 2-(aryloxy)-3-phenylpropanoic acids as peroxisome proliferator-activated receptor α/γ dual agonists able to upregulate mitochondrial carnitine shuttle system gene expression," *Journal of Medicinal Chemistry*, vol. 56, no. 1, pp. 60–72, 2012.

[196] A. C. Puhl, A. Bernardes, R. L. Silveira et al., "Mode of peroxisome proliferator-activated receptor γ activation by luteolin," *Molecular Pharmacology*, vol. 81, no. 6, pp. 788–799, 2012.

[197] Y. Li, Z. Wang, N. Furukawa et al., "T2384, a novel antidiabetic agent with unique peroxisome proliferator-activated receptor γ binding properties," *Journal of Biological Chemistry*, vol. 283, no. 14, pp. 9168–9176, 2008.

[198] C. R. Hopkins, S. V. O'Neil, M. C. Laufersweiler et al., "Design and synthesis of novel N-sulfonyl-2-indole carboxamides as potent PPAR-γ binding agents with potential application to the treatment of osteoporosis," *Bioorganic & Medicinal Chemistry Letters*, vol. 16, no. 21, pp. 5659–5663, 2006.

[199] M. V. Liberato, A. S. Nascimento, S. D. Ayers et al., "Medium chain fatty acids are selective peroxisome proliferator activated receptor (PPAR) γ activators and pan-PPAR partial agonists," *PLoS One*, vol. 7, no. 5, article e36297, 2012.

[200] J. Shang, R. Brust, S. A. Mosure et al., "Cooperative cobinding of synthetic and natural ligands to the nuclear receptor PPARγ," *eLife*, vol. 7, article e43320, 2018.

[201] S. A. Fyffe, M. S. Alphey, L. Buetow et al., "Recombinant human PPAR-β/δ ligand-binding domain is locked in an activated conformation by endogenous fatty acids," *Journal of Molecular Biology*, vol. 356, no. 4, pp. 1005–1013, 2006.

[202] S. A. Fyffe, M. S. Alphey, L. Buetow et al., "Reevaluation of the PPAR-β/δ ligand binding domain model reveals why it exhibits the activated form," *Molecular Cell*, vol. 21, no. 1, pp. 1-2, 2006.

[203] R. R. V. Malapaka, S. K. Khoo, J. Zhang et al., "Identification and mechanism of 10-carbon fatty acid as modulating ligand of peroxisome proliferator-activated receptors," *Journal of Biological Chemistry*, vol. 287, no. 1, pp. 183–195, 2011.

[204] B. M. Forman, P. Tontonoz, J. Chen, R. P. Brun, B. M. Spiegelman, and R. M. Evans, "15-Deoxy-$\Delta^{12,14}$-prostaglandin J_2 is a ligand for the adipocyte determination factor PPARγ," *Cell*, vol. 83, no. 5, pp. 803–812, 1995.

[205] B. M. Forman, J. Chen, and R. M. Evans, "Hypolipidemic drugs, polyunsaturated fatty acids, and eicosanoids are ligands for peroxisome proliferator-activated receptors α and δ," *Proceedings of the National Academy of Sciences of the United States of America*, vol. 94, no. 9, pp. 4312–4317, 1997.

[206] H. A. Hostetler, A. B. Kier, and F. Schroeder, "Very-Long-chain and branched-chain fatty acyl-CoAs are high affinity ligands for the peroxisome proliferator-activated receptor α (PPARα)," *Biochemistry*, vol. 45, no. 24, pp. 7669–7681, 2006.

[207] H. E. Popeijus, S. D. van Otterdijk, S. E. van der Krieken et al., "Fatty acid chain length and saturation influences PPARα transcriptional activation and repression in HepG2 cells," *Molecular Nutrition & Food Research*, vol. 58, no. 12, pp. 2342–2349, 2014.

[208] I. Shureiqi, W. Jiang, X. Zuo et al., "The 15-lipoxygenase-1 product 13-S-hydroxyoctadecadienoic acid down-regulates PPAR-δ to induce apoptosis in colorectal cancer cells," *Proceedings of the National Academy of Sciences of the United States of America*, vol. 100, no. 17, pp. 9968–9973, 2011.

[209] S. Naruhn, W. Meissner, T. Adhikary et al., "15-Hydroxyeicosatetraenoic acid is a preferential peroxisome proliferator-activated receptor β/δ agonist," *Molecular Pharmacology*, vol. 77, no. 2, pp. 171–184, 2010.

[210] S. Karki, P. Chakrabarti, G. Huang, H. Wang, S. R. Farmer, and K. V. Kandror, "The multi-level action of fatty acids on adiponectin production by fat cells," *PLoS One*, vol. 6, no. 11, article e28146, 2011.

[211] J. Song, C. Li, Y. Lv, Y. Zhang, W. K. Amakye, and L. Mao, "DHA increases adiponectin expression more effectively than

EPA at relative low concentrations by regulating PPARγ and its phosphorylation at Ser273 in 3T3-L1 adipocytes," *Nutrition & Metabolism*, vol. 14, no. 1, p. 52, 2017.

[212] M. Thor, K. Beierlein, G. Dykes et al., "Synthesis and pharmacological evaluation of a new class of peroxisome proliferator-activated receptor modulators," *Bioorganic & Medicinal Chemistry Letters*, vol. 12, no. 24, pp. 3565–3567, 2002.

[213] C. Salim, Y. V. Boxberg, J. Alterio, S. Féréol, and F. Nothias, "The giant protein AHNAK involved in morphogenesis and laminin substrate adhesion of myelinating Schwann cells," *Glia*, vol. 57, no. 5, pp. 535–549, 2009.

[214] D. A. Yool, J. M. Edgar, P. Montague, and S. Malcolm, "The proteolipid protein gene and myelin disorders in man and animal models," *Human Molecular Genetics*, vol. 9, no. 6, pp. 987–992, 2000.

[215] L. Szalardy, D. Zadori, E. Tanczos et al., "Elevated levels of PPAR-gamma in the cerebrospinal fluid of patients with multiple sclerosis," *Neuroscience Letters*, vol. 554, pp. 131–134, 2013.

[216] S. Mandrekar-Colucci, A. Sauerbeck, P. G. Popovich, and D. M. McTigue, "PPAR agonists as therapeutics for CNS trauma and neurological diseases," *ASN Neuro*, vol. 5, no. 5, pp. 347–362, 2013.

[217] K. A. Hanafy and J. A. Sloane, "Regulation of remyelination in multiple sclerosis," *FEBS Letters*, vol. 585, no. 23, pp. 3821–3828, 2011.

[218] J. P. Taygerly, L. R. McGee, S. M. Rubenstein et al., "Discovery of INT131: a selective PPARγ modulator that enhances insulin sensitivity," *Bioorganic & Medicinal Chemistry*, vol. 21, no. 4, pp. 979–992, 2013.

[219] A. Motani, Z. Wang, J. Weiszmann et al., "INT131: a selective modulator of PPARγ," *Journal of Molecular Biology*, vol. 386, no. 5, pp. 1301–1311, 2009.

[220] F. L. Dunn, L. S. Higgins, J. Fredrickson, and A. M. DePaoli, "Selective modulation of PPARγ activity can lower plasma glucose without typical thiazolidinedione side-effects in patients with type 2 diabetes," *Journal of Diabetes and its Complications*, vol. 25, no. 3, pp. 151–158, 2011.

[221] A. M. DePaoli, L. S. Higgins, R. R. Henry, C. Mantzoros, and F. L. Dunn, "Can a selective PPARγ modulator improve glycemic control in patients with type 2 diabetes with fewer side effects compared with pioglitazone?," *Diabetes Care*, vol. 37, no. 7, pp. 1918–1923, 2014.

[222] D. Weinstein, *PPARγ Agonists for Treatment of Multiple Sclerosis. WO2014120538A1*, 2014.

[223] D. Weinstein, A. Boyko, L. Pugliese et al., "CHS-131, a novel once daily oral treatment, decreased lesion burden of patients with relapsing-remitting course of multiple sclerosis (RRMS) in a randomized, double-blind, phase 2b, multicenter study (S50.002)," *Neurology*, vol. 88, 16 Supplement, 2017.

[224] D. Weinstein, L. Pugliese, H. Tang et al., "Once daily oral CHS-131, a novel PPARγ agonist, reduces both neuroinflammation and gray matter volume depletion in patients with relapsing-remitting multiple sclerosis: a randomized, placebo controlled double-blind, phase 2b, multicenter study," November 2019, https://onlinelibrary.ectrims-congress.eu/ectrims/2017/ACTRIMS-ECTRIMS2017/200368/david.weinstein.once.daily.oral.chs-131.a.novel.ppar.agonist.reduces.both.html.

[225] R. L. Frkic, Y. He, B. B. Rodriguez et al., "Structure–activity relationship of 2,4-dichloro-*N*-(3,5-dichloro-4-(quinolin-3-yloxy)phenyl)benzenesulfonamide (INT131) analogs for PPARγ-targeted antidiabetics," *Journal of Medicinal Chemistry*, vol. 60, no. 11, pp. 4584–4593, 2017.

[226] M. J. Khandekar, A. S. Banks, D. Laznik-Bogoslavski et al., "Noncanonical agonist PPARγ ligands modulate the response to DNA damage and sensitize cancer cells to cytotoxic chemotherapy," *Proceedings of the National Academy of Sciences of the United States of America*, vol. 115, no. 3, pp. 561–566, 2018.

[227] C. Blanquart, R. Mansouri, R. Paumelle, J.-C. Fruchart, B. Staels, and C. Glineur, "The protein kinase C signaling pathway regulates a molecular switch between transactivation and transrepression activity of the peroxisome proliferator-activated receptor α," *Molecular Endocrinology*, vol. 18, no. 8, pp. 1906–1918, 2004.

[228] R. Paumelle, C. Blanquart, O. Briand et al., "Acute antiinflammatory properties of statins involve peroxisome proliferator-activated receptor-α via inhibition of the protein kinase C signaling pathway," *Circulation Research*, vol. 98, no. 3, pp. 361–369, 2006.

[229] N.-S. Yaacob, M.-N. Norazmi, G. G. Gibson, and G. E. N. Kass, "The transcription of the peroxisome proliferator-activated receptor α gene is regulated by protein kinase C," *Toxicology Letters*, vol. 125, no. 1-3, pp. 133–141, 2001.

[230] M. Kockx, P. P. Gervois, P. Poulain et al., "Fibrates suppress fibrinogen gene expression in rodents via activation of the peroxisome proliferator-activated receptor-alpha," *Blood*, vol. 93, no. 9, pp. 2991–2998, 1999.

[231] P. Gervois, N. Vu-Dac, R. Kleemann et al., "Negative regulation of human fibrinogen gene expression by peroxisome proliferator-activated receptor α agonists via inhibition of CCAAT box/enhancer-binding protein β," *Journal of Biological Chemistry*, vol. 276, no. 36, pp. 33471–33477, 2001.

[232] A. Roy, M. Jana, M. Kundu et al., "HMG-CoA reductase inhibitors bind to PPARα to upregulate neurotrophin expression in the brain and improve memory in mice," *Cell Metabolism*, vol. 22, no. 2, pp. 253–265, 2015.

[233] D. A. Taha, C. H. De Moor, D. A. Barrett et al., "The role of acid-base imbalance in statin-induced myotoxicity," *Translational Research*, vol. 174, pp. 140–160.e14, 2016.

[234] A. Álvarez-Lueje, C. Valenzuela, J. A. Squella, and L. J. Núñez-Vergara, "Stability study of simvastatin under hydrolytic conditions assessed by liquid chromatography," *Journal of AOAC International*, vol. 88, no. 6, pp. 1631–1636, 2005.

[235] T. B. Vree, E. Dammers, I. Ulc, S. Horkovics-Kovats, M. Ryska, and I. J. Merkx, "Differences between lovastatin and simvastatin hydrolysis in healthy male and female volunteers: gut hydrolysis of lovastatin is twice that of simvastatin," *The Scientific World Journal*, vol. 3, 1343 pages, 2003.

[236] T. Prueksaritanont, L. M. Gorham, B. Ma et al., "In vitro metabolism of simvastatin in humans [SBT] identification of metabolizing enzymes and effect of the drug on hepatic P450s," *Drug Metabolism and Disposition*, vol. 25, no. 10, pp. 1191–1199, 1997.

[237] A. Roy, M. Jana, G. T. Corbett et al., "Regulation of cyclic AMP response element binding and hippocampal plasticity-related genes by peroxisome proliferator-activated receptor α," *Cell Reports*, vol. 4, no. 4, pp. 724–737, 2013.

[238] S. Pugazhenthi, M. Wang, S. Pham, C.-I. Sze, and C. B. Eckman, "Downregulation of CREB expression in Alzheimer's brain and in Aβ-treated rat hippocampal neurons," *Molecular Neurodegeneration*, vol. 6, no. 1, p. 60, 2011.

[239] S. Fusco, C. Ripoli, M. V. Podda et al., "A role for neuronal CAMP responsive-element binding (CREB)-1 in brain responses to calorie restriction," *Proceedings of the National Academy of Sciences of the United States of America*, vol. 109, no. 2, pp. 621–626, 2012.

[240] T. Gu, "CST curation set: 2234, specificities of antibodies used to purify peptides prior to LCMS," November 2019, https://www.phosphosite.org/curatedInfoAction.action?record=11076.

[241] D. E. Clark, C. E. Poteet-Smith, J. A. Smith, and D. A. Lannigan, "Rsk2 allosterically activates estrogen receptor alpha by docking to the hormone-binding domain," *The EMBO Journal*, vol. 20, no. 13, pp. 3484–3494, 2001.

[242] B. G. Shearer, H. S. Patel, A. N. Billin et al., "Discovery of a novel class of PPARδ partial agonists," *Bioorganic & Medicinal Chemistry Letters*, vol. 18, no. 18, pp. 5018–5022, 2008.

[243] S. Keil, H. Matter, K. Schönafinger et al., "Sulfonylthiadiazoles with an unusual binding mode as partial dual peroxisome proliferator-activated receptor (PPAR) γ/δ agonists with high potency and in vivo efficacy," *ChemMedChem*, vol. 6, no. 4, pp. 633–653, 2011.

[244] T. Adhikary, K. Kaddatz, F. Finkernagel et al., "Genomewide analyses define different modes of transcriptional regulation by peroxisome proliferator-activated receptor-β/δ (PPARβ/δ)," *PLoS One*, vol. 6, no. 1, article e16344, 2011.

[245] F. A. H. Batista, D. B. B. Trivella, A. Bernardes et al., "Structural insights into human peroxisome proliferator activated receptor delta (PPAR-delta) selective ligand binding," *PLoS One*, vol. 7, no. 5, article e33643, 2012.

[246] A. Ohtera, Y. Miyamae, K. Yoshida et al., "Identification of a new type of covalent PPARγ agonist using a ligand-linking strategy," *ACS Chemical Biology*, vol. 10, no. 12, pp. 2794–2804, 2015.

[247] I. M. Serafimova, M. A. Pufall, S. Krishnan et al., "Reversible targeting of noncatalytic cysteines with chemically tuned electrophiles," *Nature Chemical Biology*, vol. 8, no. 5, pp. 471–476, 2012.

[248] R. M. Miller, V. O. Paavilainen, S. Krishnan, I. M. Serafimova, and J. Taunton, "Electrophilic fragment-based design of reversible covalent kinase inhibitors," *Journal of the American Chemical Society*, vol. 135, no. 14, pp. 5298–5301, 2013.

[249] C. F. H. Allen and W. J. Humphlett, "The thermal reversibility of the Michael reaction: V. the effect of the structure of certain thiol adducts on cleavage," *Canadian Journal of Chemistry*, vol. 44, no. 19, pp. 2315–2321, 1966.

[250] H. Kim, A. Jo, S. S. Choi et al., "Rational design and synthesis of reversible covalent PPARγ antagonistic ligands inhibiting Ser273 phosphorylation," *Asian Journal of Organic Chemistry*, vol. 8, no. 9, pp. 1698–1706, 2019.

[251] J. Y. Jang, H. Kim, H.-J. Kim, S. W. Suh, S. B. Park, and B. W. Han, "Structural basis for the inhibitory effects of a novel reversible covalent ligand on PPARγ phosphorylation," *Scientific Reports*, vol. 9, no. 1, article 11168, 2019.

[252] P. S. Palkar, M. G. Borland, S. Naruhn et al., "Cellular and pharmacological selectivity of the peroxisome proliferator-activated receptor-β/δ antagonist GSK3787," *Molecular Pharmacology*, vol. 78, no. 3, pp. 419–430, 2010.

Hindawi
PPAR Research
Volume 2020, Article ID 1892375, 6 pages
https://doi.org/10.1155/2020/1892375

Research Article

Integrating Literature-Based Knowledge Database and Expression Data to Explore Molecular Pathways Connecting PPARG and Myocardial Infarction

Rongyuan Cao,[1] Yan Dong,[1] and Kamil Can Kural[2]

[1]*The Second People's Hospital, Lianyungang, Jiangsu Province 222000, China*
[2]*School of Systems Biology, George Mason University, Manassas, VA 20110, USA*

Correspondence should be addressed to Yan Dong; dongyan@gousinfo.com

Received 27 February 2020; Accepted 11 April 2020; Published 1 June 2020

Guest Editor: Anastasia Nesterova

Peroxisome proliferator-activated receptor γ (PPARG) might play a protective role in the development of myocardial infarction (MI) with limited mechanisms identified. Genes associated with both PPARG and MI were extracted from Elsevier Pathway Studio to construct the initial network. The gene expression activity within the network was estimated through a mega-analysis with eight independent expression datasets derived from Gene Expression Omnibus (GEO) to build PPARG and MI connecting pathways. After that, gene set enrichment analysis (GSEA) was conducted to explore the functional profile of the genes involved in the PPARG-driven network. PPARG demonstrated a significantly low expression in MI patients (LFC $= -0.52$; $p < 1.84e-9$). Consequently, PPARG could indicatively be promoting three MI inhibitors (e.g., SOD1, CAV1, and POU5F1) and three MI-downregulated markers (e.g., ALB, ACADM, and ADIPOR2), which were deactivated in MI cases ($p < 0.05$), and inhibit two MI-upregulated markers (RELA and MYD88), which showed increased expression levels in MI cases ($p = 0.0077$ and 0.047, respectively). These eight genes were mainly enriched in nutrient- and cell metabolic-related pathways and functionally linked by GSEA and PPCN. Our results suggest that PPARG could protect the heart against both the development and progress of MI through the regulation of nutrient- and metabolic-related pathways.

1. Introduction

Myocardial infarction (MI) and afterward heart failure are the significant causes of death and disability in the developed countries, which is characterized by acute myocardial ischemia derived from coronary artery occlusion, myocardial injury, and even necrosis [1–3]. Atherosclerotic plaque rupture with thrombus formation is determined to be the most dominant cause of myocardial infarction, which will result in an acute reduction of blood supply and imbalance in oxygen supply and demand. The prolonged ischemia will cause irreversible myocardial necrosis and heart failure [4–6]. To negate the life-threatening condition, rapid diagnoses and the proper therapy to restore the perfusion are urgent to salvage the jeopardized myocardium.

The members of the peroxisome proliferator-activated receptor (PPAR) family involve PPARα, PPARβ/δ, and PPARγ (PPARG), which might play vital roles in glucose and lipid metabolism. Among these members, PPARG is enriched in the adipose tissue and widely expressed in extra-adipose tissues, such as the heart, the vascular wall, and the skeletal muscle. PPARG can control the balance between glucose utilization and fatty acid oxidation, which is essential in the energy homeostasis in human myocardia physiology demand and postischemic remodeling [7–9].

As the nuclear hormone receptor superfamily of ligand-activated transcription factors, PPARG could recruit transcription coactivators that are necessary for the initiation of target gene transcription and may also inhibit the development and progress of myocardial infarction [10, 11]. Although some simulators of PPARG have been testified to show a protective effect on the development of myocardial infarction, a systemic literature text mining investigation has been performed to screen the genes and relevant molecular pathways

connecting PPARG to myocardial infarction. In this study, literature-based Elsevier Pathway Studio information and expression data retrieved from Gene Expression Omnibus (GEO) were integrated to explore the specific molecules and pathways connecting PPARG and myocardial infarction.

2. Materials and Methods

To explore meaningful genetic networks through which PPARG could influence the development and progress of MI, we set up the following rules for the identification of the networks: (1) For each edge (relationship) within a network, there were one or more scientific studies supporting the relationship. (2) A node (gene) demonstrated significant expression changes in the patients of MI.

2.1. Identifying PPARG-MI Connection Network. We conducted large-scale literature data mining to identify common genes that were downstream targets of PPARG and also linked to MI. The data was extracted from Elsevier Pathway Studio (http://www.pathwaystudio.com; version 12.3), the database of which is a network of interactions between molecules, processes, and diseases. Each relationship/edge is build based on the fact extracted from the literature by natural language processing (NLP) technology. A manual quality control process was enforced to remove unreliable relationships and relationships with nonspecific polarities by reading the sentences where a relationship was identified. Here, unreliable relationships refer to these with unmatched sentences, which were false positives by the NLP technique. After that, all the entities within the remaining network were tested using a mega-analysis with eight independent MI RNA expression datasets. The process is described as follows.

2.2. Selection of Gene Expression Datasets for Mega-analysis. The MI expression datasets were identified within the GEO database (https://www.ncbi.nlm.nih.gov/geo/) [12].The search was conducted using the keyword 'myocardial infarction,' where 678 studies with series data were identified and downloaded. We made an outline of the metadata of the identified datasets and selected a subset for the mega-analysis with the following criteria applied: (1) The dataset was array expression data. (2) The organism of the dataset was Homo sapiens. (3) The study design was MI case vs. healthy control. (4) The original data and the corresponding format file were downloadable. (5) The sample size was bigger than 10. Eight datasets satisfied the above criteria and were included for the mega-analysis, as shown in Table 1.

2.3. Mega-analysis Models. For each gene, the mega-analysis estimated the effect size in terms of gene expression log2 fold-change (LFC). Results from using both the random effects model and fixed effects model were compared [13]. To determine the heterogeneity of the datasets, between- and within-study variance was calculated and compared. When the total variance Q was no bigger than the expected value of the between-study variances (df), the model sets the ISq (percentage of the within-study over between-study variance) to zero. In this case, the fixed effects model, instead of the random effects model, will be selected for the mega-analysis. All analyses were performed using MATLAB (R2017a version).

2.4. Analysis of Influential Factors. To estimate the possible influence of several factors (e.g., study date, country of origin, and sample size) on the gene expression in MI patients, we conducted a multiple linear regression (MLR) analysis and reported the p values for each of these factors.

2.5. GSEA and Protein-Protein Connection. To test the functional profile of the genes involved in the PPARG-MI regulation, we conducted a Gene Set Enrichment Analysis (GSEA) [14] against the Pathway Studio pathways and Gene Ontology (GO; http://geneontology.org) terms [15]. The purpose of GSEA was to identify GO terms and Pathway Studio collected pathways enriched with the genes identified within the PPARG-MI network. Additionally, we explored the connections between the genes involved in the PPARG-MI regulation network by using Pathway Studio and constructed the protein-protein connection network (PPCN). Each relationship (edge) within the network was supported by one or more references, which were presented in the Supplementary Material (available here): Ref4PPCN. The PPCN was used to explore the potential functional linkage among the proteins identified within the PPARG-MI network.

3. Results

3.1. PPARG-MI Regulating Pathway and Mega-analysis Results. Pathway Studio literature text mining identified 30 genes that were promoted by PPARG and also upstream MI regulators (see Supplementary Material: 30 Genes). To identify these genes, we first explored all genes promoted by PPARG; then, we mined all the genes that inhibit MI; after that, we took the overlap and identified these 30 genes. Mega-analysis identified three out of these 30 genes demonstrating a significant decrease in expression levels, including SOD1, CAV1, and POU5F1 (Table 2). These genes were appended in the network connecting PPARG-MI, as shown in Figure 1 (highlighted in yellow).

Following the similar literature text mining approach, we identified 125 genes that were contradirectionally influenced by PPARG and MI (see Supplementary Material: 125 Genes). Out of these 125 genes, three demonstrated significantly increased expression levels in MI patients, including ALB, ACADM, and ADIPOR2 (Table 2). These genes were inhibited in MI while stipulated by PPARG. On the contrary, two genes (e.g., RELA and MYD88) were upregulated in MI patients, which could be suppressed by PPARG (Table 2). These pathways may partially explain the protective role of PPARG in the contradevelopment of MI. Please note that one or more previous studies supported each of these relationships presented in Figure 1. For the details of the supporting references, including relation type, polarity, reference PMID, title, and the sentences where the relation has been described, please refer to Supplementary Material: PPARG_MI_Network.

Mega-analysis showed that the expression levels of PPARG were significantly downregulated in MI patients

Table 1: The eight MI expression datasets selected for mega-analysis.

Dataset GEO ID	No. of controls	No. of cases	Country	Study age	Sample organism
GSE24519	4	34	Italy	3	Homo sapiens
GSE24591	4	34	Italy	3	Homo sapiens
GSE34198	48	49	Czech Republic	6	Homo sapiens
GSE48060	21	31	USA	6	Homo sapiens
GSE60993	7	10	South Korea	5	Homo sapiens
GSE60993	7	17	South Korea	5	Homo sapiens
GSE62646	14	84	Poland	6	Homo sapiens
GSE66360	50	49	USA	5	Homo sapiens

Note: Study age = current year − year of study + 1.

Table 2: Mega-analysis results of the eight genes involved in the PPARG-MI regulatory network.

Gene name	Random-effects model	No. of studies	LFC	*p* value	No. of samples	Country	Study age
SOD1	0	4	-0.28	0.048	0	0	1.00
RELA	0	4	0.28	0.008	0	0	1.00
POU5F1	1	5	-0.23	0.041	1.00	2.00*E*-09	2.00*E*-13
MYD88	0	3	0.23	0.047	0	0	1.00
CAV1	0	7	-0.24	0.0050	0.12	0.013	0.070
ALB	1	6	-1.35	0.0050	0.40	0.022	0.0030
ADIPOR2	0	6	-0.16	0.031	0.22	6.00*E*-04	1.00
ACADM	0	6	-0.32	0.0034	0.0056	0.000329	0.99328
PPARG	0	5	-0.52	2*e*-09	1	6.75*E*-11	5.28*E*-10

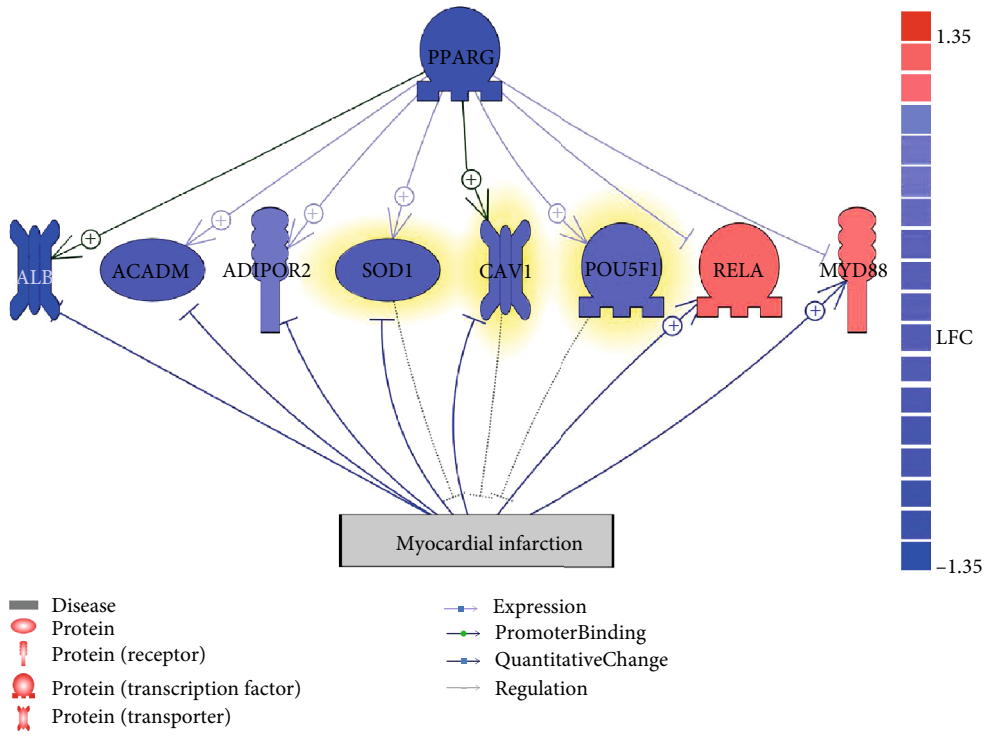

Figure 1: Functional network connecting PPARG and myocardial infarction. Entities in blue are genes with decreased expression levels from the mega-analysis using 8 MI datasets. Entities in red have an increased expression. Entities highlighted in yellow are genes regulating myocardial infarction, and the rest of the genes were targets regulated by myocardial infarction. + represents positive regulation; -| is negative.

Table 3: The GO terms enriched with nine genes within the PPARG-MI functional network.

Name	No. of entities	GO ID	Overlap	p value	Jaccard similarity
GO: response to nutrient	370	0007584	7	2.94E-07	0.019
GO: response to nutrient levels	730	0031667	7	1.53E-05	0.0096
GO: response to extracellular stimulus	761	0009991	7	1.53E-05	0.0092
GO: response to inorganic substance	803	0010035	6	0.0011	0.0074
GO: regulation of small molecule metabolic process	422	0062012	5	0.0016	0.012
GO: regulation of lipid metabolic process	441	0019216	5	0.0016	0.011
GO: cellular response to external stimulus	451	0071496	5	0.0016	0.011
GO: response to metal ion	533	0010038	5	0.0033	0.0093

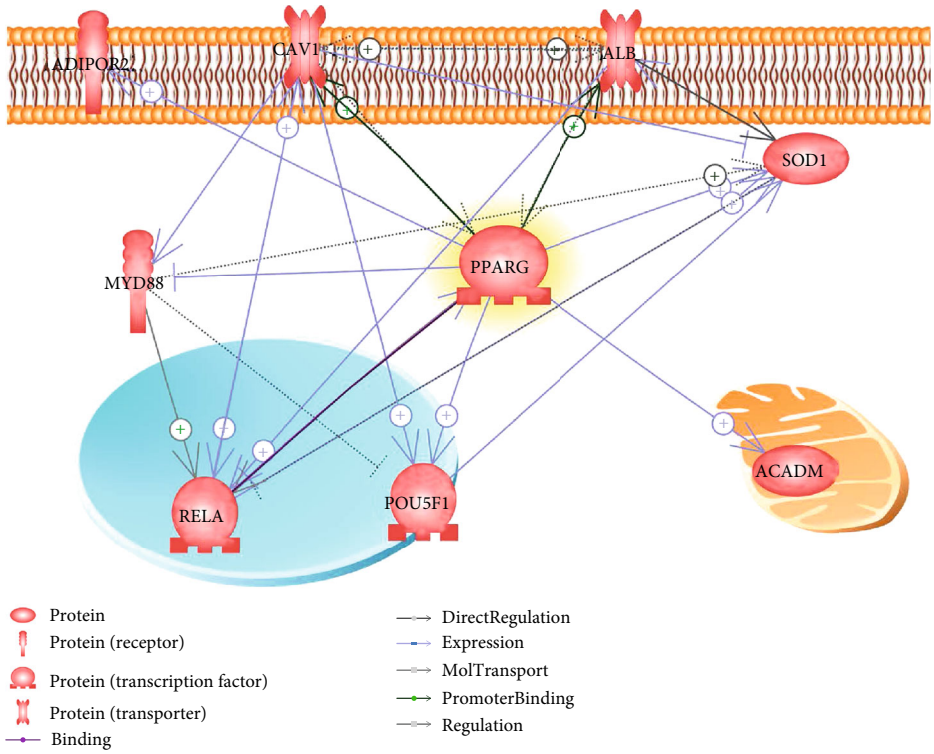

Figure 2: Protein-protein connection networks among the eight genes involved in PPARG-MI signaling pathways. The network was built using Pathway Studio (http://www.pathwaystudio.com). One or more references supported each relationship within the network. + represents positive regulation; -| is negative.

(LFC = −0.52; p value = 1.84e-9), which was calculated by using a fixed effects model. This was due to the fact that there was no significant between-study variance (PValue_Q = 0.31) according to the heterogeneity analysis.

Moreover, MLR analysis showed that two factors (country and study age) could significantly influence the expression of PPARG among different studies. For a more detailed description of the mega-analysis results of the nine genes involved in the network presented in Figure 1, please refer to Supplementary Material: Mega-analysis.

3.2. GSEA Results and PPI Network. To investigate the biological functions of the nine genes (including PPARG) within the PPARG-MI functional network (Figure 1), a GSEA was executed by using Pathway Studio. A total of eight significantly enriched GO terms (p value < 0.005, $q = 0.005$ for FDR) were identified and presented in Table 3, with details made available in Supplementary Material: GSEA. Notably, a majority of the shared GO terms highlighted by the GSEA approach were related to cell metabolic process, nutrient levels, and response to the metal ion, which were implicated with MI [16–18].

A literature-based PPI network has been constructed and presented in Figure 2. The relation between a pair of genes was identified through literature data mining. For each relationship/edge within Figure 2, there was at least one supporting reference. For the details of these references, please refer to Supplementary Material: Ref4PPCN. The PPCN showed that there were direct physical or indirect functional connection among PPARG and eight of its driven genes.

4. Discussion

This study confirmed the downregulation of PPARG in the case of myocardial infarction and revealed multiple pathways through which PPARG could regulate the development of myocardial infarction. Our results shed light on the understanding of the PPARG-MI association, suggesting PPARG as a potential therapeutic target for the treatment of myocardial infarction.

Among the eight genes identified to be driven by PPARG, ALB could be utilized as a monitor biomarker, as a low level of serum ALB is associated with increased risk of coronary artery disease and myocardial infarction [19]. ACADM could be a rate-limiting factor for the initial step of the mitochondrial fatty acid beta-oxidation catalyzation, which plays a vital role in myocardial infarction and diabetic cardiomyopathy [20].

The other six genes may be involved in the functional recovery and cellular protection involved in myocardial infarction. SOD1 overexpression, RELA blockade, and diminished MyD88-mediated inflammation can enhance functional and metabolic recovery and greatly decreased myocardial infarction [21–23], while ADIPOR2 is required for revascularization [24]. On the other hand, HIF-2α and POU5F1 (OCT4) could collaboratively promote the survival and differentiation of embryonic-like mesenchymal stem cells in myocardial infarction to repair the damaged myocardia [25]. It is worth to note that downregulated pulmonary CAV-1 expression subjected to myocardial infarction may lead to STAT3/Cyclin pathway activation, pulmonary hypertension, and lung structural remodeling development [26]. All of this evidence indicates that PPARG not only works in the progression of myocardial infarction but also plays a role in the functional recovery and cellular protection of myocardial infarction.

In addition to the exogenous activators, PPARs can also be activated by endogenous secreted ligands, such as free fatty acids or prostaglandins. It is not surprising to find that a majority of the shared pathways highlighted by the GSEA approach are related to cell metabolic process and nutrient levels, which are also implicated in the development of myocardial infarction. It is worth noting that, although detailed information should be deciphered, mitochondrial fatty acid beta-oxidation catalyzation rate limited by ACADM might be the vital energy pathway mediated by PPARG.

The PPCN showed that, besides the relation between PPARG and its eight driven genes (Figure 1), the majority of the eight genes (6 out of 8) were physically or functionally linked to each other (Figure 2). Especially, five out of the rest seven genes were connected to SOD1; the overexpression of which enhances functional and metabolic recovery and significantly decreases MI [21]. These functional connections (Figure 2) suggested that the genes connecting PPARG and MI may be also functionally linked to each other.

In this study, we propose an integrated analysis employing both literature-based knowledge database and expression data to explore the functional connection between PPARG and MI. This approach could help the exploration of the crucial genes and pathways further to decipher the association of factors in interest with a particular disease. Both the metabolic-and nutrient-associated pathways involved in the development and progress of myocardial infarction can be regulated by PPARG, which indicates that PPARG might be utilized as an essential target in myocardial infarction treatment.

This study has several limitations that need to be addressed in further work. First, the PPARG-MI connecting network was constructed using Pathway Studio only. More data sources should be employed to explore more potential relationships. Second, we used array data to study the expression variation of PPARG and its driven genes. Expression by RNA sequencing may provide higher resolution in studying the expression profile.

5. Conclusion

Literature-based knowledge database and expression data integration may significantly promote the illustration of the relevant mechanism involved in PPARG-mediated myocardial infarction protection.

Data Availability

The data in our study are available from the corresponding author upon reasonable request.

Conflicts of Interest

All the authors declare no conflict of interest.

Acknowledgments

This work was supported by the 2018 Jiangsu University Medical/Clinical Science and Technology Development Fund Project (Natural Science) (JLY20180021) and Lianyungang Second People's Hospital Middle-Aged and Young People's Fund Project (TQ201902).

Supplementary Materials

Supplementary materials were provided for this study (an excel file), including the following worksheets: PPARG_MI_Pathway, 30 Genes, 125 Genes, Mega-analysis, GSEA, and Ref4PPCN. *(Supplementary Materials)*

References

[1] L. Lu, M. Liu, R. Sun, Y. Zheng, and P. Zhang, "Myocardial infarction: symptoms and treatments," *Cell Biochemistry and Biophysics*, vol. 72, no. 3, pp. 865–867, 2015.

[2] A. Sakaguchi, C. Nishiyama, and W. Kimura, "Cardiac regeneration as an environmental adaptation," *Biochimica et Biophysica Acta (BBA) - Molecular Cell Research*, vol. 1867, no. 4, article 118623, 2020.

[3] K. Thygesen, J. S. Alpert, and H. D. White, "Universal definition of myocardial infarction," *Journal of the American College of Cardiology*, vol. 50, no. 22, pp. 2173–2195, 2007.

[4] A. O. Jackson, H. Tang, and K. Yin, "HiPS-cardiac trilineage cell generation and transplantation: a novel therapy for myocardial

infarction," *Journal of Cardiovascular Translational Research*, vol. 13, no. 1, pp. 110–119, 2020.

[5] J. Frampton, J. T. Devries, T. D. Welch, and B. J. Gersh, "Modern management of ST-segment elevation myocardial infarction," *Current Problems in Cardiology*, vol. 45, no. 3, article 100393, 2020.

[6] D. Q. Chen, X. S. Kong, X. B. Shen et al., "Identification of differentially expressed genes and signaling pathways in acute myocardial infarction based on integrated bioinformatics analysis," *Cardiovascular Therapeutics*, vol. 2019, Article ID 8490707, 13 pages, 2019.

[7] H. H. Liao, X. H. Jia, H. J. Liu, Z. Yang, and Q. Z. Tang, "The role of PPARs in pathological cardiac hypertrophy and heart failure," *Current Pharmaceutical Design*, vol. 23, no. 11, pp. 1677–1686, 2017.

[8] B. N. Finck, "The PPAR regulatory system in cardiac physiology and disease," *Cardiovascular Research*, vol. 73, no. 2, pp. 269–277, 2007.

[9] Y. F. Zhang, H. M. Xu, F. Yu et al., "Crosstalk between MicroRNAs and Peroxisome Proliferator-Activated Receptors and Their Emerging Regulatory Roles in Cardiovascular Pathophysiology," *PPAR Research*, vol. 2018, Article ID 8530371, 11 pages, 2018.

[10] E. Legchenko, P. Chouvarine, P. Borchert et al., "PPARγ agonist pioglitazone reverses pulmonary hypertension and prevents right heart failure via fatty acid oxidation," *Science Translational Medicine*, vol. 10, no. 438, article eaao0303, 2018.

[11] X. Niu, J. Zhang, L. Zhang et al., "Weighted gene co-expression network analysis identifies critical genes in the development of heart failure after acute myocardial infarction," *Frontiers in Genetics*, vol. 10, article 1214, 2019.

[12] E. Clough and T. Barrett, "The gene expression omnibus database," *Methods in Molecular Biology*, vol. 1418, pp. 93–110, 2016.

[13] M. Borenstein, L. V. Hedges, J. P. T. Higgins, and H. R. Rothstein, "A basic introduction to fixed-effect and random-effects models for meta-analysis," *Research Synthesis Methods*, vol. 1, no. 2, pp. 97–111, 2010.

[14] A. Subramanian, P. Tamayo, V. K. Mootha et al., "Gene set enrichment analysis: a knowledge-based approach for interpreting genome-wide expression profiles," *Proceedings of the National Academy of Sciences of the United States of America*, vol. 102, no. 43, pp. 15545–15550, 2005.

[15] A. W. Vesztrocy and C. Dessimoz, "A Gene Ontology tutorial in Python," *Methods in Molecular Biology*, vol. 1446, pp. 221–229, 2017.

[16] P. Pierucci, G. Misciagna, M. T. Ventura et al., "Diet and myocardial infarction: a nested case-control study in a cohort of elderly subjects in a Mediterranean area of southern Italy," *Nutrition, Metabolism, and Cardiovascular Diseases*, vol. 22, no. 9, pp. 727–733, 2012.

[17] S. Shen, H. Jiang, Y. Bei et al., "Qiliqiangxin attenuates adverse cardiac remodeling after myocardial infarction in ovariectomized mice *via* activation of PPARγ," *Cellular Physiology and Biochemistry*, vol. 42, no. 3, pp. 876–888, 2017.

[18] B. N. Plummer, H. Liu, X. Wan, I. Deschenes, and K. R. Laurita, "Targeted antioxidant treatment decreases cardiac alternans associated with chronic myocardial infarction," *Circulation Arrhythmia and Electrophysiology*, vol. 8, no. 1, pp. 165–173, 2015.

[19] L. Djousse, K. J. Rothman, L. A. Cupples, D. Levy, and R. C. Ellison, "Serum albumin and risk of myocardial infarction and all-cause mortality in the Framingham Offspring Study," *Circulation*, vol. 106, no. 23, pp. 2919–2924, 2002.

[20] A. Mitra, T. Basak, S. Ahmad et al., "Comparative Proteome Profiling during Cardiac Hypertrophy and Myocardial Infarction Reveals Altered Glucose Oxidation by Differential Activation of Pyruvate Dehydrogenase E1 Component Subunit β," *Journal of Molecular Biology*, vol. 427, no. 11, pp. 2104–2120, 2015.

[21] P. Wang, H. Chen, H. Qin et al., "Overexpression of human copper, zinc-superoxide dismutase (SOD1) prevents postischemic injuryOverexpression of human copper,zinc-superoxide dismutase (SOD1) prevents postischemic injury," *Proceedings of the National Academy of Sciences of the United States of America*, vol. 95, no. 8, pp. 4556–4560, 1998.

[22] S. Kawano, T. Kubota, Y. Monden et al., "Blockade of NF-κB improves cardiac function and survival after myocardial infarction," *American Journal of Physiology-Heart and Circulatory Physiology*, vol. 291, no. 3, pp. H1337–H1344, 2006.

[23] M. V. Singh, P. D. Swaminathan, E. D. Luczak, W. Kutschke, R. M. Weiss, and M. E. Anderson, "MyD88 mediated inflammatory signaling leads to CaMKII oxidation, cardiac hypertrophy and death after myocardial infarction," *Journal of Molecular and Cellular Cardiology*, vol. 52, no. 5, pp. 1135–1144, 2012.

[24] Y. Wang, X. L. Ma, and W. B. Lau, "Cardiovascular adiponectin resistance: the critical role of adiponectin receptor modification," *Trends in Endocrinology and Metabolism*, vol. 28, no. 7, pp. 519–530, 2017.

[25] S. Zhang, L. Zhao, J. Wang, N. Chen, J. Yan, and X. Pan, "HIF-2 α and Oct4 have synergistic effects on survival and myocardial repair of very small embryonic-like mesenchymal stem cells in infarcted hearts," *Cell Death & Disease*, vol. 8, no. 1, article e2548, 2018.

[26] J. F. Jasmin, I. Mercier, R. Hnasko et al., "Lung remodeling and pulmonary hypertension after myocardial infarction: pathogenic role of reduced caveolin expression," *Cardiovascular Research*, vol. 63, no. 4, pp. 747–755, 2004.

Hindawi
PPAR Research
Volume 2020, Article ID 2510951, 9 pages
https://doi.org/10.1155/2020/2510951

Research Article

PPARG Could Work as a Valid Therapeutic Strategy for the Treatment of Lung Squamous Cell Carcinoma

Shunbin Shi,[1] Guiping Yu,[2] Bin Huang,[2] Yedong Mi,[2] Yan Kang,[3] and Julia Pia Simon[4]

[1]*Department of Thoracic Surgery, Suzhou Ninth People's Hospital, Suzhou, Jiangsu Province 215200, China*
[2]*Department of Cardiothoracic Surgery, Jiangyin Hospital of Southeast University Medical College, Jiangyin, Jiangsu Province 214400, China*
[3]*Department of General Surgery, Children's National Medical Center, Washington, DC 20010, USA*
[4]*Neuroimaging and Informatics Institute, University of Southern California, California, Los Angeles 90007, USA*

Correspondence should be addressed to Guiping Yu; xiaoyuer97103@163.com

Received 28 February 2020; Accepted 6 April 2020; Published 1 June 2020

Guest Editor: Fuquan Zhang

Previous studies showed that PPAR-gamma (PPARG) ligands might serve as potential therapeutic agents for nonsmall cell lung cancer (NSCLC). However, a few studies reported the specific relationship between PPARG and lung squamous cell carcinoma (LSCC). Here, we made an effort to explore the relationship between PPARG and LSCC. First, we used mega-analysis and partial mega-analysis to analyze the effects of PPARG on LSCC by using 12 independent LSCC expression datasets (285 healthy controls and 375 LSCC cases). Then, literature-based molecular pathways between PPARG and LSCC were established. After that, a gene set enrichment analysis (GSEA) was conducted to study the functionalities of PPARG and PPARG-driven triggers within the molecular pathways. Finally, another mega-analysis was constructed to test the expression changes of PPARG and its driven targets. The partial mega-analysis showed a significant downregulated expression of PPARG in LSCC (LFC = −1.08, p value = 0.00073). Twelve diagnostic markers and four prognostic markers were identified within multiple PPARG-LSCC regulatory pathways. Our results suggested that the activation of PPARG expression may inhibit the development and progression of LSCC through the regulation of LSCC upstream regulators and downstream marker genes, which were involved in tumor cell proliferation and protein polyubiquitination/ubiquitination.

1. Introduction

PPARG is a ligand-activated transcription factor belonging to the family of peroxisome proliferator-activated receptors (PPARs) [1], which is widely expressed in many cells and tissues in the human body [2]. PPARG has recently attracted interest as the potential therapeutic target for a variety of malignancies [3]. A number of animal models [4], cell lines [5, 6], and clinical trials [NCT00923949, NCT01199068, NCT01199055] demonstrated that activation of PPAR-gamma impedes lung tumor progression and suggest that PPARG ligands may serve as potential therapeutic agents for nonsmall cell lung cancer (NSCLC), with the emphasis on lung adenocarcinoma [7, 8]. For instance, Ni et al.'s study showed that the activation of PPARG could inhibit the proliferation of EGFR-TKI-resistant lung adenocarcinoma cells and lead to a better survival rate [8].

So far, only a few studies explored the relationship between PPARG and lung squamous cell carcinomas (LSCC) [9, 10]. Kim et al. pointed out that the truncated splice variant of human PPAR gamma1 (hPPARG1(tr)) was strongly expressed in primary LSCC tumorous tissues, and the overexpression of hPPARG1(tr)) could increase the resistance of transfected cells to chemotherapeutic drug- and chemical-induced cell death [10]. However, to our knowledge, no study has systematically studied the role of PPARG in the pathology of LSCC.

To address this issue, we first conducted a meta-analysis to study the gene expression change of PPARG in the case of LSCC. Then, we integrated literature-based pathways

and gene set enrichment analysis (GSEA) to study the potential pathways where PPARG could exert influence on the pathologic development of LSCC. Our results may help to understand the potential roles of PPARG in the case of LSCC.

2. Materials and Methods

2.1. Selection of LSCC Expression Data in Mega-Analysis. For the initial selection, we searched the LSCC expression datasets on gene expression omnibus (GEO; https://www.ncbi.nlm.nih.gov/geo/) by using the keywords "lung squamous cell carcinoma." Then, we applied the following criteria to filter further: (1) The entry type used in the study was series; (2) The dataset was array expression data; (3) The studies were designed as a comparison between LSCC and healthy controls: and (4) The organism of the dataset was Homo sapiens. Finally, we considered the datasets for which the original data and the corresponding format files were downloadable. Since we calculated the expression using the original data as extracted above, we used the term "mega-analysis" instead of "meta-analysis.".

2.2. Mega-Analysis and Partial Mega-Analysis Models. In order to identify the relation between PPARG and LSCC, we used a mega-analysis to analyze the expression levels of PPARG in the case of LSCC. In our study, results from using both the random-effects model and the fixed-effects model were compared. To determine the heterogeneity of the datasets, between- and within-study variance was calculated and compared. When the total variance Q was no bigger than the expected value of the between-study variances (df), the model sets the ISq (percentage of the within- over between-study variance) to zero. In this case, the fixed-effects model, instead of the random-effects model, will be selected for the mega-analysis. All analyses were performed using Matlab (version R2017a; https://www.mathworks.com/products/matlab.html).

Moreover, we performed a partial mega-analysis to discover the significance of a gene presented in part of the studies/datasets (e.g., 50% of total studies) but not in all datasets, where 50% top studies/datasets were employed for the mega-analysis of a gene. Here, we define the "top datasets" for a gene as these datasets that demonstrate the bigger absolute value of effect size than the rest of the datasets. It should be mentioned that the top datasets for different genes could be different.

2.3. Analysis of Influential Factors. To estimate the possible influence of several factors (e.g., study date, country of origin, and sample size) on the gene expression in the case of MI, we conducted a multiple linear regression (MLR) analysis and reported the p values for each of these factors.

2.4. Construct PPARG-Drive Network and Gene Set Enrichment Analysis. Based on large scale literature data mining, we constructed a diagnostic and a prognostic functional network connecting PPARG and LSCC. In the diagnostic network, we identified the genes that were contra-directionally regulated by PPARG and LSCC. To achieve this goal, we used Pathway Studio (http://www.pathwaystudio.com/) to identify PPARG➔gene relationships and LSCC➔gene relationships with polarity. Each of these relationships has supported by one or two scientific references. Then we identified the overlapped genes within these relationships to construct the PPARG—LSCC diagnostic network. To increase the reliability of the identified network, we limited the genes to these that also demonstrated consistency in terms of their gene expression alteration in the case of LSCC in the mega-analysis. For the prognostic pathway, we followed the same pressure but to identify genes that were downstream targets of PPARG and upstream regulators of LSCC. The reference information supporting the relations identified in these networks was provided in the Supplementary Materials (available here), including the type of the relationship, supporting references, and related sentences from the references where the relationship has been identified.

For these genes within the diagnostic and prognostic networks built above, a gene set enrichment analysis (GSEA) was conducted using Pathway Studio (version 12.1.0.9; http://www.pathwaystudio.com/) against Gene Ontology (GO; http://geneontology.org) and Pathway Studio pathways. The purpose of GSEA was to test the functional profile of the genes involved in the PPARG-driven networks.

3. Results

3.1. Mega-Analysis Based on the Selected LSCC Expression Datasets. There were 4,643 results shown in the GEO datasets identified by the keywords "lung squamous cell carcinoma". Then, further filters were set as our criteria. A total of 12 datasets satisfied the inclusion criteria for the mega-analysis, which are listed in Table 1. The studies were distributed in 8 different countries, and the study dates ranged from 2 to 15 years ago, including 285 healthy controls and 375 LSCC cases.

The mega-analysis and partial mega-analysis results for gene PPARG are presented in Table 2. As shown in Figure 1(a), the total variance (Q) was larger than the expected between-study variance (df), the within-study variance percentage ($ISq\%$) was 45.10, the between-study variances were significant, and thus a random-effects model was selected for PPARG in the mega-analysis. However, there were no significant between-study variances ($Isq = 0$, Q test $p = 0.64$), see in Figure 1(b). Thus, the fixed-effects model was selected for PPARG in partial mega-analysis. The LFC of the gene was estimated from about half (top 50%) of the selected datasets. PPARG demonstrated significantly lower expression in the case of LSCC ($LFC = -1.08$, $p\ value = 0.00073$).

MLR analysis showed that sample size and study age were not significant influential factors for the expression levels of PPARG among the 11 LSCC datasets ($p\ value > 0.30$). However, the population region (country) was identified as a significant factor that influences the LFC of PPARG in the case of LSCC ($p\ value = 0.0045$, Figure 1(c)). This may partially explain the differential results between the partial mega-analysis and the mega-analysis.

Table 1: The 12 qualified LSCC expression datasets for mega-analysis.

GEO ID	Control (n)	Case (n)	Country	Study age	Sample organism
GSE84784	9	9	Luxembourg	2	Homo sapiens
GSE67061	8	69	China	3	Homo sapiens
GSE30219	14	61	France	5	Homo sapiens
GSE33479	27	14	USA	5	Homo sapiens
GSE32036	59	12	USA	7	Homo sapiens
GSE19188	65	27	Netherlands	9	Homo sapiens
GSE11969	5	35	Japan	10	Homo sapiens
GSE2088	30	48	Japan	10	Homo sapiens
GSE12428	28	34	Netherlands	11	Homo sapiens
GSE6044	5	14	Germany	13	Homo sapiens
GSE1987	7	17	Israel	15	Homo sapiens
GSE12472	28	35	Netherland	10	Homo sapiens

Table 2: Analysis of PPARG expression levels in LSCC datasets.

PPARG	Mega-analysis	Partial mega-analysis
Models	Random effects	Fixed effects
# study	11	5
LFC (effect size)	-0.22	-1.08
p value	0.094	0.00073
ISq (%)	45.10	0.00
p value Q	0.051	0.64
# sample	0.85	0.10
Country	0.0045	2.79e-6
Study age	0.30	0.00034

3.2. The LSCC Diagnostic Network Interfered by PPARG. Multiple molecules (12 genes) have been identified through large-scale literature data mining that was contra-directionally influenced by PPARG and LSCC, as shown in Figure 2. According to previous literature reports, a total of 8 molecules (XIAP, UBE2D1, SKP2, ACKR3, MI21, HOXA10, STAT1, and PDPN) were upregulated in LSCC (the genes at the bottom of Figure 2; the arrows with ⊕, Figure 2) but negatively affected by PPARG (the arrows with ┤, Figure 2). These eight genes also presented increased expression levels in the 12 LSCC RNA expression datasets. These results support the literature data mining results and suggest these eight genes as positive markers for LSCC. The mega-analysis results for these genes were provided in the Supplementary Materials→Mega-analysis (available here). The inhibition of these genes by PPARG could exert an anti-LSCC effect during its pathological development (Figure 2).

On the other hand, four genes (MIR223, ANGPT1, CYP2A6, and FOXA2) have been suggested to get suppressed in LSCC (the genes at the top of Figure 2, the arrows with ┤) but were stimulated by PPARG (Figure 2). These four genes also presented decreased expression levels in the mega-analysis, supporting the literature data mining results. Activation of these molecules could be due to other pathways where PPARG inhibits the progress of LA. Detailed information regarding the network presented in Figure 2 can be found in the Supplementary Materials→LSCC (available here) diagnostic network, including the type of the relationships and the supporting references.

3.3. GSEA for the Genes Involved in LSCC Diagnostic Network. The GSEA was performed using Pathway Studio with the purpose of investigating the biological functions of the 12 genes within the LSCC diagnostic network. The GSEA was also confirmed by the mega-analysis, including eight upregulated and five suppressed genes. A total of 10 out of these 12 genes were shared among the top 10 most significantly enriched pathways (p *values* < 0.012, $q = 0.05$ for FDR), which are presented in Table 3. The full 21 pathways/-gene sets enriched with p *value* < 0.047 were presented in the Supplementary Materials→GSEA1 (available here). Notably, enriched pathways highlighted by the GSEA approach are mainly related to the regulation of protein ubiquitination, the regulation of cell proliferation, and cytokine stimulus.

3.4. LSCC Prognostic Network Interfered by PPARG. As shown in Figure 3, a regulatory pathway connecting PPARG and LSCC was identified, heavily involved in the pathological development of LSCC. Based on the literature reports, three genes, TNF, NOS2, and ACE, could promote the pathological development of LSCC (highlighted in red, the arrows with ⊕, Figure 3). These three genes were deactivated by PPARG. However, according to the mega-analysis results, these genes were downregulated together with PPARG in the case of LSCC. Therefore, PPARG may not necessarily be needed for the deactivation of these genes to inhibit the progress of LSCC. The supporting references for each relation presented in Figure 3 were provided in the Supplementary Materials→LSCC_ (available here)prognostic network, which also include the type of the relationships.

In addition, an LSCC-inhibitor, STK11, has been shown to be activated by PPARG (highlighted in blue, the arrows with ┤, see Figure 3(a)). Mega-analysis showed that this gene showed slightly increased expression in the case of LSCC. Therefore, activation of PPARG may further promote the activation of STK11, which could be a blocker for the

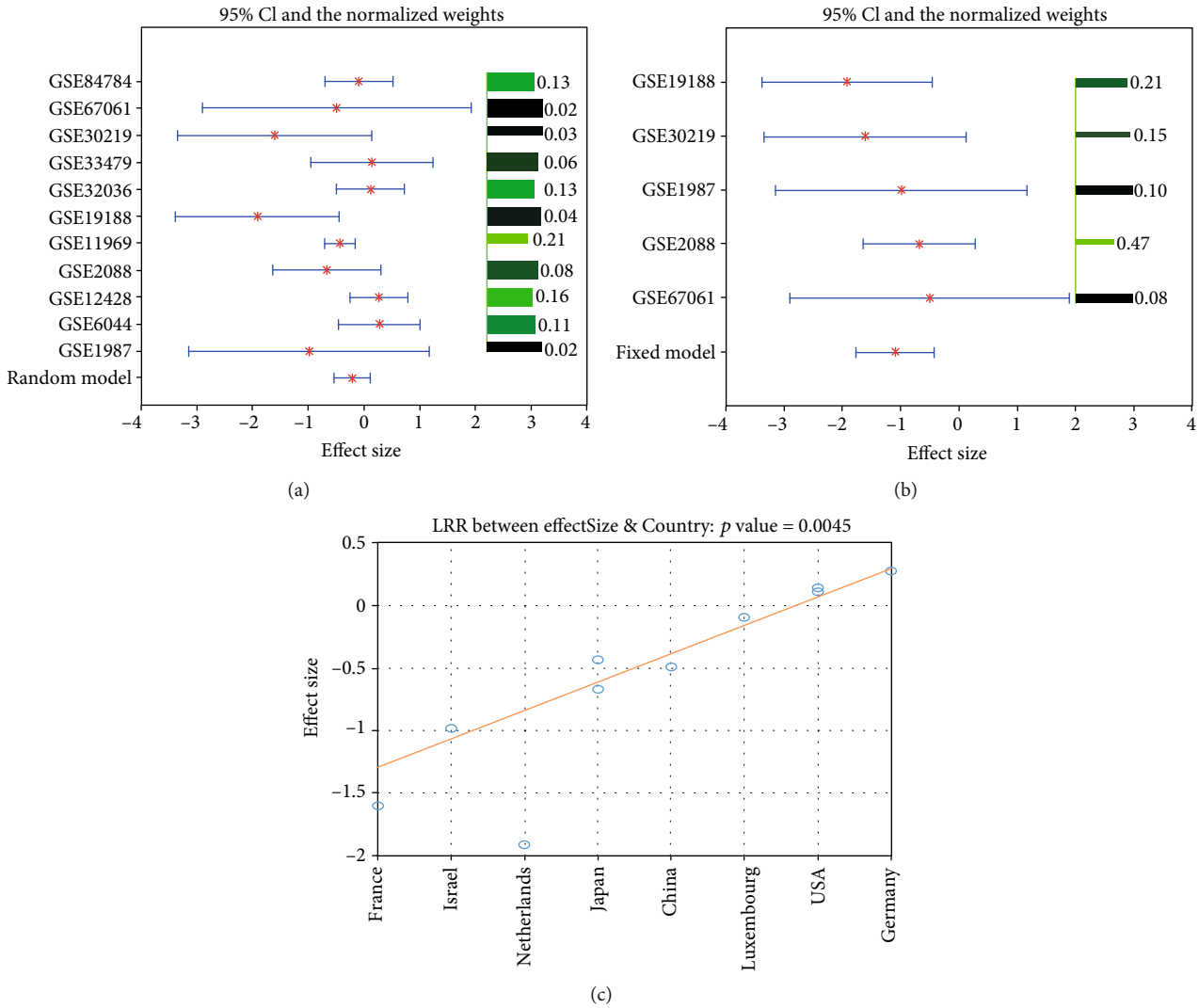

Figure 1: Mega-analysis results of PPARG using 11 LSCC RNA expression datasets. (a) Mega-analysis results from the random-effects model. (b) Partial mega-analysis results from the fixed-effects model. (c) The influence of population region (country) on the PPARG expression levels. The bar plot on the right of each figure represents the normalized weights for each dataset/study, range (0, 1); the brighter (green) the color, the bigger the weight (labeled right next to the bar). The star (in red) and lines (in blue) on the left are the mean of effect size (log fold change) and 95% confidence interval (CI) of each dataset/study, respectively.

pathologic development of LSCC. The mega-analysis results of these four genes in Figure 3 were provided in the Supplementary Materials→Mega-analysis (available here).

3.5. GSEA for the Genes Involved in LSCC Prognostic Network. GSEA results showed that the five genes (PPARG, STK11, NOS2, and TNF) were significantly enriched within 59 pathways/gene sets (p *value* < 0.044; $q = 0.05$ for FDR; see Supplementary Materials→GSEA2 (available here)). We presented the top 10 pathways (4 genes were enriched; $p < 0.0077$) in Table 4. The pathways were mainly related to cell metabolism and hormone level regulation, which was largely different from that of the LSCC diagnostic network. Also, notably, these five genes enrich more pathways than that of the 12 genes within the LSCC diagnostic network, indicating that these five genes were more functionally linked to each other.

4. Discussion

Previous studies suggested that the activation of PPARG might be associated with the inhibition of NSCLC [4–6]. However, most studies were focused on the cases of lung adenocarcinoma [4–6]. In this study, we aim to explore the possible linkage between PPARG and LSCC. First, we utilized a mega-analysis and a partial mega-analysis to analyze the potential relationship between PPARG and LSCC. Subsequently, we integrated knowledge from large-scale literature data mining and existing LSCC expression data to construct molecular networks connecting PPARG and LSCC, followed by a GAEA analysis to study the functional profile of the molecules involved in the PPARG-drive network. Our results showed that PPARG was significantly downregulated in about half of the LSCC cases, with multiple pathways

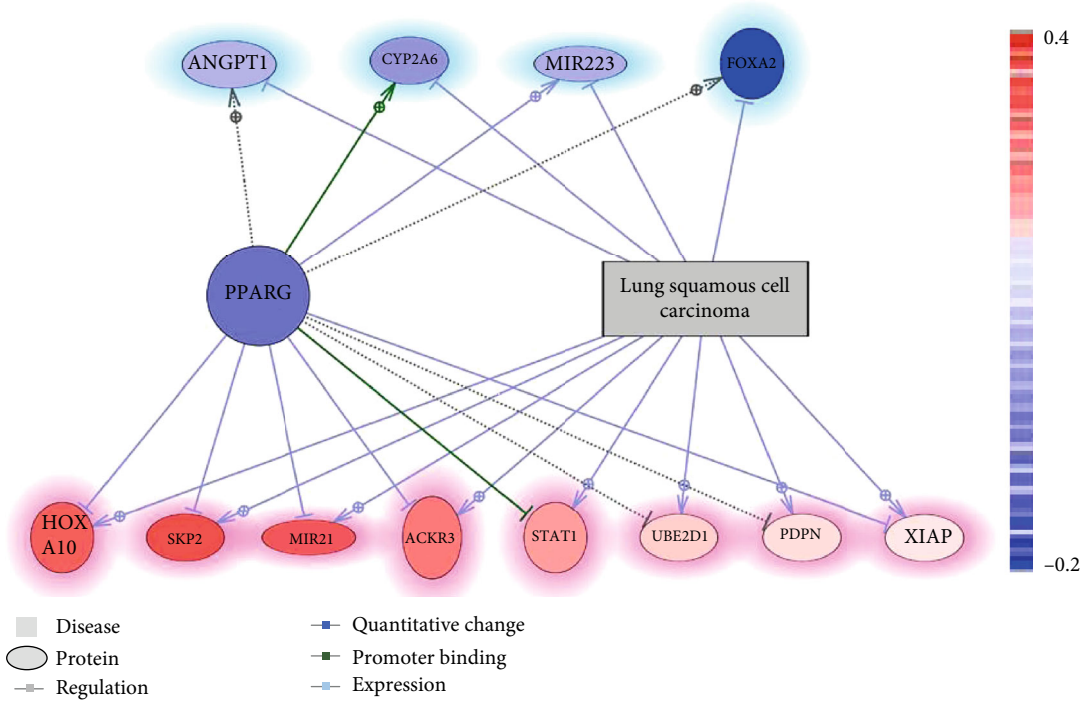

Figure 2: LSCC diagnostic network interfered with PPARG. Genes highlighted in blue (genes at the top of the figure) were literature-implicated with a downregulation in the case of LSCC, and those highlighted in red (genes at the bottom of the figure) were upregulated according to literature reports. Genes in blue represent a decreased expression level from the mega-analysis using 12 LSCC datasets, while those in red represent an increased expression level.

Table 3: The top 10 genetic pathways enriched by the 12 genes within LSCC_diagnostic network.

Name	GO ID	Overlap	p value	Jaccard similarity
GO: positive regulation of protein polyubiquitination	1902916;	3	0.00085	0.14
GO: regulation of smooth muscle cell proliferation	0048660;	5	0.0012	0.022
GO: regulation of protein polyubiquitination	1902914;	3	0.0015	0.097
GO: positive regulation of protein ubiquitination	0031398;	4	0.0036	0.029
GO: positive regulation of protein modification by small protein conjugation or removal	1903322;	4	0.0050	0.025
GO: regulation of response to cytokine stimulus	0060759;	4	0.0052	0.022
GO: regulation of cytokine-mediated signaling pathway	0001959;	4	0.0052	0.023
GO: regulation of endothelial cell proliferation	0001936;	4	0.0080	0.019
GO: regulation of protein ubiquitination	0031396;	4	0.010	0.017
GO: regulation of response to external stimulus	0032101;	6	0.011	0.0060

suggesting an inhibition role of PPARG in the pathologic development and progress of LSCC.

Notably, PPARG did not show a significant decrease in the 11 studies overall ($LFC = -0.22$; $p\ value = 0.094$), while it demonstrated significant decreased expression in 5 out of the 11 studies ($LFC = -1.08$; $p\ value = 0.00073$). These results indicate that there are influential factors that lead to different expression levels of PPARG among different studies. MLR analysis showed that the population region was a significant factor that influenced the PPARG levels (Figure 1(c)). Specifically, PPARG demonstrated low expression of $LFC = -1.60$ in the dataset from France (GSE30219), while relatively high expression in the dataset from Germany ($LFC = 0.27$; GSE6044). Notably, one of the highest (GSE12428; $LFC = 0.26$) and the lowest (GSE19188; $LFC = -1.91$) expression levels were from the Netherlands, indicating that, besides population region, there could be other factors that influence the PPARG expression levels in LSCC patients. Further investigation showed that the GSE12428 dataset was especially studying LSCC patients who smoke, while the dataset of GSE19188 contained all patients in general. It has been shown that smoking is one of the major risk factors for the development of LSCC [11], and smokers tend to have low PPARG expression levels [12]. These studies may explain the different PPARG levels in these two Netherlands datasets. Moreover, MLR results also suggest that sample size

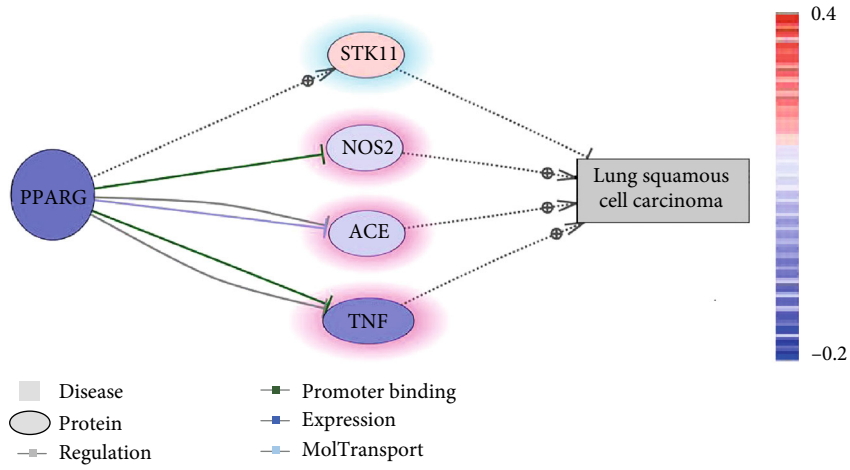

Figure 3: LSCC prognostic network interfered with PPARG. Genes in blue represent a decreased expression level from the mega-analysis using 12 LSCC datasets; entities in red represent an increased expression level. Entities highlighted in blue were literature implicated as the LSCC-inhibitors, while those highlighted in red were LSCC-promoters.

Table 4: The top 10 genetic pathways enriched by the 12 genes within LSCC_diagnostic network.

Name	GO ID	Overlap	*p* value	Jaccard similarity
GO: positive regulation of small molecule metabolic process	0062013	4	0.00054	0.023
GO: regulation of small molecule metabolic process	0062012	4	0.0036	0.0095
GO: fatty acid transport	0015908	3	0.0036	0.037
GO: receptor biosynthetic process	0032800	2	0.0036	0.22
GO: response to oxygen levels	0070482	4	0.0049	0.0073
GO: regulation of inflammatory response	0050727	4	0.0049	0.0079
GO: cellular response to organic cyclic compound	0071407	4	0.0076	0.0063
GO: regulation of hormone levels	0010817	4	0.0077	0.0060
GO: monocarboxylic acid transport	0015718	3	0.0077	0.019
CSF2 -> STAT expression targets	NONE	4	0.0077	0.055

and study date were not significant factors for the PPARG levels. Due to lack of data, we only studied the influence of three factors on the expression levels of PPARG. Further study is needed to test the expression level of PPARG in LSCC patients and the possible influential factors such as age, gender, and complication.

Functional network analysis showed that PPARG could play roles both in the development and progression of LSCC. Specifically, PPARG counter-regulated 12 molecules that were upregulated or downregulated by LSCC (Figure 2). The expression levels of eight LSCC markers (XIAP, UBE2D1, SKP2, ACKR3, MI21, HOXA10, STAT1, and PDPN) were significantly upregulated in LSCC patients [13–20] and were downregulated by PPARG [21–28]. On the other hand, PPARG could activate multiple genes [29–33] inhibited by LSCC [34–38], including MIR 223, PTEN, ANGPT1, CYP2A6, and FOXA2. It should also be noted that the relations between LSCC and the molecules in the network are supported by both the literature data mining and mega-analysis using 12 LSCC expression datasets, which strengthens the reliability of the PPARG-driven network.

GSEA analysis suggested that PPARG may influence the development of LSCC through multiple pathways (Table 3 and Table 4). Besides the regulation of cell proliferation associated with the procession of LSCC, PPARG could also regulate protein polyubiquitination and ubiquitination, which has become increasingly recognized as a controller to regulate the function and signaling of a profusion of proteins. Ubiquitination affects proteins in various cellular processes, including signal transduction, DNA repair, chromosome maintenance, transcriptional activation, cell cycle progression, cell survival, and certain immune cell functions [39]. Thus, it is not surprising that ubiquitin metabolism enzymes prominently feature either oncogenes or tumor suppressors in a variety of cancers and many pathways relevant to cancer. A previous study suggested that targeting those physiological processes may effectively abate the proliferation and facilitate the treatment of lung cancer cells [40]. In the LSCC diagnostic network (Figure 2), E2 ubiquitin-conjugating enzymes (UBE2D1), E3 ubiquitin ligases (XIAP), and SKP2 were involved in the regulation of protein ubiquitination. The expression of XIAP, UBE2D1, and SKP2 downregulated by PPARG at the transcriptional level [21, 22, 41] were

overexpressed in LSCC tissues with robust proliferation ability [13–15].

PPARG may also play a role in the progression of LSCC by interfering upstream regulators of LSCC, as shown in Figure 3. For instance, the knock-down of PPARG has been shown to deactivate STK11 [42], while the loss of STK11 could lead to the formation of LSCC [43]. Furthermore, the activation of PPARG could inhibit three promoters of LSCC, including NOS2 [44], ACE [45], and TNF [46]. Thus, increased expression of PPARG may inhibit the formation of LSCC.

The most significant contribution of this study was the identification of the two PPARG-driven networks (Figures 2 and 3) that partially explain the mechanism of the roles of PPARG in the etiology and development of LSCC. However, the integration of literature data-mine and mega-analysis may exclude potential genes/molecules connection PPARG and LSCC. Further study is needed to validate and consummate the networks identified here.

5. Conclusion

Results from this study indicated that the expression of PPARG might be suppressed in LSCC patients. Activation of PPARG expression may inhibit the development and progress of LSCC through the regulation of LSCC upstream regulators and downstream marker genes. Our results indicate the need for further study of the relationship between PPARG and LSCC.

Data Availability

The data of this study are available from the corresponding author upon reasonable request.

Conflicts of Interest

All the authors declare no conflict of interest.

Authors' Contributions

Shunbin Shi and Guiping Yu have contributed equally to this work.

Supplementary Materials

(1) GSEA1 and GAEA2 present GSEA results for the genes within Figure 2 and Figure 3, respectively. (2) Mega-analysis presents the mega-analysis results for PPARG gene and its driven genes within the Figure 2 and Figure 3. (3) Partial_Mega-analysis presents the partial mega-analysis results for PPARG; (4) LSCC_diagnostic network presents the reference information for the network presented in Figure 2. (4) LSCC_prognostic network presents the reference information for the network presented in Figure 3. *(Supplementary Materials)*

References

[1] V. Bocher, G. Chinetti, J. C. Fruchart, and B. Staels, "Role of the peroxisome proliferator-activated receptors (PPARS) in the regulation of lipids and inflammation control," *Journal de la Societe de biologie*, vol. 196, no. 1, pp. 47–52, 2002.

[2] J. Berger and D. E. Moller, "The mechanisms of action of PPARs," *Annual Review of Medicine*, vol. 53, no. 1, pp. 409–435, 2002.

[3] J. M. Peters, Y. M. Shah, and F. J. Gonzalez, "The role of peroxisome proliferator-activated receptors in carcinogenesis and chemoprevention," *Nature Reviews Cancer*, vol. 12, no. 3, pp. 181–195, 2012.

[4] N. Skrypnyk, X. Chen, W. Hu et al., "PPARα activation can help prevent and treat non-small cell lung cancer," *Cancer Research*, vol. 74, no. 2, pp. 621–631, 2014.

[5] V. G. Keshamouni, R. C. Reddy, D. A. Arenberg et al., "Peroxisome proliferator-activated receptor- γ activation inhibits tumor progression in non-small-cell lung cancer," *Oncogene*, vol. 23, no. 1, pp. 100–108, 2004.

[6] S. Kaur, A. Nag, G. Gangenahalli, and K. Sharma, "Peroxisome Proliferator Activated Receptor Gamma Sensitizes Non-small Cell Lung Carcinoma to Gamma Irradiation Induced Apoptosis," *Front Genet*, vol. 10, p. 554, 2019.

[7] Y. Susaki, M. Inoue, M. Minami et al., "Inhibitory effect of PPARγ on NR0B1 in tumorigenesis of lung adenocarcinoma," *International Journal of Oncology*, vol. 41, no. 4, pp. 1278–1284, 2012.

[8] J. Ni, L. L. Zhou, L. Ding et al., "PPARγ agonist efatutazone and gefitinib synergistically inhibit the proliferation of EGFR-TKI-resistant lung adenocarcinoma cells via the PPARγ/PTEN/Akt pathway," *Experimental Cell Research*, vol. 361, no. 2, pp. 246–256, 2017.

[9] H. Li, M. C. Weiser-Evans, and R. Nemenoff, "Anti- and Protumorigenic Effects of PPARγ in Lung Cancer Progression: A Double-Edged Sword," *PPAR Research*, vol. 2012, Article ID 362085, 12 pages, 2012.

[10] H. J. Kim, J. Y. Hwang, H. J. Kim et al., "Expression of a peroxisome proliferator-activated receptor gamma 1 splice variant that was identified in human lung cancers suppresses cell death induced by cisplatin and oxidative stress," *Clinical Cancer Research*, vol. 13, no. 9, pp. 2577–2583, 2007.

[11] M. C. Boelens, A. van den Berg, R. S. Fehrmann et al., "Current smoking-specific gene expression signature in normal bronchial epithelium is enhanced in squamous cell lung cancer," *The Journal of Pathology*, vol. 218, no. 2, pp. 182–191, 2009.

[12] B. C. Bergman, L. Perreault, D. M. Hunerdosse, M. C. Koehler, A. M. Samek, and R. H. Eckel, "Intramuscular lipid metabolism in the insulin resistance of smoking," *Diabetes*, vol. 58, no. 10, pp. 2220–2227, 2009.

[13] Y. B. Chen, J. Shu, W. T. Yang et al., "XAF1 as a prognostic biomarker and therapeutic target in squamous cell lung cancer," *Chinese Medical Journal*, vol. 124, no. 20, pp. 3238–3243, 2011.

[14] L. Hou, Y. Li, Y. Wang et al., "UBE2D1 RNA Expression Was an Independent Unfavorable Prognostic Indicator in Lung Adenocarcinoma, but Not in Lung Squamous Cell Carcinoma," *Disease Markers*, vol. 2018, Article ID 4108919, 8 pages, 2018.

[15] K. Zhong, F. Yang, Q. Han, J. Chen, and J. Wang, "Skp2 expression has different clinicopathological and prognostic implications in lung adenocarcinoma and squamous cell carcinoma," *Oncology Letters*, vol. 16, no. 3, pp. 2873–2880, 2018.

[16] B. Behnam Azad, A. Lisok, S. Chatterjee et al., "Targeted Imaging of the Atypical Chemokine Receptor 3 (ACKR3/CXCR7)

in Human Cancer Xenografts," *Journal of Nuclear Medicine*, vol. 57, no. 6, pp. 981–988, 2016.

[17] Y. Song, H. Dou, P. Wang et al., "A novel small-molecule compound diaporine A inhibits non-small cell lung cancer growth by regulating miR-99a/mTOR signaling," *Cancer Biology Therapy*, vol. 15, no. 10, pp. 1423–1430, 2014.

[18] A. Clemenceau, O. Boucherat, K. Landry-Truchon et al., "Lung cancer susceptibility genetic variants modulate HOXB2 expression in the lung," *The International Journal of Developmental Biology*, vol. 62, no. 11-12, pp. 857–864, 2018.

[19] M. Yang, H. Chen, L. Zhou, K. Chen, and F. Su, "Expression profile and prognostic values of STAT family members in non-small cell lung cancer," *American journal of translational research*, vol. 11, no. 8, pp. 4866–4880, 2019.

[20] H. Suzuki, M. Onimaru, T. Koga et al., "High podoplanin expression in cancer cells predicts lower incidence of nodal metastasis in patients with lung squamous cell carcinoma," *Pathology, Research and Practice*, vol. 207, no. 2, pp. 111–115, 2011.

[21] K. Bräutigam, J. Biernath-Wüpping, D. O. Bauerschlag et al., "Combined treatment with TRAIL and PPARγ ligands overcomes chemoresistance of ovarian cancer cell lines," *Journal of Cancer Research and Clinical Oncology*, vol. 137, no. 5, pp. 875–886, 2011.

[22] P. E. Almeida, A. B. Carneiro, A. R. Silva, and P. T. Bozza, "PPARγ Expression and Function in Mycobacterial Infection: Roles in Lipid Metabolism, Immunity, and Bacterial Killing," *PPAR Research*, vol. 2012, 383827 pages, 2012.

[23] J. Meng, Y. Ding, A. Shen et al., "Overexpression of PPARγ can down-regulate Skp2 expression in MDA-MB-231 breast tumor cells," *Molecular and Cellular Biochemistry*, vol. 345, no. 1-2, pp. 171–180, 2010.

[24] D. Zhao, Z. Zhu, D. Li, R. Xu, T. Wang, and K. Liu, "Pioglitazone Suppresses CXCR7 Expression To Inhibit Human Macrophage Chemotaxis through Peroxisome Proliferator-Activated Receptor γ," *Biochemistry*, vol. 54, no. 45, pp. 6806–6814, 2015.

[25] Y. F. Zhang, H. M. Xu, F. Yu et al., "Crosstalk between MicroRNAs and Peroxisome Proliferator-Activated Receptors and Their Emerging Regulatory Roles in Cardiovascular Pathophysiology," *PPAR Research*, vol. 2018, Article ID 8530371, 11 pages, 2018.

[26] R. Yasmeen, J. M. Meyers, C. E. Alvarez et al., "Aldehyde dehydrogenase-1a1 induces oncogene suppressor genes in B cell populations," *Biochimica et Biophysica Acta (BBA) - Molecular Cell Research*, vol. 1833, no. 12, pp. 3218–3227, 2013.

[27] V. Costa, M. A. Gallo, F. Letizia, M. Aprile, A. Casamassimi, and A. Ciccodicola, "PPARG: Gene Expression Regulation and Next-Generation Sequencing for Unsolved Issues," *PPAR Research*, vol. 2010, Article ID 409168, 17 pages, 2010.

[28] X. Zhu, Y. Chen, W. Zhu et al., "Oroxylin A inhibits Kaposi's sarcoma-associated herpes virus (KSHV) vIL-6-mediated lymphatic reprogramming of vascular endothelial cells through modulating PPARγ/Prox1 axis,," *Journal of Medical Virology*, vol. 91, no. 3, pp. 463–472, 2019.

[29] W. Ying, A. Tseng, R. C. A. Chang et al., "MicroRNA-223 is a crucial mediator of PPARγ-regulated alternative macrophage activation," *Journal of Clinical Investigation*, vol. 125, no. 11, pp. 4149–4159, 2015.

[30] B. Farrow and B. M. Evers, "Activation of PPARγ increases PTEN expression in pancreatic cancer cells," *Biochemical and Biophysical Research Communications*, vol. 301, no. 1, pp. 50–53, 2003.

[31] T. Fink, L. Abildtrup, K. Fogd et al., "Induction of adipocyte-like phenotype in human mesenchymal stem cells by hypoxia," *Stem Cells*, vol. 22, no. 7, pp. 1346–1355, 2004.

[32] J. Deng, L. Guo, and B. Wu, "Circadian Regulation of Hepatic Cytochrome P450 2a5 by Peroxisome Proliferator-Activated Receptorγ," *Drug Metabolism and Disposition*, vol. 46, no. 11, pp. 1538–1545, 2018.

[33] H. S. Kim, Y. C. Hwang, S. H. Koo et al., "PPAR-γ activation increases insulin secretion through the up-regulation of the free fatty acid receptor GPR40 in pancreatic β-cells," *PLoS One*, vol. 8, no. 1, article e50128, 2013.

[34] P. Luo, Q. Wang, Y. Ye et al., "MiR-223-3p functions as a tumor suppressor in lung squamous cell carcinoma by miR-223-3p-mutant p53 regulatory feedback loop," *Journal of Experimental & Clinical Cancer Research*, vol. 38, no. 1, p. 74, 2019.

[35] R. D. Jolly, K. G. Thompson, and B. G. Winchester, "Bovine mannosidosis–a model lysosomal storage disease," *Bovine mannosidosis–a model lysosomal storage disease*, vol. 11, no. 6, pp. 273–278, 1975.

[36] S. Yao, S. S. Dong, J. M. Ding et al., "Sex-specific SNP-SNP interaction analyses within topologically associated domains reveals ANGPT1 as a novel tumor suppressor gene for lung cancer," *Genes Chromosomes Cancer*, vol. 59, no. 1, pp. 13–22, 2019.

[37] H. Hosono, M. Kumondai, T. Arai et al., "CYP2A6 genetic polymorphism is associated with decreased susceptibility to squamous cell lung cancer in Japanese smokers," *Drug Metabolism and Pharmacokinetics*, vol. 30, no. 4, pp. 263–268, 2015.

[38] L. Tang, J. Liu, L. Zhu et al., "Curcumin Inhibits Growth of Human NCI-H292 Lung Squamous Cell Carcinoma Cells by Increasing FOXA2 Expression," *Frontiers in Pharmacology*, vol. 9, p. 60, 2018.

[39] W. H. McBride, K. S. Iwamoto, R. Syljuasen, M. Pervan, and F. Pajonk, "The role of the ubiquitin/proteasome system in cellular responses to radiation," *Oncogene*, vol. 22, no. 37, pp. 5755–5773, 2003.

[40] Y. Tang, Y. Geng, J. Luo et al., "Downregulation of ubiquitin inhibits the proliferation and radioresistance of non-small cell lung cancer cells _in vitro_ and _in vivo_," *Scientific Reports*, vol. 5, no. 1, p. 9476, 2015.

[41] S. T. Wang, H. J. Ho, J. T. Lin, J. J. Shieh, and C. Y. Wu, "Simvastatin-induced cell cycle arrest through inhibition of STAT3/SKP2 axis and activation of AMPK to promote p27 and p21 accumulation in hepatocellular carcinoma cells," *Cell Death Disease*, vol. 8, no. 2, p. e2626, 2017.

[42] J. Ji, T. F. Xue, X. D. Guo et al., "Antagonizing peroxisome proliferator-activated receptor γ facilitates M1-to-M2 shift of microglia by enhancing autophagy via the LKB1-AMPK signaling pathway," *Aging Cell*, vol. 17, no. 4, p. e12774, 2018.

[43] C. Xu, C. M. Fillmore, S. Koyama et al., "Loss of Lkb1 and Pten leads to lung squamous cell carcinoma with elevated PD-L1 expression," *Cancer Cell*, vol. 25, no. 5, pp. 590–604, 2014.

[44] T. E. Cullingford, "The ketogenic diet; fatty acids, fatty acid-activated receptors and neurological disorders," *Prostaglandins, Leukotrienes, and Essential Fatty Acids*, vol. 70, no. 3, pp. 253–264, 2004.

[45] A. Vallée, B. L. Lévy, and J. Blacher, "Interplay between the renin-angiotensin system, the canonical WNT/β-catenin pathway and PPARγ in hypertension," *Current Hypertension Reports*, vol. 20, no. 7, p. 62, 2018.

[46] W. A. Hsueh and R. Law, "The central role of fat and effect of peroxisome proliferator-activated receptor–γ on progression of insulin resistance and cardiovascular disease," *The American Journal of Cardiology*, vol. 92, no. 4A, pp. 3J–9J, 2003.

Hindawi
PPAR Research
Volume 2020, Article ID 6287468, 7 pages
https://doi.org/10.1155/2020/6287468

Research Article

PPARG Drives Molecular Networks as an Inhibitor for the Pathologic Development and Progression of Lung Adenocarcinoma

Min Zhao,[1,2] Xiaoyang Li,[3,4] Yunxiang Zhang,[3,4] Hongming Zhu,[3,4] Zhaoqing Han,[5] and Yan Kang[6]

[1]*School of Life Sciences and Biotechnology, Shanghai Jiao Tong University, Shanghai, China*
[2]*State Key Laboratory of Medical Genomics Ruijin Hospital, Shanghai Jiao Tong University School of Medicine, Shanghai, China*
[3]*Shanghai Institute of Hematology, Ruijin Hospital Affiliated to Shanghai Jiao Tong University School of Medicine, Shanghai, China*
[4]*Department of Hematology, Ruijin Hospital Affiliated to Shanghai Jiao Tong University School of Medicine, Shanghai, China*
[5]*Department of Respiratory Medicine, Shanghai Ninth People's Hospital, Shanghai Jiao Tong University School of Medicine, Shanghai, China*
[6]*Department of General Surgery, Children's National Medical Center, Washington, DC, USA*

Correspondence should be addressed to Zhaoqing Han; zhaoqinghan19@gousinfo.com

Received 28 January 2020; Accepted 25 March 2020; Published 26 April 2020

Guest Editor: Anastasia Nesterova

Previous studies showed that low PPARG expression was associated with poor prognosis of lung adenocarcinoma (LA) with limited mechanisms identified. We first conducted a large-scale literature-based data mining to identify potential molecular pathways where PPARG could exert influence on the pathological development of LA. Then a mega-analysis using 13 independent LA expression datasets and a Pathway Enrichment Analysis (PEA) was conducted to study the gene expression levels and the functionalities of PPARG and the PPARG-driven triggers within the molecular pathways. Finally, a protein-protein interaction (PPI) network was established to reveal the functional connection between PPARG and its driven molecules. We identified 25 PPARG-driven molecule triggers forming multiple LA-regulatory pathways. Mega-analysis using 13 LA datasets supported these pathways and confirmed the downregulation of PPARG in the case of LA ($p = 1.07e^{-05}$). Results from the PEA and PPI analysis suggested that PPARG might inhibit the development of LA through the regulation of tumor cell proliferation and transmission-related molecules, including an LA tumor cell suppressor MIR145. Our results suggested that increased expression of PPARG could drive multiple molecular triggers against the pathologic development and prognosis of LA, indicating PPARG as a valuable therapeutic target for LA treatment.

1. Introduction

Lung adenocarcinoma is one of the most common histological subtypes of Nonsmall-cell lung carcinoma that accounts for about 85% of all cases of lung cancer worldwide [1]. The overall 5-year survival rate of lung cancer is low even after surgical treatment (about 69.6%) [2]. Therefore, more effective strategies of therapy are necessary.

Locating on chromosome 3 (base pairs 12,287,485 to 12,434,356), PPARG encodes a member of the peroxisome proliferator-activated receptor (PPAR) subfamily of nuclear receptors—Peroxisome proliferator-activated receptor γ (PPARγ), which have been shown to possesses an antagonistic function against LA (PMID: 22843091). However, so far, limited knowledge of this PPARG-inhibiting-LA mechanism is known [3]. On the one hand, it has been shown that the expression of PPARG was reduced in LA progression cells [4], and the low PPARG expression was strictly correlated with poor prognosis of stage IA LA [3]. On the other hand, increased expression of PPARG has been positively associated with a better survival rate of LA patients [4]. Ni et al.'s work showed that overexpression of PPARγ could inhibit

the drug resistance effect of gefitinib in the treatment of LA by reducing the proliferation of gefitinib-resistant cells [4]. Susaki et al. showed that PPARG could inhibit the tumorigenic potential of NR0B1 in LA [3]. However, more studies are needed to identify the underlying mechanism of the role that PPARG plays in the pathological development of LA.

To dissect the role of PPARG in LA at the genetic level, we employed Pathway Studio (http://www.pathwaystudio.com) knowledge database to undertake large-scale literature mining effort and integrated its results with an analysis of multiple LA expression datasets. We identified a set of PPARG-driven molecular triggers, possibly contributing to inhibition of the development of LA through a quantitative regulation. Our results might add new insights into the understanding of the LA-inhibition role of PPARG.

2. Materials and Method

This study is organized as follows. First, a large-scale literature-based data mining was performed to identify genes as the disease markers and the regulators of LA. Subsequently, regulations of PPARG on these LA genes were identified under the Pathway Studio environment. After that, a mega-analysis was performed using 13 independent LA gene expression datasets to test the expression changes of PPARG and the LA genes that were regulated by PPARG. Finally, a Pathway Enrichment Analysis (PEA) has been conducted to explore the functionality of the PPARG-driven molecular triggers, with protein-protein interaction (PPI) network built. All data and analysis results were organized in an excel file named as PPARG_LA, which is downloadable at http://www.gousinfo.com/database/Data_Genetic/PPARG_LA.xlsx.

2.1. Literature-Based Pathway Analysis. Assisted by using Pathway Studio (http://www.pathwaystudio.com), we conducted a large-scale literature-based functional pathway analysis to investigate the potential biological associations between PPARG and LA. Specifically, we identified the genes influenced by PPARG and also regulating LA to build the connections between PPARG and LA. Only relationships with polarity were selected within the Pathway Studio database. Each and all of the relations identified were supported by one or more references (1255 references in total; please refer to the worksheet "PPARG-LA Regulation Pathway" within the file PPARG_LA). In the PPARG_LA→PPARG-LA Regulation Pathway, the reference information supporting the relations identified in the PPARG-LA regulatory pathways was provided, including the types of associations, the number of underlying supporting references, and the sentences where these associations had been identified and described. The expression changes of PPARG and its driven genes involved in the pathways were tested using a mega-analysis approach described as follows.

2.2. Gene Expression Data Selected for Mega-Analysis. Following the initial search with "Lung adenocarcinoma", 634 microarray expression datasets were identified on gene expression omnibus (GEO; https://www.ncbi.nlm.nih.gov/geo/) [5]. Subsequently, the following criteria were applied: (1) the organism used in the study was *Homo sapiens*; (2) the data type was microarray expression profiling; (3) the studies were limited to a comparison between LA and healthy controls; and (4) the original data and the corresponding format file were downloadable. A total of 13 datasets satisfied the inclusion criteria for the mega-analysis, which are listed in Table 1.

2.3. Mega-Analysis Models. For PPARG and the 25 genes involved in the PPARG-LA regulatory pathway, the log2 fold-change (LFC) of the gene expression level was used to indicate the effect size. Both fixed-effects and random-effects models were employed to investigate and compare the effect size (doi:10.1002/jrsm.12). The heterogeneity of the mega-analysis was analyzed to study the variance within and between different studies. In the case that the total variance (Q) was equal to or smaller than the expected between-study variance (df), the $\text{within-study variance percentage (ISq)} = 100\% \times (Q - df)/Q$ was set at 0, and a fixed-effects model was selected for the mega-analysis. Otherwise, a random-effects model was selected. Q-p represents the probability that the total variance was only due to within-study variance. The current study presented all the mega-analysis results in the worksheet "mega-analysis" of the excel file PPARG_LA (http://www.gousinfo.com/database/Data_Genetic/PPARG_LA). The full name and description of related stats were given within "mega-analysis." All analyses were performed using Matlab (version R2017a; https://www.mathworks.com/products/matlab.html). Here, we used the term "mega-analysis" instead of "meta-analysis" to reflect that the LFC of each gene was calculated from the original data instead of results within publications.

2.4. Multiple Linear Regression Analysis. A multiple linear regression (MLR) model was employed to investigate the possible influence of sample size, country of origin, and study date on the gene expression in the case of LA. p values were reported for each of these factors.

2.5. Pathway Enrichment Analysis and Protein-Protein Interaction Analysis. To test the functional profile of the genes involved in the PPARG-LA regulation pathway, a Fisher's Exact Test based pathway enrichment analysis (PEA; Pathway Studio: Find Pathways/Groups Enriched with Selected Entities) was conducted using Pathway Studio (version 12.1.0.9; http://www.pathwaystudio.com) against Gene Ontology (GO; http://geneontology.org) and Pathway Studio pathways. Statistics for the enriched pathways were provided, including false discovery rate (FDR) corrected p-value and Jaccard similarity.

Moreover, based on the PEA results, a protein-protein interaction (PPI) network was constructed. Two genes were recognized as connected if they were identified to play roles within at least one common pathway (from Pathway Studio Pathway Collection) or functional group (from GO groups).

3. Results

3.1. PPARG-LA Contradirectional Common Targets. Pathway analysis has identified multiple molecules that were

Table 1: The 13 LA expression datasets employed for mega-analysis.

Dataset GEO ID	Control (n)	Case (n)	Country	Study age	Sample Organism
GSE2088	30	9	Japan	11	Homo sapiens
GSE7670	28	27	Taiwan	13	Homo sapiens
GSE10072	49	58	USA	12	Homo sapiens
GSE31547	20	30	USA	9	Homo sapiens
GSE32863	58	58	USA	8	Homo sapiens
GSE32867	58	58	USA	8	Homo sapiens
GSE40791	90	94	USA	7	Homo sapiens
GSE43458	30	80	USA	7	Homo sapiens
GSE46539	92	92	Taiwan	4	Homo sapiens
GSE51852	4	49	Japan	6	Homo sapiens
GSE63459	32	33	USA	5	Homo sapiens
GSE68465	4	443	USA	5	Homo sapiens
GSE118370	6	6	China	1	Homo sapiens

contradirectionally influenced by PPARG and LA, as shown in Figure 1. The expression levels of these genes, including PPARG, were tested in the mega-analysis and color-coded with the literature-based pathway (see the color bar in Figure 1).

According to previous literature reports, a total of 13 molecules upregulated in LA were negatively affected by PPARG (genes highlighted in red), and a total of six molecules suppressed in LA were stimulated by PPARG (genes highlighted in blue). The detailed information regarding the network presented in Figure 1 can be found in PPARG_LA⟶PPARG-LA Regulation Pathway with each network-related entry, including the type of the relationship, supporting references, and related sentences from the references where the relationship has been identified.

To note, five LA-unregulated genes presented increased expression levels in the mega-analysis using 13 LA datasets, including COL1A1, SPP1, CXCL14, MMP9, and CCNB1. The depression of these genes by PPARG could exert an anti-LA effect during its pathological development. On the other hand, four out of six LA-suppressed genes presented decreased expression levels in the mega-analysis, including three genes (CAV1, PTEN, and FAS) and one microRNA (MIR145). The activation of these molecules could be other pathways where PPARG inhibits the progress of LA.

Notably, PPARG presented a decreased expression level (p value = 1.07e-05, LFC = −0.48). This was consistent with previous studies [4]. Heterogeneity analysis showed that there was no significant between-study variance of PPARG expression levels (ISq = 0). Therefore, the fixed-effects model was used for the mega-analysis of PPARG. Moreover, MLR analysis suggested that none of the three parameters (sample size, country of origin, and study date) was a significant influence factor for the PPARG expression changes (p value > 0.070). For detailed info of the mega-analysis results of PPARG and other molecules, please refer to PPARG_LA⟶Mega-analysis.

3.2. PPARG-LA Regulation Pathway. We also identified a regulatory pathway through which PPARG may bar the pathological development of LA, as shown in Figure 2. According to literature reports, there were seven LA promoters (highlighted in red in Figure 2) deactivated by PPARG. Out of these molecular triggers, two genes presented increased expression levels in LA patients according to the mega-analysis results, including CCR7 and TLR2.

Literature data mining also revealed three LA inhibitors that could be activated by PPARG (see Figure 2; highlighted in blue). Only one of them, MIR145, presented a decreased expression level in the case of LA according to the results of mega-analysis, which was consistent with the negative-regulation relationship between LA and MIR145 that has been identified in literature data mining (see Figure 1). For more detailed information regarding the network presented in Figure 2, please refer to PPARG_LA⟶PPARG-LA Regulation Pathway.

3.3. PEA Results and PPI Network. To investigate the biological functions of the 26 genes within the PPARG-LA regulatory pathways (Figures 1 and 2), a pathway enrichment analysis was executed by using Pathway Studio. A total of 24 out of these 26 genes were shared among the top 10 most significantly enriched pathways (p value < $1.40e^{-14}$, $q = 0.05$ for FDR), which are presented in Table 2. The full 115 pathways and GO terms enriched with p value < $1.00e^{-6}$, which encompassed all 26 genes, were presented in PPARG_LA⟶PEA. Notably, a majority of the shared pathways highlighted by the PEA approach were related to cell proliferation and cell migration, which were implicated with LA.

Based on the significantly enriched pathways identified from PEA, a PPI network has been constructed, as shown in Figure 3 The number between two entities is the number of shared pathways out of the 115 pathways from PEA results. Please note that most of the molecules paly roles with all other molecules, suggesting the shared functionality of these molecules. Specifically, PPARG plays a role within 52 pathways and connecting with other molecules through 23.03 ± 12.90 pathways on average. This supports the literature-based relationship presented in the PPARG-LA regulatory pathways (Figures 1 and 2).

4. Discussion

In this study, we aimed at exploring the possible genetic mechanisms of the linkage between PPARG and better survival in LA. First, we conducted a large-scale literature-based data mining to construct functional PPARG-LA regulatory pathways (Figures 1 and 2). The 25 genes within these literature-based pathways were identified as connected to both PPARG and LA with polarity. Then, PEA was conducted to study the pathological functions of these 25 genes. After that, an LA expression data-based mega-analysis was performed to explore the expression levels of these 25 genes in the case of LA. Our results showed that PPARG could exert influence on both the development and progression of LA, which may add new insights into the understanding of

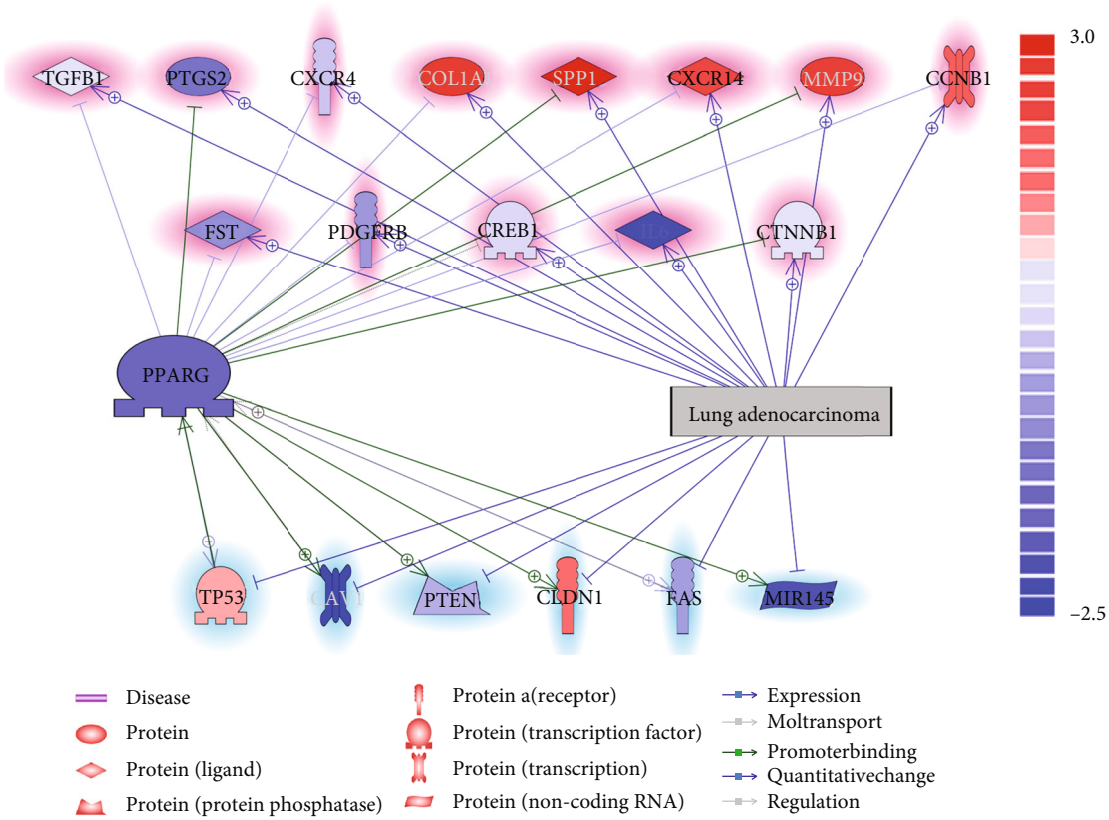

Figure 1: Contradirectional common targets of PPARG and lung adenocarcinoma according to literature that was also tested using expression data. Entities in blue represent a decreased expression level from the mega-analysis using 13 LA datasets; entities in red represent an increased expression level. Entities highlighted in blue (genes at the bottom of the figure) were literature implicated with a downregulation in the case of LA; highlighted in red (genes at the top of the figure) means they were upregulated. The polarity of the relationships was denoted as "-|" for negative effects and "-+>" for positive effects.

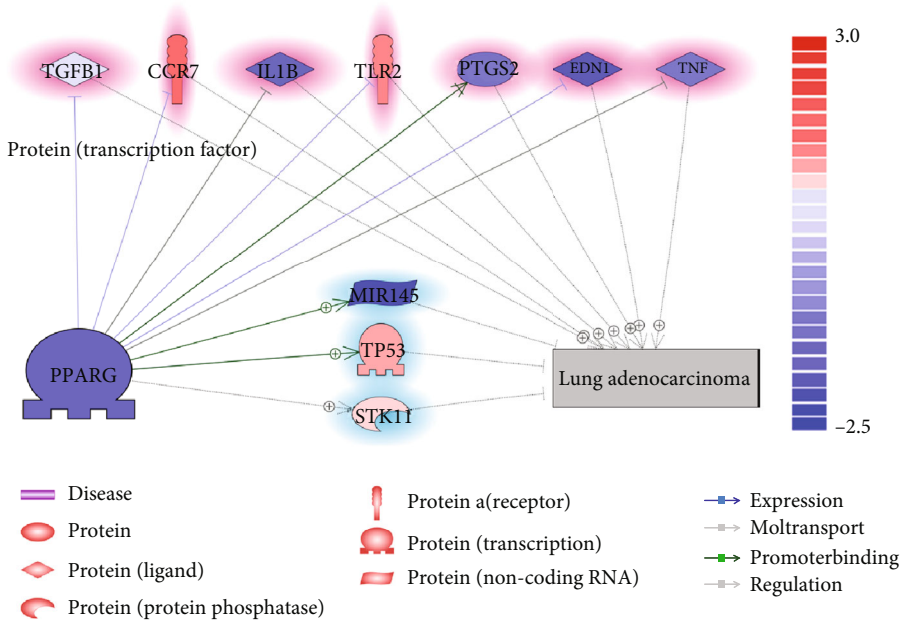

Figure 2: PPARG-LA regulatory pathways based on literature also tested by using expression data. Entities in blue represent a decreased expression level from the mega-analysis using 13 LA datasets; entities in red represent an increased expression level. Entities highlighted in blue (genes at the bottom of the figure) were literature implicated as an LA-inhibitor; highlighted in red (genes at the top of the figure) means they were LA promoter. The polarity of the relationships was denoted as "-|" for negative effects and "-+>" for positive effects.

Table 2: The top 10 genetic pathways enriched with 26 genes with the PPARG-LA regulatory pathways.

Name	GO ID	# of entities	Overlap	*p* value	Jaccard similarity
GO: response to oxygen levels	0070482	544	17	3.48*e*-18	0.031
GO: response to mechanical stimulus	0009612	334	14	2.46*e*-16	0.040
GO: response to inorganic substance	0010035	803	17	5.15*e*-16	0.021
GO: response to acid chemical	0001101	662	16	1.06*e*-15	0.024
GO: response to peptide	1901652	553	15	3.2*e*-15	0.027
GO: regulation of smooth muscle cell proliferation	0048660	215	12	3.62*e*-15	0.052
GO: response to hypoxia	0001666	424	14	3.85*e*-15	0.032
GO: positive regulation of cell migration	0030335	603	15	8.92*e*-15	0.024
GO: response to decreased oxygen levels	0036293	461	14	9.11*e*-15	0.030
GO: positive regulation of cell motility	2000147	630	15	1.4*e*-14	0.023

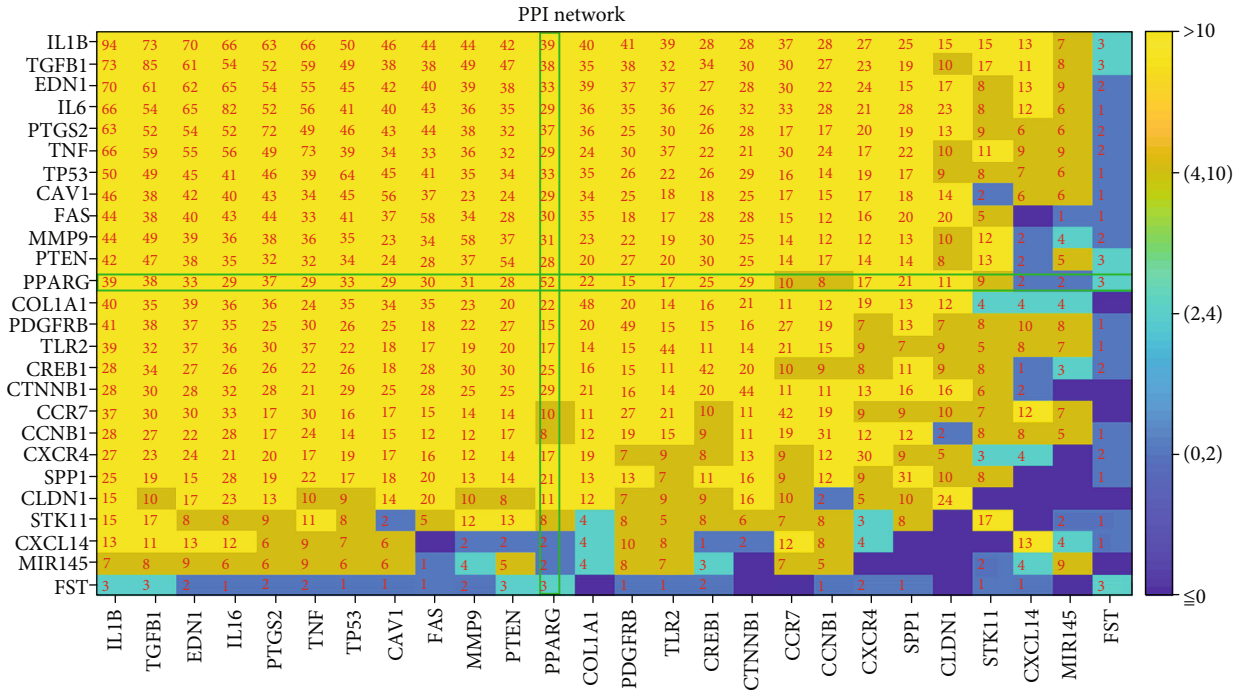

Figure 3: Protein-protein interaction networks among the 26 molecules involved in PPARG-LA regulatory pathways. The numbers between the two molecules are the number of pathways they shared out of the 115 pathways enriched by the 26 molecules.

the PPARG-LA association. We provided detailed descriptions of the PPARG-LA regulatory pathways as follows.

There were 19 molecules that have been identified as common targets but were contradirectionally regulated by PPARG and LA. These molecules have been reported to present altered expression levels in case of LA, and part of them (eight proteins and one microRNA) have been confirmed from the mega-analysis using 13 LA datasets employed in this study (please see Figure 1, the entities with body color matched with the highlighting color). With both literature and experimental data support, the pathways constructed with these molecules have high potential to be the PPARG→LA regulating channel. Specifically, the expression levels of five LA markers (i.e., COL1A1, SPP1, CXCL14, MMP9, and CCNB1) were significantly unregulated in LA patients [6–10], which were confirmed in the mega-analysis in this study. PPARG has been shown to inhibit hepatic stellate cell proliferation and COL1A1 expression in vitro and in vivo [11]. Similarly, the expressions of SPP1, CXCL14, MMP9, and CCNB1 have also been negatively regulated by PPARG [12–15]. On the other hand, PPARG could stimulate multiple molecules that inhibited by LA, including CAV1, PTEN, FAS, and MIR145. More descriptions of these PPARG regulations were provided in PPARG_LA→PPARG-LA Regulation Pathway. These pathways might partially explain the mechanisms of the development-blocking effect of PPARG on LA.

Moreover, PPARG has been shown to play roles in the prognostic pathway of LA (Figure 2). Both the literature data mining and the mega-analysis results support the

suppression of four LA promoters (IL1B, PTGS2, END1, and TNF) and stimulation of one LA inhibitors, MIR145. As an LA tumor cell suppressor [16], MIR145 was found to be involved in multiple other types of cancers, including breast cancer [17], colon cancer [18], and acute myeloid leukemia [19]. However, as shown in Figure 1, in the case of LA, the expression levels of MIR145 will be downregulated, which also got confirmed from the 13-LA-datasets mega-analysis (see PPARG_LA→Mega-analysis). PPARG could activate the expression of MIR145 by directly binding to a PPAR response element in its promoter at 1207/-1194 bp from the transcription start site [20], which could be an important mechanism underlying the LA inhibition effect of PPARG.

PEA results indicated that each of the 25 PPARG-driven molecular triggers has at least two functional pathways shared with PPARG (see Figure 3). Most of these pathways were linked to cell proliferation, cell migration, and motility, indicating that PPARG may influence the LA development and progression through the cell metabolism and motivation pathways, which are important in the etiology of LA [21]. More interestingly, we see that PPARG was enriched in all top six pathways (see Table 2). These results support the functional association between PPARG and the 25 molecular triggers identified from the literature data mining (PPARG_LA→PPARG-LA Regulation Pathway).

To note, the expression of PPARG has been downregulated in LA, which is consistent with previous findings [4]. Therefore, our results suggest that the activation of PPARG could be a valid therapeutic strategy for the treatment of LA.

One of the limitations of this study was that the PPARG-driven LA pathways built only explored the genes connecting PPARG and LA. There could be more "bridge items" (e.g., functional class and compounds) to reveal more mechanisms underlying the PPARG_LA relation.

5. Conclusion

This study confirmed the downregulation of PPARG in the case of LA and revealed multiple pathways through which PPARG could play roles as a LA blocker. Our results shed light on the understanding of the PPARG-LA association, suggesting PPARG as a valuable therapeutic target for the treatment of LA.

Data Availability

The data in our study are available from the corresponding author upon reasonable request. The supplementary data and results were available at http://www.gousinfo.com/database/Data_Genetic/PPARG_LA.

Conflicts of Interest

The authors declare that there is no conflict of interest regarding the publication of this paper.

Authors' Contributions

Min Zhao, Xiaoyang Li, and Yunxiang Zhang contributed equally to this work.

References

[1] J. Ansari, R. E. Shackelford, and H. El-Osta, "Epigenetics in non-small cell lung cancer: from basics to therapeutics," *Translational Lung Cancer Research*, vol. 5, no. 2, pp. 155–171, 2016.

[2] N. Sawabata, E. Miyaoka, H. Asamura et al., "Japanese lung cancer registry study of 11,663 surgical cases in 2004: demographic and prognosis changes over decade," *Journal of Thoracic Oncology*, vol. 6, no. 7, pp. 1229–1235, 2011.

[3] Y. Susaki, M. Inoue, M. Minami et al., "Inhibitory effect of PPARγ on NR0B1 in tumorigenesis of lung adenocarcinoma," *International Journal of Oncology*, vol. 41, no. 4, pp. 1278–1284, 2012.

[4] J. Ni, L. L. Zhou, L. Ding et al., "PPARγ agonist efatutazone and gefitinib synergistically inhibit the proliferation of EGFR-TKI-resistant lung adenocarcinoma cells via the PPARγ/PTEN/Akt pathway," *Experimental Cell Research*, vol. 361, no. 2, pp. 246–256, 2017.

[5] R. Edgar, M. Domrachev, and A. E. Lash, "Gene Expression Omnibus: NCBI gene expression and hybridization array data repository," *Nucleic Acids Research*, vol. 30, no. 1, pp. 207–210, 2002.

[6] Y. Zhang, B. Chen, Y. Wang et al., "NOTCH3 overexpression and posttranscriptional regulation by miR-150 were associated with EGFR-TKI resistance in lung adenocarcinoma," *Oncology Research Featuring Preclinical and Clinical Cancer Therapeutics*, vol. 27, no. 7, pp. 751–761, 2019.

[7] H. M. Fathallah-Shaykh, M. Rigen, L. J. Zhao et al., "Mathematical modeling of noise and discovery of genetic expression classes in gliomas," *Oncogene*, vol. 21, no. 47, article BF1205654, pp. 7164–7174, 2002.

[8] R. Shaykhiev, R. Sackrowitz, T. Fukui et al., "Smoking-induced CXCL14 expression in the human airway epithelium links chronic obstructive pulmonary disease to lung cancer," *American Journal of Respiratory Cell and Molecular Biology*, vol. 49, no. 3, pp. 418–425, 2013.

[9] Y. L. Wen and L. Li, "Correlation between matrix metalloproteinase-9 and vascular endothelial growth factor expression in lung adenocarcinoma," *Genetics and Molecular Research*, vol. 14, no. 4, pp. 19342–19348, 2013.

[10] T. Wang, X. B. Yan, J. J. Zhao et al., "Gene associated with retinoid-interferon-induced mortality-19 suppresses growth of lung adenocarcinoma tumor in vitro and in vivo," *Lung Cancer*, vol. 72, no. 3, pp. 287–293, 2011.

[11] S. Zheng and A. Chen, "Disruption of transforming growth factor-beta signaling by curcumin induces gene expression of peroxisome proliferator-activated receptor-gamma in rat hepatic stellate cells," *American Journal of Physiology-Gastrointestinal and Liver Physiology*, vol. 292, no. 1, pp. G113–G123, 2007.

[12] M. Shan, R. You, X. Yuan et al., "Agonistic induction of PPARγ reverses cigarette smoke-induced emphysema," *Journal of Clinical Investigation*, vol. 124, no. 3, pp. 1371–1381, 2014.

[13] M. Takahashi, Y. Takahashi, K. Takahashi et al., "CXCL14 enhances insulin-dependent glucose uptake in adipocytes

and is related to high-fat diet-induced obesity," *Biophysical Research Communications*, vol. 364, no. 4, pp. 1037–1042, 2007.

[14] E. L. Schiffrin, "Peroxisome proliferator-activated receptors and cardiovascular remodeling," *American Journal of Physiology-Heart and Circulatory Physiology*, vol. 288, no. 3, pp. H1037–H1043, 2005.

[15] J. Wan, Z. Xiao, S. Chao et al., "Pioglitazone modulates the proliferation and apoptosis of vascular smooth muscle cells via peroxisome proliferators-activated receptor-gamma," *Diabetology & Metabolic Syndrome*, vol. 6, no. 1, p. 101, 2014.

[16] Y. F. Chang, K. H. Lim, Y. W. Chiang et al., "STAT3 induces G9a to exacerbate HER3 expression for the survival of epidermal growth factor receptor-tyrosine kinase inhibitors in lung cancers," *BMC Cancer*, vol. 19, no. 1, article 6217, p. 959, 2019.

[17] M. Götte, C. Mohr, C. Y. Koo et al., "miR-145-dependent targeting of junctional adhesion molecule A and modulation of fascin expression are associated with reduced breast cancer cell motility and invasiveness," *Oncogene*, vol. 29, no. 50, pp. 6569–6580, 2010.

[18] J. Zhang, H. Guo, H. Zhang et al., "Putative tumor suppressor miR-145 inhibits colon cancer cell growth by targeting oncogene friend leukemia virus integration 1 gene," *Cancer*, vol. 117, no. 1, pp. 86–95, 2011.

[19] D. T. Starczynowski, R. Morin, A. McPherson et al., "Genome-wide identification of human microRNAs located in leukemia-associated genomic alterations," *Blood*, vol. 117, no. 2, pp. 595–607, 2011.

[20] A. V. Das and R. M. Pillai, "Implications of miR cluster 143/145 as universal anti-oncomiRs and their dysregulation during tumorigenesis," *Cancer Cell International*, vol. 15, no. 1, p. 92, 2015.

[21] Z. Li, J. Xia, M. Fang, and Y. Xu, "Epigenetic regulation of lung cancer cell proliferation and migration by the chromatin remodeling protein BRG1," *Oncogenesis*, vol. 8, no. 11, p. 66, 2019.

Hindawi
PPAR Research
Volume 2020, Article ID 6452182, 6 pages
https://doi.org/10.1155/2020/6452182

Research Article

Pparg may Promote Chemosensitivity of Hypopharyngeal Squamous Cell Carcinoma

Meng Lian, Jiaming Chen, Xixi Shen, Lizhen Hou, and Jugao Fang

Department of Otorhinolaryngology Head and Neck Surgery, Beijing Tongren Hospital, Capital Medical University, Beijing 100730, China

Correspondence should be addressed to Jugao Fang; fangjugao@gousinfo.com

Received 1 February 2020; Accepted 1 April 2020; Published 21 April 2020

Guest Editor: Hongbao Cao

The upregulation of peroxisome proliferator-activated receptor gamma (*PPARG*) has been shown to increase the chemosensitivity of several human cancers. This study is aimed at studying if *PPARG* sensitizes hypopharyngeal squamous cell carcinoma (HSCC) in chemotherapeutic treatments and at dissecting possible mechanisms of observed effects. We integrated large-scale literature data and HSCC gene expression data to identify regulatory pathways that link *PPARG* and chemosensitivity in HSCC. Expression levels of molecules within the *PPARG* regulatory pathways were compared in 21 patients that underwent chemotherapy for primary HSCC, including 12 chemotherapy-sensitive patients (CSP) and 9 chemotherapy-nonsensitive patients (CNSP). In the CPS group, expression levels of *PPARG* were higher than that in the CNSP group (log-fold-change = 0.50). Structured text mining identified two chemosensitivity-related regulatory pathways driven by *PPARG*. In the CSP group, expression levels for 7 chemosensitivity-promoting genes were increased, while for 13 chemosensitivity suppressing the gene expression levels were decreased. Our results support the chemosensitivity-promoting role of *PPARG* in HSCC tumor cells, most likely by affecting both cell proliferation and cell motility pathways.

1. Introduction

As one of the most common head and neck tumors, hypopharyngeal squamous cell carcinoma (HSCC) accounts for more than 160,000 new cases and 83,000 deaths annually [1]. In Europe and the United States, HSCC has been ranked as one of the most common human malignancies [2]. High risks of metastasis to cervical lymph nodes and a lack of evident clinical symptoms make it a challenge for the diagnosis and treatment of HSCC [3]. Novel therapies for HSCC are warranted.

PPARG gene encodes a member of the peroxisome proliferator-activated receptor (PPAR) subfamily of nuclear receptors. Several previous studies suggested that the upregulation of *PPARG* might induce chemosensitivity in human carcinomas [4–6]. In particular, in human nonsmall-cell lung carcinoma cells, the activation of PPARγ is capable of overcoming the NRF2-dependent chemoresistance [4]. In basal-like breast carcinoma, *PPARG* activation significantly reduces the expression of MnSOD and increases chemosensitivity [5]. In turn, the silencing of *PPARG* decreases the chemosensitivity of pancreatic cancer cells in vitro [6]. So far, the involvement of PPARG was explored in some but not other squamous cell carcinoma with location in the head or neck, with the emphasis being made on oral cancer. For example, in cell lines of oral carcinoma origin, the treatment with a synthetic retinoid, 4-hydroxyphenylretinamide was shown to result in an increase of HSCC chemosensitivity [7]. PPARG has been suggested as a target for chemoprevention in head and neck cancer prevention, which was based on consistent evidence from investigations of human tumor cell line studies, epidemiological analysis, and animal carcinogenesis models [8]. PPARG has also been suggested as a potential therapeutic target gene for oral squamous cell carcinoma [9], and the activation of PPARG was shown to downregulate several features of the neoplastic phenotype in human upper aerodigestive tract tumors [10].

In this study, we hypothesize that PPARG may play roles in HSCC chemotherapy by influencing the tumor cell chemosensitivity. To test this hypothesis, we collected

expression profiles from primary HSCC patients that underwent chemotherapy and tested the PPARG expression variations between chemotherapy-sensitive patients (CSP) and chemotherapy-nonsensitive patient (CNSP) groups. Then, we used large-scale literature data mining to identify molecular pathways that are driven by PPARG to influence the chemotherapeutical activities within the HSCC patients. Our results suggested that the increased expression of PPARG might promote the chemosensitivity of HSCC cells through multiple molecular pathways.

2. Materials and Methods

2.1. Patient Recruit and Specimen Selection. Twenty-one HSCC patients were recruited by the Department of Head and Neck Surgery, Beijing Tongren Hospital, including 12 chemotherapy-sensitive patients (CSP) and nine chemotherapy-nonsensitive patients (CNSP). All patients received two-periodic chemotherapies induced by TPF (taxane/cisplatin/5-FU). Tissue specimens were collected from each of these patients after resection during surgery. Each sample was immediately snap-frozen in liquid nitrogen and stored at -80°C. This study has been approved by the ethics committee of Beijing Tongren Hospital, and written agreement has been acquired from each participant.

2.2. RNA Extraction, cDNA Synthesis, and In Vitro Transcription. mRNA was extracted from tissue samples using TRIzol (Invitrogen), and then, RNA quantity was examined by denaturing gel electrophoresis, which revealed at least two distinct bands representing 28S and 18S ribosomal RNA, suggesting no DNA contamination or RNA degradation. First, reverse transcription was used to synthesize the first-strand cDNA, and second-strand cDNA synthesis was used to convert single-stranded cDNA into double-stranded DNA with a PrimeScript™ Double Strand cDNA Synthesis Kit (TAKARA). Second, after purification by removing RNA, primers, enzymes, etc., the double-stranded DNA was used as a template for the transcription of biotinylated cRNA in vitro. Finally, the biotinylated cRNA was purified and prepared for hybridization with a prepared microarray.

2.3. Acquirement of mRNA Expression Profiles of HSCC. For the microarray mRNA expression profile of HSCC, the Illumina Human HT-12 Bead Chip was applied for hybridization with the labeled cRNA. There are six types of internal parameters and 887 probes in this microarray for the quality control of all samples. Briefly, the cRNA samples were hatched with the Illumina Human HT-12 Bead Chip at room temperature and subjected to high-temperature washes, ethanol washes, and three washes at room temperature. After desiccation, images were collected with the Illumina Bead Chip Reader software. Illumina Genome studio-Gene Expression software was employed to filter background noise and the missing value effect in the raw data. The quantile method was used for normalization. The gene expression profile was obtained using Illumina Custom software.

2.4. Literature-Based Pathway Analysis. Large-scale literature-based functional pathway analysis was performed to investigate potential biological associations between PPARG and chemosensitivity and constructing PPARG regulatory pathways. We first identified PPARG downstream molecular targets with polarity; then, we explored the chemosensitivity upstream positive and negative regulators. Each relationship (PPARG-gene and chemosensitivity-gene relationship) has at least one reference, which is covered by Pathway Studio (https://www.pathwaystudio.com). We provided detailed information about each relationship in PPARG_HSCC→Regulatory_Pathway1 and Regulatory_Pathway2, including the types of associations, the number of underlying supporting references, and the sentences where these associations had been identified and described.

Then, we tested that expression changes of the molecules involved in the pathway to associate it with HSCC by using HSCC expression data. The expression changes of PPARG and the 20 genes involved in the PPARG-chemosensitivity regulatory pathway were compared between CSP and CNSP groups.

2.5. Gene Set Enrichment Analysis (GSEA). To test the molecular functions of the identified PPARG driven triggers that regulate the chemosensitivity in HSCC, a GSEA was conducted for each PPARG-chemosensitivity regulatory pathway; results were reported and compared.

3. Results

3.1. PPARG Expression in CSP Group. We presented the expression of PPARG for the 12 chemotherapy-sensitive HDCC patients in Figure 1. Overall, PPARG demonstrated an average 40% increase in the CSP group (LFC = 0.50). Nine out of the 12 patients presented increased expression levels compared to the CNSP group. However, there was a significant variance among the individuals within the CSP group (std = 0.75), with three of them demonstrated expression, resulting in a nonsignificant p value = 0.25. These results suggested that PPARG might not be the only factor that influences the chemotherapy sensitivity of HDCC patients.

3.2. PPARG Stimulates Chemosensitivity Promoters. As shown in Figure 1, literature-based data mining identified seven chemosensitivity promoters that have been promoted by PPARG. The expression of these molecules, including PPARG, was upregulated in the CSP group, which supports the pathway identified from the literature knowledge database. For the 54 references supporting the pathway given in Figure 1, please refer to PPARG_HSCC⟶Regulatory_Pathway1. For the expression levels of the eight molecules in Figure 1, please refer to PPARG_HSCC⟶Expression_LFC.

To explore the functionality of the molecules included in the chemosensitivity-promoting pathway presented in Figure 1, a GSEA has been conducted using against the Gene Ontology (GO). The top 10 GO terms enriched were presented in Table 1. More detailed information of the 12 enriched GO terms passed false discovery ratio (FDR) analysis ($q = 0.05$) was presented in PPARG_HSCC⟶GSEA1. From Table 1, it can be seen that the genes were mainly related to cell proliferation and cell apoptotic, suggesting that

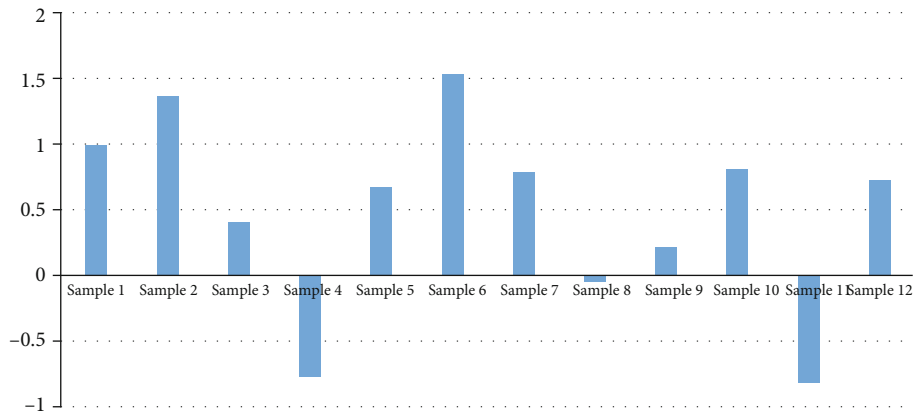

Figure 1: PPARG expression in terms of log-fold-change (LFC) in chemotherapy-sensitive patients (CSP) among each of the 12 samples.

Table 1: The top 10 GO terms enriched with the eight genes from the chemosensitivity-promoting pathway.

GO ID	Name	# of entities	Overlap	Overlapping entities	*p* value
0048662	GO: negative regulation of smooth muscle cell proliferation	82	4	PPARG; TP53; MIR145; PTEN	0.00037
0010660	GO: regulation of muscle cell apoptotic process	125	4	PPARG; TP53; MIR145; PTEN	0.0010
0090200	GO: positive regulation of release of cytochrome c from mitochondria	33	3	BAX; TNFSF10; TP53	0.0014
0030162	GO: regulation of proteolysis	997	6	PPARG; BAX; PTEN; SERPINB5; TNFSF10; TP53	0.0014
0048147	GO: negative regulation of fibroblast proliferation	40	3	BAX; PPARG; TP53	0.0020
2001235	GO: positive regulation of apoptotic signaling pathway	213	4	BAX; PTEN; TP53; TNFSF10	0.0022
0010661	GO: positive regulation of muscle cell apoptotic process	48	3	PPARG; TP53; PTEN	0.0022
0048660	GO: regulation of smooth muscle cell proliferation	215	4	PPARG; MIR145; PTEN; TP53	0.0022
0090199	GO: regulation of release of cytochrome c from mitochondria	53	3	TP53; BAX; TNFSF10	0.0024
0090403	GO: oxidative stress-induced premature senescence	4	2	TP53; ARNTL	0.0024

PPARG may promote the chemosensitivity through the regulation of cell proliferation-related pathways. To note, PPARG directly plays roles in 6 out of 10 of these GO terms.

3.3. PPARG Suppresses Chemosensitivity Inhibitors. As shown in Figure 1, literature-based data mining identified 14 chemosensitivity inhibitors that have been suppressed by PPARG. The expression of these molecules was downregulated in the CSP group, which supports the pathway identified from the literature knowledge database. For the 172 references supporting the pathway given in Figure 2, please refer to PPARG_HSCC⟶ Regulatory_Pathway2. For the expression levels of the eight molecules in Figure 2, please refer to PPARG_HSCC⟶Expression_LFC.

GSEA results showed that the GO terms enriched by the 15 genes (including PPARG) were mostly related to the regulation of cell motility and locomotion (see Table 2). The top 10 GO terms enriched were presented in Table 2. More detailed information of the 65 significantly enriched GO terms (FDR = 0.05) was presented in PPARG_HSCC⟶GSEA2. These results suggested that the promotion of the chemosensitivity by PPARG might also be through the regulation of cell motivation related pathways.

4. Discussion

PPARG has been shown to increase the chemosensitivity in several human carcinomas, including nonsmall-cell lung carcinoma, breast carcinoma, and pancreatic carcinoma [4–6]. Here, we tested the potential role of increased PPARG expression in the chemosensitivity in HSCC, integrating literature-based pathway analysis and expression data analysis. Our results showed that PPARG plays roles in both chemosensitivity-inhibiting and promoting pathways and could improve the chemosensitivity through the positive regulation of cell proliferation-related pathways and the negative regulation of cell motility-related pathways.

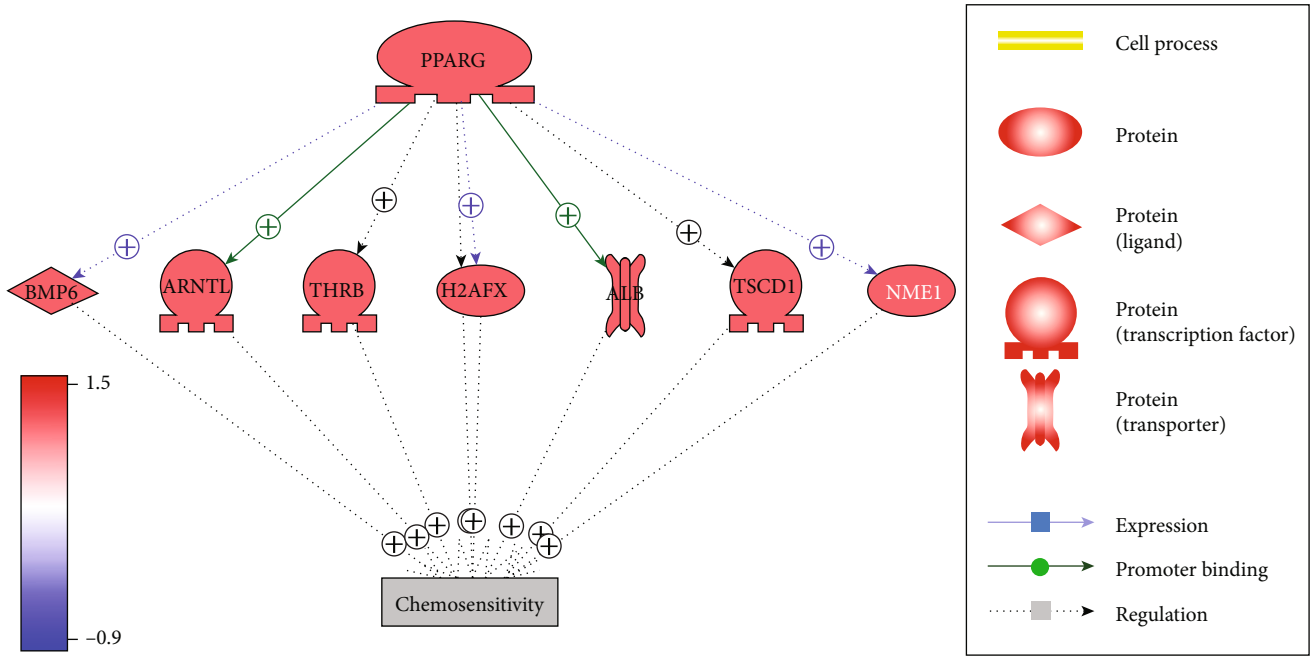

Figure 2: The chemosensitivity-promoting pathway built through literature data analysis and tested by HSCC expression data. The red color of genes represents increased expression in the chemosensitive group compared with the nonchemosensitive group.

Table 2: The top 10 GO terms enriched with the 13 genes from the chemosensitivity- inhibiting pathway.

GO ID	Name	# Of entities	Overlap	Overlapping entities	p value
2000147	GO: positive regulation of cell motility	630	9	CSF1; IGF1R; TWIST1; CCR2; RPS6KB1; EGR1; TERT; RAC1; MYC	2.37E-07
0051272	GO: positive regulation of cellular component movement	650	9	CSF1; IGF1R; TWIST1; CCR2; RPS6KB1; EGR1; TERT; RAC1; MYC	2.37E-07
0040017	GO: positive regulation of locomotion	666	9	CSF1; IGF1R; TWIST1; CCR2; RPS6KB1; EGR1; TERT; RAC1; MYC	2.37E-07
0030335	GO: positive regulation of cell migration	603	8	CSF1; IGF1R; CCR2; RPS6KB1; EGR1; TERT; RAC1; MYC	4.29E-06
0048660	GO: regulation of smooth muscle cell proliferation	215	6	IGF1R; PPARG; RPS6KB1; EGR1; TERT; MYC	1.13E-05
0071453	GO: cellular response to oxygen levels	221	6	PPARG; TWIST1; CFTR; EGR1; TERT; MYC	1.13E-05
0097305	GO: response to alcohol	460	7	PPARG; STAT3; IGF1R; RPS6KB1; CFTR; EGR1; MYC	1.69E-05
0043434	GO: response to peptide hormone	479	7	PPARG; STAT3; IGF1R; RPS6KB1; CFTR; EGR1; MYC	1.96E-05
0032870	GO: cellular response to hormone stimulus	520	7	PPARG; STAT3; IGF1R; RPS6KB1; CFTR; EGR1; MYC	3.07E-05
0048661	GO: positive regulation of smooth muscle cell proliferation	130	5	IGF1R; EGR1; TERT; MYC; RPS6KB1	3.49E-05

Literature-based pathway analysis first identified seven chemosensitivity promoters that could be stimulated by increased PPARG expression, as shown in Figure 1. Each of the relations identified in Figure 2 was supported by at least one scientific report. For instance, Takeda et al. showed that the activation of PPARG increases the expression of BMP6 and BMP7 [11], while the expression of BMP6 was positively related to the chemosensitivity of breast cancer [12]. Chuang et al. showed that PPARG could directly increase the expression of NME1 [13], and NME1 increases the chemosensitivity of multiple squamous carcinoma cells [14, 15]. More information about the pathways in Figure 2 can be found in PPARG_HSCC: Regulatory_Pathway1. Expression analysis showed that these PPARG-driven chemosensitivity promoters were all upregulated in the HSCC CSP group compared with the CSNP group, which provides supports for

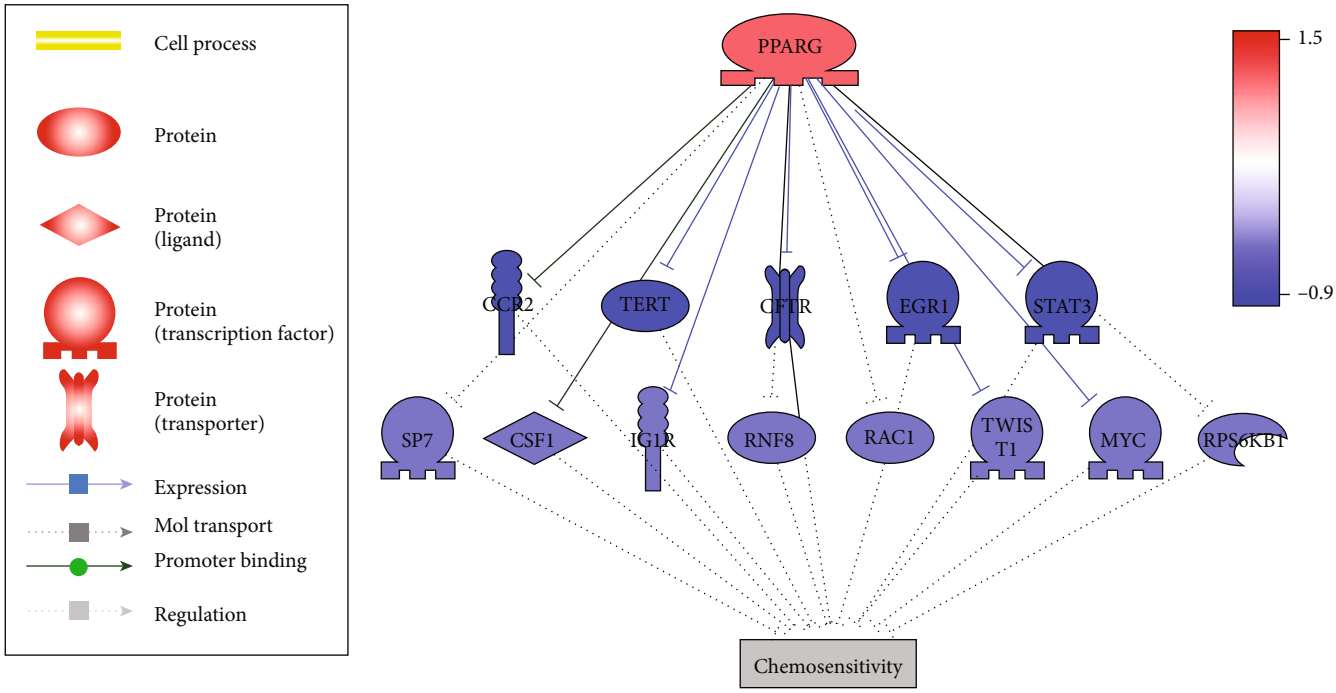

Figure 3: The chemosensitivity-inhibiting pathway built through literature data analysis and tested by HSCC expression data. The blue color of genes represents decreased expression in the chemosensitive group compared with the nonchemosensitive group.

the literature-based pathway. In addition, GSEA results showed that these PPARG-driven chemosensitivity promoters were mainly enriched within the cell proliferation-related pathways (Table 1), indicating that PPARG may influence the chemosensitivity through the regulation of carcinoma-related cell proliferation pathways.

On the other hand, literature-based pathway analysis also identified 13 chemosensitivity inhibitors that were suppressed by the activation of PPARG (Figure 2). For example, TERT was negatively correlated with chemosensitivity of hepatocellular carcinoma, bladder cancer, and head and neck cancers [16–18]. Ogawa et al. showed that PPARG ligands inhibit TERT expression through a receptor-dependent suppression of the TERT promoter [19]. Therefore, increased PPARG expression may indirectly activate chemosensitivity by suppressing its inhibitor. More pathways can be found in PPARG_HSCC→Regulatory_Pathway2. The expression of these PPARG-suppressed molecules in Figure 3 demonstrated the downregulated expressions in the HSCC CSP group, which supports the literature-based pathways for the chemosensitivity in HSCC. GSEA results showed that these molecules in Figure 3 mainly play roles in the cell motility and locomotion-related pathways (Table 2),suggesting that PPARG may also activate the chemosensitivity through the regulation of cell motivation-related pathways. Cell motivation and cell proliferation have been well connected with the etiology and prognoses of HSCC [20]. However, so far, little knowledge has been suggested regarding how cell proliferation and motivation were linked to chemosensitivity. The pathway we built and the GSEA revealed pathways indicated that the genes regulating cell proliferation and motivation might also play roles in the chemosensitivity regulation.

Expression analysis showed that PPARG demonstrated increased expression levels in CSP group (LFC = 0.50). However, due to the limited sample size, the expression level difference of PPARG between did reach statistical significance (p value = 0.25). Further study using larger datasets should be conducted to test the relation between PPARG expression and chemosensitivity in HSCC.

5. Conclusion

Our results identified potential pathways suggesting the chemosensitivity-promoting role of PPARG in HSCC cells, which may through the regulation of cell proliferation and motility-related pathways. Further studies with large datasets were guaranteed for the test of PPARG-chemosensitivity relation in HSCC.

Data Availability

The data in our study are available from the corresponding author upon reasonable request.

Conflicts of Interest

The authors declare that there is no conflict of interest regarding the publication of this paper.

Acknowledgments

This work was partially supported by the Beijing Municipal Administration of Hospitals Incubating Program (PX2018009), Beijing Administration of Traditional Chinese

Medicine (QN2018-32), Beijing Municipal Science & Technology Commission (Z141107002514003), the Capital Health Research and Development of Special (2018-2-205), and Beijing Municipal Administration of Hospitals' Ascent Plan, Code (DFL20180202).

Supplementary Materials

PPARG_HSCC: detailed results of pathway analysis and mega-analysis for PPARG and HSCC relationship study. *(Supplementary Materials)*

References

[1] K. D. Miller, A. Goding Sauer, A. P. Ortiz et al., "Cancer statistics for Hispanics/Latinos, 2018," *Cancer Journal for Clinicians*, vol. 68, no. 6, pp. 425–445, 2018.

[2] G. Marioni, "Letter to the editors: essentials for an updated epidemiology of laryngeal carcinoma," *Cancer Treatment Reviews*, vol. 38, no. 6, p. 559, 2012.

[3] C. Godballe, K. Jørgensen, O. Hansen, and L. Bastholt, "Hypopharyngeal cancer: results of treatment based on radiation therapy and salvage surgery," *The Laryngoscope*, vol. 112, no. 5, pp. 834–838, 2002.

[4] L. Zhan, H. Zhang, Q. Zhang et al., "Regulatory role of KEAP1 and NRF2 in PPARγ expression and chemoresistance in human non-small-cell lung carcinoma cells," *Free Radical Biology and Medicine*, vol. 53, no. 4, pp. 758–768, 2012.

[5] A. P. Kumar, S. Y. Loo, S. W. Shin et al., "Manganese superoxide dismutase is a promising target for enhancing chemosensitivity of basal-like breast carcinoma," *Antioxidants & Redox Signaling*, vol. 20, no. 15, pp. 2326–2346, 2014.

[6] Y. Zhang, H. Y. Luo, G. L. Liu et al., "Prognostic significance and therapeutic implications of peroxisome proliferator-activated receptor γ overexpression in human pancreatic carcinoma," *International Journal of Oncology*, vol. 46, no. 1, pp. 175–184, 2015.

[7] G. Harris, R. A. Ghazallah, D. Nascene, B. Wuertz, and F. G. Ondrey, "PPAR activation and decreased proliferation in oral carcinoma cells with 4-HPR," *Otolaryngology–Head and Neck Surgery*, vol. 133, no. 5, pp. 695–701, 2005.

[8] M. Burotto and E. Szabo, "PPARγ in head and neck cancer prevention," *Oral Oncology*, vol. 50, no. 10, pp. 924–929, 2014.

[9] S. J. Li, J. D. Cha, H. J. Kim, W. Nam, and I. H. Cha, "Expression of peroxisome proliferator-activated receptor gamma and cyclooxygenase 2 in oral squamous cell carcinoma," *International Journal of Oral and Maxillofacial Surgery*, vol. 38, no. 5, p. 533, 2009.

[10] S. K. Wright, B. R. Wuertz, G. Harris et al., "Functional activation of PPARγ in human upper aerodigestive cancer cell lines," *Molecular Carcinogenesis*, vol. 56, no. 1, pp. 149–162, 2017.

[11] M. Takeda, F. Otsuka, H. Otani et al., "Effects of peroxisome proliferator-activated receptor activation on gonadotropin transcription and cell mitosis induced by bone morphogenetic proteins in mouse gonadotrope LbetaT2 cells," *Journal of Endocrinology*, vol. 194, no. 1, pp. 87–99, 2007.

[12] W. J. Lian, G. Liu, Y. J. Liu, Z. W. Zhao, T. Yi, and H. Y. Zhou, "Downregulation of BMP6 enhances cell proliferation and chemoresistance via activation of the ERK signaling pathway in breast cancer," *Oncology Reports*, vol. 30, no. 1, pp. 193–200, 2013.

[13] C. H. Chuang, C. L. Yeh, S. L. Yeh, E. S. Lin, L. Y. Wang, and Y. H. Wang, "Quercetin metabolites inhibit MMP-2 expression in A549 lung cancer cells by PPAR-γ associated mechanisms," *The Journal of Nutritional Biochemistry*, vol. 33, pp. 45–53, 2016.

[14] L. S. Wang, K. C. Chow, Y. C. Lien, K. T. Kuo, and W. Y. Li, "Prognostic significance of nm23-H1 expression in esophageal squamous cell carcinoma," *European Journal of Cardio-Thoracic Surgery*, vol. 26, no. 2, pp. 419–424, 2004.

[15] X. Q. Yang, Z. M. Zhang, D. Wang, G. Wang, L. L. Zeng, and Z. Z. Yang, "nm23-H1-siRNA enhances the chemosensitivity to liposome-encapsulated paclitaxel in lung adenocarcinoma cells in vitro," *Zhonghua Zhong Liu Za Zhi*, vol. 33, no. 6, pp. 405–409, 2011.

[16] X. Guo, W. Wang, F. Zhou et al., "siRNA-mediated inhibition of hTERT enhances chemosensitivity of hepatocellular carcinoma," *Cancer Biology & Therapy*, vol. 7, no. 10, pp. 1555–1560, 2008.

[17] J. Zhou, W. Dai, and J. Song, "miR-1182 inhibits growth and mediates the chemosensitivity of bladder cancer by targeting hTERT," *Biochemical and Biophysical Research Communications*, vol. 470, no. 2, pp. 445–452, 2016.

[18] T. Zhao, F. Hu, X. Liu, and Q. Tao, "Blockade of telomerase reverse transcriptase enhances chemosensitivity in head and neck cancers through inhibition of AKT/ERK signaling pathways," *Oncotarget*, vol. 6, no. 34, pp. 35908–35921, 2015.

[19] D. Ogawa, T. Nomiyama, T. Nakamachi et al., "Activation of peroxisome proliferator-activated receptor gamma suppresses telomerase activity in vascular smooth muscle cells," *Circulation Research*, vol. 98, no. 7, pp. e50–e59, 2006.

[20] Y. Chen, Y. Liu, H. Ni, C. Ding, X. Zhang, and Z. Zhang, "FoxM1 overexpression promotes cell proliferation and migration and inhibits apoptosis in hypopharyngeal squamous cell carcinoma resulting in poor clinical prognosis," *Int J Oncol*, vol. 51, no. 4, pp. 1045–1054, 2017.

Hindawi
PPAR Research
Volume 2020, Article ID 9210748, 18 pages
https://doi.org/10.1155/2020/9210748

Research Article

Comparative Study of PPARγ Targets in Human Extravillous and Villous Cytotrophoblasts

Fulin Liu,[1] Christine Rouault,[2,3] Mickael Guesnon,[1] Wencan Zhu,[4] Karine Clément,[2,3,5] Séverine A. Degrelle,[1,2,6] and Thierry Fournier[1,2]

[1]*Université de Paris, INSERM, UMR-S1139 "Pathophysiology & Pharmacotoxicology of the Human Placenta, Pre & Postnatal Microbiota" (3PHM), Paris F-75006, France*
[2]*Fondation PremUp, Paris F-75006, France*
[3]*Sorbonne Université, INSERM, "Nutrition et Obesités: Approches Systémiques Research Unit", Paris F-75013, France*
[4]*UMR MIA-PARIS, AgroParisTech-Université Paris-Saclay, Paris F-75005, France*
[5]*Assistance Publique-Hôpitaux de Paris, Nutrition Department, Pitié-Salpêtrière Hospital, Paris F-75013, France*
[6]*Inovarion, Paris F-75005, France*

Correspondence should be addressed to Thierry Fournier; thierry.fournier@inserm.fr

Received 24 October 2019; Revised 26 January 2020; Accepted 11 February 2020; Published 1 April 2020

Guest Editor: Fuquan Zhang

Trophoblasts, as the cells that make up the main part of the placenta, undergo cell differentiation processes such as invasion, migration, and fusion. Abnormalities in these processes can lead to a series of gestational diseases whose underlying mechanisms are still unclear. One protein that has proven to be essential in placentation is the peroxisome proliferator-activated receptor γ (PPARγ), which is expressed in the nuclei of extravillous cytotrophoblasts (EVCTs) in the first trimester and villous cytotrophoblasts (VCTs) throughout pregnancy. Here, we aimed to explore the genome-wide effects of PPARγ on EVCTs and VCTs via treatment with the PPARγ-agonist rosiglitazone. EVCTs and VCTs were purified from human chorionic villi, cultured *in vitro*, and treated with rosiglitazone. The transcriptomes of both types of cells were then quantified using microarray profiling. Differentially expressed genes (DEGs) were filtered and submitted for gene ontology (GO) annotation and pathway analysis with ClueGO. The online tool STRING was used to predict PPARγ and DEG protein interactions, while iRegulon was used to predict the binding sites for PPARγ and DEG promoters. GO and pathway terms were compared between EVCTs and VCTs with clusterProfiler. Visualizations were prepared in Cytoscape. From our microarray data, 139 DEGs were detected in rosiglitazone-treated EVCTs (RT-EVCTs) and 197 DEGs in rosiglitazone-treated VCTs (RT-VCTs). Downstream annotation analysis revealed the similarities and differences between RT-EVCTs and RT-VCTs with respect to the biological processes, molecular functions, cellular components, and KEGG pathways affected by the treatment, as well as predicted binding sites for both protein-protein interactions and transcription factor-target gene interactions. These results provide a broad perspective of PPARγ-activated processes in trophoblasts; further analysis of the transcriptomic signatures of RT-EVCTs and RT-VCTs should open new avenues for future research and contribute to the discovery of possible drug-targeted genes or pathways in the human placenta.

1. Introduction

The human placenta serves as a critical bridge between mother and fetus and thus plays a crucial role in maternal and fetal physiology. The placenta is composed mainly of trophoblast cells, which derive from the outer layer of the blastocyst. Certain trophoblasts can be further distinguished as villous cytotrophoblasts (VCTs), whose development progresses along with that of the placenta. In the process of embryo implantation and placenta formation, VCTs that invade the maternal uterus are known as extravillous cytotrophoblasts (EVCTs); these anchor the chorionic villi. Other VCTs differentiate and fuse to form the syncytiotrophoblast layer, which has critical functions in gas and nutrient

exchange between the fetus and the mother. Defects in EVCT invasion and VCT differentiation and fusion contribute to a series of gestational diseases, such as fetus-related miscarriage [1], preterm birth [2], and preeclampsia [3]. The causes of and mechanisms behind these diseases have been the focus of much research, but as yet remain unclear.

As a member of the ligand-dependent nuclear receptor superfamily, PPARγ regulates many downstream target genes involved in lipid metabolism, cell differentiation, and tumorigenesis. PPARγ functions by forming a heterodimer with the nuclear receptor retinoid X receptor α (RXRα) and then binding to the PPAR response element (PPRE) of target genes [4]. It has been reported that a lack of PPARγ leads to defects in trophoblast differentiation and abnormal vasculogenesis in mice [5, 6], and PPAR$\gamma^{-/-}$ embryonic lethality can be rescued via PPARγ transfection in the trophoblast [7]. To be more specific, previous research showed that the activation of PPARγ inhibited the invasion of first-trimester EVCTs, which implicates PPARγ in the regulation of invasion of the decidua [8, 9]. Furthermore, the activation of PPARγ can also induce the differentiation of VCTs isolated from term placenta [10]. Taken together, the current literature on the effects of PPARγ on the regulation of EVCTs and VCTs suggests that it plays a critical role in trophoblast invasion and differentiation but also that these effects differ dramatically among different subtypes of trophoblast. PPARγ thus appears to play a crucial but poorly understood role in placental development.

To explore the role of PPARγ in biological processes, the PPARγ-agonist rosiglitazone has been widely applied to various tissues. In human placenta, rosiglitazone has been used for the study of placental metabolism [11, 12], inflammation [13, 14], antioxidant response [15, 16], and preeclampsia [17]. *In vitro* treatment with rosiglitazone has been shown to reverse inflammation of the placenta that is mediated by the PPARγ-NF-κB pathway [13]. Similarly, rosiglitazone can improve the survival rate of trophoblasts under oxidative stress via its effects on the PPARγ pathway [15]. Other investigations into the activity of this drug have identified new potential target genes of PPARγ [17, 18]. Furthermore, the activation of PPARγ in both first-trimester EVCTs and term VCTs, as described in the research cited above on the influence of PPARγ in trophoblast invasion and differentiation, was also accomplished by this PPARγ-agonist. Taken together, these studies show the enormous potential and benefit of rosiglitazone use in studies of the placenta.

In the human placenta, PPARγ is exclusively located in the nuclei of EVCTs during the first trimester and of VCTs throughout pregnancy [19–21]. To date, there is a lack of systematic research on the effects of PPARγ in these tissues and during these developmental periods. Therefore, our purpose here was to investigate the performance of PPARγ-activated trophoblasts by analyzing the transcriptomic signatures of rosiglitazone-treated EVCTs (RT-EVCTs) and VCTs (RT-VCTs). In this study, we isolated EVCTs and VCTs from first trimester and term human chorionic villi, respectively; cultured these cells with rosiglitazone; and quantified the transcriptome of each type of cell using microarray analysis, as shown in Figure 1. Our results provide abundant information on the biological processes and pathways affected by PPARγ, as well as on the specific genes and pathways targeted, and constitute an invaluable knowledge base for future research.

2. Materials and Methods

2.1. Ethics Statement. Placenta samples in this study were collected with patients' written informed consent, in compliance with the Declaration of Helsinki. Placenta tissues were collected from women with normal pregnancies during the 8-9th gestational weeks and at term (39 gestational weeks). Our ethics committee (CCPRB Paris Cochin no. 18-05) approved the collection of placentas from legal and voluntary terminations of pregnancy in the first trimester as well as of the normal term placentas.

2.2. Cell Isolation and Culture. As previously described [22], five effective first-trimester placentas were obtained for EVCT isolation. Villous tissues were rinsed and minced in Ca^{2+}-, Mg^{2+}-free Hanks' balanced salt solution for membrane removal. Mononucleated VCTs were isolated using digestion with trypsin-DNase and fractionation on a discontinuous Percoll gradient according to the protocol of Kliman et al. [23] and Alsat et al. [24]. In brief, villous tissues were digested in Hanks' balanced salt solution, containing 5 IU/mL of DNase I, 4.2 mM $MgSO_4$, 0.25% (wt/vol) trypsin powder (Difco), 100 IU/mL penicillin, 25 mM HEPES, and 100 μg/mL streptomycin (Biochemical Industry), and monitored under invert microscopy. The initial digested solution (consisting mostly of red blood cells) was discarded while the subsequent digested solution (clearly consisting of EVCTs) was retained. A discontinuous Percoll gradient (5–70% in 5% steps) was used to stratify the digested solutions; the middle layer (which included EVCTs) was retained for further analysis. The purified EVCTs were diluted with Dulbecco's modified Eagle's medium (DMEM), with 2 mM glutamine, 100 IU/mL penicillin, 100 mg/mL streptomycin, and 10% decomplemented fetal calf serum (FCS), to a final density of 0.9×10^6 cells/mL in 60 mm diameter plastic tissue culture dishes (Techno Plastic Products, Switzerland). In preparation for culturing, culture plates (Techno Plastic Products, Switzerland) were coated with Matrigel™ (7 μg/cm^2; Collaborative Biomedical Products, Le Pont de Claix, France), then seeded with EVCTs at a density of 5×10^4 cells/cm^2. To maintain continuous culture conditions, DMEM-F12 medium was used that contained 10% heat-inactivated fetal calf serum (FCS), Glutamax, 100 μg/mL streptomycin, and 100 IU/mL penicillin (Invitrogen). Plates were incubated for 2 h at 37°C and 5% CO_2; then, nonadherent EVCTs were rinsed off. At this point, fresh medium with or without 1 μM rosiglitazone (Cayman) dissolved at 1 mM in ethanol (treatment) or 0.1% ethanol (vehicle) was added for another 24 h of incubation.

VCTs were isolated from five term placentas using the following procedures. Placentas were oriented with the maternal side facing upwards, and tissues were sampled at a depth of 1.5 cm, half the distance from the edge to the centre. Villous tissues were rinsed, minced, digested, and purified using the steps described above. Culture dishes containing

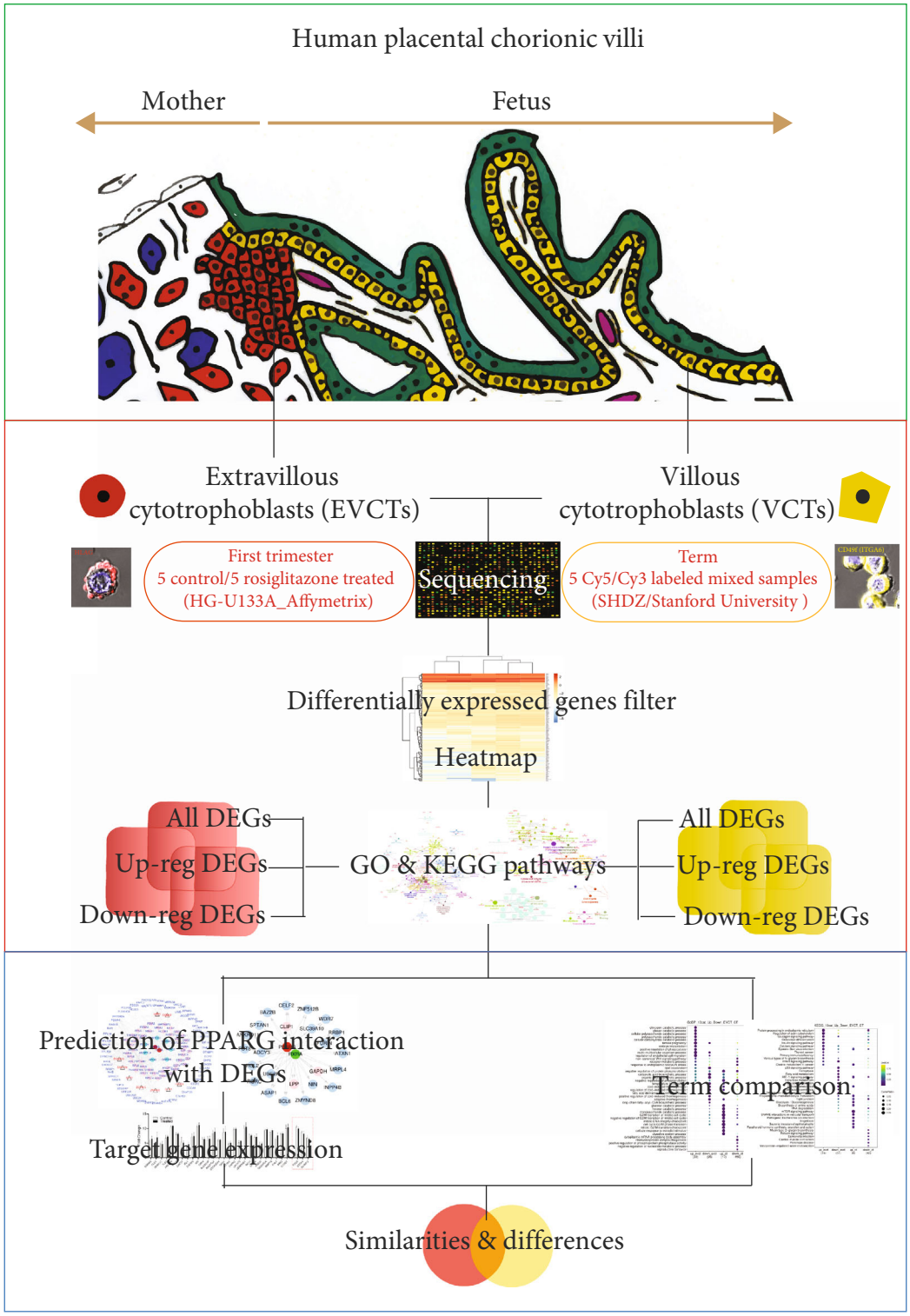

Figure 1: Summary of procedures. Extravillous cytotrophoblasts (EVCTs, HLAG+ cells) [22] and villous cytotrophoblasts (VCTs, CD49f+ cells) were isolated from human first trimester and term placental chorionic villi, respectively, treated with rosiglitazone, and analyzed using microarrays. Differentially expressed genes (DEGs) were filtered for quality control and submitted for annotation. Terms associated with DEGs and predictions of PPARγ-target genes were compared between the rosiglitazone-treated EVCTs and VCTs. PPARγ: peroxisome proliferator-activated receptor γ. The top graphic was modified from Handschuh et al. (2007).

0.9×10^6 cells/mL were placed in a humidified incubator at 37°C under 5% CO_2 for 3 h. Nonadherent VCTs were rinsed off, fresh medium with or without 1 μM rosiglitazone (Cayman) dissolved at 1 mM in ethanol (treatment) or 0.1% ethanol (vehicle) was added, and dishes were incubated for another 24 h.

2.3. Microarray Experiments. After 24 h of incubation, RT-EVCTs and control EVCTs were harvested for microarray experiments. Cell RNA was extracted using TRIzol® reagents (Invitrogen) and purified using RNeasy® Mini Kits (Qiagen). RNA integrity and purity were examined with a 2100 Bioanalyzer with the RNA 6000 LabChip kit (Agilent Technologies). The U133A 2.0 GeneChip (Affymetrix, Inc.) was used for gene expression detection according to the manufacturer's manual. From the 22,000 probe sets on the gene chip, 14,500 genes were detected.

RT-VCTs and control VCTs were likewise harvested after 24 h of incubation for microarray experiments; RNA extraction, purification, and quality control were performed as described. The SHDZ gene chip (Stanford University) was used for gene detection as described in [25]: for each sample, the MessageAmp RNA kit (Ambion) was used, with 1 μg total RNA, for RNA amplification, and 3 μg amplified RNA were then labeled with Cy-dye using the 26 CyScribe first-strand cDNA labeling kit (Amersham Biosciences). Amplified RNA from rosiglitazone-treated VCTs was labeled with Cy5, and amplified RNA from control VCTs was labeled with Cy3. A Microcon YM 30 column (Millipore) was used to purify and concentrate the labeled mixture (Cy5 and Cy3) after additional modifications with human cot-1, yeast tRNA, and poly A. The probes were denatured and the mixture was hybridized at 65°C overnight in a sealed humidified hybridization chamber, then rinsed with 1XSSC, 2XSSC, 0.03% SDS, and 0.2% SDS solutions for 2 min each. Arrays were scanned with a GenePrix 4000A microarray scanner (Axon Instruments).

2.4. Data Processing. Since gene expression in EVCTs and VCTs was detected using different microarray platforms, different procedures were followed for data processing. For EVCT gene expression, which was quantified using the GeneChip (U133A 2.0, Affymetrix) application, data processing used the following filter thresholds: (i) percentage of missing data was no more than 50%, (ii) threshold to identify up- and downregulated genes for statistical comparison was set to a fold change of 1.5, (iii) maximum false discovery rate (FDR) was set to 5%, and (iv) fold change of one gene was equal to mean of treated groups minus mean of control groups and then divided by the minimum value from all (fold change = (mean (treated) − mean (control))/minimum (treated, control)) [22]. For VCT gene expression, which was measured using the SHDZ GeneChip/Stanford University (GPL21609) application, data processing used the following filter thresholds: (i) background-corrected data were log2-transformed and subjected to the Loess normalization method [11], (ii) differentially expressed genes (DEGs) were determined via the significance analysis of microarrays (SAM) method [26], and (iii) the maximum false discovery rate (FDR) was set to 1%, without a fold change threshold imposed [27].

2.5. GO and Pathway Enrichment Analyses. ClueGO is a Cytoscape plug-in application for the functional classification of genes [28]. Our analysis used Cytoscape version 3.7.1 (The Cytoscape Consortium, New York, NY) and ClueGO version 2.5.4 (released 28 Feb 2019), with the simultaneous update of gene ontology (GO) terms. Using ClueGO, we recovered the GO terms associated with the dataset of all DEGs as well as of up- or downregulated DEGs only; this same application was also used for KEGG and Reactome pathway analysis. GO terms were compared between EVCTs and VCTs using the R package clusterProfiler (version 3.9, synced to latest GO terms and pathways) [29]. For term comparison in clusterProfiler, 10 category terms for each group were selected for inclusion in charts. Instead, ClueGO analyses were based on approximately 30 terms per group in order to generate more detailed visualizations. P values lower than 0.05 identified significant enrichment.

2.6. Protein-Protein Interaction (PPI) Network. The STRING database (https://string-db.org) was used to analyze the interactions of DEG-encoded proteins and construct a PPI network. For this, the significant confidence score was set to greater than 0.4. Cytoscape was used to visualize and organize the PPI network. Proteins interacting with PPARγ or RXRα were indicated by different colors, and shapes were used to represent different groups. Binding site interactions between transcription factors and target genes were predicted by the Cytoscape plug-in iRegulon (based on the TRANSFAC database; version 1.3). Putative regulatory regions were defined as 10 kb around transcription starting sites. The FDR was set to 0.1% to verify the interaction. The resulting chart was modified in Cytoscape using red to indicate upregulated genes and blue to indicate downregulated genes.

3. Results

3.1. Gene Expression Profiling of RT-EVCTs and RT-VCTs. Microarrays were used to characterize gene expression in EVCTs and VCTs with or without rosiglitazone treatment. Our microarray data have been deposited in the Gene Expression Omnibus public repository (https://www.ncbi.nlm.nih.gov/geo/; EVCT microarray data under accession number GSE28426, VCT microarray data under accession number GSE137434). Gene expression profiles of the rosiglitazone-treated (TRT) samples of EVCTs and VCTs were normalized (Figure 2(a)). Four of the five independent RT-EVCT samples yielded consistent results, with one sample appearing slightly different; instead, all five independent RT-VCT samples yielded similar results. Next, DEGs were detected based on thresholds for both fold change in expression levels and FDR. In RT-EVCTs, a total of 139 genes were identified as DEGs ($P < 0.05$), of which 114 genes were upregulated (red) and 25 genes were downregulated (blue). In RT-VCTs, a total of 197 genes were identified as DEGs ($P < 0.05$), of which 181 genes were upregulated (red) and 16 genes were downregulated (blue) (Figure 2(b)).

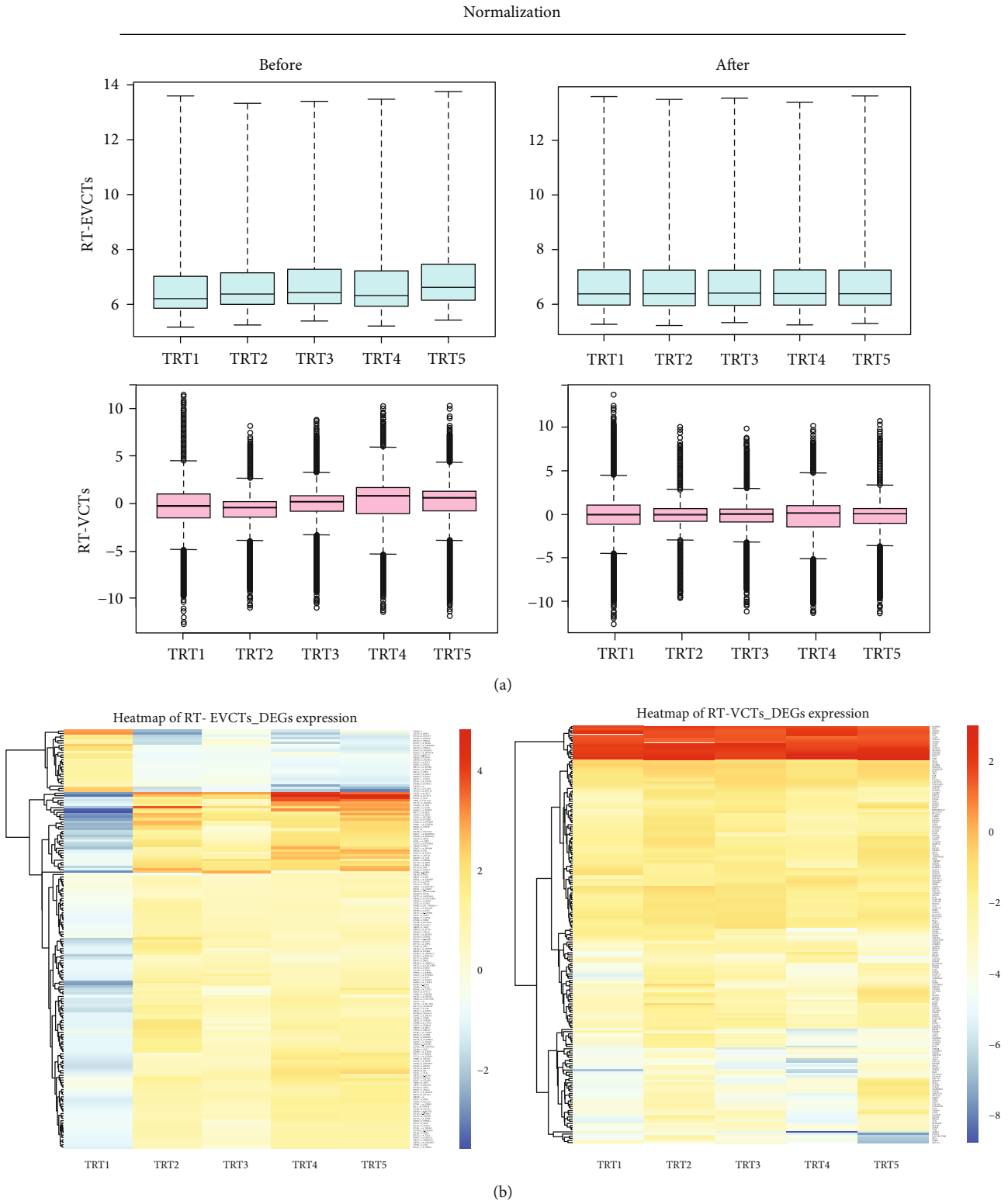

Figure 2: Microarray data normalization and DEG heatmap of RT-EVCTs and RT-VCTs. (a) RT-EVCT gene expression microarray was performed with the Affymetrix GeneChip while the RT-VCT microarray used the SHDZ/Stanford University chip. DEGs were detected based on the thresholds of 1.5-fold change and 5% FDR for the RT-EVCT microarray matrix; a threshold of 1% FDR was applied for the RT-VCT microarray matrix. The Loess normalization method was used to normalize both datasets. Box plots represent microarray data before and after normalization, with blue indicating data from RT-EVCTs and pink data from RT-VCTs. (b) Heatmaps of five independent samples of RT-EVCTs and RT-VCTs. Upregulated DEGs are represented in red and downregulated DEGs in blue. DEGs: differentially expressed genes; RT-EVCTs: rosiglitazone-treated extravillous cytotrophoblasts; RT-VCTs: rosiglitazone-treated villous cytotrophoblasts; FDR: false discovery rate; TRT: treated.

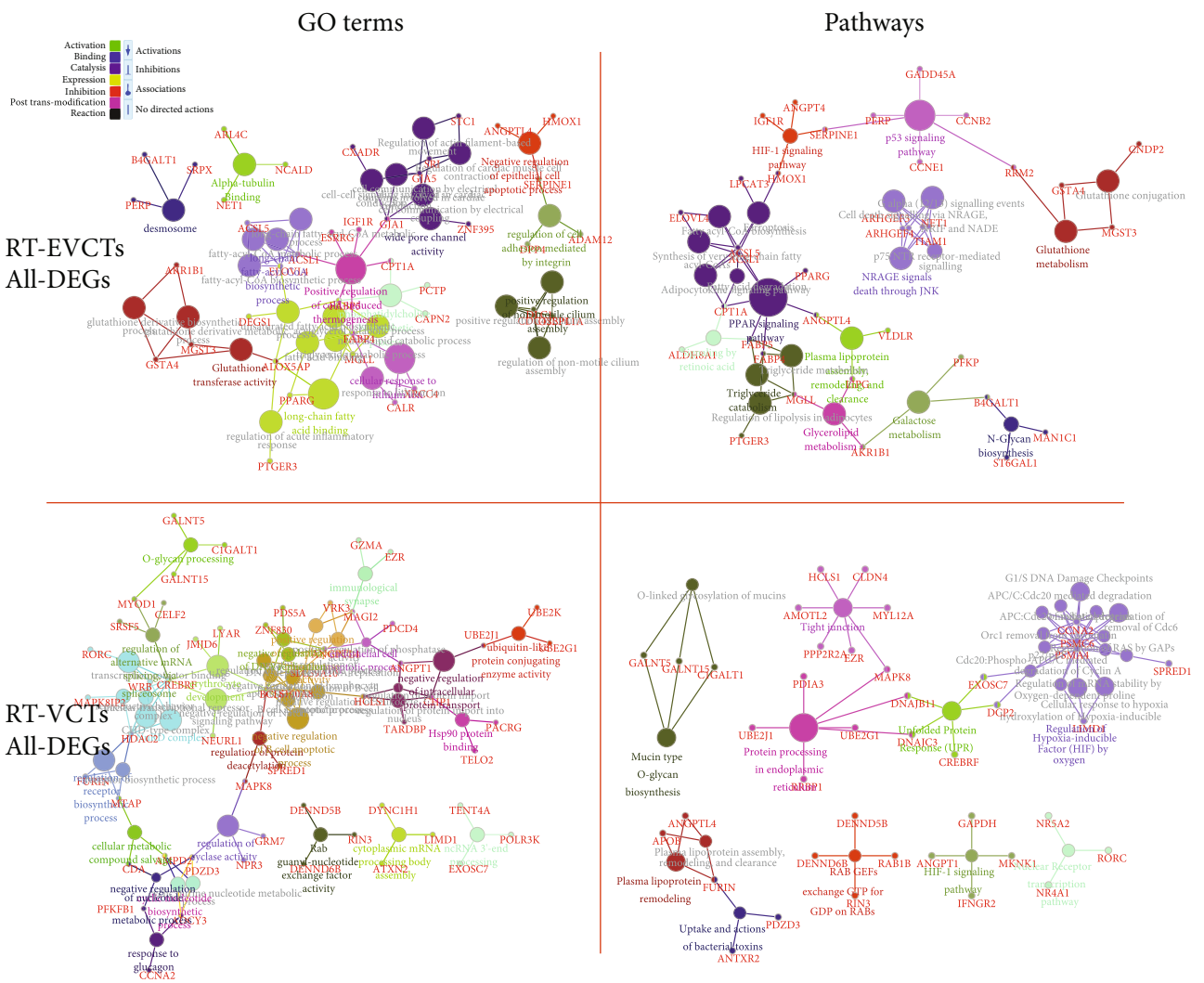

Figure 3: GO and pathway terms associated with all DEGs in RT-EVCTs and RT-VCTs. All DEGs were submitted separately according to their cell type of origin to ClueGO with the default parameters. GO and pathway enrichment were set up for analysis. DEGs were classified by three ways: by GO biological process, GO molecular function, and GO cellular component. The KEGG and Reactome database was consulted to determine pathway enrichment. An exhaustive list of all terms (including those not shown above) can be found in supplementary materials (Tables S1-S8). DEGs: differentially expressed genes; RT-EVCTs: rosiglitazone-treated extravillous cytotrophoblasts; RT-VCTs: rosiglitazone-treated villous cytotrophoblasts; GO: gene ontology; KEGG: Kyoto encyclopedia of genes and genomes.

3.2. Gene Ontology and Pathway Terms of all DEGs from RT-EVCTs and RT-VCTs. The entire set of DEGs from RT-EVCTs and RT-VCTs was separated by cell type of origin and submitted independently to ClueGO with the default parameters. GO and pathway enrichment were set up for analysis. DEGs were classified by three ways: by GO biological process, GO molecular function, and GO cellular component. Enriched pathways were identified through a search of the KEGG and Reactome databases. The results are visualized in Figure 3.

Among the DEGs identified in RT-EVCTs, the main GO biological processes represented were "negative regulation of epithelial cell apoptotic process," "long-chain fatty-acyl-CoA biosynthetic process," and "phosphatidylcholine biosynthetic process." For the same group of DEGs, the GO molecular functions were mainly classified as "alpha-tubulin binding," "wide pore channel activity," "positive regulation of cold-induced thermogenesis," "glutathione transferase activity," "long-chain fatty acid binding," "regulation of cell adhesion mediated by integrin," and "positive regulation of non-motile cilium assembly." Finally, the GO cellular component that was most associated with these DEGs was "desmosome." In the pathway enrichment analysis of RT-EVCTs, DEGs were mainly associated with the terms "HIF-1 signaling pathway," "p53 signaling pathway," "glutathione metabolism," "NRAGE signals death through JNK," "PPAR signaling pathway," "plasma lipoprotein assembly," and "remodeling and clearance".

In the analysis of GO terms associated with the RT-VCT dataset, DEGs were mainly involved in the following biological processes: "regulation of receptor biosynthetic process," "negative regulation of nucleotide metabolic process," "cyclic nucleotide biosynthetic process," and "negative regulation of B cell apoptotic process." The molecular functions of this

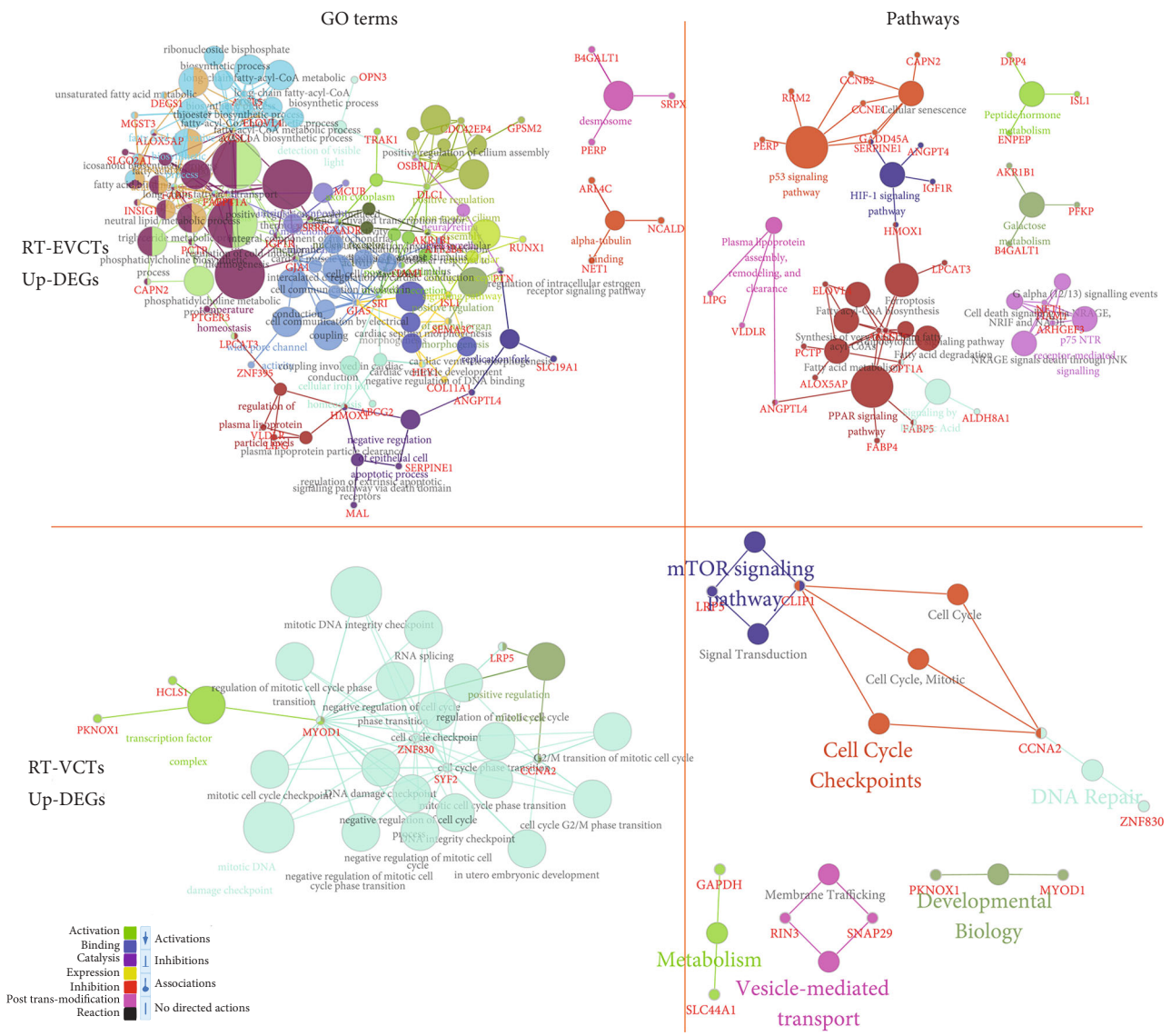

Figure 4: GO and pathway terms associated with DEGs that were upregulated in RT-EVCTs and RT-VCTs. These DEGs were submitted separately to ClueGO by their cell type of origin with the default parameters. GO and pathway enrichment were set up for analysis. Upregulated DEGs were classified by three ways: by their GO biological process, GO molecular function, and GO cellular component. The KEGG and Reactome databases were consulted to determine pathway enrichment. All additional enrichment terms (not shown above) can be found in supplementary materials (Tables S1-S8). DEGs: differentially expressed genes; RT-EVCTs: rosiglitazone-treated extravillous cytotrophoblasts; RT-VCTs: rosiglitazone-treated villous cytotrophoblasts; GO: gene ontology; KEGG: Kyoto encyclopedia of genes and genomes.

same group of DEGs were mainly linked to "negative regulation of DNA replication," "regulation of protein deacetylation," "ubiquitin-like protein conjugating enzyme activity," "Hsp90 protein binding," "negative regulation of intracellular protein transport," and "positive regulation of phosphoprotein." With respect to GO cellular components, DEGs were mainly associated with the terms "NuRD complex," "cellular metabolic compound salvage," and "immunological synapse." Finally, the pathway enrichment analysis of RT-VCTs revealed that DEGs were mainly involved in "tight junction," "regulation of HIF by oxygen," "unfolded protein response," "HIF-1 signaling pathway," "nuclear receptor transcription pathway," and "plasma lipoprotein remodeling".

3.3. GO and Pathway Terms Associated with Upregulated DEGs in RT-EVCTs and RT-VCTs. DEGs that were upregulated in RT-EVCTs and RT-VCTs were submitted separately to ClueGO following the same procedure as described above. The results are visualized in Figure 4. In RT-EVCTs, upregulated DEGs were mainly associated with the GO biological processes "fatty acid derivative biosynthetic process" and "negative regulation of epithelial cell apoptotic process," and the GO molecular functions "positive regulation of insulin secretion," "temperature homeostasis," "wide pore channel activity," "nuclear receptor activity," and "regulation of plasma lipoprotein particles levels." The main GO cellular components implicated in the activity of these DEGs were

"desmosome" and "intrinsic component of mitochondrial membrane." Finally, the pathway enrichment analysis indicated that upregulated DEGs in RT-EVCTs were mainly involved in the "p53 signaling pathway," "HIF-1 signaling pathway," "peptide hormone metabolism," "PPAR signaling pathway," "p57 NTR receptor-mediated signaling," and "signaling by retinoic acid".

Instead, from the DEGs that were upregulated in RT-VCTs, no significant GO biological process was identified. In the classification of GO molecular functions, these DEGs were mainly linked with "positive regulation of cell cycle" and "mitotic DNA damage checkpoint," and the most significant GO cellular component was "transcription factor complex." In the pathway enrichment analysis, upregulated DEGs in RT-VCTs were mainly associated with the terms "mTOR signaling pathway," "cell cycle checkpoints," "DNA repair," "developmental biology," "metabolism," and "vesicle-mediated transport".

3.4. GO and Pathway Terms Associated with Downregulated DEGs in RT-EVCTs and RT-VCTs. DEGs that were downregulated in RT-EVCTs and RT-VCTs with respect to controls were submitted to ClueGO using the same procedure as described above. Results are visualized in Figure 5. In RT-EVCTs, downregulated DEGs were mainly associated with the GO biological process "positive regulation of small molecular metabolic process;" the GO molecular functions "membrane fusion," "regulation of epithelial cell migration," "response to estriol," and "protein kinase binding;" and the GO cellular component "phosphorylase kinase complex." From the analysis of pathway enrichment based on the KEGG and Reactome database, downregulated DEGs in RT-EVCTs appeared to be mainly associated with pathways linked with "glycogen breakdown," "influenza infection," "protein processing in endoplasmic reticulum," and "regulation of actin cytoskeleton".

Instead, DEGs that were downregulated in RT-VCTs were mainly involved in the GO biological processes "cyclic nucleotide biosynthetic process," "negative regulation of nucleotide metabolic process," "ncRNA 3'-end processing," and "O-glycan processing;" the GO molecular functions "nuclear receptor activity," "histone deacetylation," "regulation of TOR signaling," "Hsp90 protein binding," "ion channel regulator activity," "nuclear envelope organization," and "peptidyl-threonine modification;" and the GO cellular component "organellar ribosome." In the pathway enrichment analysis of RT-VCTs, downregulated DEGs were mainly associated with the "HIF-1 signaling pathway," "transfer of ubiquitin from E1 to E3," "cell-cell communication," "transcription regulation of RUNX3," and "formation of NR-MED1 coactivator complex".

3.5. Comparison of GO Terms Associated with Tissue-Specific or Tissue-Generalist DEGs. Next, we wanted to determine the extent to which the cellular processes affected by rosiglitazone treatment were specific to either EVCTs or VCTs, and which instead were present in both tissue types. To do this, we characterized the up- and downregulated DEGs of RT-EVCTs and RT-VCTs separately using clusterProfiler, using information from the GO and KEGG databases, as well as the Disease Ontology (DO) and Disease Gene Network (DisGeNET) databases. Terms appearing in at least three columns were thought important in both, while terms appearing only in the RT-EVCT or RT-VCT dataset were labelled tissue-specific; significance was determined by P values less than 0.05.

In both RT-EVCTs and RT-VCTs, the GO biological processes "regulation of endothelial cell migration," "non-canonical Wnt signaling pathway," "receptor metabolic process," "negative regulation of protein phosphorylation," and "metabolism process" appeared to play important roles. Instead, processes specific to RT-EVCTs included "glycogen catabolic process," "cellular carbohydrate catabolic process," "embryo implantation," "fatty acid derivative biosynthetic process," and "long-chain fatty-acyl-CoA biosynthetic process," while those specific to RT-VCTs were "cytoplasmic mRNA processing body assembly," "ribonucleoprotein complex biogenesis," "positive regulation of phosphoprotein phosphatase activity," and "negative regulation of nucleotide metabolic process" (Figure 6(a)).

The GO molecular functions "nuclear hormone receptor binding," "long-chain fatty acid binding," "fatty acid binding," "nuclear activity," and "transcription factor activity" seemed to be important in both RT-EVCTs and RT-VCTs. Functions specific to RT-EVCTs included "steroid hormone receptor binding," "eicosanoid receptor activity," "phosphatidylinositol phosphate kinase activity," and "fatty acid ligase activity," while those specific to RT-VCTs were "Wnt-activated receptor activity," "cyclin-dependent protein kinase activity," "transferase activity," and "ubiquitin-specific protease activity" (Figure 6(b)).

Both tissue types shared the significant GO cellular components "smooth endoplasmic reticulum," "ruffle," "transcription factor complex," "apical plasma membrane," "lumen," and "cell-cell junction." Instead, the component terms "beta-catenin destruction complex," "M band," "integral component of lumenal side of endoplasmic reticulum membrane," and "A band" were found only in RT-EVCTs, while "spliceosomal complex," "Wnt signalosome," "pronucleus," "microtubule end," and "autophagosome membrane" appeared to be specific to RT-VCTs (Figure 6(c)).

Through a search of the KEGG database, the following pathways appeared to be important in both tissue types: "protein processing in endoplasmic reticulum," "glucagon signaling pathway," "Epstein-Barr virus infection," "PPAR signaling pathway," "HIF-1 signaling pathway," "progesterone-mediated oocyte maturation," and "mTOR signaling pathway." Pathway terms specific to RT-EVCTs included "primary immunodeficiency" and "fatty acid metabolism," while those specific to RT-VCTs were linked with "bacterial invasion of epithelial cells" and "parathyroid hormone synthesis, secretion, and action" (Figure 6(d)).

From the Disease Ontology database, the terms "pre-eclampsia," "HELLP syndrome," "spinocerebellar ataxia," "familial hyperlipidemia," "lipid metabolism disorder," and "musculoskeletal system cancer" were important in both EVCTs and VCTs. Terms specific to RT-EVCTs included "breast benign neoplasm," "thoracic benign neoplasm,"

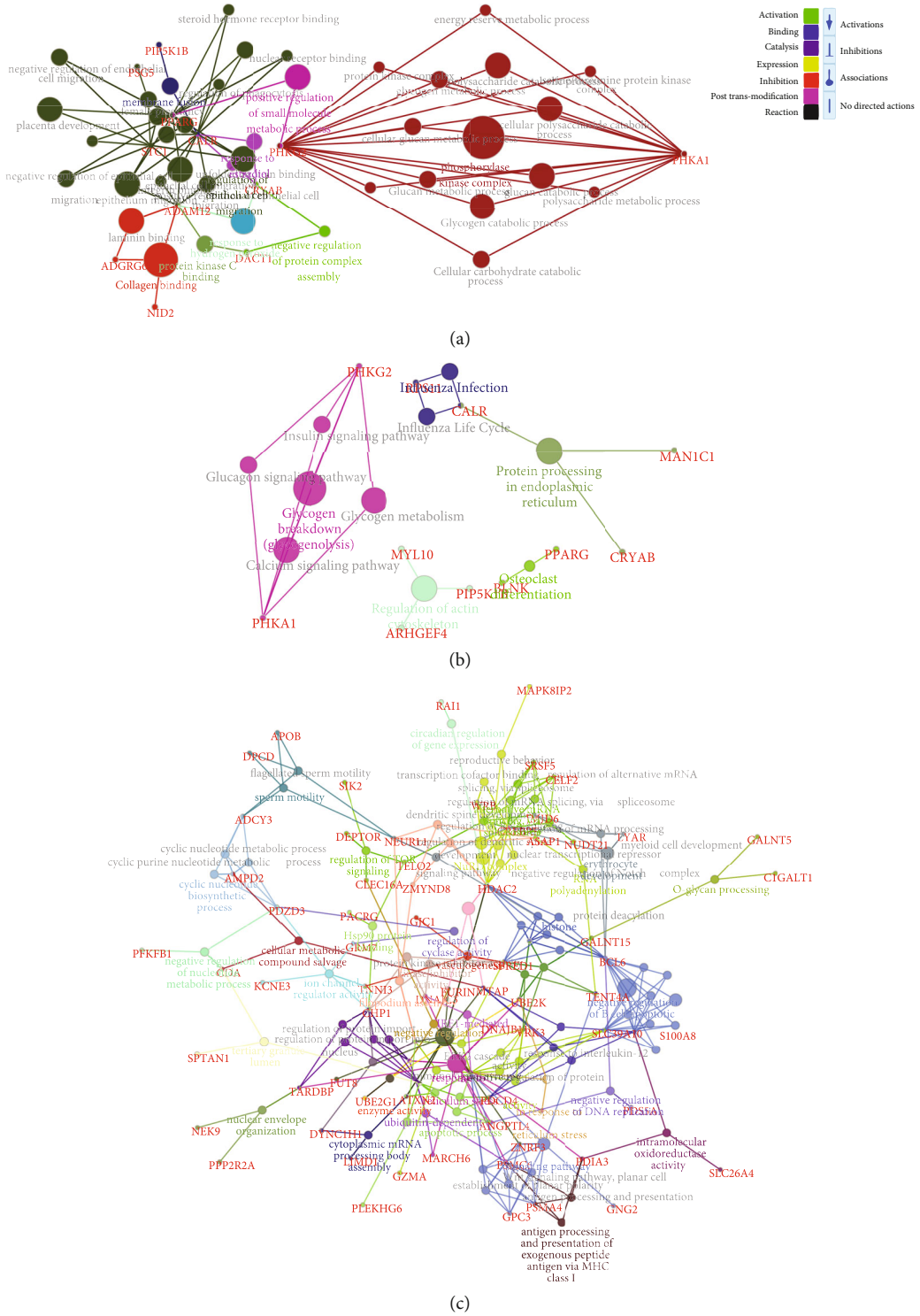

Figure 5: Continued.

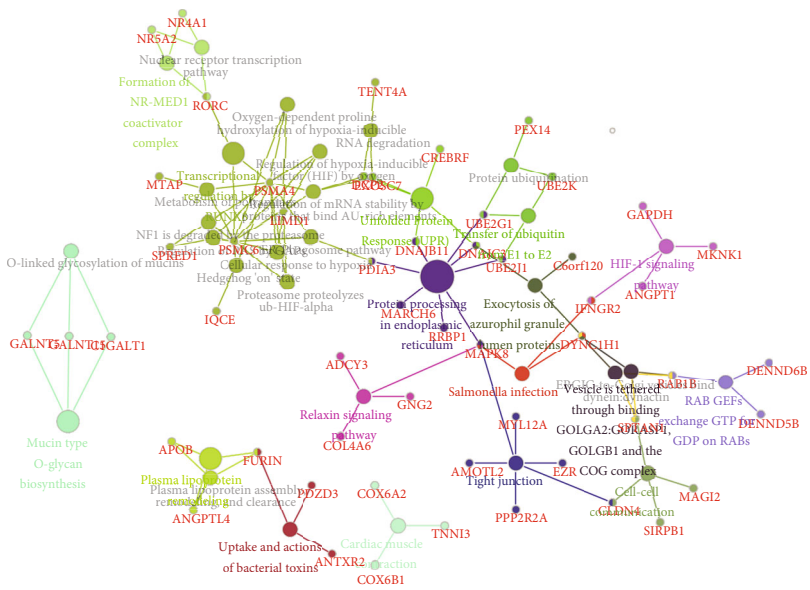

(d)

Figure 5: GO and pathway terms associated with DEGs that were downregulated in RT-EVCTs and RT-VCTs, respectively, compared to controls. Downregulated DEGs of RT-EVCTs (a, b) and RT-VCTs (c, d) were submitted to ClueGO separately, with the default parameters. GO and pathway enrichment were set up for analysis. DEGs were classified by three ways: by GO biological process, GO molecular function, and GO cellular component (a, c). Pathway enrichment was determined via comparison with the KEGG database (b, d). (a) The GO terms most associated with DEGs that were downregulated in RT-EVCTs. (b) The pathways that were most enriched among the downregulated DEGs in RT-EVCTs. (c) The GO terms most associated with DEGs that were downregulated in RT-VCTs. (d) The pathways that were most enriched among the downregulated DEGs in RT-VCTs. An exhaustive list of all associated terms (including those not pictured above) can be found in supplementary materials (Tables S1-S8). DEGs: differentially expressed genes; RT-EVCTs: rosiglitazone-treated extravillous cytotrophoblasts; RT-VCTs: rosiglitazone-treated villous cytotrophoblasts; GO: gene ontology; KEGG: Kyoto encyclopedia of genes and genomes.

"lipomatous cancer," "amyloidosis," and "vein disease," while those specific to RT-VCTs were "alveolar rhabdomyosarcoma," "osteopetrosis," "giant cell tumor," and "germ cell and embryonal cancer" (Figure 6(e)).

From a search of the DisGeNET database, the terms "preeclampsia," "hypertrophic cardiomyopathy," "immunologic deficiency syndromes," "diabetes mellitus," "vascular inflammations," "hematopoietic neoplasms," "non-alcoholic fatty liver disease," "vascular disease," "ischemic cardiomyopathy," and "triploidy syndrome" were significant for both tissue types. Instead, "chronic neutrophilic leukemia," "glycogen storage disease," and "myeloid, chronic, atypical, and BCR-ABL negative leukemia" were specific to RT-EVCTs, and "alport syndrome" and "aggressive non-Hodgkin lymphoma" were specific to RT-VCTs (Figure 6(f)).

3.6. PPARγ Interactions with DEGs of RT-EVCTs and RT-VCTs. Since the gene expression changes we observed here were caused by the activation of PPARγ by rosiglitazone, we next attempted to predict (i) the protein-protein interactions (PPI) of PPARγ with DEG-encoded proteins and (ii) the transcription factor-target gene (TF-TG) interactions of PPARγ with DEG promoters. In RT-EVCTs (Figure 7(a)), the following proteins appeared to interact directly with the PPARγ complex: MGLL, FABP5, HMOX1, SERPINE1, ABCG2, PHC1, VLDLR, INSIG1, DPP4, ANGPTL4, FAPB4, ACSL1, and CPT1A. Instead, ACSL5, PFKP, AKR1B1, LOX, GXTA4, SOWAHC, GJA1, SLC19A1, RUNX1, PERP, ENPEP, SLFN12, CDC42EP, and LIPG participated in secondary interactions. In RT-VCTs (Figure 7(b)), the PPARγ complex interacted directly with MYOD1, MAPK8, HDAC2, GAPDH, APOB, ANGPTL4, and PDCD4 and secondarily with PDIA3, MAPK8IP2, NR4A1, GNG2, and CCR1. Our analysis of TF-TG interactions in RT-EVCTs (Figure 7(c)) predicted that the target genes of the PPARγ complex were the upregulated DEGs DLC1, SEMA3C, ARL6IP5, PCTP, ISL1, ZNF395, SR1, DPP4, ALOX5AP, ANGPL4, CDC42EP4, GKN1, ATXN1, CAPN2, LPCAT3, SERPINE1, NET1, LPCAT3, CPT1A, RAB30, GADD45A, MMP19, FHL1, MMD, CCNE1, and ESRRG, as well as the downregulated DEGs ADAM12, GSTA4, PSG5, and DACT1. The same analysis of RT-VCTs (Figure 7(d)) predicted that the target genes of the PPARγ complex were the upregulated DEGs CLIP1, GAPDH, and LPP, as well as the downregulated DEGs CELF2, ZNF512B, SLC39A10, WDR7, FURIN, RRBP1, ATXN1, MRPL4, INNPP4B, ZMYND8, BCL6, ASAP1, UBE2K, RORC, RGL2, ADCY3, FUT8, ANKRD11, SPTAN1, and BAZ2B.

3.7. Expression of Genes Targeted by PPARγ in RT-EVCTs and RT-VCTs. We next filtered our datasets to examine only the DEGs targeted directly by the PPARγ complex, based on the TF-TG predictions described above. The filtered RT-EVCT database contained 26 upregulated and 4

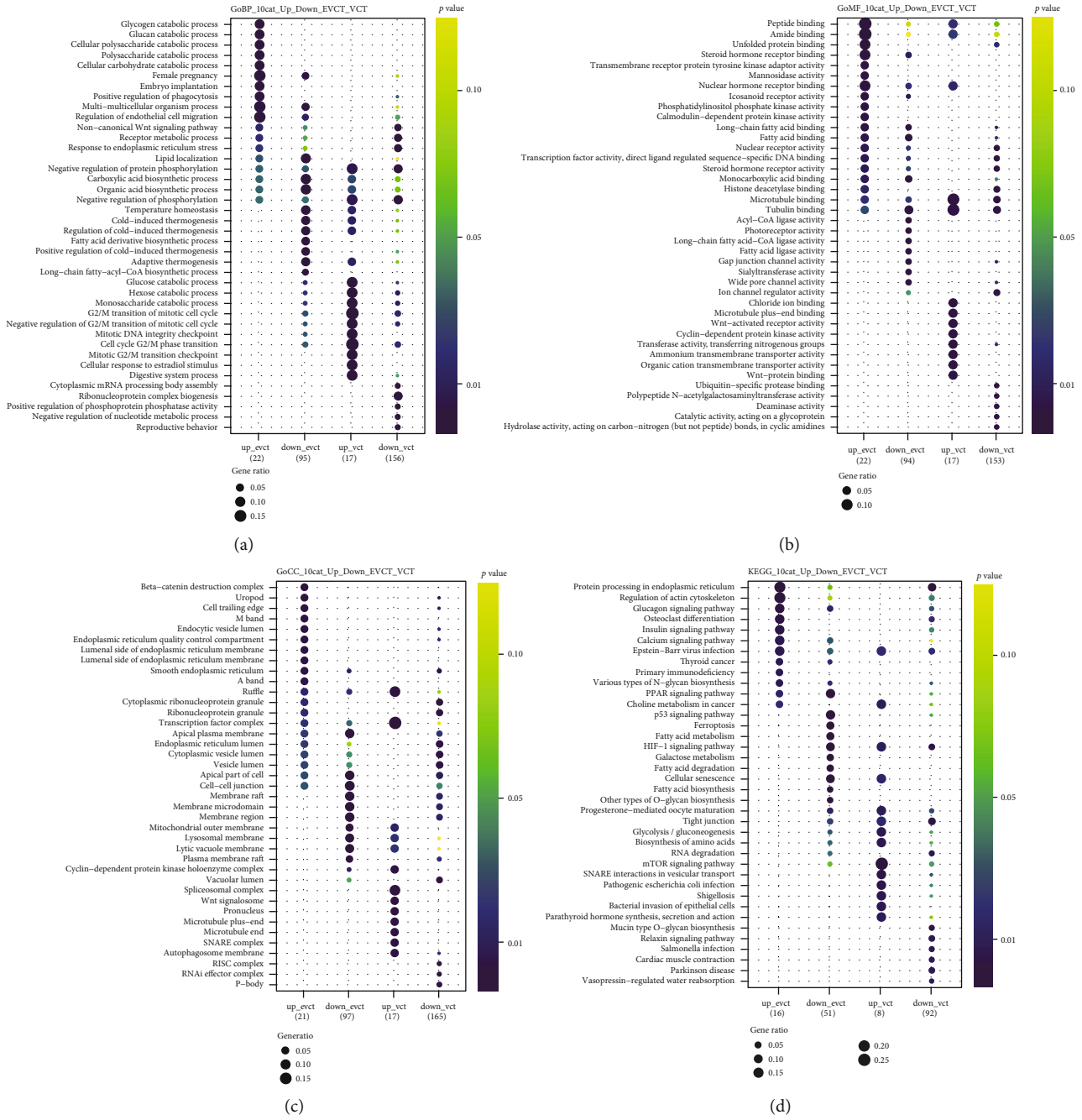

Figure 6: Continued.

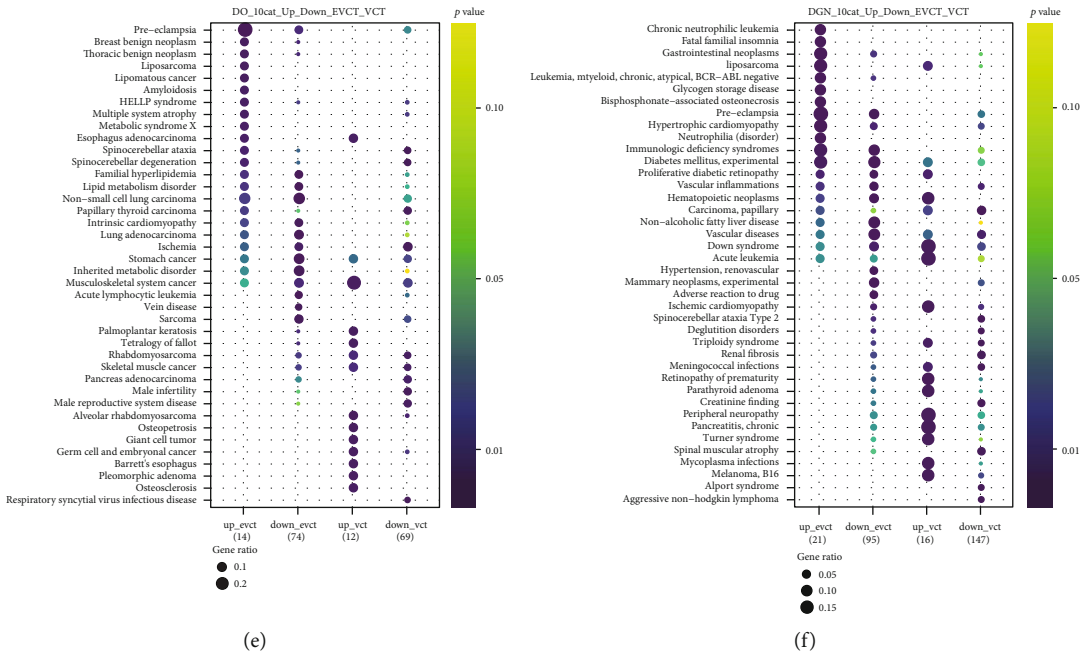

(e) (f)

Figure 6: Comparison of enriched GO terms between RT-EVCTs and RT-VCTs. Up and downregulated DEGs of RT-EVCTs and RT-VCTs were submitted separately to analysis in clusterProfiler, for a total of four groups. GO and pathway enrichment were set up for analysis. DEGs were classified by their associated (a) GO biological process, (b) GO molecular function, and (c) GO cellular component. DEGs were further compared with the (d) KEGG database to characterize pathway enrichment, (e) the Disease Ontology (DO) gene set, and (f) the Disease Gene Network (DisGeNET) database. For the purpose of visualization, the top ten categories of enriched terms were included for each gene set. A P value less than 0.05 determined significance. DEGs: differentially expressed genes; RT-EVCTs: rosiglitazone-treated extravillous cytotrophoblasts; RT-VCTs: rosiglitazone-treated cytotrophoblasts; GO: gene ontology; KEGG: Kyoto encyclopedia of genes and genomes.

downregulated DEGs (Figure 8(a)), while the filtered RT-VCT database contained 3 upregulated and 21 downregulated DEGs (Figure 8(b)). Only one target gene, ATXN1, was present in both datasets; it was upregulated in RT-EVCTs and downregulated in RT-VCTs (Figure 8).

4. Discussion

The human placenta is a critical bridge between mother and fetus, facilitating nutrient exchange and various endocrine and immunological processes. As the cells that form the main part of the placenta, trophoblasts undergo extensive cell differentiation, including invasion, migration, and fusion. Abnormalities in these physiological processes can lead to a series of gestational diseases such as preeclampsia or intrauterine growth restriction. Specifically, both of these disorders appear to be associated with irregularities in the invasion of EVCTs into the maternal uterus, a biological process that is tightly controlled both spatially and temporally [30, 31]. However, the underlying mechanism linking EVCT invasion to gestational dysfunction has yet to be fully investigated. Our team has previously shown the critical influence of activated PPARγ on trophoblasts via treatment of the natural ligands of PPARγ or its specific agonist rosiglitazone [9, 20, 22, 32]. Rosiglitazone is the first synthetic chemical compound to be developed that demonstrates high selectivity for PPARγ (Kd approximately 40 nM); concentrations of up to 100 μM of this compound have been reported to activate only PPARγ (including the PPAR$\alpha/\beta/\delta$ complex [33]). Moreover, our previous research revealed that a concentration of only 1 μM rosiglitazone led to significant alterations in trophoblast differentiation, with more than 50% inhibition of EVCT invasion [9]. In this study, we treated EVCTs and VCTs with 1 μM rosiglitazone in order to more fully understand the effects of PPARγ on gene expression in these tissues.

Our microarray results for EVCTs were published previously with the aim of identifying significant DEGs for further study [22]. However, this work provided little information about the relative enrichment of pathways and processes among these DEGs and did not include any comparisons with RT-VCTs. To more broadly determine the key genes, biological processes, and pathways affected by activated PPARγ in trophoblasts, in this study, we also analyzed gene expression changes in VCTs using microarray profiling, and, through various approaches, identified the enriched processes that were linked with these DEGs in RT-EVCTs and RT-VCTs. We were thus able to compare the similarities and differences between EVCTs and VCTs affected by activated PPARγ. In total, there were 139 DEGs in RT-EVCTs and 197 DEGs in RT-VCTs, and these were associated with enrichment in more than 200 GO and pathway terms (Tables S1-S8). Of these terms, the most significant and relevant are depicted in the figures. The majority of the terms recovered in our analysis were consistent with reports from the existing literature. For example, the terms "long-chain fatty-acyl-CoA biosynthetic process," "regulation of plasma lipoprotein particle levels," "plasma

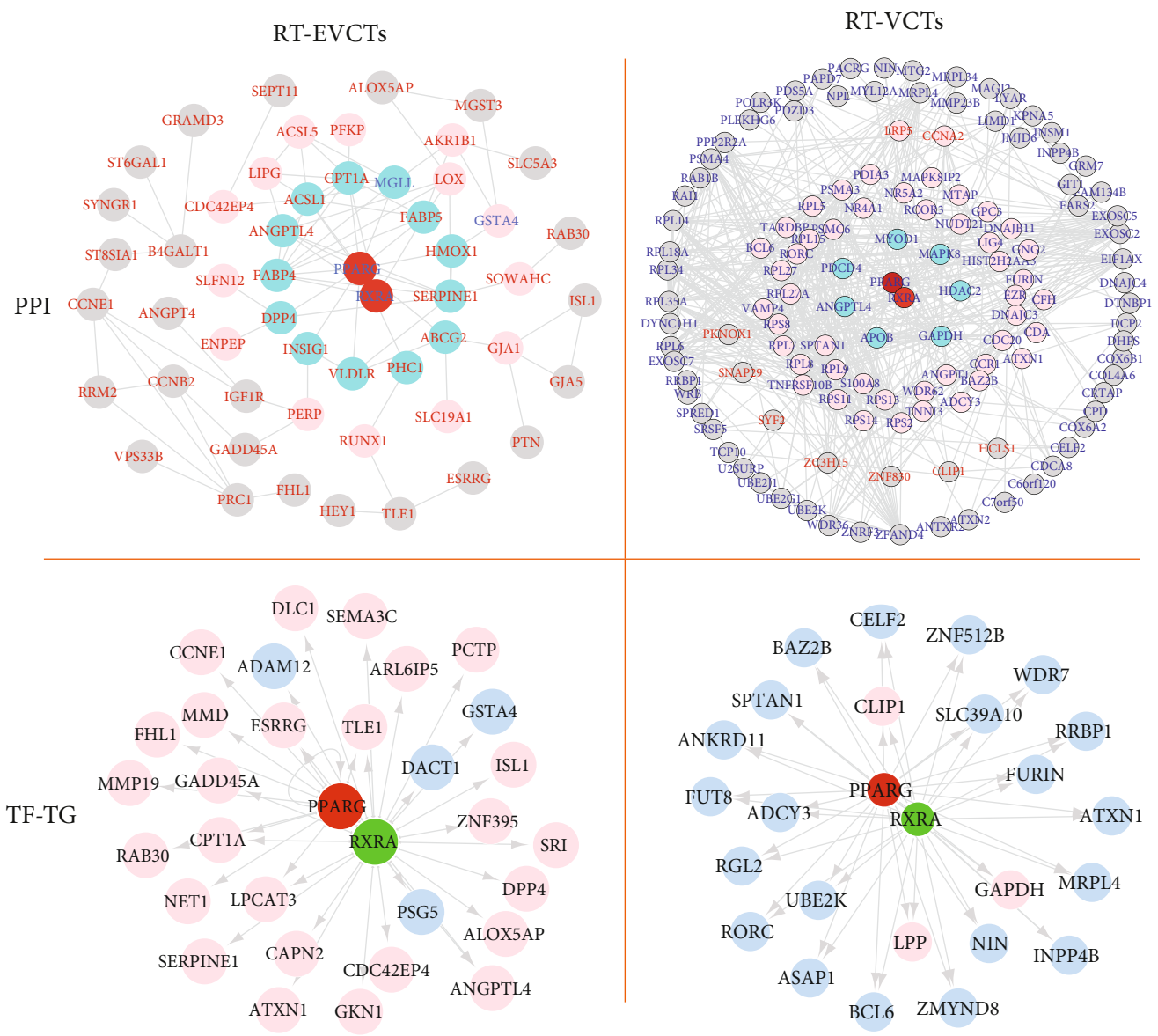

Figure 7: Interactions of the PPARγ and RXRα complex with DEGs of RT-EVCTs and RT-VCTs. Predictions were made of protein-protein interactions between PPARγ and DEG-encoded proteins, as well as of the transcription factor-target gene (TF-TG) interactions of PPARγ with DEG promoters. The PPARγ and RXRα (heterodimeric nuclear receptor partner of PPARγ) complex, together with the DEGs recovered in this study, were submitted to the STRING online tool. Visualizations were modified in Cytoscape to depict hierarchical interactions and gene expression. For hierarchical protein-protein interactions, red text represents upregulated genes, blue text represents downregulated genes, blue circles represent direct interactions with the PPARγ complex, red circles represent second-level interactions, and grey circles represent plus-level interactions. TF-TG interactions of the PPARγ complex with DEG promoters were predicted by iRegulon based on the TRANSFAC database. Red circles represent upregulated DEGs and blue circles represent downregulated DEGs. PPARγ: peroxisome proliferator-activated receptor-γ; RXRα: retinoid x receptor-α; RT-EVCTs: rosiglitazone-treated extravillous cytotrophoblasts; RT-VCTs: rosiglitazone-treated villous cytotrophoblasts; DEGs: differentially expressed genes; PPI: protein-protein-interaction; TF-TG: transcription factor-target gene.

lipoprotein remodeling," and "PPAR signaling pathway" are all associated with "fatty acid transport," which in the placenta is known to demonstrate sex-specific differences due to the PPARγ-dependent response of genes involved in lipogenesis [34]. Signaling molecules and dynamic regulation of the cytoskeleton are required in trophoblast invasion [35–37], which are related to such terms as "regulation of epithelial cell migration," "regulation of actin cytoskeleton," and "tight junction." Among the specific pathways highlighted, the HIF-1 signaling pathway is known to participate in PPARγ-mediated placental angiogenesis [16]; the P53 signaling pathway mediates trophoblast apoptosis via ligand-specific activation of PPARγ [10]; the JNK signaling pathway plays an essential role in blood-placental barrier formation [38, 39], as well as in EVCT migration and endothelial-like tube formation [40]; and the

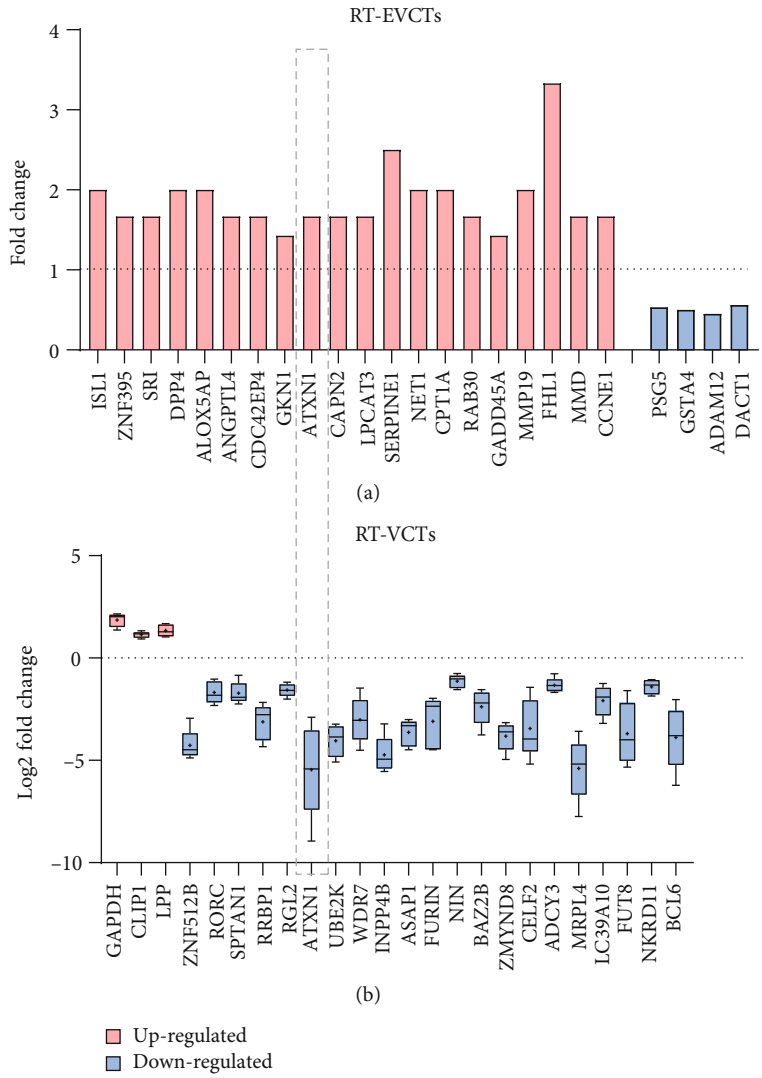

Figure 8: Expression of genes targeted by PPARγ and RXRα in RT-EVCTs and RT-VCTs. Gene symbols were retrieved from the normalized gene expression matrix, together with the log2 fold change values in each sample. With these values, boxplots were graphed for (a) RT-EVCTs and (b) RT-VCTs, with upregulation represented in red and downregulation in blue. The grey dashed box indicates the only gene found in both tissue types. PPARγ: peroxisome proliferator-activated receptor-γ; RXRα: retinoid x receptor-α; RT-EVCTs: rosiglitazone-treated extravillous cytotrophoblasts; RT-VCTs: rosiglitazone-treated cytotrophoblasts.

mTOR signaling pathway regulates adipogenic proteins in the placenta, with mTOR acting as a decidual nutrient sensor in histotrophic nutrition, which is crucial to embryo viability as well as early placental and fetal development [41]. Furthermore, our results were also consistent with the posttranscriptional modifications involved in placentation, with the terms "positive regulation of phosphoprotein," "regulation of protein deacetylation," "histone deacetylation," and "ubiquitin-like protein conjugating enzyme activity" all known from previous reports. Indeed, different subtypes of trophoblast vary in phosphorylation status depending on the stage of placental development and differentiation. For example, EVCTs require Smad2/3 phosphorylation for differentiation while the absence of pSmad2C is necessary for VCTs [42]. Downregulation of histone deacetylase-9 can repress trophoblast migration and invasion [43], and likewise, inhibition of histone acetylation in human endometrial stromal cells limits trophoblast invasion [44]. Ubiquitination of amino acid transporters expressed specifically in the plasma membrane of the trophoblast can decrease amino acid uptake, leading to abnormal development of the placenta and restricted fetal growth [45, 46]. In addition, PPARγ can be phosphorylated through activation of the downstream ERKs 1/2 or p38/c-JNK pathways [47, 48]. Rosiglitazone blocks the acetylation of lysine residues of PPARγ at positions K268ac and K293ac [49]. Atypical polyubiquitination of PPARγ reduces proteasomal degradation and guarantees the stabilization of PPARγ [50, 51].

A major aim of this study was to compare patterns of enrichment between RT-EVCTs and RT-VCTs. During EVCT invasion, noninvasive EVCTs undergo an epithelial-mesenchymal transition to acquire the invasive phenotype [52]. Invasive EVCTs then migrate away from the placenta

up to the first third of the endometrium and colonize the maternal spiral arteries. We found a comparison of these two types of trophoblasts to be particularly compelling, given the number of studies that have focused on their differences and similarities. For example, the transformation of noninvasive EVCTs into invasive EVCTs involves expression differences in adhesion molecules, which manifest themselves when EVCTs escape from the anchoring column and invade into the endometrium (decidua, spiral arteries, and myometrium) [53]. Other studies have examined differences between EVCTs and VCTs with respect to hCG secretion for the normal maintenance of pregnancy [54] and placental cytokine secretion [55]. These biological processes are apparent in the terms recovered here that were associated with "regulation of endothelial cell migration," "embryo implantation," "steroid hormone receptor binding," "secretion and action," and "preeclampsia." The main point is that these biological processes have all been reported to be regulated by PPARγ. For example, the activation of PPARγ has been found to prevent the TGF-β-induced epithelial-mesenchymal transition via inhibition of transcription of the E-cadherin and N-cadherin promoters [56]. Furthermore, PPARγ was reported to modulate basal levels of the hCGα and hCGβ subunits, resulting in differences in expression between EVCTs and VCTs [57]. Additional evidence has been obtained from studies with rosiglitazone; for example, treatment with 1 μM of the PPARγ agonist was found to decrease and increase, respectively, the number of transcripts of TGFβ2 and IL1β [32]. Such regulatory changes might be represented here by the terms "regulation of endothelial cell migration," "Wnt signaling pathway," "negative regulation of protein phosphorylation," "transcription factor activity," "PPAR signaling pathway," and "HIF-1 signaling pathway".

In general, our datasets revealed an abundance of biological processes or pathways affected by PPARγ, many of which are consistent with previous reports. This concordance should increase confidence in our results and indicate avenues for further study. However, because this study relied on DNA microarray technology, it was inherently limited by the probe set used; it is possible that some unknown genes may not have been detected effectively and certain biological processes or pathways may have been missed. Further exploration with the application of advanced technology such as RNAseq would be helpful to identify and fill in any missing gaps in our dataset.

Finally, in order to facilitate study of the mechanisms behind the molecular interactions, we attempted to predict the protein-protein interactions between the DEGs recovered here and PPARγ and RXRα. As was recently reviewed, the transcription exerted by the PPARγ and RXRα complex can be modified by different types of cofactors, such as the transcriptional corepressors SMRT (silencing mediator of retinoid and thyroid hormone receptors) and NCoR (nuclear receptor corepressor), which block transactivation or the transcriptional coactivators CREB-binding protein (CBP), histone acetyltransferase p300 (p300), and PPAR-binding protein (PBP), which have the opposite effect [58]. We propose that the interaction with PPARγ might affect the transcription complex formed by PPARγ and RXRα, their cofactors or transcription partners, which could then lead to alterations in the regulation of different transcription circuits. Our results provided evidence for direct protein-protein and protein-promoter interaction with the PPARγ complex. Among the proteins that appear to interact directly with PPARγ, several have been experimentally verified, including ANGPTL4 [59–61], ABCG2 [62], APOB [63], CCNE1 [64], CPT1B [65], FABP4 [66–69], HMOX1 [70], and SERPINE1 [71, 72]. Many of the TF-TG interactions, which were predicted using the position weight matrix algorithm, have not been previously reported and await further verification. Our interaction matrix (Figure 7) also revealed more extensive upstream-to-downstream signaling pathways, such as the PPARγ-MAPK-MMP signaling pathway. Commonly, phosphorylated PPARγ stimulates the MAPK-activated pathway, leading to the activation of extracellular signal-regulated kinases (ERKs) that then induce the upregulation of matrix metalloproteinase (MMP) [73–75]. Here, only a single DEG, ATXN1, was found in both types of rosiglitazone-treated trophoblast, but with opposing responses in RT-EVCTs and RT-VCTs: this gene was upregulated in RT-EVCTs and downregulated in RT-VCTs. It has been reported that the ATXN1 protein family can regulate remodeling of the extracellular matrix [76], which indicates a potential involvement in trophoblast differentiation. However, further research is needed to determine if this gene is solely responsible for the different responses of the two distinct cell types to PPARγ activation. In addition to the direct target genes predicted here, the genes in secondary relationships should be paid equal attention in terms of potential regulation by other target genes. For example, our previous research has shown the key role of LOX1, through secondary interactions, in cytotrophoblast invasion [22].

5. Conclusions

To our knowledge, our results reveal for the first time the widespread effects of PPARγ activation in EVCTs and VCTs, highlighting extensive changes in gene expression and the biological processes and pathways affected. This study provides a broad perspective of PPARγ-influenced biological processes in trophoblasts and facilitates further study, particularly into potential drug-targeted genes or pathways in the human placenta.

Data Availability

Our microarray data have been deposited in the Gene Expression Omnibus public repository (https://www.ncbi.nlm.nih.gov/geo/); EVCT microarray data under accession number GSE28426, VCT microarray data under accession number GSE137434).

Conflicts of Interest

The authors declare that there are no conflicts of interest that could affect the impartiality of the reported research.

Authors' Contributions

Séverine A. Degrelle and Thierry Fournier contributed equally to this work.

Acknowledgments

The authors wish to thank the consenting patients and the clinical staff midwives of Cochin Port Royal for providing placental tissues and Dr. Danièle Evain-Brion, former director of the Unit, for her support, as well as Lindsay Higgins for English editing (http://www.englishservicesforscientists.com). This work was carried out with the funding support of INSERM, University of Paris Descartes, and RSI Professions Libérales Provinces, 44 boulevard de la Bastille, 75578 Paris Cedex 12, as well as the China Scholarship Council (CSC) in Chegongzhuang Avenue, Beijing 100044, P. R China.

Supplementary Materials

Differentially expressed genes (DEGs) were selected from the EVCT microarray data under accession number GSE28426 and VCT microarray data under accession number GSE137434. These genes were subsequently enriched according to the gene ontology (GO) terms. The terms of the enriched results were shown in detail in Tables S1-S8. Table S1-S4 shows the terms of GO biological process, GO cellular component, GO molecular function, and pathways of DEGs from the EVCT microarray data, respectively, while Table S5-S8 shows the terms of GO biological process, GO cellular component, GO molecular function, and pathways of DEGs from the VCT microarray data, respectively. Table S1_EVCT_DEGs_Go_Biological Process. Table S2_EVCT_DEGs_Go_Cellular Component. Table S3_EVCT_DEGs_Go_Molecular Function. Table S4_EVCT_DEGs_Pathways. Table S5_VCT_DEGs_Go_Biological Process. Table S6_VCT_DEGs_Go_Cellular Component. Table S7_VCT_DEGs_Go_Molecular Function. Table S8_VCT_DEGs_Pathways. *(Supplementary Materials)*

References

[1] J. Buchrieser, S. A. Degrelle, T. Couderc et al., "IFITM proteins inhibit placental syncytiotrophoblast formation and promote fetal demise," *Science*, vol. 365, no. 6449, pp. 176–180, 2019.

[2] C. A. Labarrere, H. L. DiCarlo, E. Bammerlin et al., "Failure of physiologic transformation of spiral arteries, endothelial and trophoblast cell activation, and acute atherosis in the basal plate of the placenta," *American Journal of Obstetrics and Gynecology*, vol. 216, no. 3, pp. 287.e1–287.e16, 2017.

[3] L. Ji, J. Brkić, M. Liu, G. Fu, C. Peng, and Y.-L. Wang, "Placental trophoblast cell differentiation: physiological regulation and pathological relevance to preeclampsia," *Molecular Aspects of Medicine*, vol. 34, no. 5, pp. 981–1023, 2013.

[4] V. Chandra, P. Huang, Y. Hamuro et al., "Structure of the intact PPAR-γ-RXR-α nuclear receptor complex on DNA," *Nature*, vol. 456, no. 7220, pp. 350–356, 2008.

[5] Y. Barak, M. C. Nelson, E. S. Ong et al., "PPARγ is required for placental, cardiac, and adipose tissue development," *Molecular Cell*, vol. 4, no. 4, pp. 585–595, 1999.

[6] N. Kubota, Y. Terauchi, H. Miki et al., "PPARγ mediates high-fat diet-induced adipocyte hypertrophy and insulin resistance," *Molecular Cell*, vol. 4, no. 4, pp. 597–609, 1999.

[7] S. Z. Duan, C. Y. Ivashchenko, S. E. Whitesall et al., "Hypotension, lipodystrophy, and insulin resistance in generalized PPARγ-deficient mice rescued from embryonic lethality," *The Journal of Clinical Investigation*, vol. 117, no. 3, pp. 812–822, 2007.

[8] T. Fournier, L. Pavan, A. Tarrade et al., "The role of PPAR-γ/RXR-α heterodimers in the regulation of human trophoblast invasion," *Annals of the New York Academy of Sciences*, vol. 973, pp. 26–30, 2002.

[9] A. Tarrade, K. Schoonjans, L. Pavan et al., "PPARγ/RXRα heterodimers control human trophoblast invasion," *The Journal of Clinical Endocrinology and Metabolism*, vol. 86, no. 10, pp. 5017–5024, 2001.

[10] W. T. Schaiff, M. G. Carlson, S. D. Smith, R. Levy, D. M. Nelson, and Y. Sadovsky, "Peroxisome proliferator-activated receptor-γ modulates differentiation of human trophoblast in a ligand-specific manner," *The Journal of Clinical Endocrinology and Metabolism*, vol. 85, no. 10, pp. 3874–3881, 2000.

[11] Q. Zhao, D. Yang, L. Gao et al., "Downregulation of peroxisome proliferator-activated receptor gamma in the placenta correlates to hyperglycemia in offspring at young adulthood after exposure to gestational diabetes mellitus," *Journal of Diabetes Investigation*, vol. 10, no. 2, pp. 499–512, 2019.

[12] J. R. Chen, O. P. Lazarenko, M. L. Blackburn et al., "Maternal obesity programs senescence signaling and glucose metabolism in osteo-progenitors from rat and human," *Endocrinology*, vol. 157, no. 11, pp. 4172–4183, 2016.

[13] L. Kadam, B. Kilburn, D. Baczyk, H. R. Kohan-Ghadr, J. Kingdom, and S. Drewlo, "Rosiglitazone blocks first trimester *in-vitro* placental injury caused by NF- κB-mediated inflammation," *Scientific Reports*, vol. 9, no. 1, article 2018, 2019.

[14] L. Kadam, N. Gomez-Lopez, T. N. Mial, H. R. Kohan-Ghadr, and S. Drewlo, "Rosiglitazone regulates TLR4 and rescues HO-1 and NRF2 expression in myometrial and decidual macrophages in inflammation-induced preterm birth," *Reproductive Sciences*, vol. 24, no. 12, pp. 1590–1599, 2017.

[15] H. R. Kohan-Ghadr, B. A. Kilburn, L. Kadam et al., "Rosiglitazone augments antioxidant response in the human trophoblast and prevents apoptosis," *Biology of Reproduction*, vol. 100, no. 2, pp. 479–494, 2019.

[16] J. Zhang, X. Peng, A. Yuan, Y. Xie, Q. Yang, and L. Xue, "Peroxisome proliferator-activated receptor γ mediates porcine placental angiogenesis through hypoxia inducible factor-, vascular endothelial growth factor- and angiopoietin-mediated signaling," *Molecular Medicine Reports*, vol. 16, no. 3, pp. 2636–2644, 2017.

[17] L. Liu, X. Zhuang, M. Jiang, F. Guan, Q. Fu, and J. Lin, "ANGPTL4 mediates the protective role of PPARγ activators in the pathogenesis of preeclampsia," *Cell Death & Disease*, vol. 8, no. 9, article e3054, 2017.

[18] Y. Lin, K. M. Bircsak, L. Gorczyca, X. Wen, and L. M. Aleksunes, "Regulation of the placental BCRP transporter by PPARγ," *Journal of Biochemical and Molecular Toxicology*, vol. 31, no. 5, article e21880, 2017.

[19] T. Fournier, J. Guibourdenche, K. Handschuh et al., "PPARγ and human trophoblast differentiation," *Journal of Reproductive Immunology*, vol. 90, no. 1, pp. 41–49, 2011.

[20] T. Fournier, P. Therond, K. Handschuh, V. Tsatsaris, and D. Evain-Brion, "PPARγ and early human placental development," *Current Medicinal Chemistry*, vol. 15, no. 28, pp. 3011–3024, 2008.

[21] T. Fournier, K. Handschuh, V. Tsatsaris, J. Guibourdenche, and D. Evain-Brion, "Role of nuclear receptors and their ligands in human trophoblast invasion," *Journal of Reproductive Immunology*, vol. 77, no. 2, pp. 161–170, 2008.

[22] N. Segond, S. A. Degrelle, S. Berndt et al., "Transcriptome analysis of PPARγ target genes reveals the involvement of lysyl oxidase in human placental cytotrophoblast invasion," *PLoS One*, vol. 8, no. 11, article e79413, 2013.

[23] H. J. Kliman, J. E. Nestler, E. Sermasi, J. M. Sanger, and J. F. Strauss III, "Purification, characterization, and *in vitro* differentiation of cytotrophoblasts from human term Placentae," *Endocrinology*, vol. 118, no. 4, pp. 1567–1582, 1986.

[24] E. Alsat, V. Mirlesse, C. Fondacci, M. Dodeur, and D. Evain-Brion, "Parathyroid hormone increases epidermal growth factor receptors in cultured human trophoblastic cells from early and term placenta," *The Journal of Clinical Endocrinology and Metabolism*, vol. 73, no. 2, pp. 288–295, 1991.

[25] C. Henegar, J. Tordjman, V. Achard et al., "Adipose tissue transcriptomic signature highlights the pathological relevance of extracellular matrix in human obesity," *Genome Biology*, vol. 9, no. 1, article R14, 2008.

[26] V. G. Tusher, R. Tibshirani, and G. Chu, "Significance analysis of microarrays applied to the ionizing radiation response," *Proceedings of the National Academy of Sciences of the United States of America*, vol. 98, no. 9, pp. 5116–5121, 2001.

[27] C. Rouault, K. Clément, M. Guesnon et al., "Transcriptomic signatures of villous cytotrophoblast and syncytiotrophoblast in term human placenta," *Placenta*, vol. 44, pp. 83–90, 2016.

[28] G. Bindea, B. Mlecnik, H. Hackl et al., "ClueGO: a Cytoscape plug-in to decipher functionally grouped gene ontology and pathway annotation networks," *Bioinformatics*, vol. 25, no. 8, pp. 1091–1093, 2009.

[29] G. Yu, L. G. Wang, Y. Han, and Q. Y. He, "clusterProfiler: an R package for comparing biological themes among gene clusters," *OMICS*, vol. 16, no. 5, pp. 284–287, 2012.

[30] B. Huppertz, "Placental origins of Preeclampsia," *Hypertension*, vol. 51, no. 4, pp. 970–975, 2008.

[31] J. M. Roberts and D. W. Cooper, "Pathogenesis and genetics of pre-eclampsia," *Lancet*, vol. 357, no. 9249, pp. 53–56, 2001.

[32] T. Fournier, K. Handschuh, V. Tsatsaris, and D. Evain-Brion, "Involvement of PPARγ in human trophoblast invasion," *Placenta*, vol. 28, Supplement A, pp. S76–S81, 2007.

[33] J. M. Lehmann, L. B. Moore, T. A. Smith-Oliver, W. O. Wilkison, T. M. Willson, and S. A. Kliewer, "An antidiabetic thiazolidinedione is a high affinity ligand for peroxisome proliferator-activated receptor γ (PPARγ)," *The Journal of Biological Chemistry*, vol. 270, no. 22, pp. 12953–12956, 1995.

[34] M. Gimpfl, J. Rozman, M. Dahlhoff et al., "Modification of the fatty acid composition of an obesogenic diet improves the maternal and placental metabolic environment in obese pregnant mice," *Biochimica et Biophysica Acta - Molecular Basis of Disease*, vol. 1863, no. 6, pp. 1605–1614, 2017.

[35] A. J. Ridley, M. A. Schwartz, K. Burridge et al., "Cell migration: integrating signals from front to back," *Science*, vol. 302, no. 5651, pp. 1704–1709, 2003.

[36] C. Chakraborty, L. M. Gleeson, T. McKinnon, and P. K. Lala, "Regulation of human trophoblast migration and invasiveness," *Canadian Journal of Physiology and Pharmacology*, vol. 80, no. 2, pp. 116–124, 2002.

[37] P. Bischoff, A. Meisser, and A. Campana, "Paracrine and Autocrine Regulators of Trophoblast Invasion– A Review," *Placenta*, vol. 21, Supplement A, pp. S55–S60, 2000.

[38] V. Nadeau and J. Charron, "Essential role of the ERK/MAPK pathway in blood-placental barrier formation," *Development*, vol. 141, no. 14, pp. 2825–2837, 2014.

[39] J. Charron, V. Bissonauth, and V. Nadeau, "Implication of MEK1 and MEK2 in the establishment of the blood-placenta barrier during placentogenesis in mouse," *Reproductive Biomedicine Online*, vol. 25, no. 1, pp. 58–67, 2012.

[40] N. Lala, G. V. Girish, A. Cloutier-Bosworth, and P. K. Lala, "Mechanisms in decorin regulation of vascular endothelial growth factor-induced human trophoblast migration and acquisition of endothelial Phenotype1," *Biology of Reproduction*, vol. 87, no. 3, p. 59, 2012.

[41] S. L. Roberti, R. Higa, V. White, T. L. Powell, T. Jansson, and A. Jawerbaum, "Critical role of mTOR, PPARγ and PPARδ signaling in regulating early pregnancy decidual function, embryo viability and feto-placental growth," *Molecular Human Reproduction*, vol. 24, no. 6, pp. 327–340, 2018.

[42] S. Haider, V. Kunihs, C. Fiala, J. Pollheimer, and M. Knofler, "Expression pattern and phosphorylation status of Smad2/3 in different subtypes of human first trimester trophoblast," *Placenta*, vol. 57, pp. 17–25, 2017.

[43] D. Xie, J. Zhu, Q. Liu et al., "Dysregulation of HDAC9 represses trophoblast cell migration and invasion through TIMP3 activation in preeclampsia," *American Journal of Hypertension*, vol. 32, no. 5, pp. 515–523, 2019.

[44] C. Estella, I. Herrer, S. P. Atkinson et al., "Inhibition of histone deacetylase activity in human endometrial stromal cells promotes extracellular matrix remodelling and limits embryo invasion," *PLoS One*, vol. 7, no. 1, article e30508, 2012.

[45] F. J. Rosario, K. G. Dimasuay, Y. Kanai, T. L. Powell, and T. Jansson, "Regulation of amino acid transporter trafficking by mTORC1 in primary human trophoblast cells is mediated by the ubiquitin ligase Nedd4-2," *Clinical Science*, vol. 130, no. 7, pp. 499–512, 2016.

[46] Y. Y. Chen, F. J. Rosario, M. A. Shehab, T. L. Powell, M. B. Gupta, and T. Jansson, "Increased ubiquitination and reduced plasma membrane trafficking of placental amino acid transporter SNAT-2 in human IUGR," *Clinical Science*, vol. 129, no. 12, pp. 1131–1141, 2015.

[47] H. S. Camp and S. R. Tafuri, "Regulation of peroxisome proliferator-activated receptor gamma activity by mitogen-activated protein kinase," *The Journal of Biological Chemistry*, vol. 272, no. 16, pp. 10811–10816, 1997.

[48] E. Hu, J. B. Kim, P. Sarraf, and B. M. Spiegelman, "Inhibition of adipogenesis through MAP kinase-mediated phosphorylation of PPARγ," *Science*, vol. 274, no. 5295, pp. 2100–2103, 1996.

[49] L. Qiang, L. Wang, N. Kon et al., "Brown remodeling of white adipose tissue by SirT1-dependent deacetylation of Pparγ," *Cell*, vol. 150, no. 3, pp. 620–632, 2012.

[50] J. J. Li, R. Wang, R. Lama et al., "Ubiquitin ligase NEDD4 regulates PPARγ stability and adipocyte differentiation in 3T3-L1 Cells," *Scientific Reports*, vol. 6, no. 1, 2016.

[51] M. Watanabe, H. Takahashi, Y. Saeki et al., "The E3 ubiquitin ligase TRIM23 regulates adipocyte differentiation via stabilization of the adipogenic activator PPARγ," *Elife*, vol. 4, 2015.

[52] S. DaSilva-Arnold, J. L. James, A. Al-Khan, S. Zamudio, and N. P. Illsley, "Differentiation of first trimester cytotrophoblast to extravillous trophoblast involves an epithelial-mesenchymal transition," *Placenta*, vol. 36, no. 12, pp. 1412–1418, 2015.

[53] L. K. Harris, C. J. Jones, and J. D. Aplin, "Adhesion molecules in human trophoblast - a review. II. Extravillous trophoblast," *Placenta*, vol. 30, no. 4, pp. 299–304, 2009.

[54] K. Handschuh, J. Guibourdenche, V. Tsatsaris et al., "Human chorionic gonadotropin expression in human trophoblasts from early placenta: comparative study between villous and extravillous trophoblastic cells," *Placenta*, vol. 28, no. 2-3, pp. 175–184, 2007.

[55] K. Naruse, B. A. Innes, J. N. Bulmer, S. C. Robson, R. F. Searle, and G. E. Lash, "Secretion of cytokines by villous cytotrophoblast and extravillous trophoblast in the first trimester of human pregnancy," *Journal of Reproductive Immunology*, vol. 86, no. 2, pp. 148–150, 2010.

[56] A. K. Reka, H. Kurapati, V. R. Narala et al., "Peroxisome proliferator-activated receptor-gamma activation inhibits tumor metastasis by antagonizing Smad3-mediated epithelial-mesenchymal transition," *Molecular Cancer Therapeutics*, vol. 9, no. 12, pp. 3221–3232, 2010.

[57] K. Handschuh, J. Guibourdenche, M. Cocquebert et al., "Expression and regulation by PPARγ of hCG α- and β-subunits: comparison between villous and invasive extravillous trophoblastic cells," *Placenta*, vol. 30, no. 12, pp. 1016–1022, 2009.

[58] X. Ma, D. Wang, W. Zhao, and L. Xu, "Deciphering the roles of PPARγ in adipocytes via dynamic change of transcription complex," *Frontiers in Endocrinology*, vol. 9, 2018.

[59] S. Yamagishi, T. Matsui, K. Nakamura, M. Takeuchi, and H. Inoue, "Telmisartan inhibits advanced glycation end products (AGEs)-elicited endothelial cell injury by suppressing AGE receptor (RAGE) expression via peroxisome proliferator-activated receptor-gammaactivation," *Protein and Peptide Letters*, vol. 15, no. 8, pp. 850–853, 2008.

[60] J. G. Chen, X. Li, H. Y. Huang et al., "Identification of a peroxisome proliferator responsive element (PPRE)-like *cis* -element in mouse plasminogen activator inhibitor-1 gene promoter," *Biochemical and Biophysical Research Communications*, vol. 347, no. 3, pp. 821–826, 2006.

[61] S. Mandard, F. Zandbergen, N. S. Tan et al., "The direct peroxisome proliferator-activated receptor target fasting-induced adipose factor (FIAF/PGAR/ANGPTL4) is present in blood plasma as a truncated protein that is increased by fenofibrate treatment," *The Journal of Biological Chemistry*, vol. 279, no. 33, pp. 34411–34420, 2004.

[62] I. Szatmari, G. Vámosi, P. Brazda et al., "Peroxisome proliferator-activated receptor γ-regulated ABCG2 expression confers cytoprotection to human dendritic cells," *The Journal of Biological Chemistry*, vol. 281, no. 33, pp. 23812–23823, 2006.

[63] N. Xu, B. Ahren, J. Jiang, and P. Nilsson-Ehle, "Down-regulation of apolipoprotein M expression is mediated by phosphatidylinositol 3-kinase in HepG2 cells," *Biochimica et Biophysica Acta*, vol. 1761, no. 2, pp. 256–260, 2006.

[64] W. K. Leung, A. H. Bai, V. Y. Chan et al., "Effect of peroxisome proliferator activated receptor gamma ligands on growth and gene expression profiles of gastric cancer cells," *Gut*, vol. 53, no. 3, pp. 331–338, 2004.

[65] A. Baldan, J. Relat, P. F. Marrero, and D. Haro, "Functional interaction between peroxisome proliferator-activated receptors-alpha and Mef-2C on human carnitine palmitoyltransferase 1β (CPT1β) gene activation," *Nucleic Acids Research*, vol. 32, no. 16, pp. 4742–4749, 2004.

[66] U. H. Park, S. K. Yoon, T. Park, E. J. Kim, and S. J. Um, "Additional sex comb-like (ASXL) proteins 1 and 2 play opposite roles in adipogenesis via reciprocal regulation of peroxisome proliferator-activated receptor γ," *The Journal of Biological Chemistry*, vol. 286, no. 2, pp. 1354–1363, 2011.

[67] L. Sarov-Blat, R. S. Kiss, B. Haidar et al., "Predominance of a proinflammatory phenotype in monocyte-derived macrophages from subjects with low plasma HDL-cholesterol," *Arteriosclerosis, Thrombosis, and Vascular Biology*, vol. 27, no. 5, pp. 1115–1122, 2007.

[68] Y. Rival, A. Stennevin, L. Puech et al., "Human adipocyte fatty acid-binding protein (aP2) gene promoter-driven reporter assay discriminates nonlipogenic peroxisome proliferator-activated receptor γ ligands," *The Journal of Pharmacology and Experimental Therapeutics*, vol. 311, no. 2, pp. 467–475, 2004.

[69] D. B. Savage, C. P. Sewter, E. S. Klenk et al., "Resistin / Fizz3 expression in relation to obesity and peroxisome proliferator-activated receptor-gamma action in humans," *Diabetes*, vol. 50, no. 10, pp. 2199–2202, 2001.

[70] G. Krönke, A. Kadl, E. Ikonomu et al., "Expression of heme oxygenase-1 in human vascular cells is regulated by peroxisome proliferator-activated receptors," *Arteriosclerosis, Thrombosis, and Vascular Biology*, vol. 27, no. 6, pp. 1276–1282, 2007.

[71] J. C. Yoon, T. W. Chickering, E. D. Rosen et al., "Peroxisome proliferator-activated receptor γ target gene encoding a novel angiopoietin-related protein associated with adipose differentiation," *Molecular and Cellular Biology*, vol. 20, no. 14, pp. 5343–5349, 2000.

[72] N. Marx, T. Bourcier, G. K. Sukhova, P. Libby, and J. Plutzky, "PPARγ activation in human endothelial cells increases plasminogen activator inhibitor type-1 Expression," *Arteriosclerosis, Thrombosis, and Vascular Biology*, vol. 19, no. 3, pp. 546–551, 1999.

[73] X. Lan, L. J. Fu, J. Zhang et al., "Bisphenol A exposure promotes HTR-8/SVneo cell migration and impairs mouse placentation involving upregulation of integrin-β1 and MMP-9 and stimulation of MAPK and PI3K signaling pathways," *Oncotarget*, vol. 8, no. 31, pp. 51507–51521, 2017.

[74] L. Liu, Y. Wang, C. Shen et al., "Benzo(a)pyrene inhibits migration and invasion of extravillous trophoblast HTR-8/SVneo cells via activation of the ERK and JNK pathway," *Journal of Applied Toxicology*, vol. 36, no. 7, pp. 946–955, 2016.

[75] M. Cohen, A. Meisser, L. Haenggeli, and P. Bischof, "Involvement of MAPK pathway in TNF-α-induced MMP-9 expression in human trophoblastic cells," *Molecular Human Reproduction*, vol. 12, no. 4, pp. 225–232, 2006.

[76] Y. Lee, J. D. Fryer, H. Kang et al., "ATXN1 protein family and CIC regulate extracellular matrix remodeling and lung alveolarization," *Developmental Cell*, vol. 21, no. 4, pp. 746–757, 2011.